UNIVERSITY OF CALIFORNIA

SANTA CRUZ

Surface Modification of Medical Grade PVC to Prevent Biofilm Formation Using Copper-Free Azide-Alkyne Cycloadditions

A thesis submitted in partial satisfaction
of the requirements for the degree of

MASTER OF SCIENCE

in

CHEMISTRY

by

Jerin Tasnim

March 2021

The Thesis of Jerin Tasnim is approved:

_____

Professor Rebecca Braslau, Advisor

_____

Professor Bakthan Singaram, Chair

_____

Assistant Professor Jevgenij Raskatov

_____

Quentin Williams
Interim Vice Provost and Dean of Graduate Studies

Table of Contents

List of Figures, Tables and Schemes

Abstract

Surface Modification of Medical Grade PVC to Prevent Biofilm Formation Using Copper-Free Azide-Alkyne Cycloadditions

Jerin Tasnim

Covalent surface modification of medical grade PVC tubing was performed using copper-free azide-alkyne cycloaddition reactions to prepare anti-fouling surfaces. PVC azide surface was synthesized by nucleophilic substitution of labile chlorine with sodium azide in the presence of phase transfer catalyst in aqueous media to minimize loss of plasticizer. Electron-poor alkynes with different functionality (zwitterionic, polyethylene oxide, polyfluoro and quaternary amines) were synthesized and covalently attached to the PVC azide surface by thermal azide-alkyne cycloaddition reactions. The reaction progress was monitored by ATR-FTIR spectroscopy. Static contact angle, surface free energy, contact angle hysteresis and atomic force microscopic images were taken for each modified surface. Except for the C_6F_{13} polyfluoro group, the other functional groups containing zwitterionic, polyethylene oxide and quaternary ammonium display hydrophilic properties with the initial SCA in the range of 35-80° due to the strong surface charges. All the modified PVC surfaces maintain their wetting properties against vigorous water rinsing for long period of time (over 60 minutes of sonication) confirming strong

covalent bonding of the functional groups to the surface. The antifouling activity of these modified endotracheal tubing samples was evaluated by bacterial adherence assay using *Pseudomonas aeruginosa*, a gram-negative opportunistic and nosocomial pathogen. Although the adherence assays demonstrate that high polyfluoro (di-ester of C_6F_{13}) and long quaternary amine functionality samples slightly reduced *P. aeruginosa* adherence to endotracheal tubing, the inhibition was not as strong as expected. X-Ray Photoelectron Spectroscopy revealed a pre-existing silicone coating on the original commercial samples, dampening the effects of biofilm inhibition from the chemical modification procedures.

Acknowledgements

I would like to thank the University of California, Santa Cruz for giving me the opportunity to become a tiny part of this wonderful campus. I would like to thank my advisor professor Rebecca Braslau. Thank you for giving me the opportunity to work in your lab. I have learnt many things from you. I have just one request, please do not make your student to work on a project where you cannot provide the core ingredient of the research. Collaboration is wonderful if both collaborators work with the same interest and pace.

I also want to thank my thesis committee: Professor Bakthan Singaram, and Professor Jevgenji Raskatov. Thanks for your advice in the past years. I have learned a lot from you.

I want to thank our collaborators Prof. Chalongrat Daengngm at Prince of Songkla University in Thailand, Dr. Kyle Floyd and Prof. Fitnat Yildiz at Microbiology and Environmental Toxicology Department at University of California. Many thanks for your help for surface characterization on modified PVC tubing. I would like to thank Dr. Monica Neuburger at Eurofins EAG Material Science in Sunnyvale, California for the XPS data. Without this data, I would never know the main reason behind lower antifouling activity of the modified surfaces. It has been a great experience working with you.

I also want to thank Dr. Jack Lee for helping with NMR and Li Zhang for helping with MS and ATR-FTIR. I also want to thank Karen for being very helpful and approachable.

Last but most importantly, I would like to thank my family and my friends. My husband Asif Islam, you have taught me in every aspects of life for the last 7 years. Thanks for bringing so much fun and happiness in my life. I would like to thank my family: my parents, my brother and my sister for being very supportive. Thanks to my son Areeb. You have completed me. I love you all.

1. Introduction: A Review on Surface Modification of Poly(vinyl Chloride)

Poly(vinyl chloride) (PVC) is the third most widely produced thermoplastic in the world.[1, 2] About 40 million metric tons of PVC is produced each year globally, in the United Stated 7.2 million metric tons was produced in 2019.[3] This production is expected to grow to nearly 60 million metric tons by 2025.

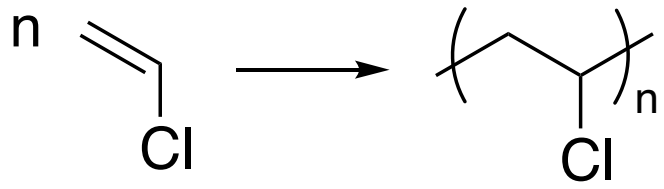

Figure 1.1: Vinyl chloride is polymerized to form PVC

1.1 PVC: Synthesis and Use

In 1872, German scientist Eugen Baumann synthesized PVC by leaving a container of vinyl chloride in sunlight.[4] Pure PVC is a rigid materials which limits its application. In 1926, American scientist Waldo Lonsbury Samon at the B. F. Goodrich company first plasticized PVC by blending the powder form with different additives to make it flexible.[5]

PVC is synthesized by polymerization of vinyl chloride monomer (**Figure 1.1**). About 80% of PVC is produced by suspension polymerization, 12% by emulsion polymerization and 8% by bulk polymerization.[6, 7] Generally, PVC is used in two different forms: rigid and flexible. Rigid or unplasticized PVC is used for construction

pipes, doors, windows and sheets. Different additives such as plasticizers, heat stabilizers, UV stabilizers, impact modifiers, thermal modifiers, fillers, flame retardants, biocides, blowing agents, smoke suppressors and pigments are added to the PVC products, depending on the required performance.[8] Normally, plasticizer is physically blended with PVC to make flexible PVC products like toys, tubing, clothing, bendable construction materials and food packaging.[9-13] These plasticizers can leach out from the polymer matrix. Exposed plasticizer contaminates environment and also causes serious health concerns in human.[14-18] Flexible PVC also covers a wide range of medical devices due to its low cost and durability.

Health care-associated infections (HCAIs), previously known as hospital-acquired infections, are one of the top five causes of death in the United States. The term HCAI is generally referred to as a type of infection that patients acquire while in a health care facility, which can appear within 2 to 30 days after receiving care.[19] Multiple studies show that the most HCAIs are categorized as Central Line Associated Blood Stream Infections (CLABSIs), Ventilator Associated Pneumonia (VAP), Catheter Associated Urinary Tract Infections (CAUTIs) or Surgery Site Infections (SSIs).[20, 21] A 2002 study by the Centers for Disease Control and Prevention found 1.7 million patients acquire HCAIs while receiving health care, and 100,000 patients died as a result.[22] About 65% of HCAIs are due to biofilm formation.[23]

1.2 Biofilm Formation

Biofilms are communities of microorganisms which can adhere to living or inert surfaces, surrounded by self-produced extracellular polymeric membranes. Biofilm formation is a complex process involving physical, chemical and biological influences.[24] First, (1) bacterial or microorganism cells are transported from bulk liquid to the surface of medical devices and adhere to the walls (**Figure 1.2**). This adhesion can be both reversible and irreversible. If the adherence is reversible, the microorganism can easily detached by small shear forces or their own motility.[25] (2) After attachment, the microorganisms starts to produce an extracellular polymeric membrane (EPS) which acts as a glue to hold the biofilm together and protects bacterial colonies from detrimental changes from surrounding microenvironment. (3 and 4, can happen both steps simultaneously or one earlier) Cell division, cellular growth and EPS production helps biofilms to grow stronger, larger and morphologically complex in structure. Finally, (5) dissemination and recolonization happen to the biofilms either as a fraction of the whole bacterial colonies, or even single cell can disperse. Small colonies of fragmented biofilms can be carried to the lungs, acting as a source of ventilator associated pneumonia.[26]

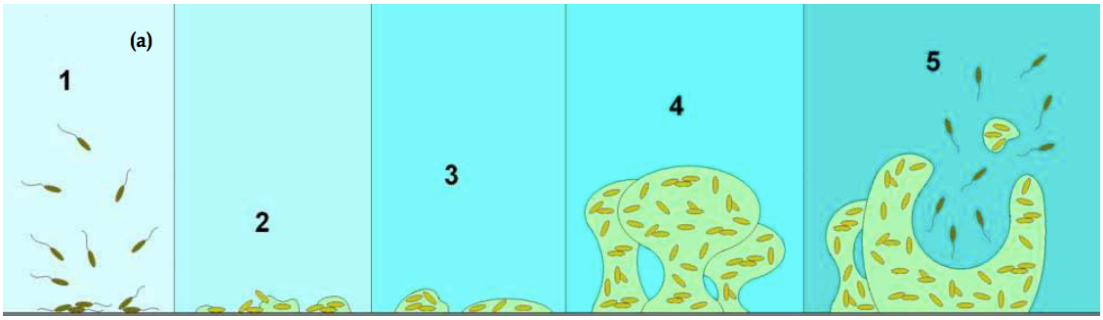

Figure 1.2: Biofilm formation process, adapted from reference 24

1.3 Bacteria Repelling and Antiadhesive surfaces

The requirement of antibacterial materials has increased for the reduction of infections. A variety of strategies have been adopted to make antifouling material surfaces (**Figure 1.3**).[27] The earliest stage of infection involves bacterial adhesion on surfaces. So, no bacterial colonies can grow if they cannot adhere on the surface. Antimicrobial surface modification can work in two different ways: antifouling or biocidal. Antifouling surfaces generally prevent initial bacterial adhesion by changing the surface properties, such as making super hydrophilic or hydrophobic or ultrasmooth surfaces, static repulsion, and lowering surface free energies. Biocidal surfaces are generally designed to kill bacteria rather than lowering initial adhesion. Surface coatings with silver or antibiotics act as biocides.

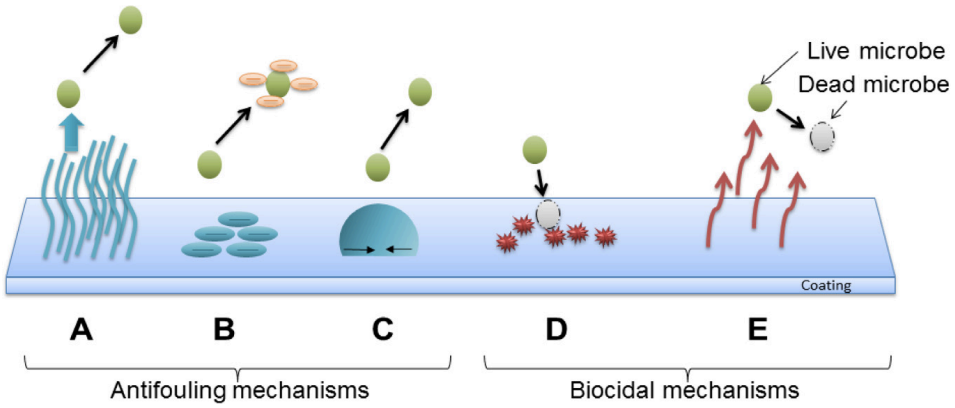

Figure 1.3: Different approaches towards antimicrobial surfaces: A. Surface grafting to create electrostatic repulsion to avoid initial bacterial adhesion. B. Creating charges on coating C. Lowering free energies. D. Biocide release such as silver ions or antibiotics to kill microbials and D. Biocide coating able to kill microbes on contact, adapted from reference 27

The initial adhesion of microbes to the colonized surface depends on Van der Walls, electrostatic and hydrophobic forces.[28] Biofilms show high resistance to antibiotic and biocide treatment, which makes device-related infections extremely difficult to cure.[29, 30] Initial bacterial adhesion to biomedical surfaces depends not only the biological features, but also on physicochemical factors, such as the surface properties of the device (hydrophilicity, roughness and porosity) and environmental factors (fluid flow conditions, temperature and pH).[31] The hydrophobicity of the device surface plays an important role in a wide range microbial infections.[32]

Biomedical devices are generally made of silicon polymers, stainless steel or poly(vinyl chloride) (PVC).[33, 34] Among all the plastics used in medical applications, more than 25% are PVC, including plasma and blood bags, tubing and associated intravenous fluid bags, endotracheal tubing, dialysis equipment and catheters.[35, 36]

1.4 Covalent Modification of PVC Surfaces

Several strategies have been previously investigated to make anti-fouling PVC surfaces. Among these are surface coatings, grafts and gamma-ray treatment. Surface modification can be either covalent or non-covalent. In covalent surface modification, new functionality or active groups are attached to the surface through covalent bonds.[37] In non-covalent surface modification, active materials are generally physically blended with the PVC. Covalent surface modification of PVC is one of the most attractive techniques to introduce antifouling properties as nothing leaches out from the polymeric matrix.

1.4.1 PVC Surface Modification by Thiols

PVC surface modification by nucleophilic substitution of chlorine atoms on the PVC backbone by aromatic or aliphatic thiols has been described. McCoy et al. worked on surface modification of unplasticized PVC film by treatment with 4-aminothiophenol, where potassium carbonate or cesium carbonate was used as the base in different ratios of DMF/H_2O solution (4:1, 5:1 and 6:1 v/v).[38] They studied the effects of static immersion versus sonication of the PVC film to enhance the degree of

chemical modification; extended sonication compromised the integrity of the PVC surface. The density of modification of the PVC surface can be increased using tetrabutylammonium bromide (TBAB) as a phase transfer catalyst. Mijangos et al. demonstrated surface modification of PVC film by substitution reactions with *p*-mercaptobenzyl alcohol (**Figure 1.4, 1a-b**).[39, 40] Another example is the work of Grohens et al. where thiophenols were used for surface modification (**Figure 1.4, 1b-f**).[41] Adhesion of *E. coli* and *S. aureus*, gram negative and gram positive representative bacterium, responsible for potential nosocomial infections, to pure and modified PVC sample was quantified. The more hydrophobic *S. aureus* strain has a higher affinity towards PVC than the hydrophilic *E. coli*, irrespective of the chemical surface modification.

Modification with polyfluorinated moieties results in PVC capable of resisting protein adhesion and bacterial adherence, important for the initial stages of biofilm formation.[37, 42-45] Sacristan et al. used fluorinated thiophenols for surface modification (**Figure 1.4, 1g-i**).[46] McCoy et al. demonstrated nucleophilic substitution by fluorinated thiol onto unplasticized PVC film (**Figure 1.4, 1j-m**),[47] demonstrating that lowering the surface energy by fluorination increases the contact angle, thus significantly reducing bacterial adhesion.

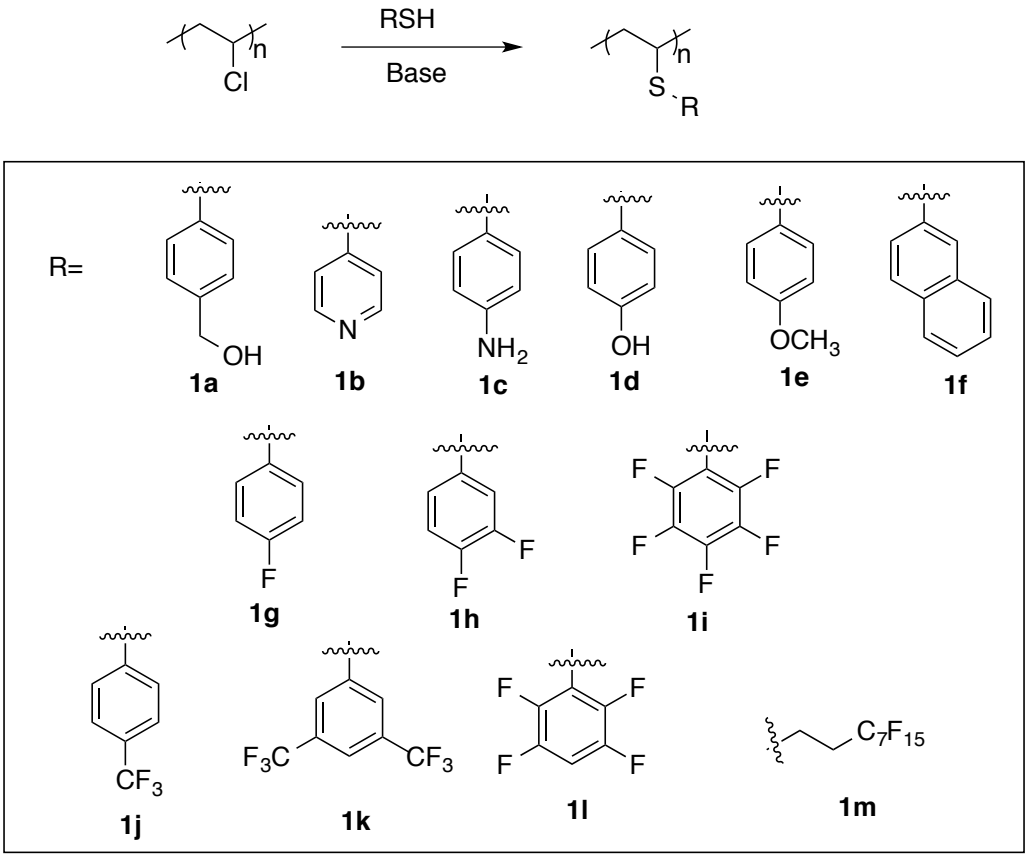

Figure 1.4: PVC surface modification by thiols

In 2020, Abdallh et al. modified PVC surfaces with thiol containing a Schiff base moiety (**Figure 1.5**).[48] The Schiff base was then coordinated with Cu (II). The modified PVC surface showed good photostability under UV irradiation compared to a pristine surface.

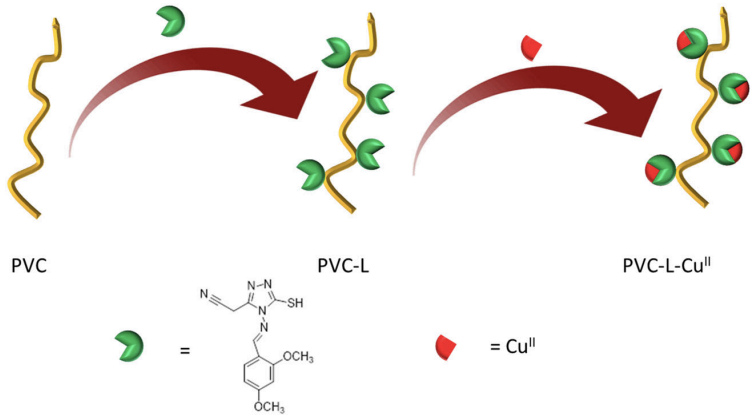

Figure 1.5: Cartoon representation of PVC surface modification by thiol containing a Schiff base, adapted from reference 48

1.4.2 PVC Surface Modification by Amines

Jayakrishnan et al. modified PVC resin by nucleophilic substitution of chlorine by ethylenediamine.[49] Dehydrochlorination and cross-linked polymers can be formed using this bifunctional nucleophile, which is also a good base. The authors suggested that by lowering the reaction time (less than one hour at 80 °C), formation of cross-linked polymer was avoided, as the aminated polymer product was still soluble in THF. On the other hand, prolonged reaction time makes crosslinked PVC, determined by its insolubility in THF. Amine functionalized PVC was then treated with hexamethylene diisocyanate, followed by addition of poly(ethyleneglycol) (PEG_{600}), to prepare an anti-fouling PVC surface (**Figure 1.6**). However, the possibility of HCl elimination by amines was not discussed. The surface modification was studied by contact angle

measurements and XPS analysis. Static platelet adhesion studies showed significantly less platelet adhesion on the modified compared to the bare PVC surface.

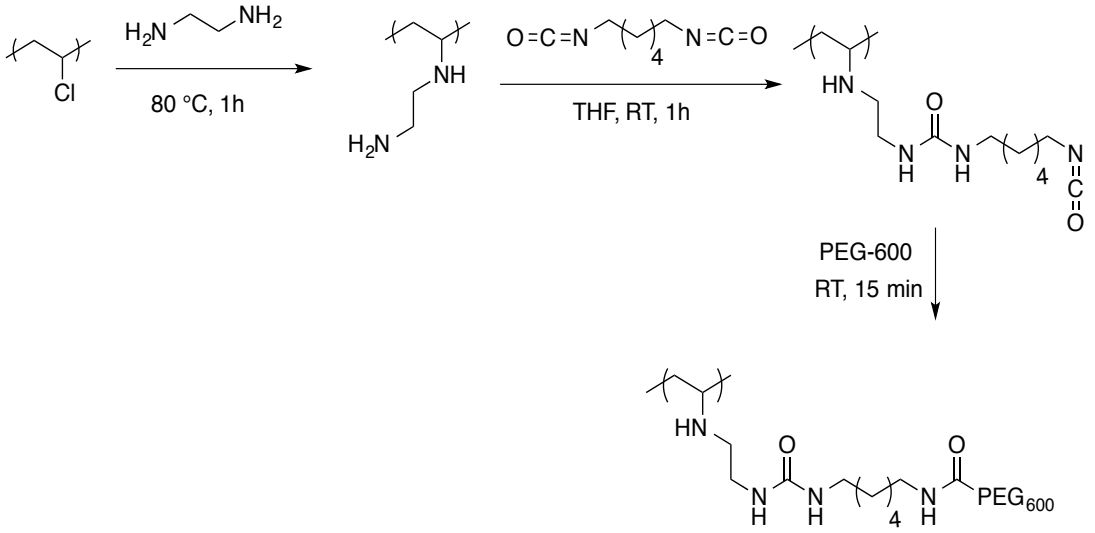

Figure 1.6: Grafting PEG onto PVC[49]

Dong et al. established a technique to introduce a coating onto the PVC surface by attaching the zwitterionic polymer: poly(3-sulfopropylmethacrylate-methacrylatoethyl trimethyl ammonium chloride–glycidyl methacrylate) (PSTG), synthesized by free-radical random co-polymerization with positively charged [2-(methacryloyloxy)-ethyl] trimethylammonium chloride, negatively charged 3-sulfopropyl methacrylate potassium, and glycidyl methacrylate (GMA) (**Figure 1.7**).[50] Nucleophilic substitution of chlorine with only one end of ethylenediamine was claimed to introduce a free amino group onto the PVC surface. However, evidence

(higher protein and platelet adsorption on amino functionalized PVC) was provided indicating crosslinking or elimination was avoided. The amino-functionalized PVC film was immersed into a PSTG solution to presumably attach the PSTG coating by amine opening of some of the epoxide moieties. A denser coating on the PVC surface was obtained when the percent of GMA in the PSTG copolymer was high, as more ring opening of the epoxy groups is possible. The modified PVC surface showed good anti-fouling properties: less protein adsorption and platelet adhesion were observed compared to unmodified PVC.

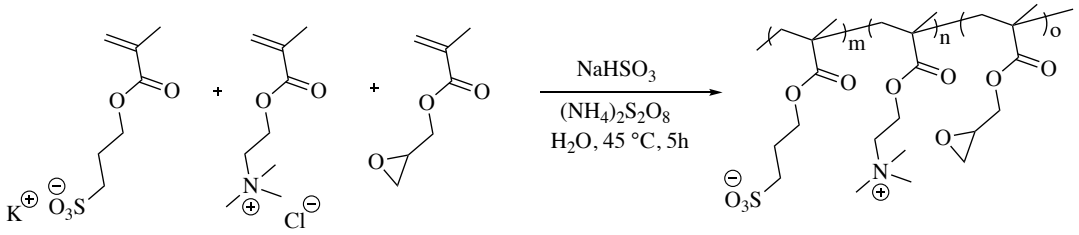

Figure 1.7: Random co-polymerization to form zwitterionic PSTG[50]

Sulfonated functionalized PVC membranes were synthesized by Easton et al. by a two-step process.[51] First, a PVC sheet was exposed to ethylenediamine solution. The possibility of crosslinking and elimination was not discussed. Then the modified PVC was exposed to conc. sulfuric acid solution (**Figure 1.8**). Conductivity and water uptake were increased significantly with the modified PVC membrane compared to the unmodified PVC membrane.

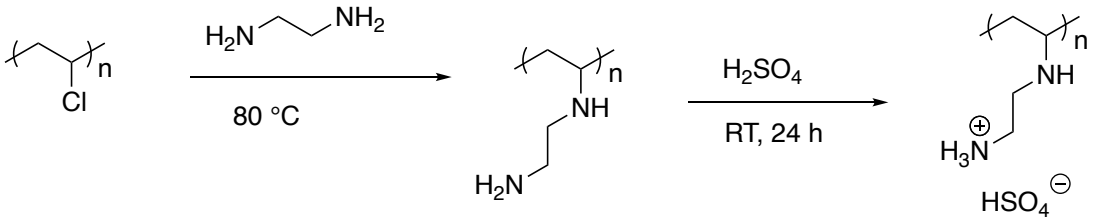

Figure 1.8: Easton's claimed synthesis of sulfonate group-functionalized PVC membrane[51]

In the work by Singh et al,[52] PVC sheets were purportedly cross-linked with multifunctional amines, such as ethylenediamine, diethylenetriamine, and ethanolamine (**Figure 1.9**). At the same time, concurrent elimination formed dienes which were trapped by maleic anhydride in a Diels-Alder reaction followed by hydrolysis, to form modified PVC bearing cyclic dicarboxylic acids. The modified PVC was characterized by elemental analysis, FTIR spectroscopy and thermal analysis. Due to the presence of free carboxylic groups, the authors suggested this modified PVC can be used for cation exchange. They also suggested it could be used as a hydrogel in chromatography, as it showed absorption capacities in different electrolytic solutions.

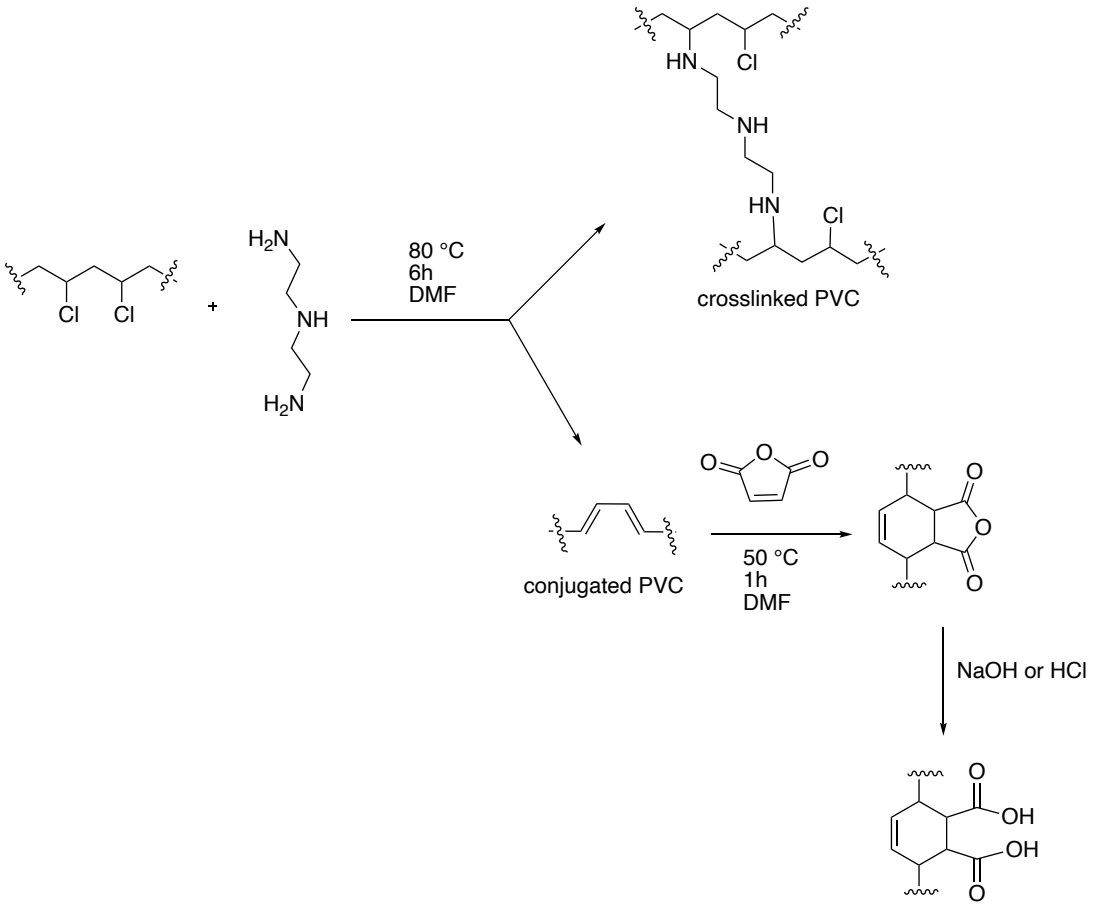

Figure 1.9: PVC modification by multifunctional amines followed by trapping of dienes with maleic anhydride and hydrolysis[52]

In a different study, the direct quaternization of a PVC ultrafiltration membrane was performed by treatment with trimethylamine solution.[53] The authors noted that by exposing the PVC membrane to a concentrated solution of trimethylamine resulted in dehydrochlorination rather than substitution reaction. The authors observed both elimination and substitution products. However, the modified

PVC membrane showed some antimicrobial activities against *E. coli* bacteria. Nucleophilic substitution of chlorine on PVC by aromatic[54] and aliphatic[55] amines was also demonstrated. However, the possibilities of dehydrochlorination and crosslinking of PVC were not discussed.[56-58]

1.4.3 PVC Surface Modification by Cycloaddition

Kebir et al. modified unplasticized PVC film by nucleophilic substitution of random chlorine atoms of PVC by sodium azide followed by Cu^{I} catalyzed azide alkyne cycloaddition.[59] Hydroxyethyl cellulose, methylcellulose, dextran and PEG containing alkynes were synthesized and grafted onto the PVC surfaces containing azide (PVC-N_3) (**Figure 1.10**). Among these polymer bearing polysaccharides and PEG functional group; hydroxyethyl cellulose, methylcellulose and PEG surfaces displayed high antifouling against *Escherichia coli*.

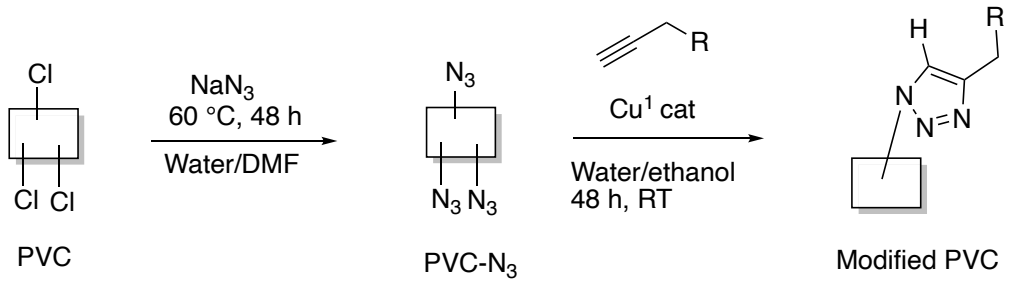

Figure 1.10: PVC surface modification with polysaccharides and PEG functional groups by Cu mediated azide alkyne cycloaddition[59]

Bakker et al. modified PVC with ferrocene pendant groups in order to prepare ion electron transducers for electrochemical ion sensors.[60] The modified PVC surface was synthesized by copper catalyzed cycloaddition between PVC azide and ethynylferrocene.

Finn et al. also modified medical grade PVC tubing by a copper catalyzed cycloaddition reaction.[61] To substitute the chlorine of PVC by azide and cyanide, a phase transfer catalyst (PTC) was used. Then the PVC surface was modified by copper catalyzed azide-alkyne cycloaddition or tetrazole formation. XPS studies showed modification occurred only at the surface of the tubing (**Figure 1.11**).

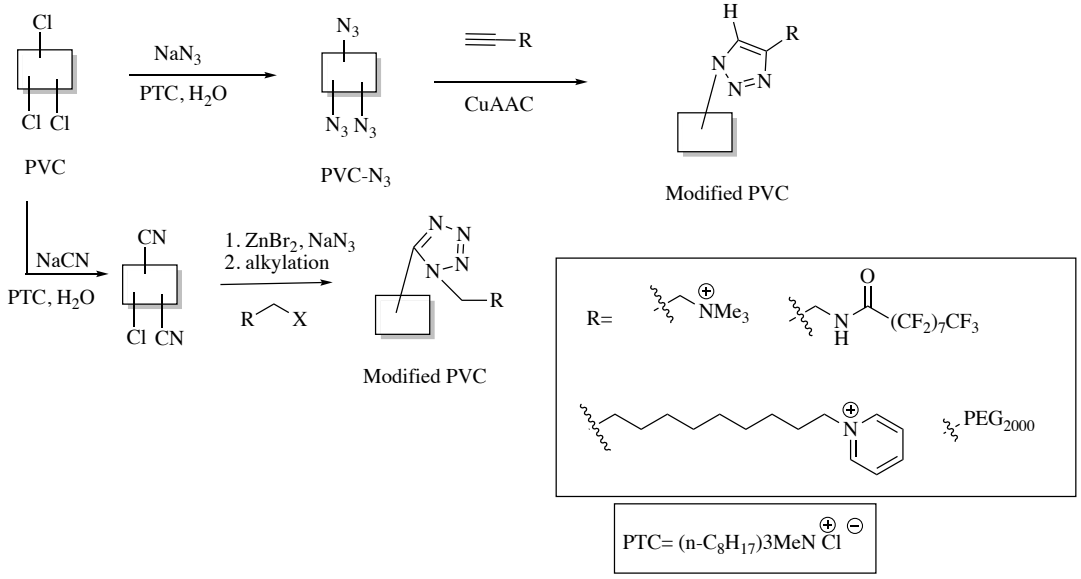

Figure 1.11: Medical grade PVC modification with the CuAAC reaction[61]

The surface of a plasticized PVC membrane was modified with different lengths of poly(ethylene glycol) (PEG) chains (PEG_{600} and PEG_{1000}) attached to cysteine molecules using the copper catalyzed cycloaddition reaction (**Figure 1.12**).[62] Surface modification with PEG derivatives increased the hydrophilicity of the membrane, as confirmed by contact angle measurements. The main purpose of the cysteine functionality was to release active nitric oxide (NO) after transnitrosation with *S*-nitrosoproteins present in blood to increase antifouling properties. However *in vitro* analysis showed NO release from cysteine did not make the surface antifouling.

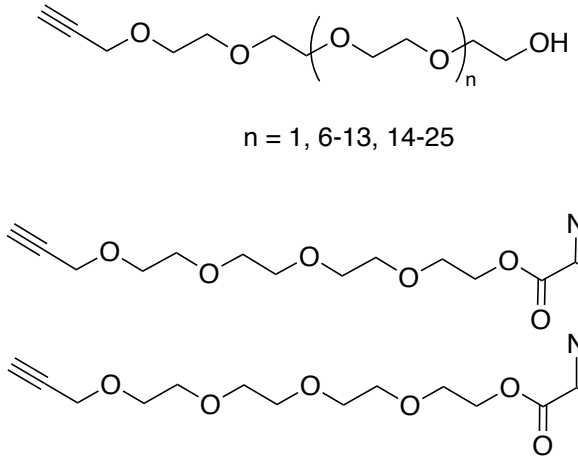

Figure 1.12: Compounds used to modify PVC membrane by CuAAC[62]

1.4.4 PVC Surface Grafting

Surface grafting is another robust technique to alter the surface properties of PVC. Generally, there are two different types of surface grafting techniques; “grafting from” and “grafting to”.[63] “Grafting from” is the process where polymer an initiator

present on the surface reacts with monomer that polymerizes. “Grafting to” is the process where preformed polymer chains with reactive functional groups are covalently bonded to the surface. Using “grafting from” polymerization techniques, different hydrophilic polymers such as poly(acrylic acid) (PAA), poly(dimethyl acrylamide) (PDMA), poly(2-hydroxy methacrylate) (PHEMA), poly(2-hydroxyethyl acrylate) (PHEA), poly(dimethylaminoethyl acrylate) (PDMAEMA) and poly(4-vinylpyridine) (P4VP) were covalently attached to plasticized PVC sheets and tubing (**Figure 1.13**).[64] First, the initiator (AIBN) was physically absorbed on the PVC surface and then radical polymerization with different monomers were carried out in hydrophilic media (**Figure 1.14**). However, the effects of the grafts on the bulk properties and antifouling properties were not explored.

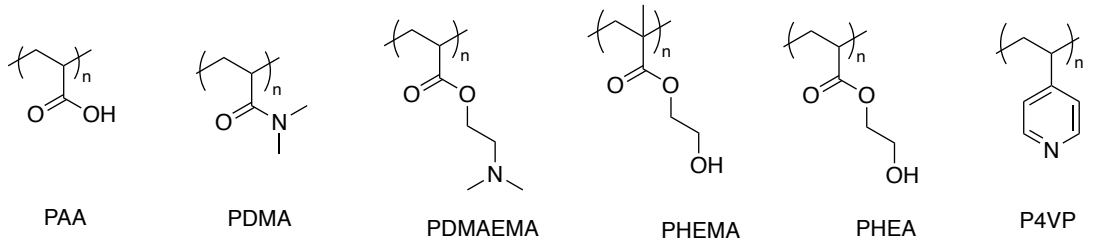

Figure 1.13: Structure of polymers grafted from the surfaces of PVC sheets and tubing[64]

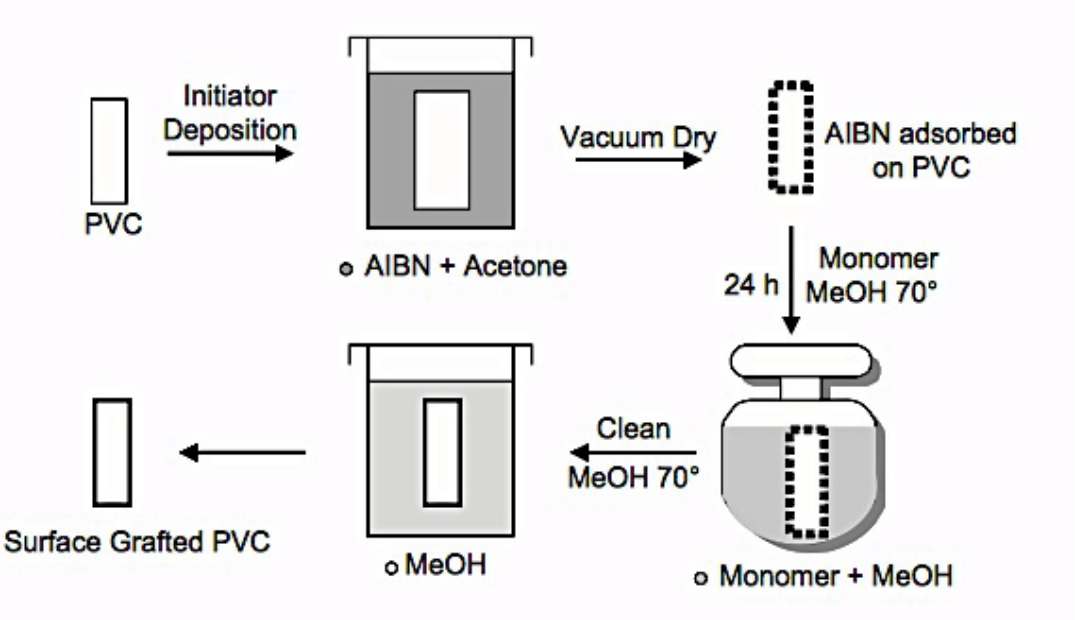

Figure 1.14: Schematic diagram of surface grafting onto PVC adapted from reference 64

1.4.4.1 PVC Surface Modification by Atom Transfer Radical Polymerization (ATRP)

Surface initiated radical polymerization has become one of the robust techniques to make polymer brushes off of the PVC surface. Percec et al. demonstrated that graft copolymerization can be initiated directly from structural defects in PVC chains in solution (**Figure 1.15**).[65] Using a similar method, unplasticized PVC sheets were modified by Huang et al. by a photo-mediated ATRP method.[66] They used structural defects of allylic and tertiary chlorides in commercial PVC, using an initiator activated by an $Ir(ppy)_3$ photoredox catalyst irradiated with blue LED light (460-470 nm). Methyl methacrylate (MMA), methacrylic acid (MAA), oligo (ethylene

glycol) methyl ether methacrylate (OEGMA) and pentafluorophenyl methacrylate (PFMA) were used as monomers for ATRP. The presence of both the catalyst $Ir(ppy)_3$ and light were crucial for surface modification. This ATRP was performed without a deoxygenation procedure and was compatible with acidic monomer methyl acrylic acid (MAA).

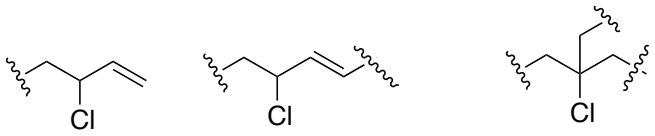

Figure 1.15: Structural defects present in PVC

Brooks et al. demonstrated another surface-initiated atom transfer radical polymerization (SI-ATRP) on unplasticized PVC sheets (**Figure 1.16**).[67] First, free amino groups were introduced onto the PVC surface by reaction with 4-aminothiophenol. Then epoxide ring opening with a mixture of glycidol and 1-sulfate-2,3-epoxypropane by the thioaniline functionalized PVC incorporated free hydroxyl and sulfate groups onto the PVC surface. The hydroxyl groups reacted with 2-chloropropionyl chloride to introduce the ATRP initiators. Finally, poly(*N, N*-dimethylacrylamide) (PDMA) was grafted onto the modified PVC surface by traditional surface initiated (SI-ATRP) in a glove box. To verify the 'living' nature of the PDMA brush, the authors performed a chain extension using *N*-isopropylacrylamide (NIPAM) with PVC-g-PDMA as the macroinitiator. The modified copolymer brush was characterized by ATR-FTIR, atomic electron microscopy (AEM) and GPC.

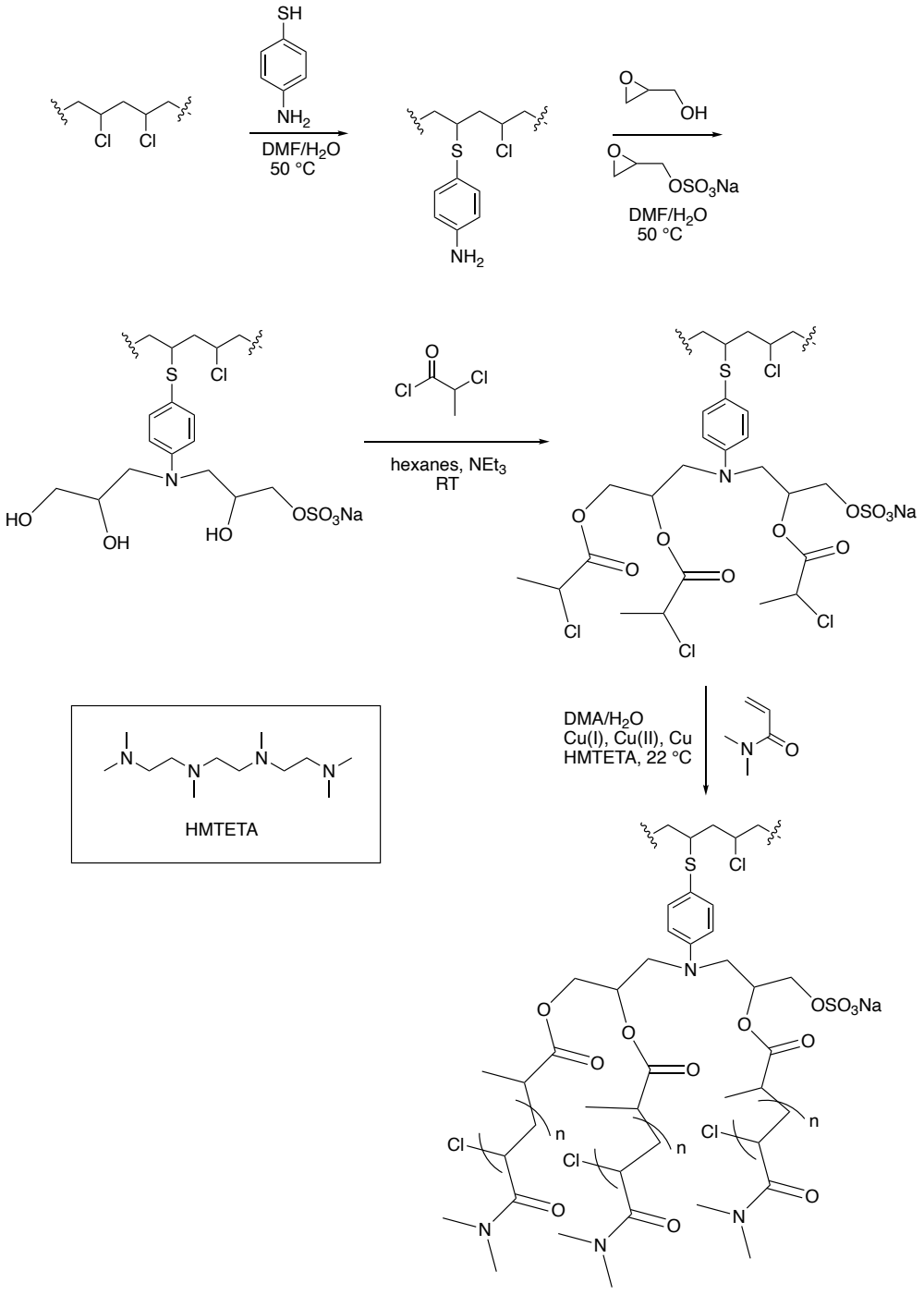

Figure 1.16: Addition of an ATRP initiator onto PVC followed by SI-ATRP[67]

Poly(ionic liquid) brushes on a PVC membrane was prepared by Du et al. using ATRP.[68] In the first step of a two-step process, poly(2-hydroxyethylmethacrylate) (PHEMA) was grafted onto the PVC membrane by aqueous ATRP (**Figure 1.17**). Then poly(1-butyl-3-vinylimidazolium bromide) (PBVIm-Br) was grafted on the PHEMA modified PVC membrane by ATRP. The grafting density increased with increased reaction time, and the modified PVC membrane showed significant changes in surface hydrophilicity. Antifouling properties of the modified PVC membranes were tested using bovine serum albumin (BSA) as a model foulant. The BSA rejection increased with higher grafting density on the PVC membrane, compared to pristine PVC membrane.

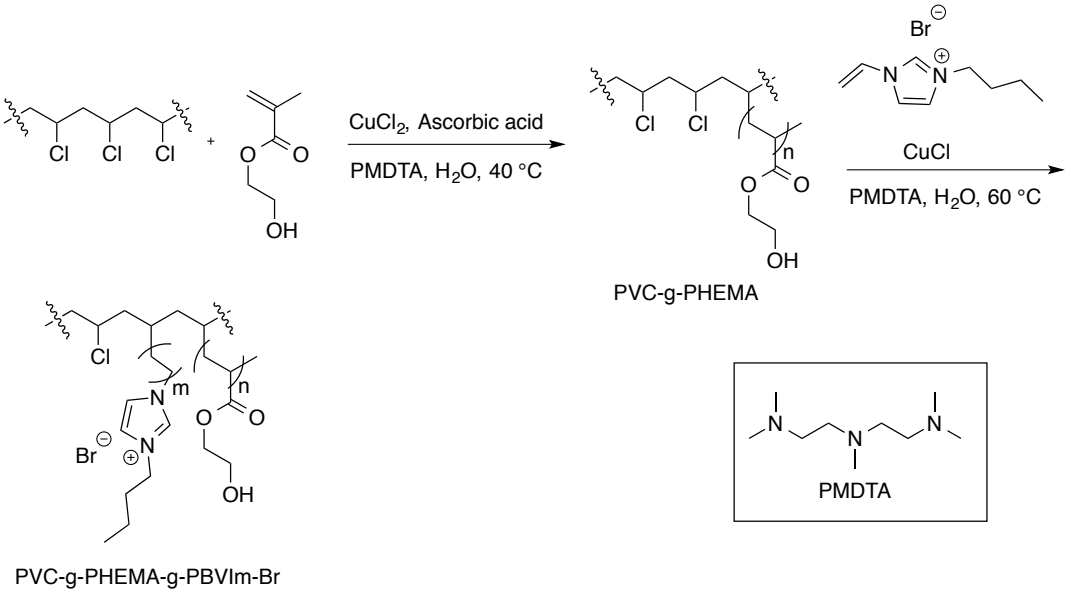

Figure 1.17: Poly(ionic liquid) brushes on PVC membrane using ATRP[68]

Poly(ethylene glycol) methyl ether methacrylate (PEGMA) grafted PVC was synthesized by Liu et al. by ATRP.[69] PVC was mixed with 5-20% PVC-g-PEGMA and cast as a solution to prepare a blend of PVC/PVC-g-PEGMA as an ultrafiltration membrane. The authors found the pore size and contact angle lowered up to 10% PVC-g-PEGMA and stayed almost constant until 20% PVC-g-PEGMA was incorporated into the membrane. They used sodium alginate (SA) as a model foulant to investigate the antifouling properties of the modified membrane by clogging the membrane. Their result suggested surface hydrophilicity and roughness plays important roles in antifouling properties of the membrane.

In 2020, Diacon et al. modified PVC surfaces with acrylic acid functionality by ATRP for biomedical applications.[70] The PVC membrane was first iodinized, as carbon-iodine bonds are easy to break for the polymer initiation step. Then direct graft polymerization was performed with acrylic acid monomer in aqueous media. The modified surface showed lower contact angles as well as changes in thermal resistance.

1.4.5 PVC Surface Modification by Thiocyanate

Thiocyanates has been used for nucleophilic substitution of chloride in PVC. Plasticized medical grade PVC sheets have been modified by Jayakrishnan et al. using sodium thiocyanate in the presence of tetrabutylammonium hydrogen sulphate

(TBAH) as a phase transfer catalyst in aqueous media.[71] The modified PVC surface showed a significant lower contact angle (50 degrees) compared to the control PVC (72 degrees). Anti-bacterial properties of the modified PVC were measured by exposing it to *Staphylococcus aureus* and *Staphylococcus epidermidis* bacteria strains. Significant reductions of bacterial adhesion were observed with the modified PVC sheets.

Yoshioka el al. analyzed the covalent modification of both plasticized and un-plasticized PVC pellets by nucleophilic substitution with thiocyanate in the presence of the phase transfer catalyst tetrabutylammonium bromide (TBAB).[56, 72] The authors suggested both substitution/dehydrochlorination reaction are accelerated by the presence of TBAB. They also found high temperature (about 190 degrees) facilitates elimination reaction, while lower temperatures below 150 degrees facilitates substitution reaction, depending on the reaction concentrations and nucleophile type.

1.4.6 PVC Surface Modification by Gamma rays

Commercially available PVC tubing was grafted with poly(ethylene glycol)methacrylate (PEGMA) by using a gamma-ray source in the presence of air.[73] The initiation is based on homolytic breakage of some of the C-Cl bonds to generate carbon free radicals. In the presence of air, these carbon radicals react with oxygen to generate peroxides and hydroperoxides on PVC tubing. Using heat, these peroxides

and hydroperoxides decompose to give oxyradicals, which react with the double bond of monomers to propagate grafting from the PVC surface (**Figure 1.18**).

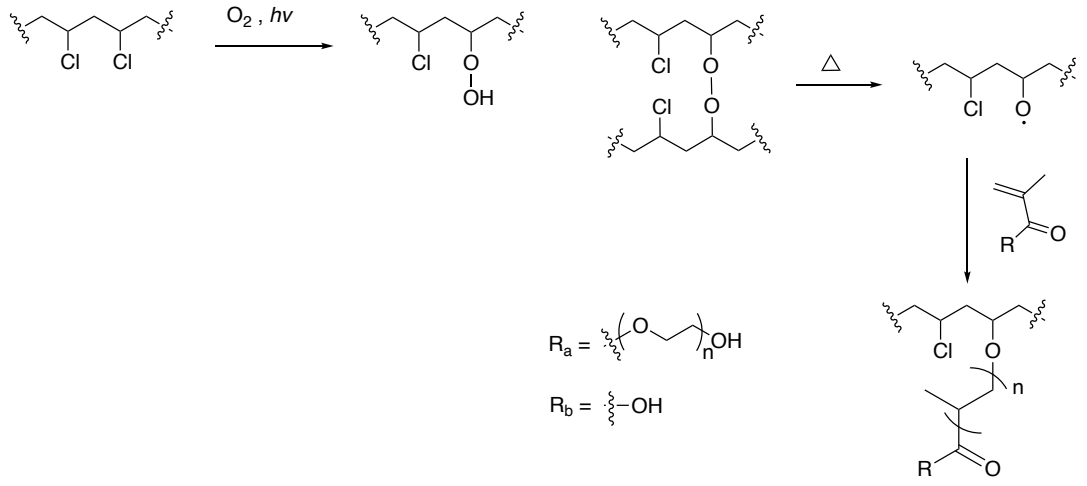

Figure 1.18: PVC surface modification using Gamma-ray with monomers R_a[73-75] and R_b[75, 76]

N-Vinylimidazole (Vim) was grafted from medical grade PVC catheters using the same technique to make bactericidal surfaces (**Figure 1.19**).[77] Then the PVC-g-Vim copolymer was quaternized by reaction with methyl iodides. The antimicrobial test of modified PVC surface was performed using *E. coli* (gram negative) and *S. aureus* (gram positive) bacteria. The modified PVC surface was able to prevent *S. aureus* bacteria adhesion but was not able to prevent *E. coli* adhesion. The authors suggested that the presence of thicker peptidoglycan layer with negatively charged polysaccharide on gram positive bacteria makes them more responsive towards positively charged modified PVC surfaces. On the other side, lipopolysaccharide membrane coating on

gram negative bacteria makes the less vulnerable towards positively charged imidazole PVC surface.

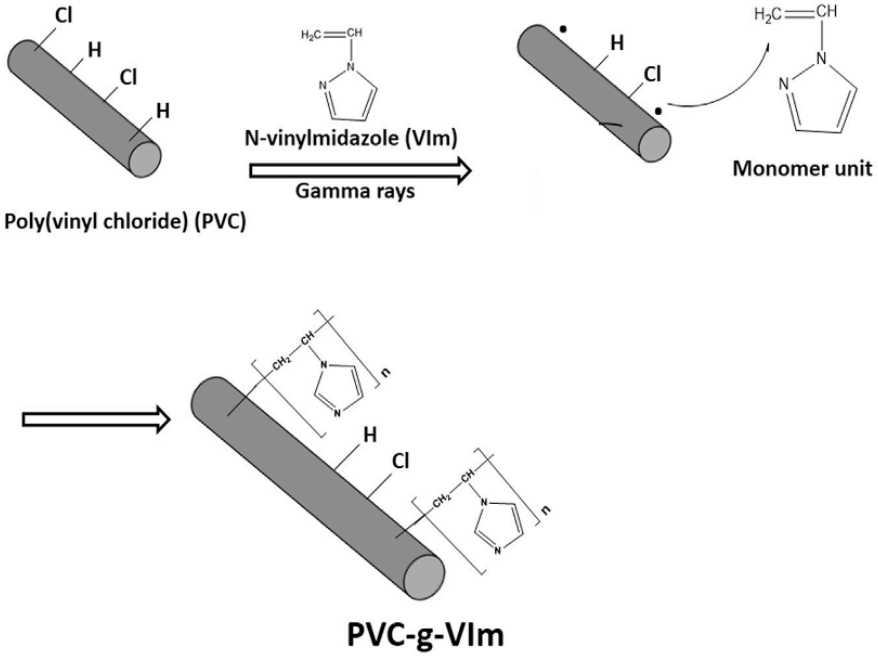

Figure 1.19: PVC surface modification with N-vinylimidazole by gamma ray adopted from reference 77

Burillo et al. also modified PVC urinary catheters by gamma-ray radiation .[75] They were able to perform both single and binary grafting of PEGMA and acrylic acid (AAc) to obtain PVC-g-PEGMA, PVC-g-AAc, PVC-g-PEGMA-g-AAc and PVC-g-AAc-g-PEGMA copolymers. The authors previous studies showed single grafted PVC-g-PEGMA and PVC-g-AAc catheters were able to prevent bacterial (*E. coli* and *S. aureus*)

adhesion after socking in ciprofloxacin.[74] But the effect of binary grafting on PVC catheters to prevent bacterial adhesion was not discussed.

1.5 Non-covalent Modification of PVC surface

The PVC surface can be modified covalently or non-covalently. In the covalent modification technique, new functionalities are incorporated by covalent bonding onto the PVC polymer matrix. As the new functionalities are covalently bonded with the polymer, nothing leaches out over time. Generally non-covalent surface modification is achieved by incorporating new materials by physically blending or adding material onto the PVC polymer surface. That is why these types of materials can leach out over time. Depending on the type or mechanism of interaction between modified PVC surface and the bacteria, non-covalent surface modification can work as contribute to antifouling or as biocides.[27] Antifouling surfaces generally lower the initial bacterial adhesion without killing the bacteria.[78] The mechanism of antifouling surfaces can be achieved by:

A. Static repulsion: where the modified surfaces provide some kind of physical barrier for the adhesion of bacteria, protein or microbes.

B. Lowering surface free energy: lowering the surface free energy results in significantly lower the bacterial adhesion and

C. Electrostatic repulsive force: charges present on the modified surface and can reduce microbial adhesion.

Biocidal PVC surfaces are designed to kill microbes instead of lowering initial adhesion. These types of coating can release biocides such as silver ions and antibiotics to kill the microbes.[79] Also, there is another type of biocidal coating where the microbes die in contact with modified surfaces such as quaternary amines.[80, 81]

1.5.1 Silver

Silver has been one of the most commonly used biocides for medical devices since the 19th century. It is also approved by the FDA. Pure silver, silver alloys (with gold or palladium), silver nanoparticles, and polymers containing silver are the most common forms of silver coats in medical devices. Generally, metallic silver oxidizes in aqueous environments and releases silver Ag(I) cations, which are strongly very biocidal. The biocidal mechanism of Ag(I) ions can occur in three different ways:[82]

1. **Protein dysfunction and loss of enzyme activity**: The presence of small amounts of Ag(I) can destroy Fe-S containing dehydratases in the bacteria *in vitro* and also inhibit these enzymes *in vivo*, thus preventing the growth of bacteria.[83]
2. **Reactive oxygen species and antioxidant depletion**: Increased amounts of Fe are observed when metal ions destroy Fe-S complexes in the cytoplasm. This excess Fe can form reactive oxygen species, which can destroy DNA and inhibit enzyme activity that is important for cell growth.[84, 85]

3. **Impaired membrane function**: Ag(I) is cytotoxic to cell membranes because of the coordination power with electronegative groups of the membranes of the bacteria. Transmission electron microscopy of *Staphylococcus aureus* and *E. coli* suggested that the integrity of the cell membrane is compromised in presence of Ag(I) ion.[86, 87]

Use of a silver alloy coating is one of the most common techniques to prepare antifouling catheter surfaces.[88] Studies showed silver coatings in the form of silver and silver oxide, including hydrogel, can significantly reduce catheter associated bacterial attachment.[89]

Incorporation of $AgNO_3$ in medical grade plasticized PVC to prepare antifouling surfaces were studied.[90] Sedlarikova et al. used thermoplastic compounding technique to add different amounts of $AgNO_3$ to make PVC-$AgNO_3$ composites films. The $AgNO_3$ distribution was not uniform in the PVC matrix, and a decrease of mechanical properties was observed with an increase in $AgNO_3$. Good antimicrobial activity was observed for both gram positive (*Staphylococcus aureus*) and gram negative (*E. coli*, *Pseudomonas aeruginosa*, *Klebsiella pneumoniae*) bacteria, with even 3 wt % addition of $AgNO_3$.

Ag nanoparticles are another popular form of Ag. Uses includes antimicrobial, drug delivery, optical and electronic fields. Che et al. synthesized spherical shaped Ag nanoparticles by a borohydride reduction method; the antimicrobial activity was

investigated against *E. coli* bacteria.[91] Proteomic studies revealed that the Ag nanoparticles destroy bacterial membranes by a similar way as Ag ions by impaired membrane function. Also, Ag nanoparticles are more potent than Ag ions, as only nanomolar level concentrations were required to act as effective antimicrobial agents.

Balazs et al. modified medical grade PVC endotracheal tubing by oxygen glow discharge plasma followed by a two-step post-plasma treatment with sodium hydroxide and silver nitrate solution to incorporate Ag ions onto the tubing.[92] XPS analysis showed the presence of more oxygenated groups on the modified surface, which increased the surface hydrophilicity, although the amount of oxygenated groups were independent of the time of exposure to the plasma treatment. However longer expose times increased the surface roughness. Antifouling studies against four different stains of *Pseudomonas aureus* showed reduced bacterial adhesion.[93] Later, two-step chemical modification was performed using NaOH hydrolysis of phthalate plasticizer to make sodium phthalate, followed by replacement of the sodium ion with Ag ion using $AgNO_3$ solution (**Figure 1.20**). This modified PVC surface incorporating Ag ion was able to inhibit bacterial adhesion completely up to 72 hours, independent as to if the tubing was pre-treated with plasma or not.

Step 1: Creation of disodium phthalate by saponification

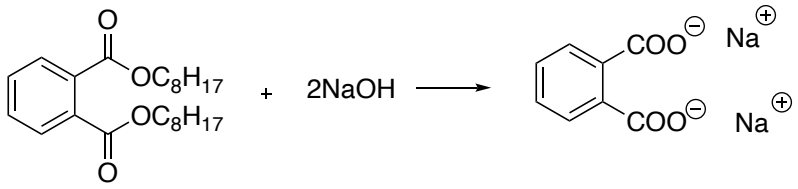

Step 2: Exchange with silver ions

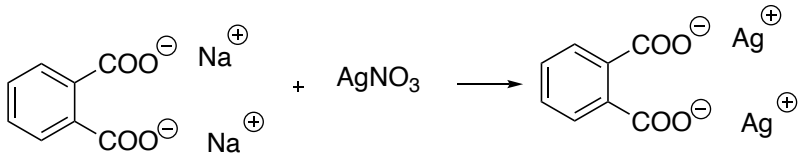

Figure 1.20: Modification of endotracheal tubing by NaOH and $AgNO_3$[92, 93]

1.5.2 PVC Surface Modification by Laser Treatment

In 2020, Krylach et al. modified the surface of PVC films deposited on copper foil using nanosecond laser radiation to make microscale laboratory devices for bactericidal treatments.[94] The PVC polymer was applied to copper foil by rotation spin coating, and then the surface was microtextured by nanosecond laser pulses. Changes in the surface microtopography resulted in lower contact angles. But in a week, the contact angle became high, indicating degradation of the polymer coating.

1.5.3 Addition of Nanoparticles (NPs)

Zhao et al. modified PVC ultrafiltration membranes with silver embedded nano sized titanium dioxide (Ag-n-TiO_2) particles to improve antifouling properties.[95] The modified membrane not only showed enhanced permeability, hydrophilicity and retention capability but also *in situ* antibacterial properties against *E. coli* (**Figure**

1.21). The authors suggested the reason for the excellent antifouling properties may be related to the release of silver ions and reactive oxygen species (ROS) from Ag-n-TiO_2.

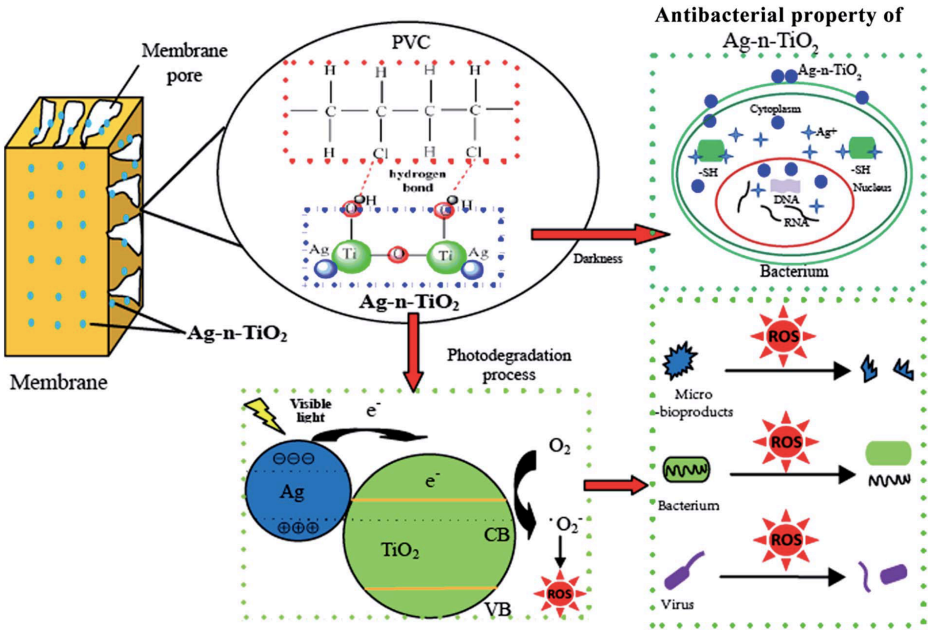

Figure 1.21: Schematic illustration of antifouling properties of Ag-n-TiO_2/PVC membrane adopted from reference 95

Another example of incorporation of TiO_2 nanoparticles into PVC membranes was carried out by Jafarzadeh et al.[96] Contact angle measurements revealed increasing hydrophilicity with increasing amounts of TiO_2. Antifouling properties of membranes were investigated by filtration of a bovine serum albumin (BSA) solution

and the improved flux recovery. But rejection of BSA decreased as the content of TiO_2 increased.

Alsalhy et al. modified PVC ultrafiltration membranes incorporating TiO_2 nanoparticles (NP) to treat refinery wastewater.[97] Due to the presence of TiO_2 nanoparticles, the hydrophilicity of the membrane increased significantly, lowering the contact angle. The modified membrane showed increased water permeability, tensile strength and fouling resistance compared to pure PVC. It also showed enhance performance in terms of turbidity, total suspended solid (TSS), oil and grease, heavy metals and chemical oxygen demand (COD) rejection.

Zine oxide has been found as an antifouling agent for a wide variety of bacteria, especially gram positive.[98] With decreasing size of the zinc oxides particles into the nanoscale region an increase in bacteria inhibition was observed. The main reason is with decreasing size of the particles, an increase in surface areas allows greater interaction with the surrounding environment. Nair et al. observed an increased antibacterial effect on *S. aureus* and *Escherichia coli* when exposed to ZnO nanoparticles of decreasing size.[99] Similar results were also found when ZnO nanoparticle size was reduced from 2 μm to 45 nm.[100] Webster et al. incorporated ZnO nanoparticles into PVC films with different weight % concentration and observed the effect on *Staphylococcus aureus*.[101] Optical density readings and crystal violet staining showed reduced amounts of bacterial attachment with increasing amount of

ZnO nanoparticles in the PVC film. Live/dead bacteria assays also confirmed less active bacteria on ZnO incorporated surfaces compared to unmodified PVC. The authors suggested release of zinc ions from ZnO nanoparticles is the main reason for these antibacterial properties.[102] Vatanpour et al. modified PVC ultrafiltration membranes by incorporating different weight % of ZnO nanoparticles.[103] Their results showed as low as 3 wt% of ZnO nanoparticles added to a PVC ultrafiltration membrane can increase flux recovery above 90%, and BSA rejection was enhanced up to 97%. Zendehnam et al. prepared PVC cation exchange membranes by incorporating ZnO nanoparticles.[104] The modified membrane with ZnO nanoparticles showed less *E. coli* adhesion compared to pure PVC. The effect of addition of ZnO nanoparticles into food grade PVC films to make antifouling packaging was studied by Xing et al.[105] Their studies showed ZnO coated PVC films exhibit inhibition effects on the growth of *E. coli* and *S. aureus*. ZnO coating was found to be more effective against gram positive *S. aureus* than gram negative *E. coli*. However antifungal activity against *Aspergillus flavus* and *Penicillum citrinum* was not observed.

Jiang et al. established a versatile gold nanoparticle (AuNP) based surface coating technique onto different types of surfaces, such as PVC, polystyrene (PS), polypropylene (PP), polyethylene (PE), polydimethylsiloxane (PDMS) and silica (SiO_2).[106] Gold nanoparticles (AuNPs) conjugated with 4,6-diamino-2-pyrimidinethiol (DAPT) was used as the antimicrobial agent for the coating. Different polymer

substrates were first treated with oxygen plasma to create negative charges on the surfaces, and then dipped into a solution of positively charged AuDAPT: resulting in electrostatic self-assembly (**Figure 1.22**). Then the unbound AuNPs were removed by washing with ultrasonication (USC) in phosphate buffered solution (PBS) for 30 minutes (X5). The *in vitro* and *in vivo* studies showed immobilized AuDAPT was able to eradicate gram negative bacteria and was not toxic to a variety of human cells. The non-leaching properties of this coating make it a much safer option for internal applications such as implantable medical devices.

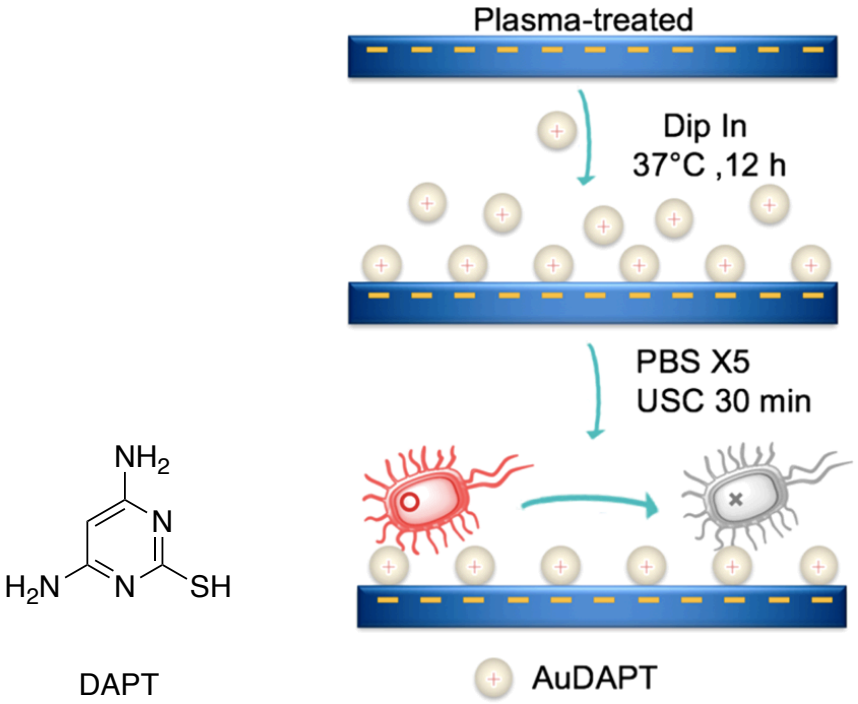

Figure 1.22: AuDAPT based antimicrobial coatings[106]

1.5.4 Antibiotics

Nitrofurazone or nitrofural (trade name Furacin™) is a commercially available antibiotic (**Figure 1.23**). Nitrofural impregnated catheters are commercially available medical devices. Studies show that the antimicrobial properties of nitrofural are due to interference with DNA synthesis, by inhibiting enzymes that are involved with glycolysis.[107] Nitrofural impregnated foley catheters are found to be more antifouling compared to silver alloy coated catheters.[88, 108] Although nitrofural has antifouling properties, it cannot be used for short term applications due to discomfort issues. Nitrofural is related to mammary tumors, testicular degradation and degeneration of articular cartilage in animals.[109] The use of nitrofuran is currently discontinued in the U.S. and is included in California's list of toxic chemicals.[110] Minocycline, rifampicin and sparfloxacin are some antimicrobial agents used for urinary catheter coatings (**Figure 1.23**). Another review showed externally impregnated chlorhexidine/silver sulfadiazine catheters lowered the risk of catheter related bloodstream infections.[111] Minocycline-rifampicin impregnated silicone catheters were found to be very efficient as an antimicrobial coating in preventing bacterial growth, compared to uncoated catheters over a period of 7-12 weeks.[112, 113]

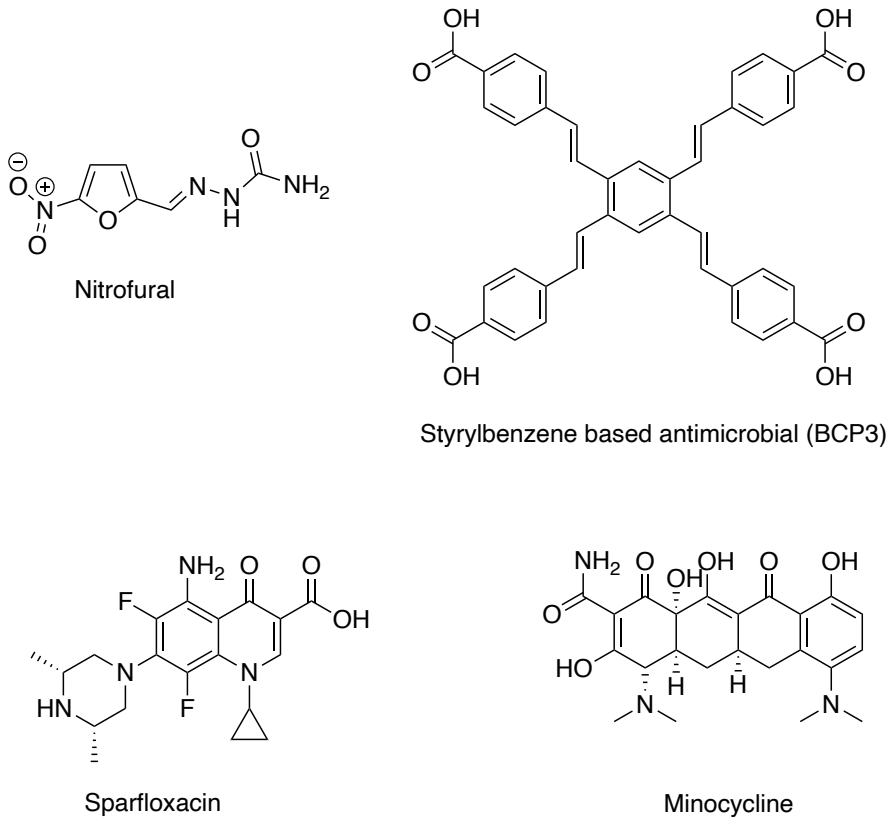

Figure 1.23: Commonly studied antibiotics that have been used as antimicrobial agents for surface modification

Another recent study incorporated 1,3,5-tri-styrylbenzene based antimicrobials (BCP3) on PVC endotracheal tubing (**Figure 1.23**).[114] Styrylbenzene based derivatives of antibiotics such as BCP3 are active against the large conductance mechanosensitive ion channel (MscL) family of protein in bacterial target.[115] This MscL transmembrane protein is only found in bacteria, but not in the human genome, making it an ideal drug target. BCP3 was incorporated by blending it with poly(lactic-

co-glycolic acid) in tetrahydrofuran and dipping segment of endotracheal tubing into that solution for short period of time. *In vitro* studies demonstrated a concentration dependent release of BCP3 from the coating over 31 days, but the highest release was in the first 24 hours. Bacterial assays against *S. aureus* and *P. aeruginosa* showed modified tubing inhibited the growth of *S. aureus* significantly, but not *P. aeruginosa*. *In vitro* studies against the L929 fibroblast cell showed high concentrations of BCP3 (1 mg/mL) did not cause any significant cytotoxicity. Antibiotic loaded medical devices inhibit bacterial growth on surfaces and can be a potent alternative to antifouling surfaces. However regular use of antibiotics for prevention rather than treatment can result in antibiotic resistance and even cause system toxicity.[116] Different studies demonstrated subinhibitory concentrations of some antibiotics enhance rather inhibit biofilm formation by bacteria, and result in the evolution of antibiotic resistant bacteria.[117, 118]

1.5.5 Nitric Oxide Releasing Coatings

Nitric oxide (NO) has been well-known as an antimicrobial agent since the 1990s.[119] The antimicrobial mechanism of nitric oxide generally involves DNA cleavage, lipid peroxidation, tyrosine nitration and nitrosation of thiols and amines.[120] Some common NO donors are *S*-nitrosoglutathione (GSNO) and *S*-nitrosothiols such as *N*-Nitroso-*N*-acetyl-DL-penicillamine (SNAP) (**Figure 1.24**). Generally, polymers are impregned with nitric oxide releasing donors that can release small amounts of NO,

as it has a short half-life. Schoenfisch et al. modified xerogels with *S*-nitrosothiol as an NO donor coated with PVC.[121] Nitric oxide fluxes ranging from 20-50 pmol/cm^2 were able to inhibit both gram positive and gram negative bacteria, resulting in about 50% lower adhesion. However, higher concentrations of the NO payload (1700 nmol/cm^2) were required to prevent ≥80% bacteria adhesion, which may cause cytotoxicity to mammalian cells.

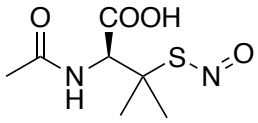

S-Nitroso-*N*-acetylpenicillamine (SNAP)

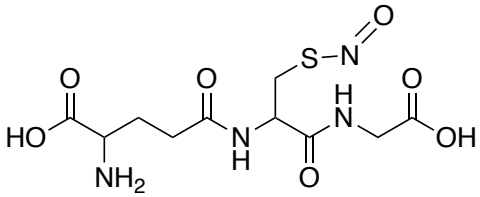

S-Nitrosoglutathione (GSNO)

Figure 1.24: Structure of two commonly studied NO donors: *S*-nitroso-*N*-acetylpenicillamine and *S*-nitrosoglutathione

Meyerhoff et al. modified biomedical grade PVC extracorporeal circuit tubing using diazeniumdiolated dibutylhexanediamine as an NO donor, mixed with a poly(lactic-co-glycolic acid) coating (**Figure 1.25**).[122] Earlier studies by the same research group exhibited NO release *in vitro* between 7 to 18 X 10^{-10} mol/cm^{2}min for up to 7 days.[123] However, NO release was significantly lower after 7 days and was pH sensitive. Another similar study on plasticized PVC film, impregnated with *N*-

diazeniumdiolated dibutylhexanediamine as an NO donor, showed higher NO release with a surface flux of $17 \pm 0.5 \times 10^{-10}$ mol/cm^{2}min required to prevent a significant amount of platelet adhesion.[123, 124]

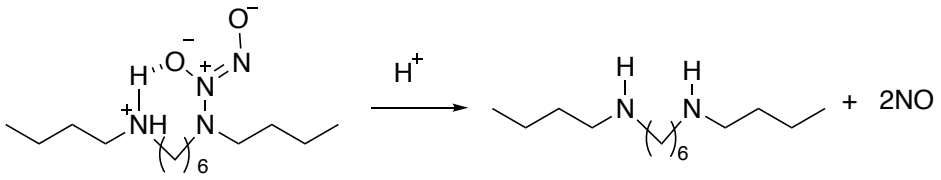

Figure 1.25: Diazeniumdiolated dibutylhexanediamine releases NO[123]

Weng et al. modified medical grade PVC catheters with a dopamine-based metal organic framework known as a HKUST-1 (**H**ong **K**ong **U**niversity of **S**cience and **T**echnology, also called MOF-199) coating.[125] First, a piece of PVC tubing was submerged into a solution of dopamine to create a polydopamine film, which acts as a nucleation center for copper ion (Cu^{2+}) for further HKUST-1 coating. This HKUST-1 coating can decompose *S*-nitrosothiols (RSNOs) to generate NO. The modified PVC surface was able to reduce *S. aureus* and *E. coli* bacterial adhesion about 95% compared to unmodified PVC. Another similar study found that copper ions embedded into PVC polymeric films were able to generate NO from *S*-nitroso-*N*-acetyl-D-penicillamine (SNAP).[126] However NO can interact with superoxides, which are generally produced in tissues during oxidative stress, generating highly cytotoxic

peroxynitrite ($ONOO^-$). Therefore it is very important to control the release of NO concentration over time.[127]

1.6 Conclusion

PVC is one of the most widely used polymers in medical devices due to its availability, flexibility, cost efficiency and heat tolerance. The surface of PVC is hydrophobic, which makes it ideal for initial bacterial adhesion, ultimately leading to biofilm formation. Biofilms are one of the main reasons for hospital acquired and post-surgery infections. Biofilms also show high resistance to antibiotics and biocides which makes device related infections extremely difficult to cure. High concentrations of biocides such as silver ions and antibiotics are required to diminish medical device related infections, which may cause concurrent toxicity to human cells. Altering the PVC surface properties to decrease initial bacterial adhesion is one of the most effective strategies towards providing antifouling surfaces for medical applications.

1.7 References

1. Geyer, R.; Jambeck, J. R.; Law, K. L., Production, use, and fate of all plastics ever made. *Science advances* **2017,** *3* (7), 1700782.

2. Fischer, I.; Schmitt, W. F.; Porth, H.-C.; Allsopp, M. W.; Vianello, G., Poly(Vinyl Chloride). In *Ullmann's Encyclopedia of Industrial Chemistry*, 2014; pp 1-30.

3. Garside, M. U.S. PVC production volume 1990-2019. https://www.statista.com/statistics/975603/us-polyvinyl-chloride-production-volume/#statisticContainer (accessed January 11, 2021).

4. Wikipedia Eugen Baumann. https://en.wikipedia.org/wiki/Eugen_Baumann (accessed January 12, 2021).

5. Wikipedia Waldo Semon. https://en.wikipedia.org/wiki/Waldo_Semon (accessed January 12, 2021).

6. Carroll, W. F.; Johnson, R. W.; Moore, S. S.; Paradis, R. A., 4 - Poly(Vinyl Chloride). In *Applied Plastics Engineering Handbook (Second Edition)*, Kutz, M., Ed. William Andrew Publishing: 2017; pp 73-89.

7. Wypych, G., 2 - PVC MANUFACTURE TECHNOLOGY. In *PVC Degradation and Stabilization (Third Edition)*, Wypych, G., Ed. ChemTec Publishing: Boston, 2015; pp 25-45.

8. Walters, P.; Cadogan, D. F.; Howick, C. J., Plasticizers. In *Ullmann's Encyclopedia of Industrial Chemistry*, 2020; pp 1-27.

9. Zhang, X.; Li, Y.; Hankett, J. M.; Chen, Z., The molecular interfacial structure and plasticizer migration behavior of “green” plasticized poly(vinyl chloride). *Physical Chemistry Chemical Physics* **2015,** *17* (6), 4472-4482.

10. Wang, Q.; Storm, B. K., Migration of Additives from Poly(vinyl chloride) (PVC) Tubes into Aqueous Media. *Macromolecular Symposia* **2005,** *225* (1), 191-204.

11. Hakkarainen, M., Migration of Monomeric and Polymeric PVC Plasticizers. In *Chromatography for Sustainable Polymeric Materials: Renewable, Degradable and Recyclable*, Albertsson, A.-C.; Hakkarainen, M., Eds. Springer Berlin Heidelberg: Berlin, Heidelberg, 2008; pp 159-185.

12. Tüzüm Demir, A. P.; Ulutan, S., Migration of phthalate and non-phthalate plasticizers out of plasticized PVC films into air. *Journal of Applied Polymer Science* **2013,** *128* (3), 1948-1961.

13. Marcilla, A.; Garcia, S.; Garcia-Quesada, J. C., Migrability of PVC plasticizers. *Polymer Testing* **2008,** *27* (2), 221-233.

14. Golshan, M.; Hatef, A.; Socha, M.; Milla, S.; Butts, I. A. E.; Carnevali, O.; Rodina, M.; Sokołowska-Mikołajczyk, M.; Fontaine, P.; Linhart, O.; Alavi, S. M. H., Di-(2-ethylhexyl)-phthalate disrupts pituitary and testicular hormonal functions to reduce sperm quality in mature goldfish. *Aquatic Toxicology* **2015,** *163*, 16-26.

15. Liu, T.; Li, N.; Zhu, J.; Yu, G.; Guo, K.; Zhou, L.; Zheng, D.; Qu, X.; Huang, J.; Chen, X.; Wang, S.; Ye, L., Effects of di-(2-ethylhexyl) phthalate on the hypothalamus-pituitary-ovarian axis in adult female rats. *Reproductive Toxicology* **2014,** *46*, 141-147.

16. North, M. L.; Takaro, T. K.; Diamond, M. L.; Ellis, A. K., Effects of phthalates on the development and expression of allergic disease and asthma. *Annals of Allergy, Asthma & Immunology* **2014,** *112* (6), 496-502.

17. Shapiro, G. D.; Dodds, L.; Arbuckle, T. E.; Ashley-Martin, J.; Fraser, W.; Fisher, M.; Taback, S.; Keely, E.; Bouchard, M. F.; Monnier, P.; Dallaire, R.; Morisset, A. S.; Ettinger, A. S., Exposure to phthalates, bisphenol A and metals in pregnancy and the association with impaired glucose tolerance and gestational diabetes mellitus: The MIREC study. *Environment International* **2015,** *83*, 63-71.

18. Schaedlich, K.; Schmidt, J.-S.; Kwong, W. Y.; Sinclair, K. D.; Kurz, R.; Jahnke, H.-G.; Fischer, B., Impact of di-ethylhexylphthalate exposure on metabolic programming in P19 ECC-derived cardiomyocytes. *Journal of Applied Toxicology* **2015,** *35* (7), 861-869.

19. Revelas, A., Healthcare - associated infections: A public health problem. *Nigerian Medical Journal* **2012,** *53* (2), 59-64.

20. Messina, A. F.; Berman, D. M.; Ghazarian, S. R.; Patel, R.; Neustadt, J.; Hahn, G.; Sibinga, E. M. S., The Management and Outcome of Spinal Implant-related

Infections in Pediatric Patients A Retrospective Review. *Pediatric Infectious Disease Journal* **2014,** *33* (7), 720-723.

21. **CDC** Healthcare-associated Infections. https://www.cdc.gov/hai/infectiontypes.html (accessed January 12, 2021).

22. Klevens, R. M.; Edwards, J. R.; Richards, C. L.; Horan, T. C.; Gaynes, R. P.; Pollock, D. A.; Cardo, D. M., Estimating Health Care-Associated Infections and Deaths in U.S. Hospitals, 2002. *Public Health Reports* **2007,** *122* (2), 160-166.

23. Moreira, J. M. R.; Ponmozhi, J.; Campos, J. B. L. M.; Miranda, J. M.; Mergulhão, F. J., Micro- and macro-flow systems to study Escherichia coli adhesion to biomedical materials. *Chemical Engineering Science* **2015,** *126*, 440-445.

24. Salek, M. M.; Martinuzzi, R. J., Numerical simulation of fluid flow and hydrodynamic analysis in commonly used biomedical devices in biofilm studies. *Numerical Simulations: Examples and Applications in Computational Fluid Dynamics* **2010**, 193-212.

25. Ofek, I.; Doyle, R. J., Principles of Bacterial Adhesion. In *Bacterial Adhesion to Cells and Tissues*, Ofek, I.; Doyle, R. J., Eds. Springer US: Boston, MA, 1994; pp 1-15.

26. Safdar, N.; Crnich, C. J.; Maki, D. G., The Pathogenesis of Ventilator-Associated Pneumonia: Its Relevance to Developing Effective Strategies for Prevention. *Respiratory Care* **2005,** *50* (6), 725.

27. Singha, P.; Locklin, J.; Handa, H., A review of the recent advances in antimicrobial coatings for urinary catheters. *Acta Biomaterialia* **2017,** *50*, 20-40.

28. Bos, R.; van der Mei, H. C.; Busscher, H. J., Physico-chemistry of initial microbial adhesive interactions – its mechanisms and methods for study. *FEMS Microbiology Reviews* **1999,** *23* (2), 179-230.

29. Abreu, A. C.; Tavares, R. R.; Borges, A.; Mergulhão, F.; Simões, M., Current and emergent strategies for disinfection of hospital environments. *Journal of Antimicrobial Chemotherapy* **2013,** *68* (12), 2718-2732.

30. Russell, A. D., Biocide use and antibiotic resistance: the relevance of laboratory findings to clinical and environmental situations. *The Lancet Infectious Diseases* **2003,** *3* (12), 794-803.

31. Simões, L. C.; Simões, M.; Vieira, M. J., Adhesion and biofilm formation on polystyrene by drinking water-isolated bacteria. *Antonie van Leeuwenhoek* **2010,** *98* (3), 317-329.

32. Doyle, R. J., Contribution of the hydrophobic effect to microbial infection. *Microbes and Infection* **2000,** *2* (4), 391-400.

33. Lawrence, E. L.; Turner, I. G., Materials for urinary catheters: a review of their history and development in the UK. *Medical Engineering & Physics* **2005,** *27* (6), 443-453.

34. Hron, P., Hydrophilisation of silicone rubber for medical applications. *Polymer International* **2003,** *52* (9), 1531-1539.

35. Veerachamy, S.; Yarlagadda, T.; Manivasagam, G.; Yarlagadda, P. K., Bacterial adherence and biofilm formation on medical implants: A review. *Proceedings of the Institution of Mechanical Engineers, Part H: Journal of Engineering in Medicine* **2014,** *228* (10), 1083-1099.

36. Seil, J. T.; Rubien, N. M.; Webster, T. J.; Tarquinio, K. M., Comparison of quantification methods illustrates reduced Pseudomonas aeruginosa activity on nanorough polyvinyl chloride. *Journal of Biomedical Materials Research Part B: Applied Biomaterials* **2011,** *98B* (1), 1-7.

37. Zhang, X.; Shi, F.; Niu, J.; Jiang, Y.; Wang, Z., Superhydrophobic surfaces: from structural control to functional application. *Journal of Materials Chemistry* **2008,** *18* (6), 621-633.

38. McCoy, C. P.; Irwin, N. J.; Hardy, J. G.; Kennedy, S. J.; Donnelly, L.; Cowley, J. F.; Andrews, G. P.; Pentlavalli, S., Systematic optimization of poly(vinyl chloride) surface modification with an aromatic thiol. *European Polymer Journal* **2017,** *97*, 40-48.

39. Hidalgo, M.; Reinecke, H.; Mijangos, C., PVC containing hydroxyl groups: I. Synthesis, characterization, properties and crosslinking. *Polymer* **1999,** *40* (12), 3525-3534.

40. Reinecke, H.; Mijangos, C., PVC modification with pyridine groups. Synthesis, characterization and transformation to ionomers. *Macromolecular Chemistry and Physics* **1998,** *199* (10), 2199-2204.

41. Herrero, M.; Quéméner, E.; Ulvé, S.; Reinecke, H.; Mijangos, C.; Grohens, Y., Bacterial adhesion to poly(vinyl chloride) films: Effect of chemical modification and water induced surface reconstruction. *Journal of Adhesion Science and Technology* **2006,** *20* (2-3), 183-195.

42. Pagliaro, M.; Ciriminna, R., New fluorinated functional materials. *Journal of Materials Chemistry* **2005,** *15* (47), 4981-4991.

43. Kawakami, H.; Takahashi, T.; Nagaoka, S.; Nakayama, Y., Albumin adsorption to surface of annealed fluorinated polyimide. *Polymers for Advanced Technologies* **2001,** *12* (3-4), 244-252.

44. Tsibouklis, J.; Graham, P.; Eaton, P. J.; Smith, J. R.; Nevell, T. G.; Smart, J. D.; Ewen, R. J., Poly(perfluoroalkyl methacrylate) Film Structures: Surface Organization Phenomena, Surface Energy Determinations, and Force of Adhesion Measurements. *Macromolecules* **2000,** *33* (22), 8460-8465.

45. Tsibouklis, J.; Stone, M.; Thorpe, A. A.; Graham, P.; Peters, V.; Heerlien, R.; Smith, J. R.; Green, K. L.; Nevell, T. G., Preventing bacterial adhesion onto surfaces: the low-surface-energy approach. *Biomaterials* **1999,** *20* (13), 1229-1235.

46. Corrales, M.; Bierbrauer, K.; Sacristan, J.; Mijangos, C., Surface Modification of PVC Membranes Using Fluorothiophenol Compounds. *Macromolecular Chemistry and Physics* **2010,** *211* (18), 1990-1998.

47. McCoy, C. P.; Cowley, J. F.; Gorman, S. P.; Andrews, G. P.; Jones, D. S., Reduction of Staphylococcus aureus and Pseudomonas aeruginosa colonisation on PVC through covalent surface attachment of fluorinated thiols. *Journal of Pharmacy and Pharmacology* **2009,** *61* (9), 1163-1169.

48. Abdallh, M.; Bufaroosha, M.; Ahmed, A.; Ahmed, D. S.; Yousif, E., Modification of Poly (vinyl chloride) Substrates via Schiff's Base for Photochemical Applications. *Journal of Vinyl and Additive Technology* **2020**.

49. Balakrishnan, B.; Kumar, D. S.; Yoshida, Y.; Jayakrishnan, A., Chemical modification of poly(vinyl chloride) resin using poly(ethylene glycol) to improve blood compatibility. *Biomaterials* **2005,** *26* (17), 3495-3502.

50. Zhang, L.; Tang, M.; Zhang, J.; Zhang, P.; Zhang, J.; Deng, L.; Lin, C.; Dong, A., One simple and stable coating of mixed-charge copolymers on poly(vinyl chloride) films to improve antifouling efficiency. *Journal of Applied Polymer Science* **2017,** *134* (12), 44632.

51. Allan, J. T. S., The sulfonation of polyvinyl chloride: Synthesis and characterization for proton conducting membrane applications. *Journal of Membrane Science* **2015,** *489*, 175-182.

52. Singh, A.; Rawat, M. S. M.; Pande, C. S., Chemical modification and characterization of poly(vinyl chloride) by crosslinking of multifunctional amines. *Journal of Applied Polymer Science* **2010,** *118* (2), 876-880.

53. Wu, C.; Wang, Z.; Liu, S.; Xie, Z.; Chen, H.; Lu, X., Simultaneous permeability, selectivity and antibacterial property improvement of PVC ultrafiltration membranes via in-situ quaternization. *Journal of Membrane Science* **2018,** *548*, 50-58.

54. Al-Daeif, Y.; Yousif, E.; Nabi, M. A., Synthesis of New Polymers Derived from Poly (Vinyl Chloride) and Study Their Optical Properties. *Journal of Al-Nahrain University* **2012,** *15* (2), 79-83.

55. Ameer, A. A.; Abdallh, M. S.; Ahmed, A. A.; Yousif, E. A., Synthesis and Characterization of Polyvinyl Chloride Chemically Modified by Amines. *Open Journal of Polymer Chemistry* **2013,** *3*, 11-15.

56. Kameda, T.; Fukuda, Y.; Grause, G.; Yoshioka, T., Chemical modification of rigid poly(vinyl chloride) by the substitution with nucleophiles. *Journal of Applied Polymer Science* **2010,** *116* (1), 36-44.

57. Starnes, W. H., Structural and mechanistic aspects of the thermal degradation of poly(vinyl chloride). *Progress in Polymer Science* **2002,** *27* (10), 2133-2170.

58. Starnes, W. H.; Ge, X., Mechanism of Autocatalysis in the Thermal Dehydrochlorination of Poly(vinyl chloride). *Macromolecules* **2004,** *37* (2), 352-359.

59. Lafarge, J.; Kébir, N.; Schapman, D.; Gadenne, V.; Burel, F., Design of bacteria repellent PVC surfaces using the click chemistry. *Cellulose* **2013,** *20* (6), 2779-2790.

60. Pawlak, M.; Grygolowicz-Pawlak, E.; Bakker, E., Ferrocene Bound Poly(vinyl chloride) as Ion to Electron Transducer in Electrochemical Ion Sensors. *Analytical Chemistry* **2010,** *82* (16), 6887-6894.

61. Beveridge, J. M.; Chenot, H. M.; Crich, A.; Jacob, A.; Finn, M. G., Covalent Functionalization of Flexible Polyvinyl Chloride Tubing. *Langmuir* **2018,** *34* (35), 10407-10412.

62. Pawlak, M.; Grygolowicz-Pawlak, E.; Crespo, G. A.; Mistlberger, G.; Bakker, E., PVC-Based Ion-Selective Electrodes with Enhanced Biocompatibility by Surface Modification with “Click” Chemistry. *Electroanalysis* **2013,** *25* (8), 1840-1846.

63. Zhao, B.; Brittain, W. J., Polymer brushes: surface-immobilized macromolecules. *Progress in Polymer Science* **2000,** *25* (5), 677-710.

64. McGinty, K. M.; Brittain, W. J., Hydrophilic surface modification of poly(vinyl chloride) film and tubing using physisorbed free radical grafting technique. *Polymer* **2008,** *49* (20), 4350-4357.

65. Percec, V.; Asgarzadeh, F., Metal-catalyzed living radical graft copolymerization of olefins initiated from the structural defects of poly(vinyl chloride). *Journal of Polymer Science Part A: Polymer Chemistry* **2001,** *39* (7), 1120-1135.

66. Huang, Z.; Feng, C.; Guo, H.; Huang, X., Direct functionalization of poly(vinyl chloride) by photo-mediated ATRP without a deoxygenation procedure. *Polymer Chemistry* **2016,** *7* (17), 3034-3045.

67. Zou, Y.; Kizhakkedathu, J. N.; Brooks, D. E., Surface Modification of Polyvinyl Chloride Sheets via Growth of Hydrophilic Polymer Brushes. *Macromolecules* **2009,** *42* (9), 3258-3268.

68. Cheng, Y.-Y.; Du, C.-H.; Wu, C.-J.; Sun, K.-X.; Chi, N.-P., Improving the hydrophilic and antifouling properties of poly(vinyl chloride) membranes by atom transfer radical polymerization grafting of poly(ionic liquid) brushes. *Polymers for Advanced Technologies* **2018,** *29* (1), 623-631.

69. Wu, H.; Li, T.; Liu, B.; Chen, C.; Wang, S.; Crittenden, J. C., Blended PVC/PVC-g-PEGMA ultrafiltration membranes with enhanced performance and antifouling properties. *Applied Surface Science* **2018,** *455*, 987-996.

70. Rusen, E.; Raluca, Ş.; Busuioc, C.; Diacon, A., Hydrophilic modification of polyvinyl chloride with polyacrylic acid using ATRP. *RSC Advances* **2020,** *10* (59), 35692-35700.

71. James, N. R.; Jayakrishnan, A., Surface thiocyanation of plasticized poly(vinyl chloride) and its effect on bacterial adhesion. *Biomaterials* **2003,** *24* (13), 2205-2212.

72. Kameda, T.; Fukuda, Y.; Grause, G.; Yoshioka, T., Chemical modification of flexible and rigid poly(vinyl chloride) by nucleophilic substitution with thiocyanate

using a phase-transfer catalyst. *Materials Chemistry and Physics* **2010,** *124* (1), 163-167.

73. Arenas, E.; Bucio, E.; Burillo, G.; Lopez, G. P., Radiation grafting of poly(ethylene glycol) methacrylate onto poly(vinyl chloride) tubes. *Designed Monomers & Polymers* **2007,** *10* (5), 459-467.

74. Islas, L.; Alvarez-Lorenzo, C.; Magariños, B.; Concheiro, A.; Castillo, L. F. d.; Burillo, G., Singly and binary grafted poly(vinyl chloride) urinary catheters that elute ciprofloxacin and prevent bacteria adhesion. *International Journal of Pharmaceutics* **2015,** *488* (1), 20-28.

75. Islas, L.; Ruiz, J.-C.; Muñoz-Muñoz, F.; Isoshima, T.; Burillo, G., Surface characterization of poly(vinyl chloride) urinary catheters functionalized with acrylic acid and poly(ethylene glycol) methacrylate using gamma-radiation. *Applied Surface Science* **2016,** *384*, 135-142.

76. Zuñiga-Zamorano, I.; Meléndez-Ortiz, H. I.; Costoya, A.; Alvarez-Lorenzo, C.; Concheiro, A.; Bucio, E., Poly(vinyl chloride) catheters modified with pH-responsive poly(methacrylic acid) with affinity for antimicrobial agents. *Radiation Physics and Chemistry* **2018,** *142*, 107-114.

77. Meléndez-Ortiz, H. I.; Alvarez-Lorenzo, C.; Concheiro, A.; Jiménez-Páez, V. M.; Bucio, E., Modification of medical grade PVC with N-vinylimidazole to obtain bactericidal surface. *Radiation Physics and Chemistry* **2016,** *119*, 37-43.

78. Campoccia, D.; Montanaro, L.; Arciola, C. R., A review of the biomaterials technologies for infection-resistant surfaces. *Biomaterials* **2013,** *34* (34), 8533-8554.

79. Fuchs, A. D.; Tiller, J. C., Contact-Active Antimicrobial Coatings Derived from Aqueous Suspensions. *Angewandte Chemie International Edition* **2006,** *45* (40), 6759-6762.

80. Poverenov, E.; Shemesh, M.; Gulino, A.; Cristaldi, D. A.; Zakin, V.; Yefremov, T.; Granit, R., Durable contact active antimicrobial materials formed by a one-step covalent modification of polyvinyl alcohol, cellulose and glass surfaces. *Colloids and Surfaces B: Biointerfaces* **2013,** *112*, 356-361.

81. He, W.; Zhang, Y.; Li, J.; Gao, Y.; Luo, F.; Tan, H.; Wang, K.; Fu, Q., A Novel Surface Structure Consisting of Contact-active Antibacterial Upper-layer and Antifouling Sub-layer Derived from Gemini Quaternary Ammonium Salt Polyurethanes. *Scientific Reports* **2016,** *6* (1), 32140.

82. Lemire, J. A.; Harrison, J. J.; Turner, R. J., Antimicrobial activity of metals: mechanisms, molecular targets and applications. *Nature Reviews Microbiology* **2013,** *11* (6), 371-384.

83. Xu, F. F.; Imlay, J. A., Silver(I), Mercury(II), Cadmium(II), and Zinc(II) Target Exposed Enzymic Iron-Sulfur Clusters when They Toxify *Escherichia coli*. *Applied and Environmental Microbiology* **2012,** *78* (10), 3614-3621.

84. Park, H.-J.; Kim, J. Y.; Kim, J.; Lee, J.-H.; Hahn, J.-S.; Gu, M. B.; Yoon, J., Silver-ion-mediated reactive oxygen species generation affecting bactericidal activity. *Water Research* **2009,** *43* (4), 1027-1032.

85. Imlay, J. A., Pathways of Oxidative Damage. *Annual Review of Microbiology* **2003,** *57* (1), 395-418.

86. Jung, W. K.; Koo, H. C.; Kim, K. W.; Shin, S.; Kim, S. H.; Park, Y. H., Antibacterial Activity and Mechanism of Action of the Silver Ion in Staphylococcus aureus and Escherichia coli. *Applied and Environmental Microbiology* **2008,** *74* (7), 2171.

87. Yamanaka, M.; Hara, K.; Kudo, J., Bactericidal Actions of a Silver Ion Solution on Escherichia coli, Studied by Energy-Filtering Transmission Electron Microscopy and Proteomic Analysis. *Applied and Environmental Microbiology* **2005,** *71* (11), 7589.

88. Johnson, J. R.; Johnston, B.; Kuskowski, M. A., *In Vitro* Comparison of Nitrofurazone- and Silver Alloy-Coated Foley Catheters for Contact-Dependent and Diffusible Inhibition of Urinary Tract Infection-Associated Microorganisms. *Antimicrobial Agents and Chemotherapy* **2012,** *56* (9), 4969-4972.

89. Lederer, J. W.; Jarvis, W. R.; Thomas, L.; Ritter, J., Multicenter cohort study to assess the impact of a silver-alloy and hydrogel-coated urinary catheter on symptomatic catheter-associated urinary tract infections. *Journal of wound, ostomy, and continence nursing : official publication of The Wound, Ostomy and Continence Nurses Society* **2014,** *41* (5), 473-480.

90. Merchan, M.; Sedlarikova, J.; Vesel, A.; Sedlarik, V.; Pastorek, M.; Sáha, P., Characterization of Antibacterial, Mechanical, and Structural Properties of Polyvinyl Chloride/Silver Nitrate Composites Prepared by Thermoplastic Compounding. *International Journal of Polymer Analysis and Characterization* **2010,** *15* (6), 360-369.

91. Lok, C.-N.; Ho, C.-M.; Chen, R.; He, Q.-Y.; Yu, W.-Y.; Sun, H.; Tam, P. K.-H.; Chiu, J.-F.; Che, C.-M., Proteomic Analysis of the Mode of Antibacterial Action of Silver Nanoparticles. *Journal of Proteome Research* **2006,** *5* (4), 916-924.

92. Balazs, D. J.; Triandafillu, K.; Chevolot, Y.; Aronsson, B.-O.; Harms, H.; Descouts, P.; Mathieu, H. J., Surface modification of PVC endotracheal tubes by oxygen glow discharge to reduce bacterial adhesion. *Surface and Interface Analysis* **2003,** *35* (3), 301-309.

93. Balazs, D. J.; Triandafillu, K.; Wood, P.; Chevolot, Y.; van Delden, C.; Harms, H.; Hollenstein, C.; Mathieu, H. J., Inhibition of bacterial adhesion on PVC endotracheal tubes by RF-oxygen glow discharge, sodium hydroxide and silver nitrate treatments. *Biomaterials* **2004,** *25* (11), 2139-2151.

94. Krylach, I. V.; Kudryashov, S. I.; Olekhnovich, R. O.; Fokina, M. I.; Sitnikova, V. E.; Moskvin, M. K.; Shchedrina, N. N.; Uspenskaya, M. V., Fabrication of a Functional Relief on the Surface of a Polyvinyl Chloride Film by Nanosecond Laser Microtexturing. *Optics and Spectroscopy* **2020,** *128* (8), 1251-1255.

95. Yu, Z.; Zhao, Y.; Gao, B.; Liu, X.; Jia, L.; Zhao, F.; Ma, J., Performance of novel a Ag-n-TiO2/PVC reinforced hollow fiber membrane applied in water purification: in situ antibacterial properties and resistance to biofouling. *RSC Advances* **2015,** *5* (118), 97320-97329.

96. Behboudi, A.; Jafarzadeh, Y.; Yegani, R., Preparation and characterization of TiO2 embedded PVC ultrafiltration membranes. *Chemical Engineering Research and Design* **2016,** *114*, 96-107.

97. Al-Ani, F. H.; Alsalhy, Q. F.; Raheem, R. S.; Rashid, K. T.; Figoli, A., Experimental Investigation of the Effect of Implanting TiO(2)-NPs on PVC for Long-Term UF Membrane Performance to Treat Refinery Wastewater. *Membranes (Basel)* **2020,** *10* (4), 77.

98. Söderberg, T. A.; Sunzel, B.; Holm, S.; Elmros, T.; Hallmans, G.; Sjöberg, S., Antibacterial effect of zinc oxide in vitro. *Scandinavian Journal of Plastic and Reconstructive Surgery and Hand Surgery* **1990,** *24* (3), 193-197.

99. Nair, S.; Sasidharan, A.; Divya Rani, V. V.; Menon, D.; Nair, S.; Manzoor, K.; Raina, S., Role of size scale of ZnO nanoparticles and microparticles on toxicity toward bacteria and osteoblast cancer cells. *Journal of Materials Science: Materials in Medicine* **2009,** *20 Suppl 1*, S235-41.

100. Padmavathy, N.; Vijayaraghavan, R., Enhanced bioactivity of ZnO nanoparticles-an antimicrobial study. *Science and Technology of Advanced Materials* **2008,** *9* (3), 035004.

101. Seil, J. T.; Webster, T. J., Reduced Staphylococcus aureus proliferation and biofilm formation on zinc oxide nanoparticle PVC composite surfaces. *Acta Biomaterialia* **2011,** *7* (6), 2579-2584.

102. Seil, J. T.; Webster, T. J. In *Zinc oxide nanoparticle and polymer antimicrobial biomaterial composites*, Proceedings of the 2010 IEEE 36th Annual Northeast Bioengineering Conference (NEBEC), 26-28 March 2010; 2010; pp 1-2.

103. Rabiee, H.; Vatanpour, V.; Farahani, M. H. D. A.; Zarrabi, H., Improvement in flux and antifouling properties of PVC ultrafiltration membranes by incorporation of zinc oxide (ZnO) nanoparticles. *Separation and Purification Technology* **2015,** *156*, 299-310.

104. Zarrinkhameh, M.; Zendehnam, A.; Hosseini, S. M., Electrochemical, morphological and antibacterial characterization of PVC based cation exchange membrane modified by zinc oxide nanoparticles. *Journal of Polymer Research* **2013,** *20* (11), 283.

105. Li, X.; Xing, Y.; Jiang, Y.; Ding, Y.; Li, W., Antimicrobial activities of ZnO powder-coated PVC film to inactivate food pathogens. *International Journal of Food Science & Technology* **2009,** *44* (11), 2161-2168.

106. Zheng, W.; Jia, Y.; Chen, W.; Wang, G.; Guo, X.; Jiang, X., Universal Coating from Electrostatic Self-Assembly to Prevent Multidrug-Resistant Bacterial Colonization on Medical Devices and Solid Surfaces. *ACS Applied Materials & Interfaces* **2017,** *9* (25), 21181-21189.

107. Ona, K. R.; Courcelle, C. T.; Courcelle, J., Nucleotide excision repair is a predominant mechanism for processing nitrofurazone-induced DNA damage in Escherichia coli. *Journal of Bacteriology* **2009,** *191* (15), 4959-4965.

108. Kilonzo, M.; Vale, L.; Pickard, R.; Lam, T.; N'Dow, J., Cost Effectiveness of Antimicrobial Catheters for Adults Requiring Short-term Catheterisation in Hospital. *European Urology* **2014,** *66* (4), 615-618.

109. National Center for Biotechnology Information. PubChem Compound Summary for CID 5447130, Nitrofurazone. https://pubchem.ncbi.nlm.nih.gov/compound/Nitrofurazone. (accessed January 11, 2021).

110. Nitrofurazone https://oehha.ca.gov/chemicals/nitrofurazone (accessed January 11, 2021).

111. Ramritu, P.; Halton, K.; Collignon, P.; Cook, D.; Fraenkel, D.; Battistutta, D.; Whitby, M.; Graves, N., A systematic review comparing the relative effectiveness of antimicrobial-coated catheters in intensive care units. *American Journal of Infection Control* **2008,** *36* (2), 104-117.

112. Darouiche, R. O.; Raad, I. I.; Heard, S. O.; Thornby, J. I.; Wenker, O. C.; Gabrielli, A.; Berg, J.; Khardori, N.; Hanna, H.; Hachem, R., A comparison of two antimicrobial-impregnated central venous catheters. *New England Journal of Medicine* **1999,** *340* (1), 1-8.

113. Hanna, H.; Benjamin, R.; Chatzinikolaou, I.; Alakech, B.; Richardson, D.; Mansfield, P.; Dvorak, T.; Munsell, M. F.; Darouiche, R.; Kantarjian, H., Long-term silicone central venous catheters impregnated with minocycline and rifampin decrease rates of catheter-related bloodstream infection in cancer patients: a prospective randomized clinical trial. *Journal of Clinical Oncology* **2004,** *22* (15), 3163-3171.

114. Ozcelik, B.; Pasic, P.; Sangwan, P.; Be, C. L.; Glattauer, V.; Thissen, H.; Boulos, R. A., Evaluation of the Novel Antimicrobial BCP3 in a Coating for Endotracheal Tubes. *ACS Omega* **2020,** *5* (18), 10288-10296.

115. Barh, D.; Jain, N.; Tiwari, S.; Parida, B. P.; D'Afonseca, V.; Li, L.; Ali, A.; Santos, A. R.; Guimarães, L. C.; de Castro Soares, S.; Miyoshi, A.; Bhattacharjee, A.; Misra, A. N.; Silva, A.; Kumar, A.; Azevedo, V., A novel comparative genomics analysis for common drug and vaccine targets in Corynebacterium pseudotuberculosis and other CMN group of human pathogens. *Chemical biology & drug design* **2011,** *78* (1), 73-84.

116. Campoccia, D.; Montanaro, L.; Speziale, P.; Arciola, C. R., Antibiotic-loaded biomaterials and the risks for the spread of antibiotic resistance following their prophylactic and therapeutic clinical use. *Biomaterials* **2010,** *31* (25), 6363-6377.

117. Wang, Q.; Sun, F.-J.; Liu, Y.; Xiong, L.-R.; Xie, L.-L.; Xia, P.-Y., Enhancement of biofilm formation by subinhibitory concentrations of macrolides in icaADBC-positive and-negative clinical isolates of Staphylococcus epidermidis. *Antimicrobial agents and chemotherapy* **2010,** *54* (6), 2707-2711.

118. Hoffman, L. R.; D'Argenio, D. A.; MacCoss, M. J.; Zhang, Z.; Jones, R. A.; Miller, S. I., Aminoglycoside antibiotics induce bacterial biofilm formation. *Nature* **2005,** *436* (7054), 1171-1175.

119. Nathan, C. F.; Hibbs, J. B., Role of nitric oxide synthesis in macrophage antimicrobial activity. *Current Opinion in Immunology* **1991,** *3* (1), 65-70.

120. Fang, F. C., Antimicrobial actions of nitric oxide. *Nitric Oxide* **2012,** *27*, S10.

121. Nichols, S. P.; Schoenfisch, M. H., Nitric oxide flux-dependent bacterial adhesion and viability at fibrinogen-coated surfaces. *Biomaterials Science* **2013,** *1* (11), 1151-1159.

122. Handa, H.; Major, T. C.; Brisbois, E. J.; Amoako, K. A.; Meyerhoff, M. E.; Bartlett, R. H., Hemocompatibility comparison of biomedical grade polymers using rabbit thrombogenicity model for preparing nonthrombogenic nitric oxide releasing surfaces. *Journal of Materials Chemistry B* **2014,** *2* (8), 1059-1067.

123. Handa, H.; Brisbois, E. J.; Major, T. C.; Refahiyat, L.; Amoako, K. A.; Annich, G. M.; Bartlett, R. H.; Meyerhoff, M. E., In vitro and in vivo study of sustained nitric oxide release coating using diazeniumdiolate-doped poly(vinyl chloride) matrix with poly(lactide-co-glycolide) additive. *Journal of Materials Chemistry B* **2013,** *1* (29), 3578-3587.

124. Lantvit, S. M.; Barrett, B. J.; Reynolds, M. M., Nitric oxide releasing material adsorbs more fibrinogen. *Journal of Biomedical Materials Research Part A* **2013,** *101* (11), 3201-3210.

125. Zhang, Y.; Zhao, Q.; Li, W.; Liu, J.; Chen, J.; Fan, Y.; Weng, Y., Substrate Independent Liquid Phase Epitaxy of HKUST-1 as Anticoagulant and Antimicrobial Coating. *Advanced Materials Interfaces* **2020,** *7* (12), 1902011.

126. Neufeld, M. J.; Ware, B. R.; Lutzke, A.; Khetani, S. R.; Reynolds, M. M., Water-Stable Metal–Organic Framework/Polymer Composites Compatible with Human Hepatocytes. *ACS Applied Materials & Interfaces* **2016,** *8* (30), 19343-19352.

127. Friedman, A.; Friedman, J., New biomaterials for the sustained release of nitric oxide: past, present and future. *Expert Opinion on Drug Delivery* **2009,** *6* (10), 1113-1122.

2 Surface Modification of Medical Grade PVC Tubing

2.1 Introduction

PVC is one of the most widely used polymeric materials in the medical industry. Anti-infective biomaterials have become one of the primary strategies to prevent medical device related infections. PVC surface modification can be achieved by a combination of both covalent and non-covalent treatments. In non-covalent surface modification, additives are most likely to leach out from polymer matrix over time, and can be toxic to humans. Covalent surface modification to introduce active groups and/or functionalities to form an antifouling PVC surface has become the most successful approach to prevent medical device related infections. The PVC surface is hydrophobic in nature, which allows bacterial cells and proteins to easily accumulate onto the surfaces and generate biofilms. Thus, the alteration of PVC surfaces to reduce initial bacterial adhesion was the main objective of this study. Literature studies showed that by increasing hydrophilicity, such as introducing zwitterionic groups, long chain polyethylene oxide (PEO), quaternary amines, etc. on the PVC surface directly reduces bacterial adhesion. These ionic groups create a hydration layer on the surface to repel foulants.[1, 2] This hydration layer is generally formed by hydrogen bonding or solvation process. Water molecules are released when protein approaches to this surface. The Polymer dehydration process increases enthalpy, but polymer chain compression decreases entropy. According to thermodynamics, these

two events happening together are unfavorable, and foulants are repealed by steric repulsion.[3, 4]

This study herein is based on surface modification of medical PVC endotracheal tubing using copper-free azide-alkyne cycloaddition. Medical endotracheal tubing was initially provided by our collaborator Dr. Chalongrat Daengngam (designated as vendor A). Later when he was unable to provide more, endotracheal tubing was obtained from Bangladesh (designated as vendor B). Labile chlorine atoms on the surface of PVC tubing were substituted by azide in aqueous media in the presence of a phase transfer catalyst. Electron poor alkynes containing different functionalities (zwitterionic, polyethyleneoxide (PEO), quaternary ammonium bromides and perfluoro groups) were synthesized, followed by thermal azide-alkyne cycloaddition to modify the PVC surface (**Scheme 1, Table 1**). The reaction progress was monitored by ATR-FTIR. The physical characterization of chemically modified PVC tubing (static contact angle, surface free energy, contact angle hysteresis and AFM images) was carried out to probe the modified surface properties by our collaborator Prof. Chalongrat Daengngm at Prince of Songkla University in Thailand. Bacterial adherence assays were performed by me in Prof. Fitnat Yildiz's lab at Microbiology and Environmental Toxicology Department at University of California, Santa Cruz under the guidance of postdoctoral scholar Dr. Kyle Floyd. *Pseudomonas aeruginosa* strain PA01, a Gram-negative opportunistic

respiratory pathogen, was used for bacterial adherence assay. X-Ray Photoelectron Spectroscopic (XPS) analysis was performed by Dr. Monica Neuburger at Eurofins EAG Material Science in Sunnyvale, California on unmodified tubing from both sources (Vendor A and Vencor B).

2.2 Azidation of PVC Tubing

Most procedures in the literature for azide nucleophilic substitution of labile secondary chlorine in PVC entail reaction of soluble PVC chains in organic solvents (THF, DMSO, DMF, ethanol).[5, 6] In order to keep the tubing flexible, surface azidation of medical endotracheal tubing was performed in aqueous solution to minimize loss of plasticizer. The use of phase transfer catalysts facilitates this substitution reaction;[7] a modified procedure of Finn[8] using Aliquat® 336 was adopted.

During the reaction, the degree of azidation was monitored by ATR-FTIR, as reflected by the increasing azide peak intensity at ~2100 cm^{-1}. The degree of azidation increases with temperature (50 to 80 °C) and reaction time (4-16 hours, **Figure 2.1**). Above 85 °C, sometimes complete dissolution of PVC tubing was eventually observed, as has also been reported by others.[9] Discoloration of the PVC tubing increases with extended reaction times, thus six hours at 80 °C was chosen as the optimized reaction conditions. This yellowing is likely due to thermal or base mediated dehydrochlorination.[10-12] Use of high concentrations ($>$ 0.4 M) of phase transfer

catalyst facilitated azidation, but was accompanied by both discoloration and enhanced rigidity of the tubing.

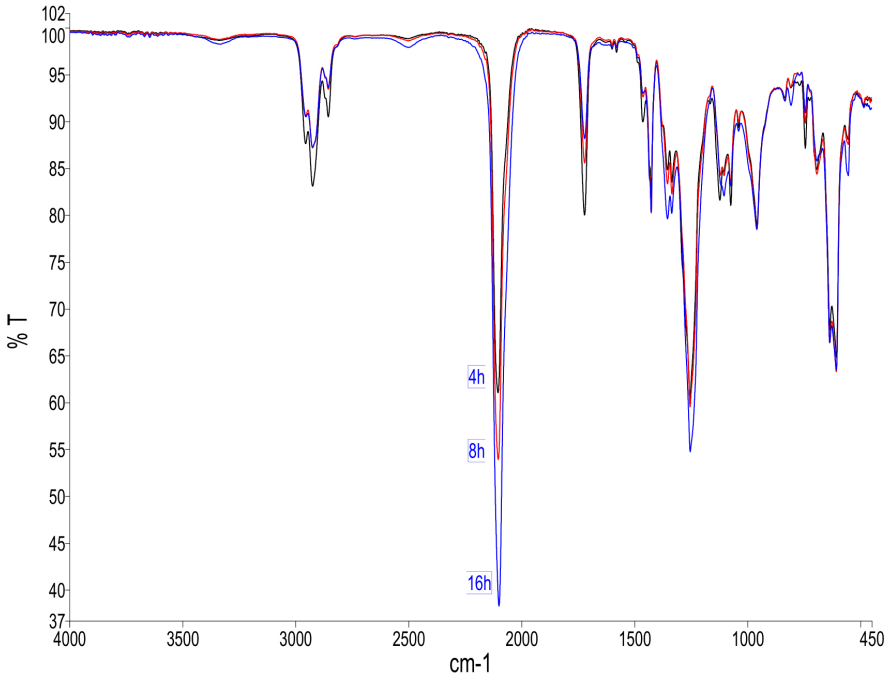

Figure 2.1: Degree of azidation monitored by ATR-FTIR as a function of time: 4, 8 and 16 hours

2.3 Small Molecule Model Reaction

A model reaction was performed before applying the cycloaddition to azidized PVC tubing (**Figure 2.2**). The main reason was to test the thermal reactivity of the alkyne bearing electron-poor groups with azide. The reaction progress was monitored by NMR. It took approximately 23 hours to complete the reaction. The model azide-alkyne cycloaddition on azidized PVC was monitored by ATR-FTIR (**Figure 2.3, Figure 2.4**) by disappearance of the strong azide pick ~2100 cm^{-1}.

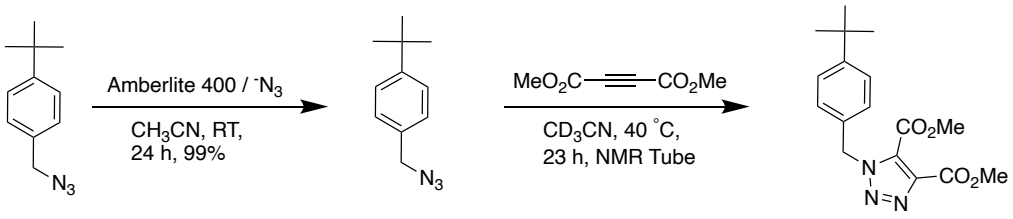

Figure 2.2: Small molecule model reaction

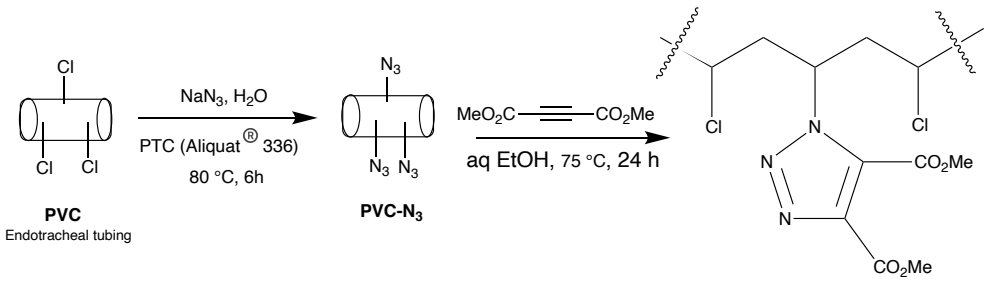

Figure 2.3: Model thermal azide alkyne cycloaddition on azidized PVC tubing

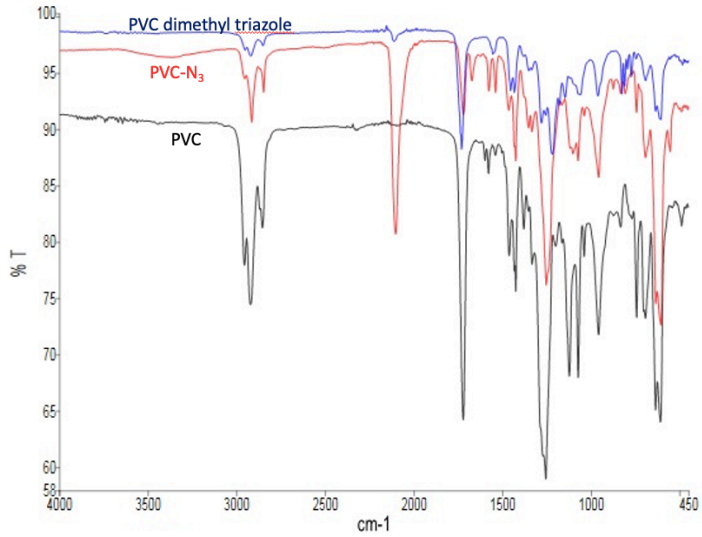

Figure 2.4: Model thermal azide-alkyne cycloaddition on azide functionalized PVC tubing monitored by ATR-FTIR

2.4 Thermal Azide-Alkyne Cycloadditions on Azide Functionalized PVC Tubing

Copper-catalyzed azide-alkyne cycloaddition is an extremely popular technique to chemically attach two moieties together. However, removal of the toxic copper residue is always challenging. An alternative is the thermal azide-alkyne cycloaddition, which is controlled by the highest occupied molecular orbital (HOMO) of the azide and the lowest unoccupied molecular orbital (LUMO) of the alkyne. The LUMO can be lowered by direct attachment of electron poor groups to the alkyne.[9] Thus copper-free thermal azide-alkyne cycloadditions were performed on azide-functionalized PVC tubing, to append functionality onto the surface. The alkyne was dissolved in solvent and mixed with azidized PVC tubing for 48 hours. Alkynes bearing two electron-withdrawing ester groups require approximately 24 hours at 75 °C. The reaction progress was again monitored by ATR-FTIR, by following the disappearance of the azide peak ~2100 cm^{-1} (**Figure 2.5**). Water was used as solvent, except for alkynes bearing quaternary amines (isopropyl alcohol was added as a co-solvent) and polyfluro chains (2,2,2-trifluroethanol was added as a co-solvent).

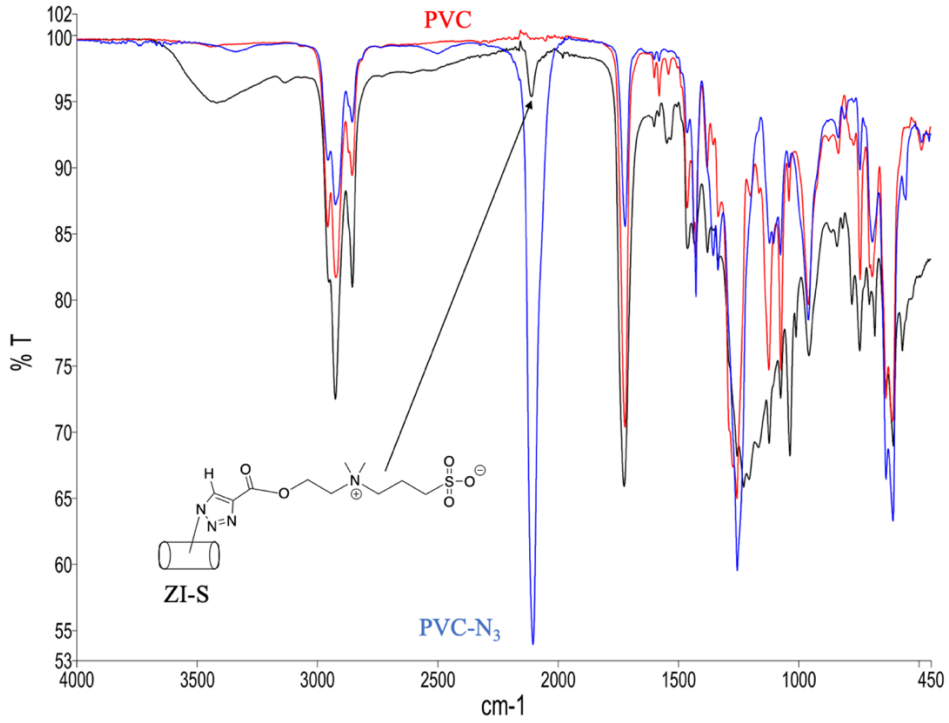

Figure 2.5: Thermal azide-alkyne cycloaddition of an alkyne bearing a zwitterionic group as monitored by ATR-FTIR

2.5 Attempt to Add Fluorophore to Confirm Surface Modification

In order to confirm surface modification, a fluorophore tethered electron poor (ester group) alkyne was synthesized and attached to PVC tubing by thermal azide-alkyne cycloaddition (**Figure 2.6**). 2-Aminoethanol was allowed to react with dansyl chloride to produce 5-(dimethylamino)-*N*-(2-hydromethyl)-1-napthalene-1-sulfonamide (a).[13] Then DCC coupling with propiolic acid gave the fluorophore containing an electron poor alkyne (b). Thermal azide-alkyne cycloaddition was performed with the fluorophore containing electron poor alkyne and azidized PVC

tubing. The reaction was monitored by ATR-FTIR (disappearance of the azide peak ~2100 cm^{-1}). The fluorophore attached tubing (c) was very fluorescent under UV light (**Figure 2.7**). However organic solvent was required to dissolve the alkyne, which may lead to removal of plasticizer from the PVC tubing. Also, a control reaction was performed by dipping PVC tubing without any azide group into the solution containing the fluorescent alkyne. PVC tubing also absorbed the dye and was fluorescent under UV light. Due to concern about use of solvent effect and fluorescent dye adsorption onto unmodified tubing, the attempt to confirm surface modification under UV light was failed.

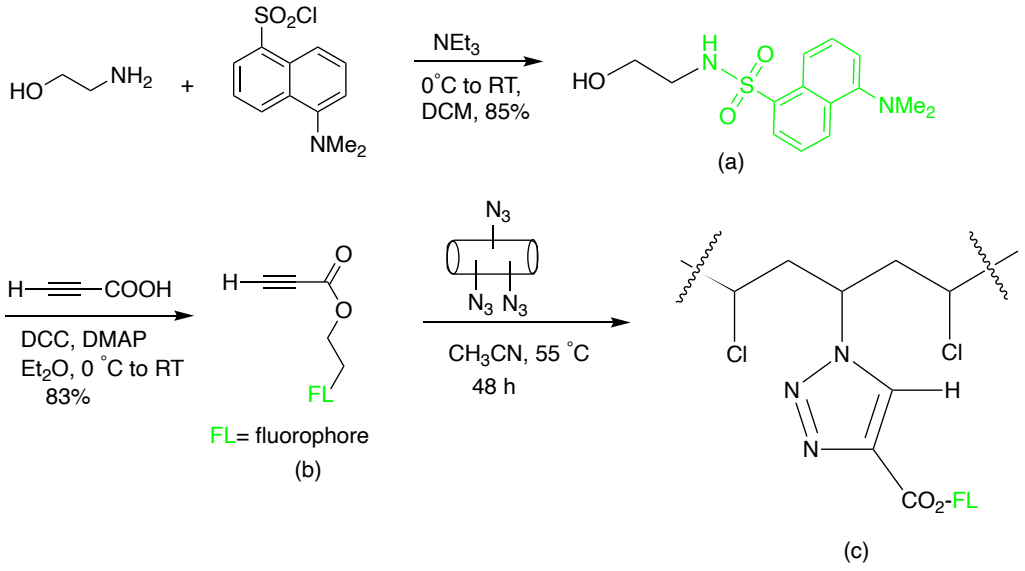

Figure 2.6: Fluorophore attachment on PVC tubing by thermal azide-alkyne cycloaddition

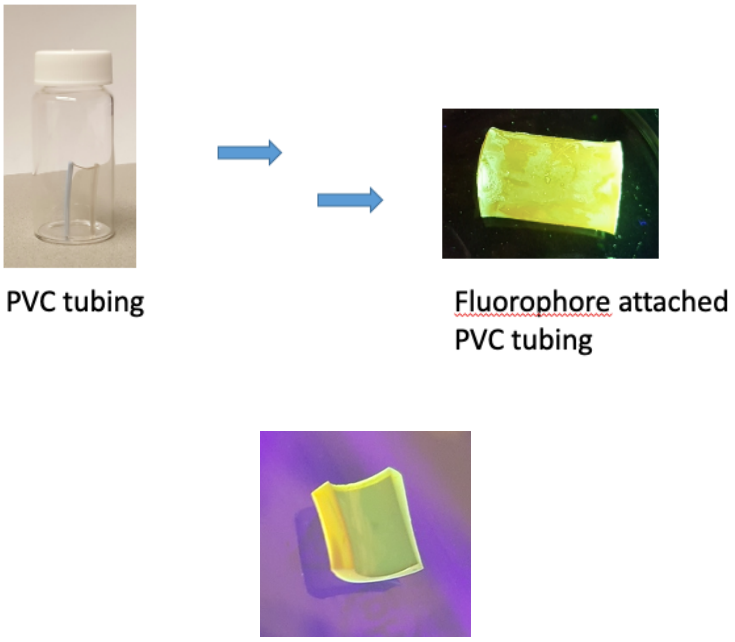

Figure 2.7: Fluorophore attached PVC tubing

2.6 Physical Properties of Modified PVC Tubing

A variety of PVC surfaces modified with zwitterionic groups, polyethylene oxide (PEO), quaternary amines or perfluoro species were prepared using short, medium and long tethers (**Scheme 1**, **Table 1**).

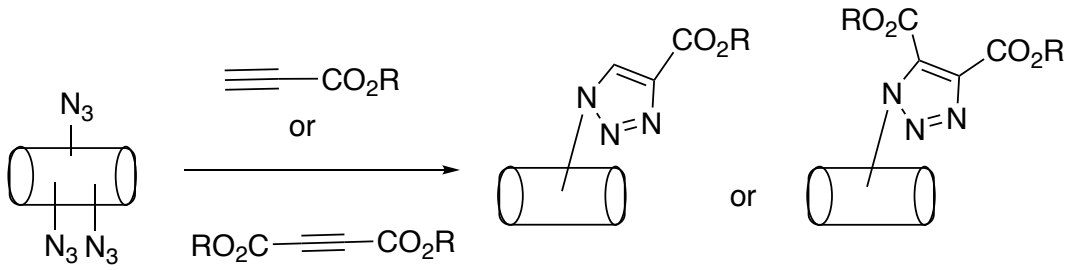

Scheme 1: Thermal azide-alkyne cycloaddition reactions

Table 1: Abbreviations of modified PVC surfaces

Name	Ester	Structure of R
Zwitterionic-Small ZI-S	Mono	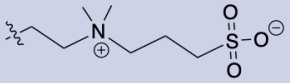
Zwitterionic-Large ZI-L	Mono	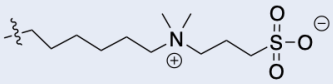
PEO_{2000}	Mono	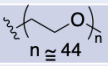
Quaternary Amine Small QA-S	Mono	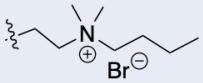
Quaternary Amine Medium QA-M	Mono	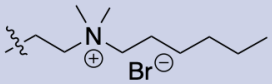
Quaternary Amine Large QA-L	Mono	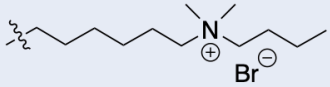
Perfluoro ester Small PF-S	Di	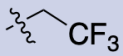
Perfluoro ester Medium PF-M	Mono	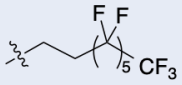
Perfluoro ester Large PF-L	Di	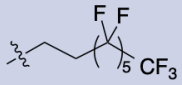

*Small, Medium and Large refer to the relative tether length between ester oxygen and functionality on the alkoxy of the ester group

2.6.1 Surface Robustness

Surface modification of the medical PVC tubing by azidation followed by thermal azide alkyne cycloadditions was confirmed by contact angle measurements.

Shown in **Figure 2.9**, the resulting static contact angle (SCA) values of the samples reveal a broad variety of surface wetting states, ranging from hydrophilic to hydrophobic as a result of the introduced alkyne functional groups. The pristine PVC surface shows moderate hydrophobic behavior, with an initial SCA of 100.7±1.3°; however, the wetting state switches to hydrophilic with an initial SCA of 35.6±1.7° once treated with azide group is introduced. This may be due to the polar character of the azide group as indicated by the resonance structure (**Figure 2.8**). All functional groups that contain quaternary ammonium salts display hydrophilic properties, with initial SCA in the range of 60-80° due to the strong zwitterionic charges on the surface. The relatively small change among hydrocarbon chains in samples QA-S, QA-M and QA-L is not sufficient to impart more hydrophobic properties on the surface. However, the presence of sulfonic groups with the quaternary ammonium in samples **ZI-S** and **ZI-L** result in slight increases in the surface hydrophobicity. **PEO_{2000}** functional groups shows hydrophobic properties with an initial SCA of 98.6±1.3°. The diester displaying two C_6F_{13} groups, **PF-L**, exhibits the highest hydrophobic surface with an initial SCA 115.5±1.8°, while the corresponding C_6F_{13} mono ester (**PF-M**) and diester with CF_3 end group (**PF-S**) show progressively small SCA values.

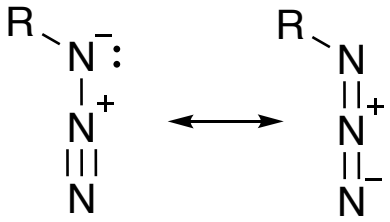

Figure 2.8: Azide resonance structure

In term of grafting durability, all functional groups maintain their wetting properties against vigorous rinsing with water. Although slight fluctuations were observed, no significant changes of the SCA values are observed over 60 min duration of ultrasonic cleaning, indicating strong bonding of the functional groups on the PVC tube surface.

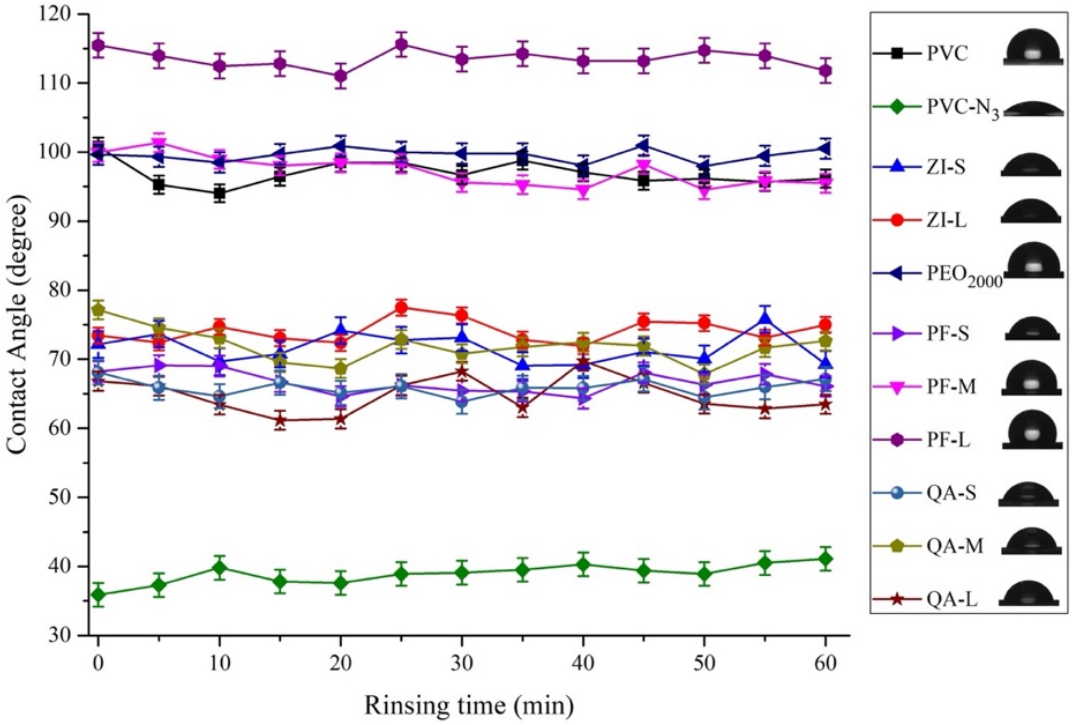

Figure 2.9: Modified PVC surface robustness test

2.6.2 Surface Free Energy

The surface energies of the funtionalized PVC tubing are presented in **Figure 2.10**. It was expected that fluorous functional groups would impact hydrophobicity in low values of surface energy. Apparently the CF_3 end group (**PF-S**) is not sufficiently fluorous to impact this property. In general, fluoropolymer surfaces with low surface energy and friction reduce the ability to be colonized by fouling organisms. Minimal surface energies in the range of 20-30 mJ/m are the most effective values, while microbial adhesion starts to increase with growing surface energy values.[14] The surface energy of PEO reaches that low (20.7 mJ/m) value as it is polar.

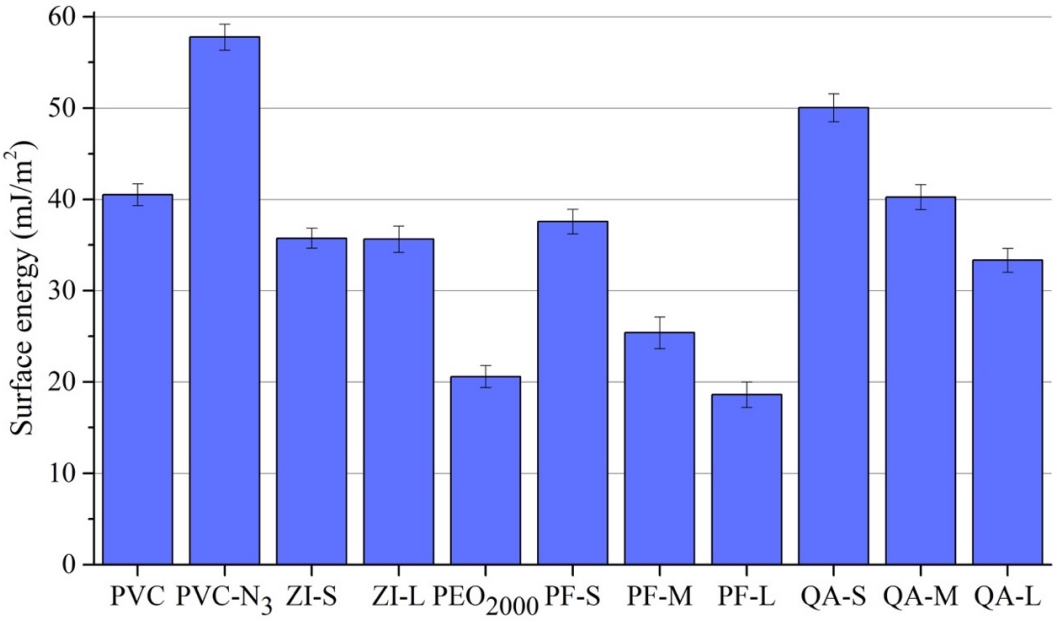

Figure 2.10: Surface free energy of surface modified PVC tubing

2.6.3 Contact Angle Hysteresis

Contact angle hysteresis (CAH) measures the difference between advancing and receding contact angles. It reveals information about dynamic wetting properties of the surface and surface adhesion for all of the modified PVC surfaces (**Figure 2.11**). High hysteresis is usually associated with high adhesion. The SCA along cannot be used to accurately predict the properties of a surface. A better prediction for bacterial adhesion properties should account for both the advancing and the receding contact angles and CAH,[15, 16] associated with work required for both the removal of liquid or microorganisms from a solid surface, stemming from several underlying physicochemical interactions. Typically, low CAH and high receding contact angles are favorable for anti-bacterial adhesion properties. This analysis suggests the sample bearing one or two C_6F_{13} groups as well as the polyether PEO_{2000} should show biofilm resistance, although the "untreated" PVC sample also displays low CAH and a high receding angle due to presence of silicone coating.

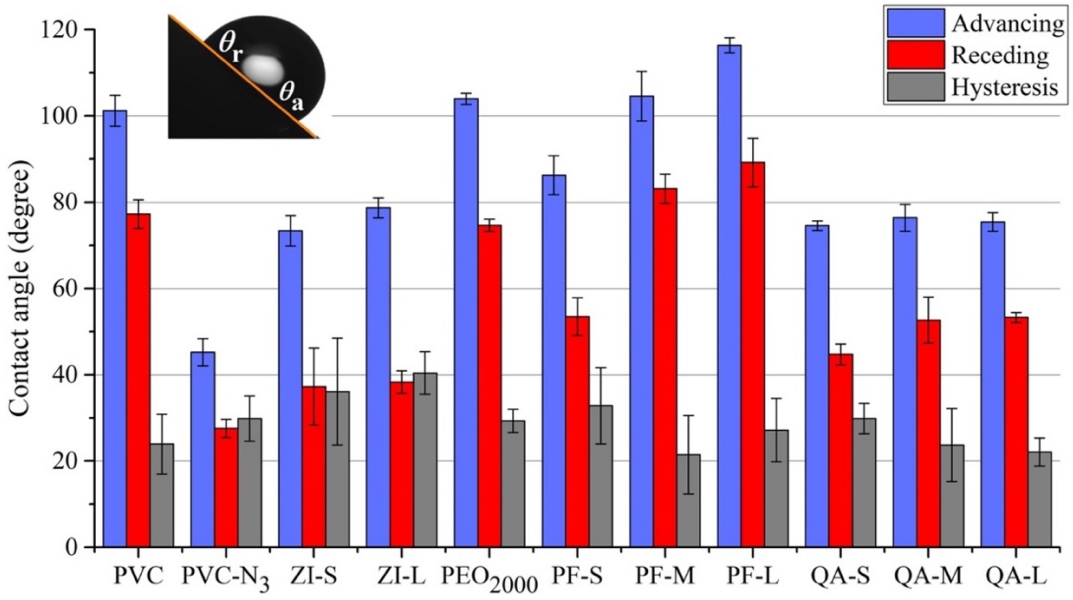

Figure 2.11: Advancing and receding contact angles and contact angle hysteresis (CAH)

2.6.4 Atomic Force Microscopic (AFM) Images

Three-dimensional surface nanotopography of PVC endotracheal tube samples grafted with various surface functional groups and the corresponding root-mean-square (rms) surface roughness are presented in **Figure 2.12** and **Figure 2.13**. The untreated PVC surface is comparatively smooth with minimum rms roughness of 7.4±0.8 nm. The initial azide treatment imparts a slightly high surface roughness. All of the quaternary amine functionalized samples show relatively consistent surface morphology and roughness, similar to the azido-functionalized sample. The perfluoro groups display an increase of surface roughness, especially the diester **PF-L**, which shows a distinctively high surface roughness around 148±13 nm.

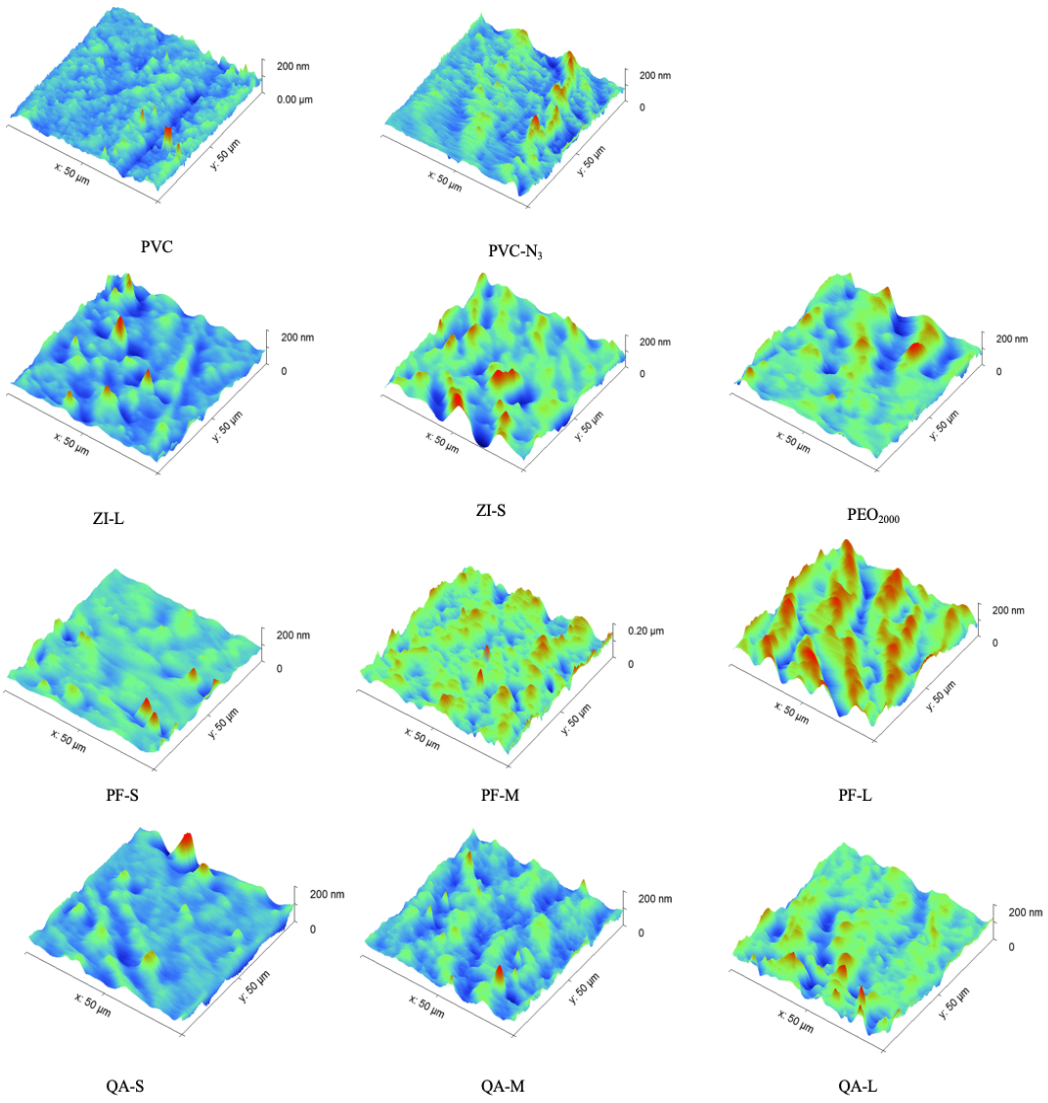

Figure 2.12: AFM images of modified PVC tubing

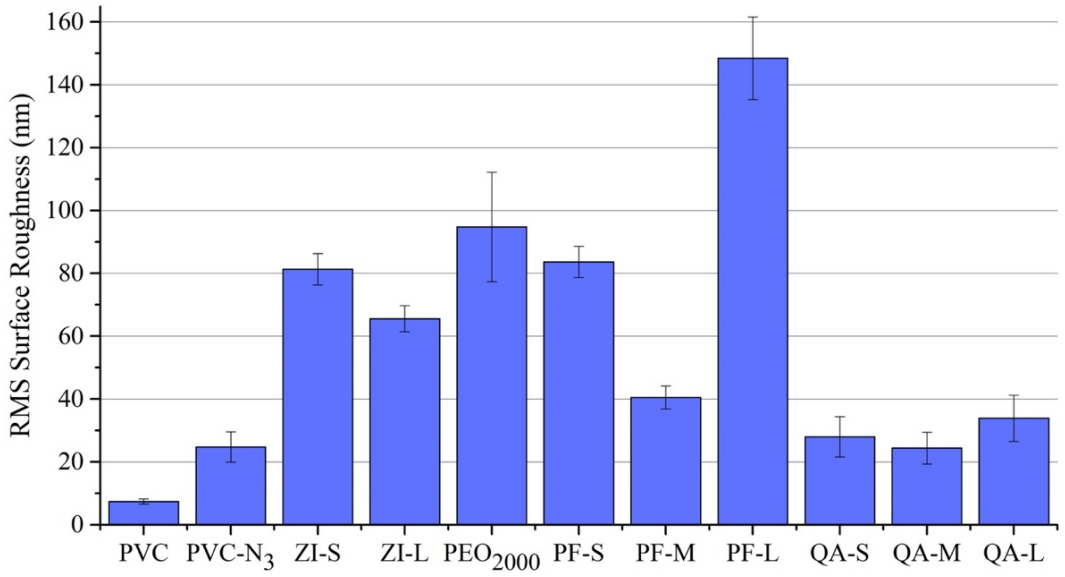

Figure 2.13: Root mean square roughness of modified PVC tubing

2.6.5 *Pseudomonas aeruginosa* Adherence Assays

The antifouling activity of modified endotracheal tubing was evaluated by a bacterial adherence assay using the Gram-negative opportunistic and nosocomial pathogen *Pseudomonas aeruginosa*. Bacterial adherence to select modified tubing samples (**ZI-L**, **PEO_{2000}**, **PF-L**, **QA-S**, **QA-M**, and **QA-L**), was compared to unmodified PVC and PVC-N_3 control samples after static growth for 24 hours at 37°C (**Figure 2.14**). Average *P. aeruginosa* colony forming units (cfu) adhered to the unmodified PVC and PVC-N_3 control samples, were observed to be $9.93x10^6 \pm 7.62x10^5$ and $1.18x10^7 \pm 5.31x10^6$ respectively. All modified tubing samples demonstrated bacterial adherence to varying degrees; with average observed cfu (± SEM) of $1.19x10^7 \pm 4.18x10^6$ for **ZI-L** treated, $9.64x10^6 \pm 2.01x10^6$ for **PEO_{2000}** treated, $5.13x10^6 \pm 3.76x10^5$ for **PF-L** treated,

$5.57x10^6 \pm 1.83x10^6$ for **QA-S** treated, $4.97x10^6 \pm 2.15x10^6$ for **QA-M** treated, and $6.05x10^6 \pm 2.11x10^5$ for **QA-L** treated samples. When compared to the PVC-N_3 control, both **PF-L** and **QA-L** treatments resulted in significantly reduced bacterial adherence to the tubing samples. This may be due to high polyfluoro **PF-L** (di-ester of C_6F_{13}) functionalization on the PVC surface with low surface free (19.7 mJ/m) energy and high roughness (148±13 nm) to reduce the ability to be colonized by fouling organisms. Similarly, long chain substituted quaternary amine **QA-L** has a lower surface free energy, high CAH and high roughness to reduce the ability to be colonized by bacteria. While not statistically significant, **QA-S** and **QA-M** treatments showed a trend towards reduced bacterial adherence to the tubing. Observation of only a slight trend towards reduced adherence among the quaternary amine samples could be affected by the pH of the media. These adherence assays were performed under a neutral pH of 7.4, and in general, only at a low pH (<4) can the QA modified surface can stay positively charged and inhibit positively charged protein interactions to reduce the fouling ratio.[17] Surprisingly, zwitterionic treatments (**ZI-S** and **ZI-L**) were observed to be non-repellent to *P. aeruginosa*, and exhibited high bacterial adhesion. Mixed charge zwitterionic surfaces can immobilize proteins. When cation-anion surfaces are designed to have net null charge on the surface, they still have the ability to absorb many proteins, even when some of them are unable to absorb on fully cationic or fully anionic supports under similar conditions.[18] Overall, these adherence

assays demonstrate that high polyfluoro **PF-L** (di-ester of C_6F_{13}) and long quaternary amine functionality **QA-L** samples slightly reduced *P. aeruginosa* adherence to endotracheal tubing, yet further studies will need to be conducted on uncoated PVC to establish the impacts of this modification on adherence of other nosocomial bacterial pathogens. The *Pseudomonas aeruginosa* adherence assays result did not show big difference on un-modified and modified tubing. So, x-ray photoelectron spectra (XPS) were taken to investigate the presence of any pre-existing antifouling coating on un-modified tubing.

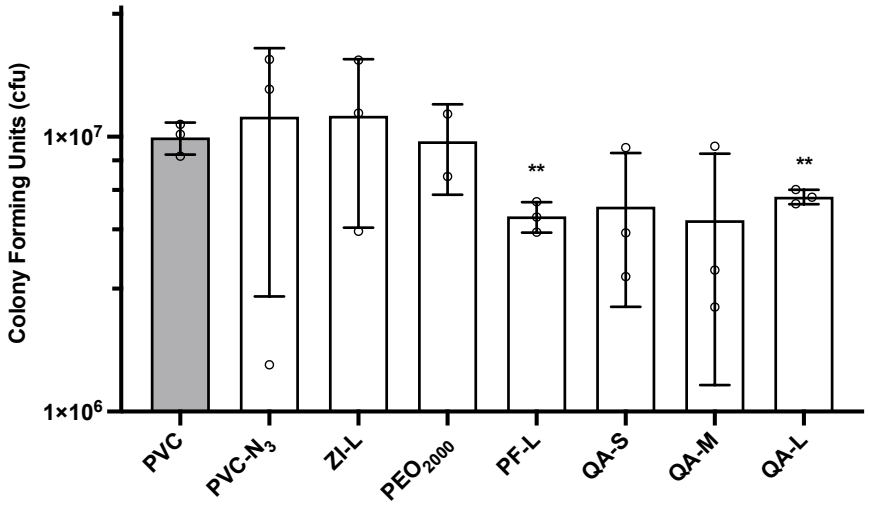

Figure 2.14: Endotracheal tube adherence assay using Pseudomonas aeruginosa, data was obtained by me under Dr. Kyle Floyd's mentorship

Bacterial adherence to unmodified (PVC) and modified endotracheal tubing, with equivalent surface areas, after 24-hour static culture at 37°C. Colony forming units (cfu) were determined by vortexing the tubing samples in 1 mL sterile PBS, after two washes with PBS, and serial dilution and plating on LB

agar medium in triplicate for each biological replicate. Data presented as the mean ± SEM of cfu determined from three tubing biological replicates. Statistical analysis: Student's *t*-Test comparing modified samples to the unmodified PVC control, PF-L $p = 0.0048$ and QA-L $p = 0.0080$.

2.7 X-Ray Photoelectron Spectroscopic Analysis

X-Ray Photoelectron Spectroscopic (XPS) analysis was performed by Dr. Monica Neuburger at Eurofins EAG Material Science in Sunnyvale, California on unmodified tubing from both sources (Vendor A and Vencor B, **Figure 2.15**) to investigate the possibility of a pre-existing antifouling coating on the surface. The walls of both tubing pieces were composed primarily of carbon (C) with low levels of chlorine (Cl) and varying amount of oxygen (O) and silicone (Si). Low to trace amounts of calcium (Ca) and zinc (Zn) were also observed (**Table 2**). The sample from Vendor A had significantly higher levels of Si and O with correspondingly lower levels of C and Cl. Silicon was found as silicone on both samples. The higher levels of Si found on the Vendor A sample indicates it had a thicker layer of silicone. A very recent clinical trial report showed silicone coated PVC endotracheal tubing is associated with lower biofilm formation compared to uncoated PVC tubing.[19] The presence of silicone coating on both commercial tubings could be the main reason that our chemically modified surfaces did not showed significant differences in antifouling properties. No real differences were observed between the carbon functionalities observed between the two commercial samples. Carbon was found primarily as hydrocarbon and/or silicone (C-C, C-H, CHx-Si) with lower levels of carbon-oxygen and carbon-chlorine

functionalities (**Table 3**). Calcium and Zn do not exhibit significant shifts in binding energy with bonding partner (i. e. chlorides, hydroxides, and/or oxides); however, the sample stoichiometry suggests they were present as chlorides, hydroxides, and/or oxides. Zn found in tubing from vendor B could possibly be ZnO and act as antifouling agent.[20] Oxygen was found incorporated as organic species on both samples found with the silicone polymer coating.

Table 2: Atomic Concentrations (in atomic %) [a, b, c]

	C	O	F	Si	Cl	Ca	Zn
vendor B	80.2	9.6	-	2.4	6.2	1.3	0.3
vendor A	63.5	20.7	-	14.0	1.5	0.2	?

[a] Normalized to 100% of the elements detected. XPS does not detect H or He.
[b] A dash line "-" indicates the element is not detected.
[c] A question mark "?" indicates species may be present at or near the detection limit of the measurement.

Table 3: Carbon and Chlorine Chemical States (in % of Total C[a] and Cl[a])

	Carbon				Chlorine	
	C-C, C-H	C-O, C-Cl	O-C=O		inorganic Cl	organic Cl
vendor B	89	8	3		43	57
vendor A	91	6	3		30	70

[a] Values in this table are percentages of the total atomic concentration of the corresponding element shown in Table 1.

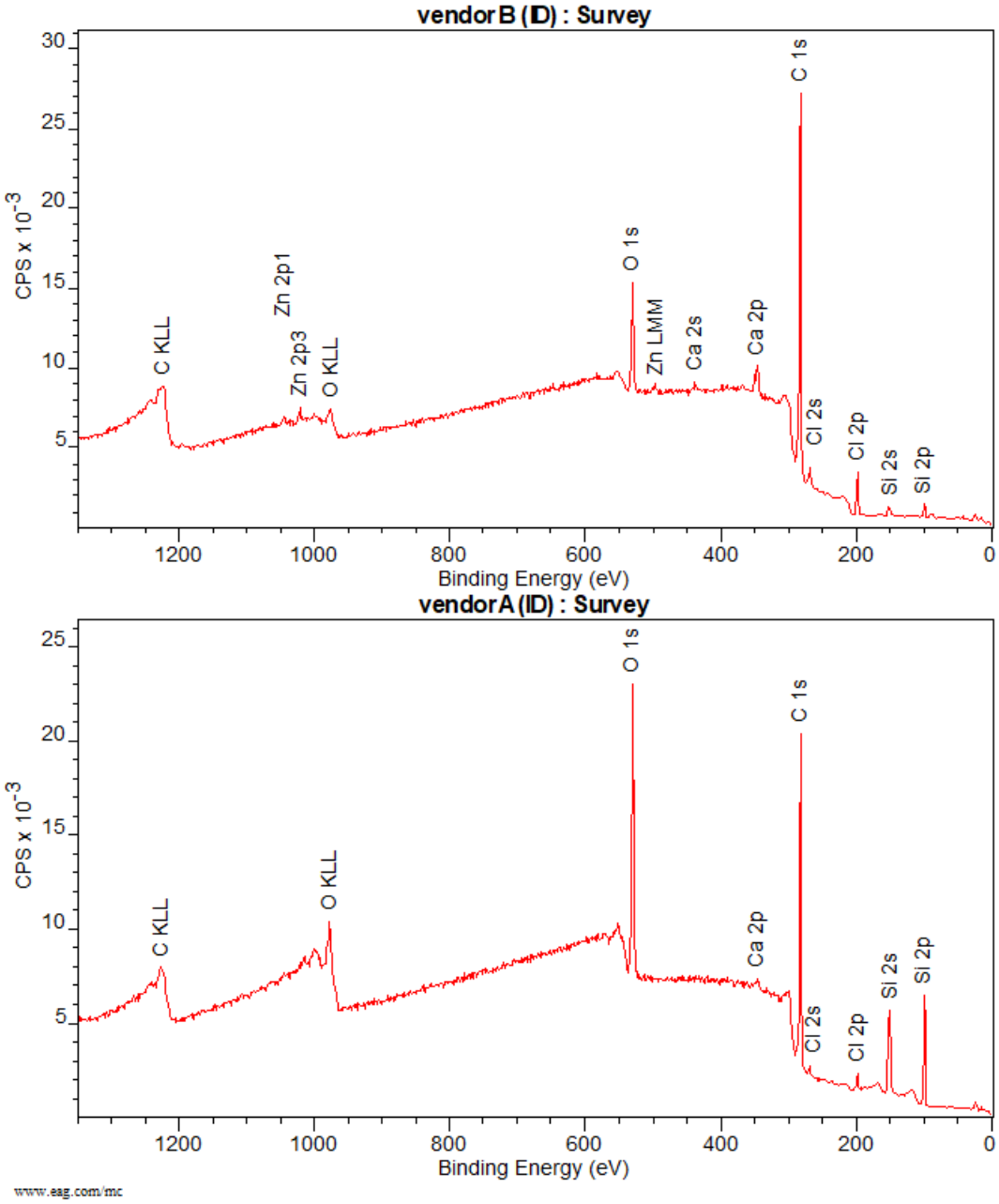

Figure 2.15: XPS of unmodified tubing from vendor B (upper) and vendor A (lower)

2.8 Conclusion

Electron-poor alkynes with different functionalities (zwitterionic, PEO, polyfluoro and quaternary amines) were synthesized and covalently attached to medical grade PVC azidized surfaces by copper-free azide-alkyne cycloaddition reaction. All the modified PVC surfaces exhibit hydrophilic properties except high polyfluoro functionalized **PF-L** compared to the unmodified tubing. All of the modified PVC surfaces maintain their wetting properties against vigorous water rinsing for 60 minutes of sonication indicating covalent bonding of the functional groups to the PVC surface. The perfluoro groups display an increase of surface roughness, especially the diester **PF-L**, while the quaternary amine functionalized samples show relatively consistent surface morphology and roughness, similar to the azido-functionalized sample. Zwitterionic samples were not repellent to *Pseudomonas aeruginosa*, whereas the other modified PVC tubings exhibit moderate bacteria repellent effects. The presence of a silicone coating on both of the un-modified tubings could be the main reason that the chemically modified surfaces did not showed large differences in antifouling properties. Further work on plasticized PVC devoid of a silicone coating is needed to clearly determine the antibacterial adhesion properties resulting from appending various functionality by thermal azide-alkyne cycloaddition onto the surface of medical grade PVC tubing.

2.9 References

1. Chen, S.; Li, L.; Zhao, C.; Zheng, J., Surface hydration: Principles and applications toward low-fouling/nonfouling biomaterials. *Polymer* **2010,** *51* (23), 5283-5293.

2. Wang, R. L. C.; Kreuzer, H. J.; Grunze, M., Molecular Conformation and Solvation of Oligo(ethylene glycol)-Terminated Self-Assembled Monolayers and Their Resistance to Protein Adsorption. *The Journal of Physical Chemistry B* **1997,** *101* (47), 9767-9773.

3. Li, L.; Chen, S.; Zheng, J.; Ratner, B. D.; Jiang, S., Protein Adsorption on Oligo(ethylene glycol)-Terminated Alkanethiolate Self-Assembled Monolayers: The Molecular Basis for Nonfouling Behavior. *The Journal of Physical Chemistry B* **2005,** *109* (7), 2934-2941.

4. Jeon, S. I.; Lee, J. H.; Andrade, J. D.; De Gennes, P. G., Protein—surface interactions in the presence of polyethylene oxide: I. Simplified theory. *Journal of Colloid and Interface Science* **1991,** *142* (1), 149-158.

5. Martínez, G., Synthesis of PVC-g-PS through stereoselective nucleophilic substitution on PVC. *Journal of Polymer Science Part A: Polymer Chemistry* **2006,** *44* (8), 2476-2486.

6. Earla, A.; Braslau, R., Covalently Linked Plasticizers: Triazole Analogues of Phthalate Plasticizers Prepared by Mild Copper-Free “Click” Reactions with Azide-Functionalized PVC. *Macromolecular Rapid Communications* **2014,** *35* (6), 666-671.

7. Jayakrishnan, A.; Sunny, M. C., Phase transfer catalysed surface modification of plasticized poly(vinyl chloride) in aqueous media to retard plasticizer migration. *Polymer* **1996,** *37* (23), 5213-5218.

8. Beveridge, J. M.; Chenot, H. M.; Crich, A.; Jacob, A.; Finn, M. G., Covalent Functionalization of Flexible Polyvinyl Chloride Tubing. *Langmuir* **2018,** *34* (35), 10407-10412.

9. Pascoal, M.; Brook, M. A.; Gonzaga, F.; Zepeda-Velazquez, L., Thermally controlled silicone functionalization using selective Huisgen reactions. *European Polymer Journal* **2015,** *69*, 429-437.

10. Starnes, W. H., Structural and mechanistic aspects of the thermal degradation of poly(vinyl chloride). *Progress in Polymer Science* **2002,** *27* (10), 2133-2170.

11. Starnes, W. H.; Ge, X., Mechanism of Autocatalysis in the Thermal Dehydrochlorination of Poly(vinyl chloride). *Macromolecules* **2004,** *37* (2), 352-359.

12. Kameda, T.; Fukuda, Y.; Grause, G.; Yoshioka, T., Chemical modification of rigid poly(vinyl chloride) by the substitution with nucleophiles. *Journal of Applied Polymer Science* **2010,** *116* (1), 36-44.

13. Cheng, Y.; Hao, J.; Lee, L. A.; Biewer, M. C.; Wang, Q.; Stefan, M. C., Thermally controlled release of anticancer drug from self-assembled γ-substituted amphiphilic poly (ε-caprolactone) micellar nanoparticles. *Biomacromolecules* **2012,** *13* (7), 2163-2173.

14. Marshall, K. C.; Bitton, G., *Adsorption of microorganisms to surfaces*. Wiley: 1980.

15. Schmidt, D. L.; Brady, R. F.; Lam, K.; Schmidt, D. C.; Chaudhury, M. K., Contact Angle Hysteresis, Adhesion, and Marine Biofouling. *Langmuir* **2004,** *20* (7), 2830-2836.

16. Erbil, H. Y., Bioadhesion to solids: contact angle hysteresis effect. **2013,** *291* (2), 355-360.

17. Cheng, Y.-Y.; Du, C.-H.; Wu, C.-J.; Sun, K.-X.; Chi, N.-P., Improving the hydrophilic and antifouling properties of poly(vinyl chloride) membranes by atom transfer radical polymerization grafting of poly(ionic liquid) brushes. *Polymers for Advanced Technologies* **2018,** *29* (1), 623-631.

18. Santos, J. C. S. d.; Barbosa, O.; Ortiz, C.; Berenguer-Murcia, A.; Rodrigues, R. C.; Fernandez-Lafuente, R., Importance of the Support Properties for Immobilization or Purification of Enzymes. *ChemCatChem* **2015,** *7* (16), 2413-2432.

19. Thorarinsdottir, H. R.; Kander, T.; Holmberg, A.; Petronis, S.; Klarin, B., Biofilm formation on three different endotracheal tubes: a prospective clinical trial. *Critical Care* **2020,** *24* (1), 382.

20. Söderberg, T. A.; Sunzel, B.; Holm, S.; Elmros, T.; Hallmans, G.; Sjöberg, S., Antibacterial effect of zinc oxide in vitro. *Scandinavian Journal of Plastic and Reconstructive Surgery and Hand Surgery* **1990,** *24* (3), 193-197.

3 Experimentals

3.1 Materials and General Methods

All reagents and solvents were used as received unless otherwise noted. Dry CH_2Cl_2 was obtained by distillation over CaH_2. Nuclear magnetic resonance (NMR) spectra were recorded on a Bruker Advance III HD four channel 500 MHz Oxford Magnet NMR spectrometer with automation. Fourier transform infrared spectra were recorded in different deuterated solvents with a PerkinElmer Spectrum One spectrometer in NaCl plates. Fourier transform infrared (FTIR) spectra were also recorded in attenuated total reflection (ATR) mode to investigate changes in chemical functional groups on the PVC tubing with a PerkinElmer Spectrum Two spectrometer. High-resolution mass spectrometry (HRMS) was recorded with a Thermo Scientific LTQ-Orbitrap Velos Pro Mass spectrometer. Medical endotracheal tubing was initially provided by our collaborator Dr. Chalongrat Daengngam (designated as vendor A, Mallinckrodt™, I. D. 7.0 mm). Later when he was unable to provide more, endotracheal tubing was obtained from Bangladesh (designated as vendor B, TornadoCare™, I. D. 7.0 mm). The physical characterization of chemically modified PVC tubing (static contact angle, surface free energy, contact angle hysteresis and AFM images) was carried out by Prof. Chalongrat Daengngm at Prince of Songkla University in Thailand. Bacterial adherence assays were performed by me in Prof. Fitnat Yildiz's lab at Microbiology and Environmental Toxicology Department at

University of California, Santa Cruz under the guidance of postdoctoral scholar Dr. Kyle Floyd. X-Ray Photoelectron Spectroscopic (XPS) analysis was performed by Dr. Monica Neuburger at Eurofins EAG Material Science in Sunnyvale, California on unmodified tubing from both sources (Vendor A and Vencor B).

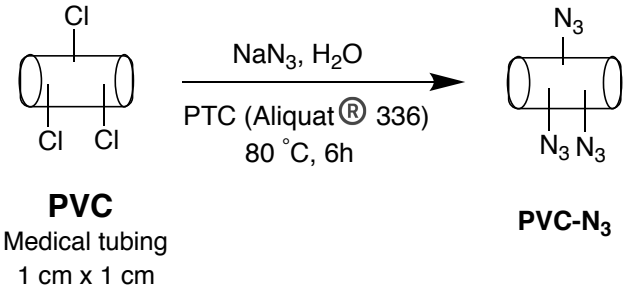

3.1.1 Surface modified PVC-N_3

Following a modified procedure of Finn,[3] sodium azide (1.180 g, 18.15 mmol), Aliquat® 336 (0.0730 g, 0.1806 mmol) and 40 mL of DI water were put in a 100 mL round bottom flask equipped with a magnetic stir bar. The reaction flask was submerged into an oil bath at 80 °C. After 20 minutes, 10 small pieces of PVC endotracheal tubing (TornadoCare™, 1cm x 1cm each) were added to the reaction mixture and stirred at 80 °C. After 6 hours, the liquid was removed, and the PVC pieces were washed several times with DI water. The surface modified **PVC-N_3** tubing pieces were dried in an oven at 45 °C for 24 hours. ATR-FTIR confirmed the presence of the distinct azide peak (2106 cm^{-1}) on the PVC surface.

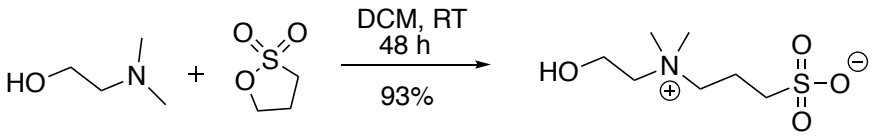

2.51

Preparation of 3-[Dimethyl-(2-hydroxyethyl)ammonio]-1-propanesulfonate (2.51)[4]

Dimethylamino-1-ethanol (3.649 g, 40.94 mmol) and 1,3-propane sultone (5.000 g, 40.94 mmol) were dissolved in 30 mL of dichloromethane (DCM) at room temperature. Crystals started to appear after 10 minutes. The reaction mixture was covered and allowed to stand. After 2 days, the reaction mixture was diluted with 50 mL of DCM and the liquid removed by vacuum filtration. The solid was washed with 200 mL of DCM, transferred into a beaker, suspended into 2-propanol and washed with 3 x 100 mL of 2-propanol under vacuum filtration. To remove trace amounts of 2-propanol, the solid was then washed with 100 mL of diethyl ether and dried under vacuum and then oven dried at 45 °C for 24 hours. The product was obtained as a white crystalline solid (8.112 g, 93.91% yield).

Melting point: 244-248 °C.

IR (Nujol): 3293 (br), 2922 (s), 1460 (s), 1376 cm^{-1}.

^{1}H NMR (500 MHz, D_2O): δ 4.00-3.95 (m, 2H), 3.50-3.44 (m, 4H), 3.11 (s, 6H), 2.91 (t, *J* = 5 Hz, 2H) ppm.

^{13}C NMR (125 MHz, D_2O, DEPT): δ 65.1 (CH_2), 63.4 (CH_2), 55.3 (CH_2), 51.4 (2XCH_3), 47.3 (CH_2), 18.2 (CH_2) ppm.

HRMS: m/z calculated for $C_7H_{18}NO_4S$ $[M+H]^+$ 212.0951, found 212.0951.

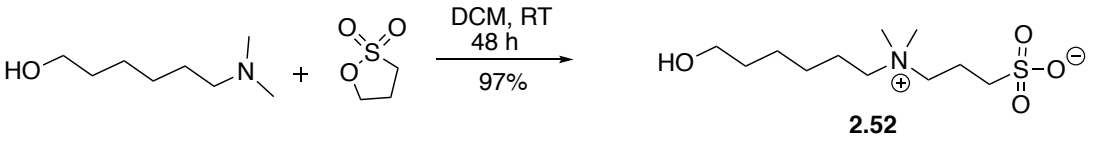

2.52

Preparation of 3-[Dimethyl-(6-hydroxyhexyl)-ammonio]-1-propanesulfonate (2.52)

Following the similar procedure to make **2.51**, dimethylamino-1-hexanol (1.000 g, 6.885 mmol) and 1,3-propane sultone (0.8410 g, 6.891 mmol) were dissolved into 15 mL of dichloromethane (DCM) at room temperature. Crystals started to appear after 15 minutes. The reaction mixture was covered and allowed to stand. After 3 days, 30 mL of DCM was added and the liquid was removed by vacuum filtration. The solid was washed with an additional 200 mL of DCM, 3 x 100 mL of 2-propanol, 100 mL of diethyl ether, and oven dried at 45 °C for 24 hours. The product was obtained as white crystalline solid (1.790 g, 97.28% yield).

Melting point: 180-182 °C.

IR (Nujol): 3392 (br), 2922 (s), 1448 (s), 1376 (s) cm^{-1}.

^1H NMR (500 MHz, D_2O): δ 3.54 (t, *J* = 5 Hz, 2H), 3.40 (t, *J* = 5 Hz, 2H), 3.27 (t, *J* = 5 Hz, 2H), 3.03 (s, 6H), 2.92 (t, *J* = 5 Hz, 2H,), 2.19-2.12 (m, 2H), 1.78-1.68 (m, 2H), 1.55-1.47 (m, 2H), 1.39-1.30 (m, 4H) ppm.

^{13}C NMR (125 MHz, D_2O, DEPT): δ 62.2 (CH_2), 62.0 (CH_2), 61.5 (CH_2), 50.5 (2 x CH_3), 47.2 (CH_2), 30.9 (CH_2), 25.2 (CH_2), 24.4 (CH_2), 21.7 (CH_2), 18.1 (CH_2) ppm.

HRMS: m/z calculated for $C_{11}H_{26}NO_4S$ $[M+H]^+$ 268.1577, found 268.1575.

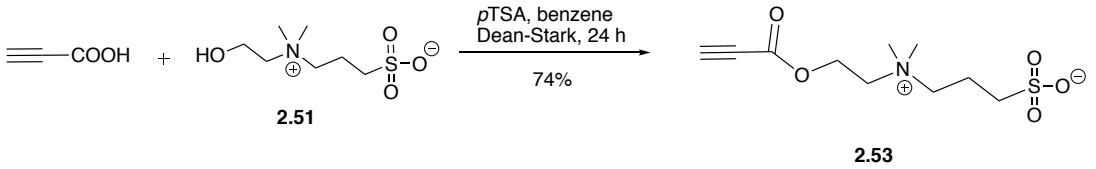

Preparation of 2-propynoic acid, 3′-[dimethyl-(2-ethyl)ammonio]- 1′-propanesulfonate ester (2.53)

Propiolic acid (0.6630 g, 9.465 mmol), 3-[Dimethyl-(2-hydroxyethyl)ammonio]-1-propanesulfonate (**2.51**) (0.2000 g, 0.9466 mmol), *p*-toluenesulfonic acid monohydrate (*p*-TSA) (0.0111 g, 0.0584 mmol) and 5 mL of benzene were put in a 15mL round bottom flask and refluxed at 90 °C for 24 hours with a Dean Stark apparatus. The reaction mixture was cooled, concentrated, poured into a mortar and triturated with 5 x 50 mL of diethyl ether. The product was isolated as a light brown powder (0.1830 g, 73.49% yield).

Melting point: 199-205 °C.

IR (Nujol): 2922 (s), 2107 (m), 1711 (s), 1460 (s), 1376 (s) cm^{-1}.

^1H NMR (500 MHz, D_2O): δ 4.63-4.56 (s, 2H), 3.75-3.71 (s, 2H), 3.65 (s, 1H), 3.51-3.46 (m, 2H), 3.13 (s, 6H), 2.93-2.89 (m, 2H), 2.21-2.16 (m, 2H) ppm.

^{13}C NMR (125 MHz, D_2O, DEPT): δ 152.9 (4°), 78.9 (CH), 73.2 (4°), 63.4 (CH_2), 61.7 (CH_2), 59.5 (CH_2), 51.4 (2XCH_3), 47.3 (CH_2), 18.3 (CH_2) ppm.

HRMS: m/z calculated for $C_{10}H_{18}NO_4S$ $[M+H]^+$ 264.0900, found 264.0900.

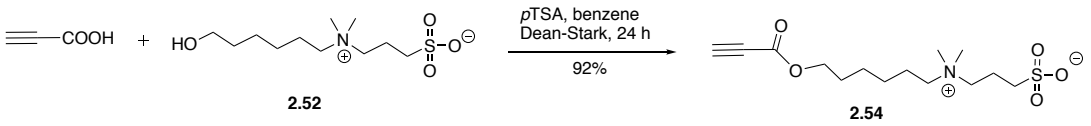

Preparation of 2-propynoic acid, 3′-[dimethyl-(6-ethyl)ammonio]-1′-propanesulfonate ester (2.54)

Propiolic acid (3.484 g, 49.74 mmol), 3-[dimethyl-(6-hydroxyhexylyl)ammonio]-1-propanesulfonate (**2.52**) (1.332 g, 4.982 mmol), *p*-toluene sulfonic acid monohydrate (*p*-TSA) (0.0570 g, 0.2985 mmol) and 15 mL of benzene were put in a 100 mL round bottom flask and refluxed at 90 °C for 24 hours with a Dean Stark apparatus. The reaction mixture was cooled, concentrated and poured into a mortar and triturated with 5 x 50mL of diethyl ether. The product was isolated as light brown powder (1.460 g, 92.41% yield).

Melting point: 100-106 °C.

IR (Nujol): 2931 (s), 2103 (m), 1714 (s), 1462 (s), 1374 (s) cm^{-1}.

^{1}H NMR (500 MHz, D_2O): δ 4.24-4.17 (t, 2H), 3.40 (s, 1H), 3.42-3.38 (m, 2H), 3.29-3.25 (m, 2H), 3.04 (s, 6H), 2.94-2.89 (t, 2H), 2.18-2.13 (m, 2H), 1.75-1.60 (m, 4H), 1.43-1.32 (m, 4H) ppm.

^{13}C NMR (125 MHz, D_2O, DEPT): δ 154.55 (4°), 77.54 (CH), 73.9 (4°), 67.22 (CH_2), 64.15 (CH_2), 62.08 (CH_2), 50.56 (2XCH_3), 47.28 (CH_2), 27.22 (CH_2), 25.00 (CH_2), 24.50 (CH_2), 21.70 (CH_2), 18.15 (CH_2) ppm.

HRMS: m/z calculated for $C_{14}H_{26}NO_5S$ $[M+H]^+$ 320.1527, found 320.1526.

3.1.2 Attachment of zwitterionic functionalities to PVC surface by thermal azide-alkyne cycloaddition

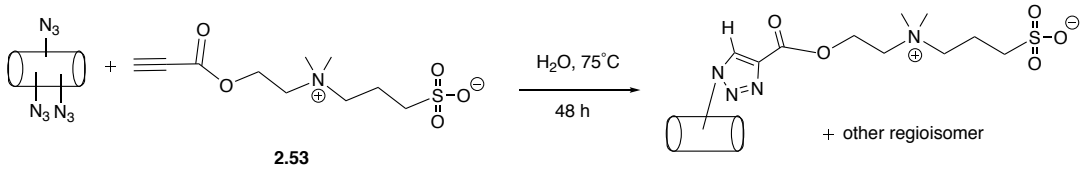

PVC surface modified by zwitterionic 2-propynoic acid, 3′-[dimethyl-(2-ethyl)ammonio]- 1′-propanesulfonate ester (PVC-ZI-S)

2-propynoic acid, 3′-[dimethyl-(2-ethyl)ammonio]- 1′-propanesulfonate ester (**2.53**) (0.2200 g, 0.8355 mmol) was dissolved in 2 mL of water, and PVC-N_3 tubing (1 cm x 1cm) was added and the reaction mixture was heated at 75 °C. Reaction progress was monitored by ATR-FTIR (disappearance of the azide peak at 2106 cm^{-1}). After 48 hours, the piece of tubing was removed from reaction mixture and washed several times with DI water. The modified PVC tubing with **z**witter**i**onic functionality **s**mall chain spacing (two carbon) "**PVC-ZI-S**" was dried in an oven at 45 °C for 24 hours.

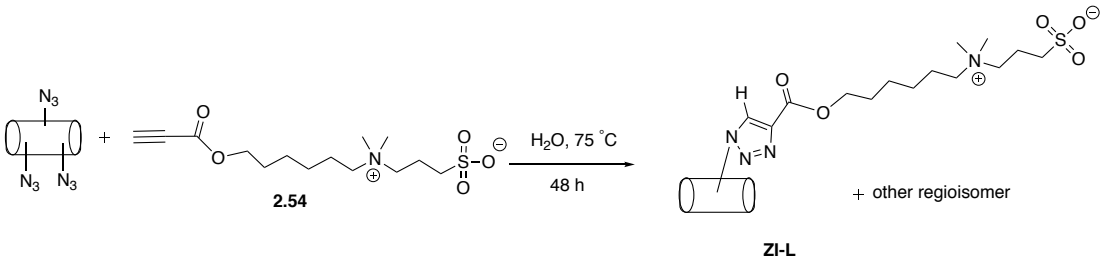

PVC surface modified by zwitterionic 2-propynoic acid, 3′-[dimethyl-(6-ethyl)ammonio]-1′-propanesulfonate ester (PVC-ZI-L)

2-Propynoic acid, 3′-[dimethyl-(6-ethyl)ammonio]-1′-propanesulfonate ester **2.54** (0.2300 g, 0.7201 mmol) was dissolved in 2 mL of water and PVC-N_3 (1 cm x 1 cm) was added to the reaction mixture and heated at 75 °C. Reaction progress was monitored by ATR-FTIR (disappearance of the azide peak at 2106 cm^{-1}). After 48 hours, the piece of tubing was removed and washed several times with DI water. The modified PVC tubing with **z**witter**i**onic functionality **l**ong chain spacing (six carbon) "**PVC-ZI-L**" was dried in an oven at 45 °C for 24 hours.

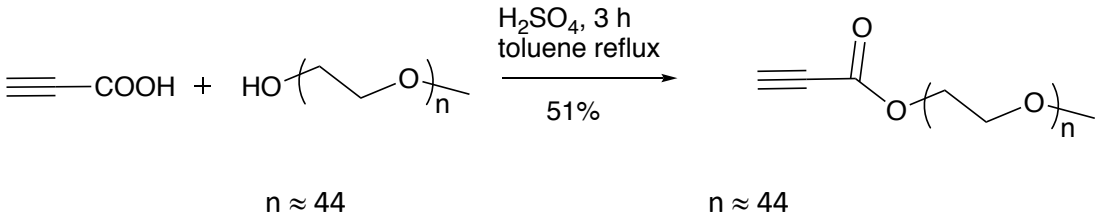

Preparation of methoxy poly(ethylene glycol) 2000 prop-2-ynoate (**PEO_{2000}**)

Following a modified procedure of Higa,[5] propiolic acid (2.100 g, 30.00 mmol), methoxy poly(ethylene glycol) 2000 (20.00 g, 10.00 mmol), 6 drops of concentrated

sulfuric acid and 40 mL of toluene were put in a 250 mL round bottom flask. The reaction mixture was stirred at reflux for 3 hours, concentrated in *vacuo* and diluted with 100 mL of ethyl acetate. The solution was transferred to a 500 mL separatory funnel and washed with 2 x 25 mL of saturated sodium bicarbonate ($NaHCO_3$) solution. The aqueous layer was separated and extracted with 2 x 100 mL of ethyl acetate. The combined organic layer was dried over $MgSO_4$ and concentrated. The product was isolated as an off-white colored waxy solid of varying chain length (10.52 g, 51.26%).

^{1}H NMR (500 MHz, $CDCl_3$): δ 4.04-4.02 (m, 2H), 3.57-3.20 (m, 176H), 3.13-3.10 (m, 4H), 3.08 (s, 1H) ppm.

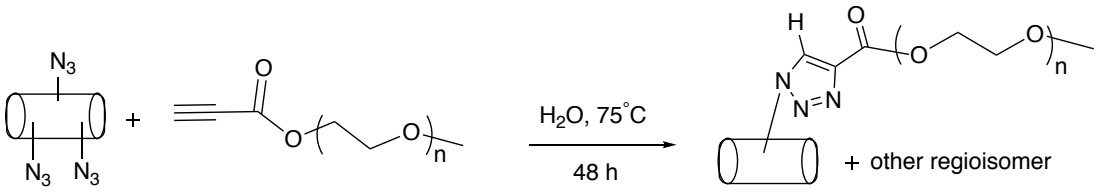

n ≈ 44 **PEO_{2000}**

3.1.3 Surface modified by methoxy poly(ethylene glycol) 2000 prop-2-ynoate (PVC-PEO_{2000})

Methoxy poly(ethylene glycol) 2000 prop-2-ynoate (PEO_{2000}) (1.252 g, 0.6181 mmol) was dissolved in 2 mL of water and a piece of PVC-N_3 tubing (1 cm x 1 cm) was added to the reaction mixture and heated at 75 °C. Reaction progress was monitored

by ATR-FTIR (disappearance of the azide peak at 2106 cm^{-1}). After 48 hours, the piece of tubing was removed and washed several times with DI water. The modified PVC tubing with **p**oly(**e**thylene glyc**o**l) 2000 prop-2-ynoate (**PEO_{2000}**) was dried in an oven at 45 °C for 24 hours.

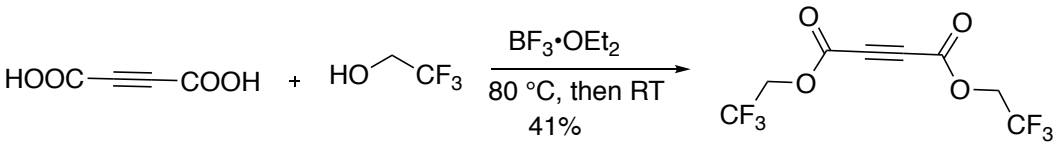

2.56

Preparation of 2-butynedioic acid, 1,4-bis(2,2,2-trifluoroethyl) ester (2.56)

Following a modified procedure of Weaver,[6] acetylene dicarboxylic acid (2.000 g, 17.54 mmol), 2,2,2-trifluoroethanol (17.54 g, 175.3 mmol) and BF_3•OEt_2 (5.226 g, 4.6 mL, 36.8226 mmol) were put in a 100 mL round bottom flask with a reflux condenser and heated at 80 °C for 5 hours and stirred at room temperature overnight. The reaction mixture was diluted with 100 mL of diethyl ether, washed with 5 x 50 mL of water and 50 mL of brine. The organic layer was dried with sodium sulphate and concentrated. The resulting crude product was purified by silica gel chromatography (hexanes : diethyl ether = 9 : 1) to provide the product as a colorless liquid (2.03 g, 40.7%).

TLC: 90:10 hexanes/diethyl ether, UV, yellow with $KMnO_4$ stain, R_f = 0.43.

IR (Nujol): 2987 (m), 1746 (s), 1410 (m), 1297 (s), 1238 (s), 1297 (s), 1164 (s) cm^{-1}.

^{1}H NMR (500 MHz, $CDCl_3$): δ 4.68-4.59 (q, J = 5 Hz, 4H) ppm.

^{13}C NMR (125 MHz, $CDCl_3$): δ 149.6 (4 °), 123.1 (q, $^{1}J_{C\text{-}F}$ = 240 Hz, CF_3), 75.0 (4 °), 61.7 (q, $^{2}J_{C\text{-}F}$ = 32 Hz, CH_2) ppm.

^{19}F NMR (470 MHz, $CDCl_3$): δ -73.6 (CF_3) ppm.

HRMS: m/z calculated for $C_8H_5F_6O_4$ $[M+H]^+$ 279.0087, found 279.0114.

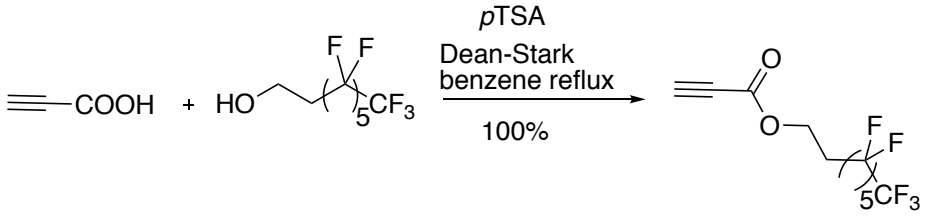

2.57

Preparation of 2-propyonic acid, 3,3,4,4,5,5,6,6,7,7,8,8,8-tridecafluoro-1-*n*-octanyl ester (2.57)

Propiolic acid (0.3000 g, 4.283 mmol), 3,3,4,4,5,5,6,6,7,7,8,8,8-tridecafluoro-1-*n*-octanol (1.715 g, 4.711 mmol) and para-toluene sulfonic acid monohydrate (0.0814 g, 0.4279 mmol) and 10 mL of benzene were put in a 100 mL round bottom flask with a reflux condenser and refluxed for 24 hours. After cooling the reaction mixture was diluted with 100 mL of diethyl ether, washed with 3 x 30 mL of water and 30 mL of brine. The organic layer was dried with sodium sulphate and concentrated. The resulting crude product was purified by silica gel chromatography (hexanes : diethyl ether = 9 : 1) to give the product as a colorless liquid (1.782 g, 99.98% yield).

TLC: 90 : 10 hexanes/diethyl ether, UV, yellow with $KMnO_4$ stain, R_f = 0.53.

IR (Nujol): 3284 (m), 2129 (m), 1720 (s), 1232 (s), 1142 (s) cm^{-1}.

^1H NMR (500 MHz, $CDCl_3$): δ 4.51 (t, *J* = 5.0 Hz, 2H), 2.95 (s, 1H), 2.60-2.50 (m, 2H) ppm.

^{13}C NMR (125 MHz, $CDCl_3$, DEPT): δ 152.0 (4°), 75.6 (CH), 73.9 (4°), 57.8 (CH_2), 30.2 (t, $^2J_{C-F}$ = 20 Hz, CH_2) ppm.

^{19}F NMR (470 MHz, $CDCl_3$): δ -81.0 (CF_3), -113.7 (CF_2), -122.0 (CF_2), -123.0 (CF_2), -123.7 (CF_2), -126.3 (CF_2) ppm.

HRMS: m/z calculated for $C_{11}H_6F_{13}O_2$ $[M+H]^+$ 417.0155, found 417.0157.

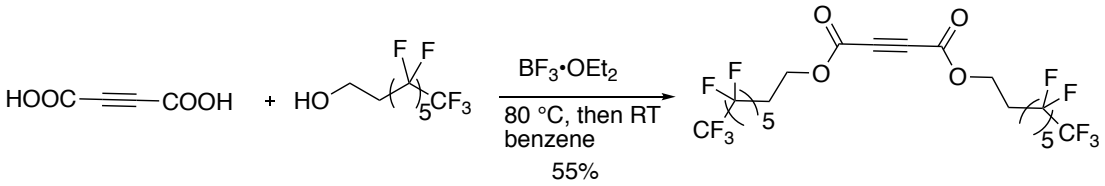

2.58

Preparation of 2-butynedioic acid, 1,5-bis(3,3,4,4,5,5,6,6,7,7,8,8,8-tridecafluoroctayl) ester (2.58)

Following a modified procedure of Weaver,[6] acetylene dicarboxylic acid (2.000 g, 17.54 mmol), 3,3,4,4,5,5,6,6,7,7,8,8,8-tridecafluoro-1-*n*-octanol (17.15 g, 52.61 mmol) and $BF_3.OEt_2$ (5.226 g, 4.55 mL, 36.82 mmol) were put in a 100 mL round bottom flask with a reflux condenser and heated at 80 °C for 6 hours and then stirred at room temperature overnight. The reaction mixture was diluted with 100 mL of

diethyl ether, washed with 5 x 50 mL of water and 50 mL of brine. The organic layer was dried with sodium sulphate and concentrated. The resulting crude product was purified by silica gel chromatography (hexanes : diethyl ether = 4 : 1) to give the product as a white crystalline solid (7.918 g, 56.01% yield).

TLC: 80:20 hexanes/diethyl ether, UV, yellow with $KMnO_4$ stain, R_f = 0.33.

Melting point: 52-53 °C.

IR (Nujol): 2913 (s), 1733 (s), 1458 (s), 1378 (s), 1292 (s), 1144 (s) cm^{-1}.

^1H NMR (500 MHz, $CDCl_3$): δ 4.57 (t, *J* = 5.0 Hz, 2H), 2.63-2.52 (m, 2H) ppm.

^{13}C NMR (125 MHz, $CDCl_3$, DEPT): δ 151.0 (4°), 74.7 (4°), 58.6 (CH_2), 30.3 (CH_2) ppm.

^{19}F NMR (470 MHz, $CDCl_3$): δ -81.3 (CF_3), -113.9 (CF_2), -122.1 (CF_2), -123.2 (CF_2), -123.8 (CF_2), -126.5 (CF_2) ppm.

HRMS: m/z calculated for $C_{20}H_9F_{26}O_4$ $[M+H]^+$ 807.0080, found 807.0078.

3.1.4 Attachment of polyfluoro functionalities to PVC surface by thermal azide-alkyne cycloaddition

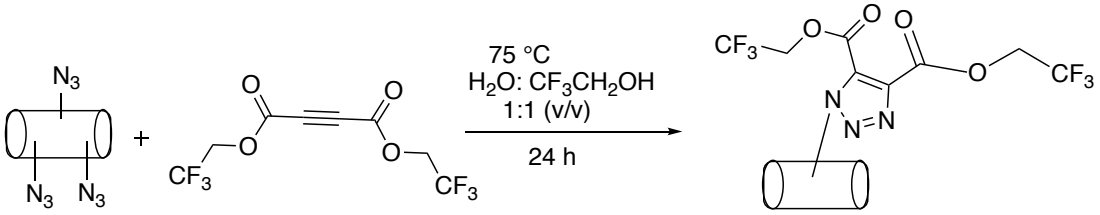

2.56 **PF-S**

PVC surface modified by 2-butynedioic acid,1,4-bis(2,2,2-trifluoroethyl) ester (2.56) (**PF-S**)

2-butynedioic acid,1,4-bis(2,2,2-trifluoroethyl) ester (**2.56**) (2.000 g, 7.192 mmol) was dissolved in 5 mL of 2,2,2-trifluoroethanol and 5 mL of water. PVC-N_3 tubing (5 pieces, 1 cm x 1 cm each) were added to the reaction mixture and heated at 75 °C. Reaction progress was monitored by ATR-FTIR (disappearance of the azide peak at 2106 cm^{-1}). After 24 hours, the pieces of tubing were removed and washed several times with DI water. The modified PVC tubing was named as **p**oly**f**luoro with **s**mall fluorine functionality "**PF-S**" and dried in an oven at 45 °C for 24 hours.

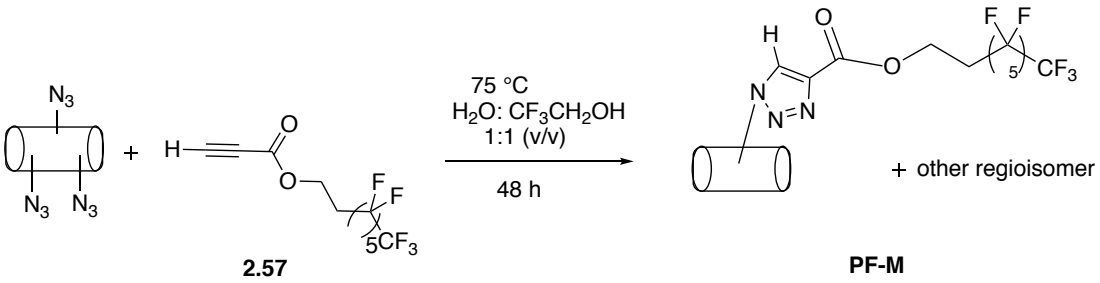

PVC surface modified by 2-propynoic acid, 3,3,4,4,5,5,6,6,7,7,8,8,8-tridecafluoro-1-*n*-octanyl ester (2.57) (**PF-M**)

2-Propynoic acid, 3,3,4,4,5,5,6,6,7,7,8,8,8-tridecafluoro-1-*n*-octanyl ester (**2.57**) (2.422 g, 5.820 mmol) was dissolved in 7 mL of 2,2,2-trifluoroethanol and 7 mL of water. PVC-N_3 tubing (5 pieces, 1 cm x 1 cm each) was added to the reaction mixture and heated at 75 °C. Reaction progress was monitored by ATR-FTIR (disappearance of

the azide peak at 2106 cm^{-1}). After 48 hours, the pieces of tubing were removed and washed several times with DI water. The modified PVC tubing was named as **p**oly**f**luoro with **m**edium fluorine functionality "**PF-M**" and dried in an oven at 45 °C for 24 hours.

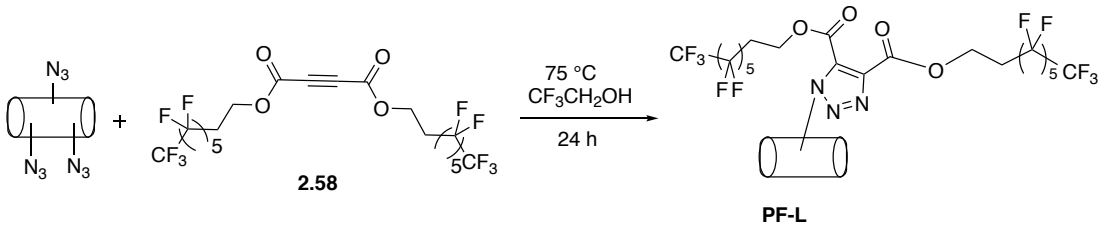

PVC surface modified by 2-butynedioic acid, 1,5-bis(3,3,4,4,5,5,6,6,7,7,8,8,8-tridecafluorooctyl) ester (2.58) (PF-L)

2-Butynedioic acid, 1,5-bis(3,3,4,4,5,5,6,6,7,7,8,8,8-tridecafluorooctayl) ester (**2.58**) (3.000 g, 3.721 mmol) was dissolved in 10 mL of 2,2,2-trifluoroethanol. PVC-N_3 tubing (5 pieces, 1 cm x 1 cm each) were added to the reaction mixture and heated at 75 °C. Reaction progress was monitored by ATR-FTIR (disappearance of the azide peak at 2106 cm^{-1}). After 24 hours, the pieces of tubing were removed and washed several times with DI water, and dried in an oven at 45 °C for 24 hours. The modified PVC tubing was named **p**oly**f**luoro **l**arge fluorous group "**PF-L**".

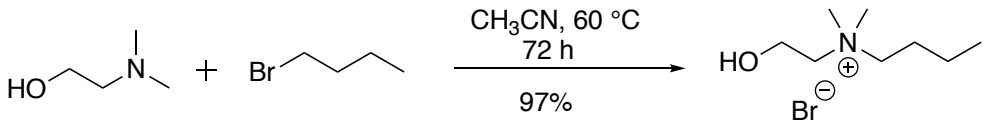

2.59

Preparation of *N*-butyl-*N*-(2-hydroxyethyl)-*N*,*N*-dimethylammonium bromide (2.59)

Following a modified procedure of Ventura,[7] *N*,*N*-dimethylaminoethanol (4.100 g, 45.99 mmol) was placed in a 48 ml Ace pressure tube in 10 mL of anhydrous acetonitrile. 1-Bromo-butane (6.302 g, 45.99 mmol) was added slowly to the reaction mixture, the tube securely capped and then heated in an oil bath at 60 °C. After 72 hours the reaction mixture was concentrated, and washed three times with 30 mL of diethyl ether. After evaporating solvent, the product was obtained as a white crystalline solid (10.20 g, 98.08 % yield).

Melting point: 112-114 °C.

IR (Nujol): 3219 (s), 2931 (s), 1466 (s), 1376 (s), 1047 (s), 920 (s) cm^{-1}.

^{1}H NMR (500 MHz, D_2O): δ 3.98 (s, 2H), 3.43 (t, *J* = 5.0 Hz, 2H), 3.34-3.29 (m, 2H), 3.07 (s, 6H), 1.75-1.67 (m, 2H), 1.37-1.27 (m, 2H), 0.89 (t, *J* = 5.0 Hz, 3H) ppm.

^{13}C NMR (125 MHz, D_2O): δ 65.3 (CH_2), 64.8 (CH_2), 55.3 (CH_2), 51.3 (2 x CH_3), 23.9 (CH_2), 19.0 (CH_2), 12.7 (CH_3) ppm.

HRMS: m/z calculated for $C_8H_{21}BrNO$ $[M+H]^+$ 226.0802, found 226.0777.

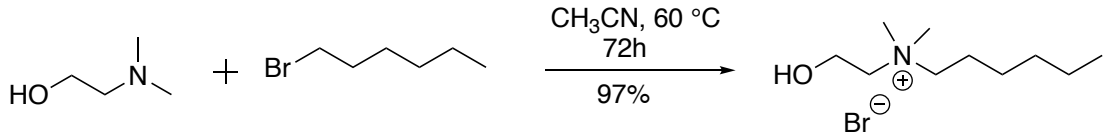

2.61

Preparation of *N*-hexyl-*N*-(2-hydroxyethyl)-*N*,*N*-dimethylammonium bromide (2.61)

Following a modified procedure of Ventura,[7] *N*,*N*-dimethylaminoethanol (4.100 g, 45.99 mmol) was placed in a 48 ml Ace pressure tube in 10 mL of anhydrous acetonitrile. 1-Bromo-hexane (7.593 g, 45.99 mmol) was added slowly to the reaction mixture, the tube was securely capped and heated in an oil bath at 60 °C. After 72 hours the reaction mixture was concentrated and washed two times with 30 mL of diethyl ether. After removing the solvent by evaporation, the product was obtained as a clear oil (11.22 g, 95.98% yield).

IR (Neat): 3366 (s), 2926 (s), 1462 (s), 1380 (s), 1088 (s) cm^{-1}.

^{1}H NMR (500 MHz, $CDCl_3$): δ 4.07 (s, 2H), 3.73-3.68 (m, 2H), 3.58-52 (m, 2H), 3.34 (s, 6H), 1.39-1.23 (m, 6H), 1.37-1.27 (m, 2H), 0.85 (t, *J* = 5.0 Hz, 3H) ppm.

^{13}C NMR (125 MHz, $CDCl_3$, DEPT): δ 66.0 (CH_2), 65.5 (CH_2), 55.8 (CH_2), 52.1 (2 x CH_3), 31.2 (CH_2), 25.8 (CH_2), 22.7 (CH_2), 22.3 (CH_2), 13.9 (CH_3) ppm.

HRMS: m/z calculated for $C_{10}H_{25}BrNO$ $[M+H]^+$ 254.1114, found 254.1114.

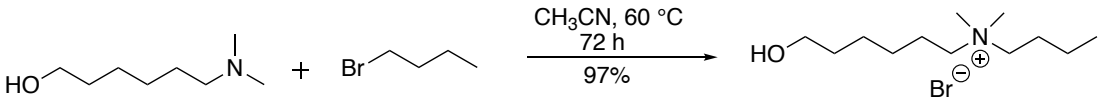

2.63

Preparation of *N*-butyl-*N*-(6-hydroxyhexyl)-*N*,*N*-dimethylammonium bromide (2.63)

N,*N*-Dimethylamino-1-hexanol (3.180 g, 21.89 mmol) was placed in a 48 ml Ace pressure tube in 10 mL of anhydrous acetonitrile. 1-Bromo-butane (3.000 g, 21.89 mmol) was added slowly to the reaction mixture, the tube was securely capped and heated in an oil bath at 60 °C. After 72 hours the reaction was concentrated and washed two times with 50 mL of diethyl ether. The product was obtained as a clear oil (6.071 g, 98.22% yield).

IR (Neat): 3383 (s), 2939 (s), 1636 (s), 1486(s), 1058 (s) cm^{-1}.

^{1}H NMR (500 MHz, CD_3OD): δ 3.61-3.57 (t, *J* = 5.0 Hz, 2H), 3.39-3.33 (m, 4H), 3.12 (s, 6H), 1.85-1.73 (m, 4H), 1.63-1.56 (m, 2H), 1.53-1.40 (m, 6H), 1.05 (t, *J* = 5.0 Hz, 3H) ppm.

^{13}C NMR (125 MHz, CD_3CN, DEPT): δ 63.7 (CH_2), 63.5 (CH_2), 60.8 (CH_2), 50.4 (2 x CH_3), 32.2 (CH_2), 25.7 (CH_2), 25.1 (CH_2), 24.1 (CH_2), 22.1 (CH_2), 19.3 (CH_2), 13.0 (CH_3) ppm.

HRMS: m/z calculated for $C_{12}H_{29}BrNO$ $[M+H]^+$ 282.1428, found 282.1265.

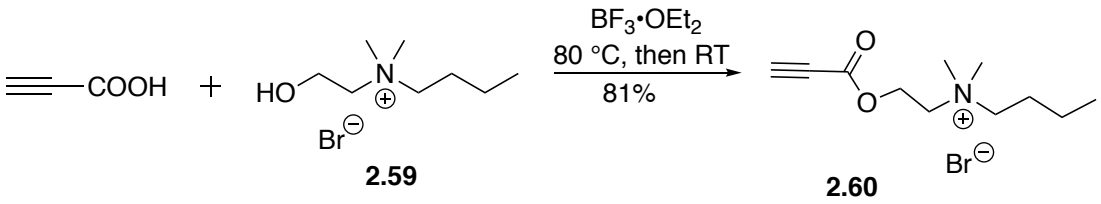

Preparation of 2-propynoic acid, 5-*N*-butyl-*N*-ethyl-*N*,*N*-dimethylammonium bromide ester (2.60)

Propiolic acid (8.006 g, 114.2 mmol), *N*-butyl-*N*-(2-hydroxyethyl)-*N*,*N*-dimethylammonium bromide (**2.59**) (5.170 g, 22.86 mmol), and boron trifluoride diethyl etherate (9.7 g, 8.5 mL, 69 mmol) were put in a 250 mL round bottom flask. The reaction mixture was stirred at 80 °C for 6 hours, and then allowed to stir overnight at room temperature. The reaction mixture was cooled and poured into a mortar and triturated with 5 x 50 mL of diethyl ether. The product was isolated as a light brown thick oil (5.193 g, 81.78% yield).

IR (Nujol): 3258 (s), 2969 (s), 2116 (s), 1722 (s), 1617 (s), 1484 (s), 1232 (s), 1026 (s) cm^{-1}.

^{1}H NMR (500 MHz, CD_3CN): δ 4.55 (s, 2H), 3.62 (t, *J* = 5.0 Hz, 2H), 3.56 (s, 1H), 3.34-3.28 (m, 2H), 3.08 (s, 6H), 1.77-1.69 (m, 2H), 1.43-1.34 (m, 2H), 0.99 (t, *J* = 5.0 Hz, 3H) ppm.

^{13}C NMR (125 MHz, CD_3CN, DEPT): δ 151.5 (4°), 77.3 (4°), 73.5 (CH), 65.0 (CH_2), 61.6 (CH_2), 59.2 (CH_2), 51.2 (2 x CH_3), 24.0 (CH_2), 19.1 (CH_2), 12.8 (CH_3) ppm.

HRMS: m/z calculated for $C_{11}H_{21}BrNO_2$ $[M+H]^+$ 278.0751, found 278.0746.

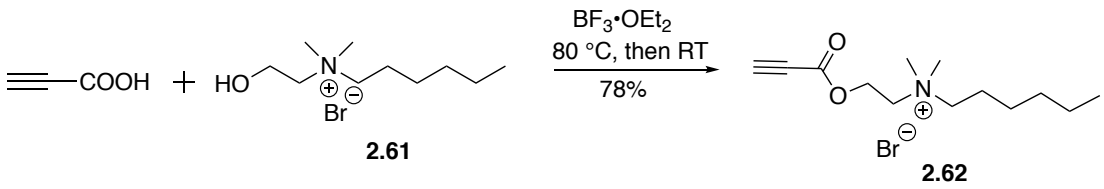

Preparation of 2-propynoic acid, 5-*N*-hexyl-*N*-ethyl-*N*,*N*-dimethylammonium bromide ester (2.62)

Propiolic acid (0.7285 g, 10.40 mmol), *N*-hexyl-*N*-(2-hydroxyethyl)-*N*,*N*-dimethylammonium bromide (**2.61**) (0.5282 g, 2.080 mmol), and boron trifluoride diethyl etherate (0.88 g, 0.77 mL, 6.2 mmol) were put in a 100 mL of round bottom flask. The reaction mixture was stirred at 80 °C for 8 hours, and then allowed to stir overnight at room temperature. The reaction mixture was cooled and poured into a mortar and triturated with 5 x 40 mL of diethyl ether. The product was isolated as a light brown thick oil (0.4902 g, 77.04% yield).

IR (Nujol): 3228 (s), 2926 (s), 2112 (s), 1726 (s), 1462 (s), 1245 (s), 1064 (s) cm^{-1}.

^{1}H NMR (500 MHz, CD_3OD): δ 4.66 (s, 2H), 3.95 (s, 1H), 3.79-3.73 (m, 2H), 3.45-3.38 (m, 2H), 3.18 (s, 6H), 1.87-1.76 (m, 2H), 1.46-1.35 (m, 6H), 0.99-0.93 (m, 3H) ppm.

^{13}C NMR (125 MHz, CD_3OD, DEPT): δ 151.5 (4°), 77.4 (4°), 73.5 (CH), 65.1 (CH_2), 61.5 (CH_2), 58.8 (CH_2), 50.5 (2 x CH_3), 30.9 (CH_2), 25.5 (CH_2), 22.2 (CH_2), 22.1 (CH_2), 12.8 (CH_3) ppm.

HRMS: m/z calculated for $C_{13}H_{24}BrNO_2$ $[M+H]^+$ 306.1061, found 306.1057.

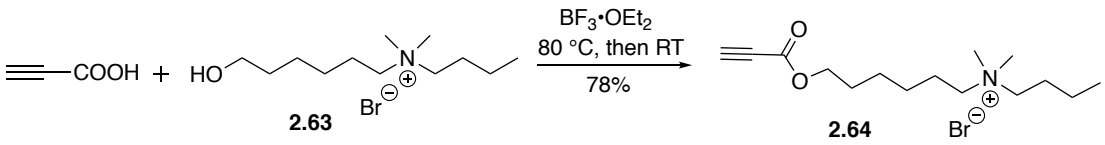

Preparation of 2-propynoic acid, 5-*N*-butyl-*N*-hexyl-*N*,*N*-dimethylammonium bromide ester (2.64)

Propiolic acid (7.829 g, 111.8 mmol), *N*-butyl-*N*-(2-hydroxyethyl)-*N*,*N*-dimethylammonium bromide (**2.63**) (6.310 g, 22.35 mmol), and boron trifluoride diethyl etherate (9.5 g, 8.3 mL, 67 mmol) were put in a 250 mL of round bottom flask. The reaction mixture was stirred at 80 °C for 8 hours, and then allowed to stir overnight at room temperature. The reaction mixture was cooled and poured into a mortar and triturated with 5 x 70 mL of diethyl ether. The product was isolated as a light brown thick oil (7.101 g, 95.06% yield).

IR (Neat): 3251 (s), 2952 (s), 2112 (s), 1709 (s), 1628 (s), 1486 (s), 1245 (s), 1069 (s) cm^{-1}.

^{1}H NMR (500 MHz, CD_3OD): δ 4.55 (s, 2H), 3.62 (t, *J* = 5.0 Hz, 2H), 3.56 (s, 1H), 3.34-3.28 (m, 2H), 3.08 (s, 6H), 1.77-1.69 (m, 2H), 1.43-1.34 (m, 2H), 0.99 (t, *J* = 5.0 Hz, 3H) ppm.

^{13}C NMR (125 MHz, CD_3OD, DEPT): δ 153.0 (4°), 76.0 (4°), 74.3 (CH), 65.9 (CH_2), 63.8 (CH_2), 49.8 (2 x CH_3), 27.7 (CH_2), 25.4 (CH_2), 24.9 (CH_2), 24.0 (CH_2), 21.9 (CH_2), 19.2 (CH_2), 12.6 (CH_3) ppm.

HRMS: m/z calculated for $C_{15}H_{29}BrNO_2$ $[M+H]^+$ 334.1376, found 334.1368.

3.1.5 Attachment of group bearing quaternary amine functionality to the surface of PVC by thermal azide-alkyne cycloadditions

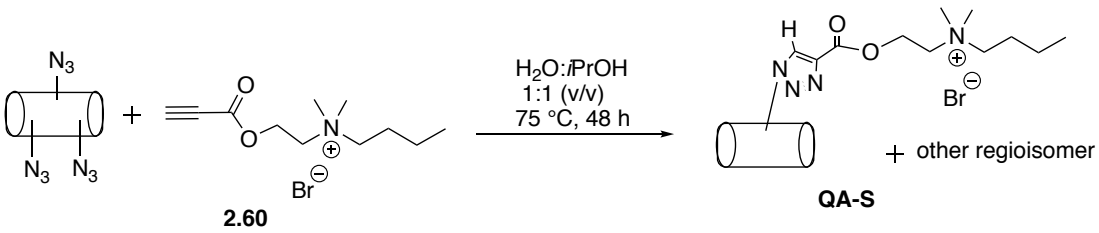

PVC tubing surface modified by 2-propynoic acid, 5-*N*-butyl-*N*-ethyl-*N*,*N*-dimethylammonium bromide ester (2.60) (**QA-S**)

2-propynoic acid, 5-*N*-butyl-*N*-ethyl-*N*,*N*-dimethylammonium bromide ester (**2.60**) (3.410 g, 12.26 mmol) was dissolved in 6 mL of 2-propanol and 12 mL of water. PVC-N_3 tubing (10 pieces, 1 cm x 1 cm each) was added to the reaction mixture and heated at 75 °C. Reaction progress was monitored by ATR-FTIR (disappearance of the azide peak at 2106 cm^{-1}). After 48 hours, the pieces of tubing were removed and washed several times with DI water and dried in an oven at 45 °C for 24 hours. The modified PVC tubing bearing **q**uaternary **a**mine functionality **s**mall molecular weight was named "**QA-S**".

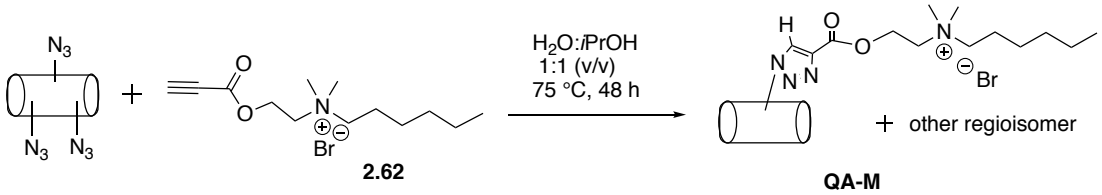

PVC surface modified by 2-propynoic acid, 5-*N*-hexyl-*N*-ethyl-*N*,*N*-dimethylammonium bromide ester (2.62) (**QA-M**)

2-propynoic acid, 5-*N*-hexyl-*N*-ethyl-*N*,*N*-dimethylammonium bromide ester (**2.62**) (1.900 g, 6.024 mmol) was dissolved in 6 mL of 2-propanol and 6 mL of water. PVC-N_3 tubing (5 pieces, 1 cm x 1 cm each) was added to the reaction mixture and heated at 75 °C. Reaction progress was monitored by ATR-FTIR (disappearance of the azide peak at 2106 cm^{-1}). After 48 hours, the pieces of tubing were removed and washed several times with DI water and dried in an oven at 45 °C for 24 hours. The modified PVC tubing bearing **q**uaternary **a**mine functionality **m**edium molecular weight was named as "**QA-M**".

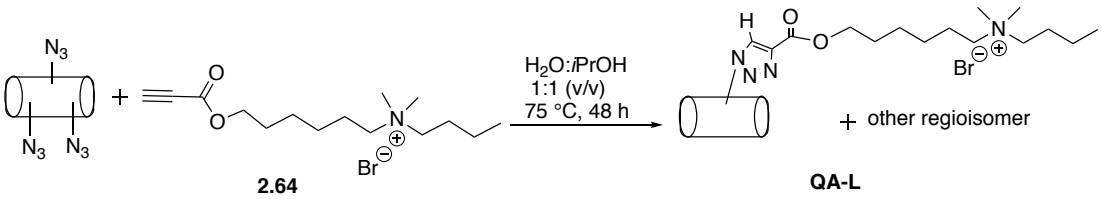

PVC surface modified by 2-propynoic acid, 5-*N*-butyl-*N*-ethyl-*N*,*N*-dimethylammonium bromide ester (2.64) (**QA-L**)

2-propynoic acid, 5-*N*-butyl-*N*-ethyl-*N*,*N*-dimethylammonium bromide ester (**2.64**) (1.510 g, 4.517 mmol) was dissolved in 6 mL of 2-propanol and 6 mL of water. PVC-N_3 tubing (5 pieces, 1 cm x 1 cm each) was added to the reaction mixture and heated at 75 °C. Reaction progress was monitored by ATR-FTIR (disappearance of the azide peak at 2106 cm^{-1}). After 48 hours, the pieces of tubing were removed and washed several times with DI water and dried in an oven at 45 °C for 24 hours. The modified PVC tubing bearing **q**uaternary **a**mine functionality **l**arge molecular weight was named "**QA-L**".

3.2 Surface Characterization

The robustness of grafted functional groups on PVC surfaces were evaluated through the change of surface wetting properties upon multiple rinsing cycles. Here, the samples were rinsed vigorously for 5 min in a sonicator bath filled with DI water. The samples were then dried with air blow and subsequently measured for their static contact angles (SCA) using an optical contact angle measurement system (Dataphysics OCA-15EC) with test droplet volume of 10 µl, placed on multiple locations for each sample surface. The rinsing and SCA measurement cycles were repeated for a number of time until the total cumulative ultrasonic rinsing duration is 60 min.

The information of the initial SCA values can be used to determine for sample surfaces energy based on Owens–Wendt–Rabel-and-Kaelble (OWRK) method.[1-2] This method assumes that surface energy is composed of dispersive and polar forces.

Therefore, it is necessary to add more types of test liquids of known surface tensions, in order to calculate the dispersive and polar parts of surface energy of the solid. The test liquids used here were DI water, ethylene glycol and formamide. The SCA measurement and data interpretation was done on the Dataphysics OCA-15EC system.

The surface adhesion properties of the chemically modified PVC were examined through the adherence of water droplet on an inclined sample. Whereby, the contact angle hysteresis (CAH) was evaluated from the difference between advancing (θ_a) and receding (θ_r) contact angles, measured using the same optical contact angle measurement system equipped with a tilted stage. Surface topography of the samples was evaluated in nanoscale level by atomic force microscope (AFM, Nanosurf Easyscan 2). The root-mean-square (rms) surface roughness was determined from the height information of the scanned area. XPS of both unmodified tubing (vendor A and B) were taken with PHI Quantum 2000 instrument using monochromated alk$_\alpha$ 1486.6 eV x-ray source.

3.3 *Pseudomonas aeruginosa* Adherence Assays

Preparation of Inoculum:

Pseudomonas aeruginosa strain PA01 was used for these analyses. The strain was struck onto a LB (pH 7.4) agar plate, and incubated at 37°C overnight. The following day, 5 single colonies were inoculated into 5mL of liquid LB (pH7.4), and the

culture was incubated at 37°C with 200rpm shaking overnight. The following day, the overnight culture was diluted 1:100 in 30mL of Mueller Hinton broth (pH 7.4, cation adjusted).

Preparation of Endotracheal Tubing:

Endotracheal tube pieces were placed individually into wells of a 24-well culture plate. Tubing pieces were then sterilized by exposure to UV light in a biosafety cabinet for 15 minutes on each side.

Adherence Assay:

Following sterilization, tubing pieces were oriented in the bottom of their well such that the internal surface of the tubing was facing upwards. Then 1mL of the bacterial suspension in Mueller Hinton broth ($7.9 \times 10^7 \pm 9.5 \times 10^6$ CFU/mL) was added to each well, plates were covered and incubated statically at 37°C for 24 hours. Following incubation, tubing pieces were removed from the culture, and was 2x by submersion in 2mL of 1x phosphate buffered saline (PBS) to remove non-adherent bacteria. Tubing pieces were then placed in a 2mL micro-centrifuge tube containing 1mL PBS and three glass beads, and then vortexed for 10 minutes to remove adherent cells. Samples were then serially diluted and plated to determine CFU/mL, with each dilution plated in triplicate. CFU/mL were also determined for the remaining biofilm culture (in technical duplicate), to ensure no treatments inhibited bacterial growth. For adherence assays, three pieces of PVC and two pieces of PVC-N_3 were used as

controls (one piece of each was also incubated without bacteria to ensure sterility). One piece each of tubing samples Zwi-S, Zwi-L, PEO_{2000}, PF-S, and PF-M were used for analysis. Data was then plotted and analyzed with Graphpad Prism, and is presented as the mean ± standard deviation. Statistical analysis: one-way ANOVA with Dunnett's correction for multiple comparisons, with the mean of each sample compared to the PVC control: PVC-N_3 ****p = <0.0001, Zwi-S ***p = 0.0008, Zwi-L ****p = <0.0001, PEO2000 ****p = <0.0001, PFS ns - not significant, PF-M *p = 0.0127.

3.4 References

1. Owens, D. K.; Wendt, R. C., Estimation of the surface free energy of polymers. *Journal of Applied Polymer Science* **1969,** *13* (8), 1741-1747.

2. Kaelble, D. H., Dispersion-Polar Surface Tension Properties of Organic Solids. *The Journal of Adhesion* **1970,** *2* (2), 66-81.

3. Beveridge, J. M.; Chenot, H. M.; Crich, A.; Jacob, A.; Finn, M. G., Covalent Functionalization of Flexible Polyvinyl Chloride Tubing. *Langmuir* **2018,** *34* (35), 10407-10412.

4. Vasudevamurthy, M. K.; Lever, M.; George, P. M.; Morison, K. R., Betaine structure and the presence of hydroxyl groups alters the effects on DNA melting temperatures. *Biopolymers* **2009,** *91* (1), 85-94.

5. Higa, C. M.; Tek, A. T.; Wojtecki, R. J.; Braslau, R., Nonmigratory internal plasticization of poly(vinyl chloride) via pendant triazoles bearing alkyl or polyether esters. *Journal of Polymer Science Part A: Polymer Chemistry* **2018,** *56* (21), 2397-2411.

6. Weaver, M. G.; Bai, W.-J.; Jackson, S. K.; Pettus, T. R. R., Diels–Alder Construction of Regiodifferentiated meta-Amino Phenols and Derivatives. *Organic Letters* **2014,** *16* (5), 1294-1297.

7. e Silva, F. A.; Siopa, F.; Figueiredo, B. F. H. T.; Gonçalves, A. M. M.; Pereira, J. L.; Gonçalves, F.; Coutinho, J. A. P.; Afonso, C. A. M.; Ventura, S. P. M., Sustainable

design for environment-friendly mono and dicationic cholinium-based ionic liquids. *Ecotoxicology and Environmental Safety* **2014,** *108*, 302-310.

4 Addendum: Contribution to Other Published Work

Contribution to other projects from Braslau lab in which I am a co-author, but are not included in the thesis are described as follows.

1. Skelly, P. W.; Sae-Jew, J.; Kitos Vasconcelos, A. P.; Tasnim, J.; Li, L.; Raskatov, J. A.; Braslau, R. *J. Org. Chem.* **2019**, *84* (21), 13615–13623. Relative Rates of Metal-Free Azide-Alkyne Cycloadditions: Tunability over 3 Orders of Magnitude. I synthesized three alkynes for Huisgen thermal cycloaddition, which were then utilized by others to determine the relative rates of various alkynes in reacting with a model azide.

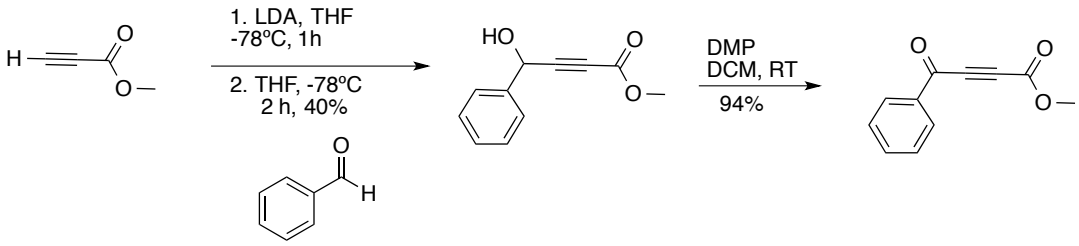

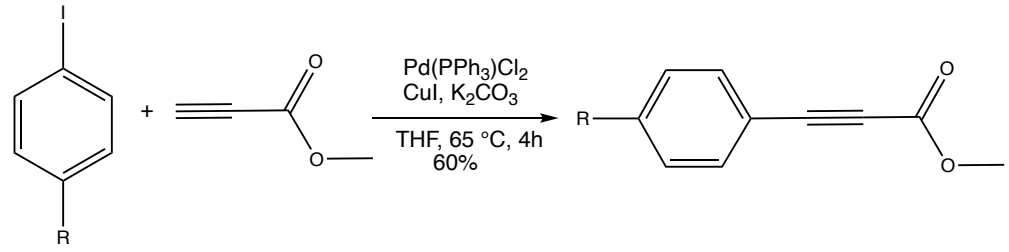

5 Appendix

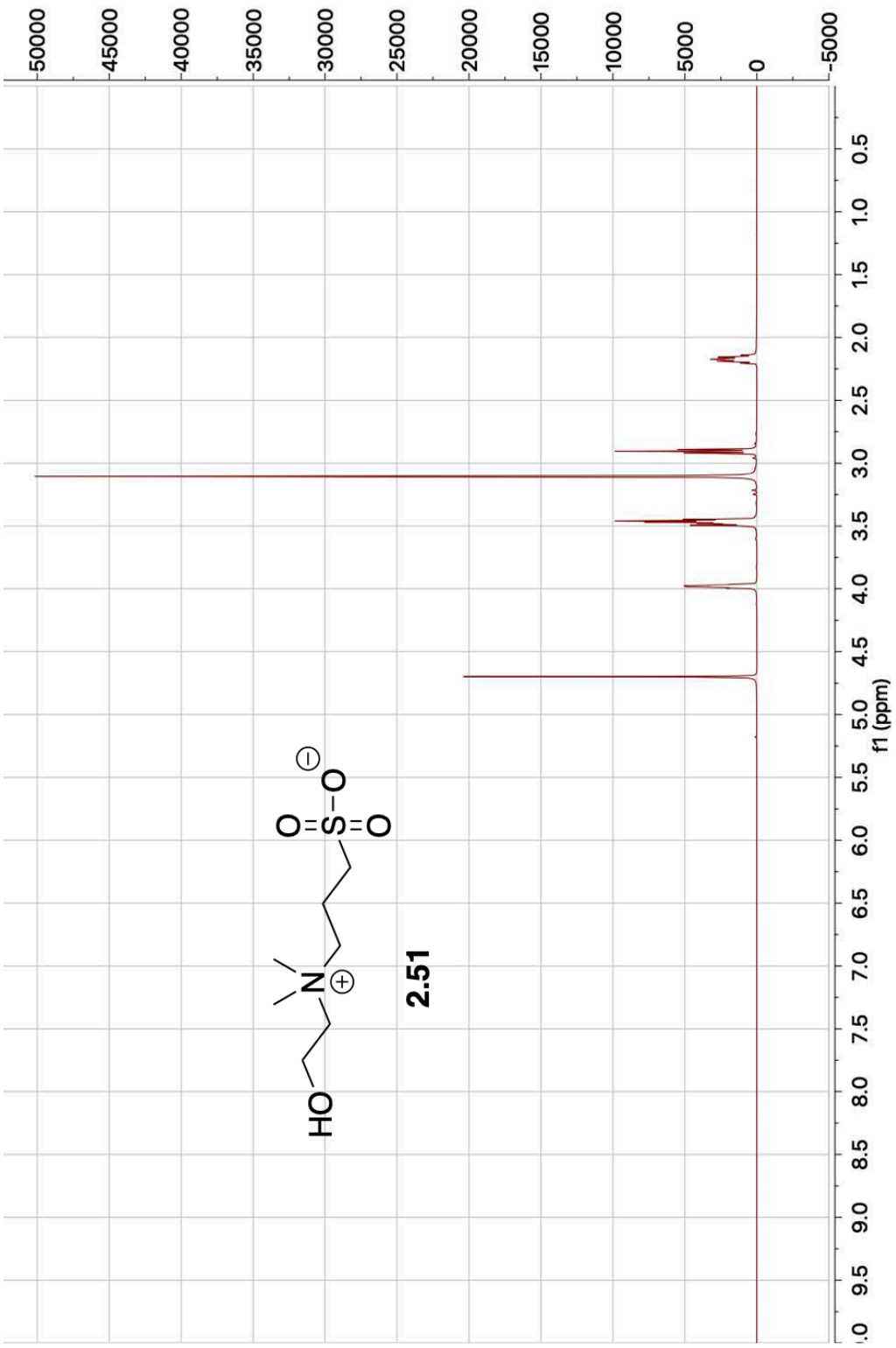
50000
45000
40000
35000
30000
25000
20000
15000
10000
5000
0
-5000
0.5
1.0
1.5
2.0
2.5
3.0
3.5
4.0
4.5
5.0
5.5
6.0
6.5
7.0
7.5
8.0
8.5
9.0
9.5
f1 (ppm)
HO
N
O=S=O
O
2.51

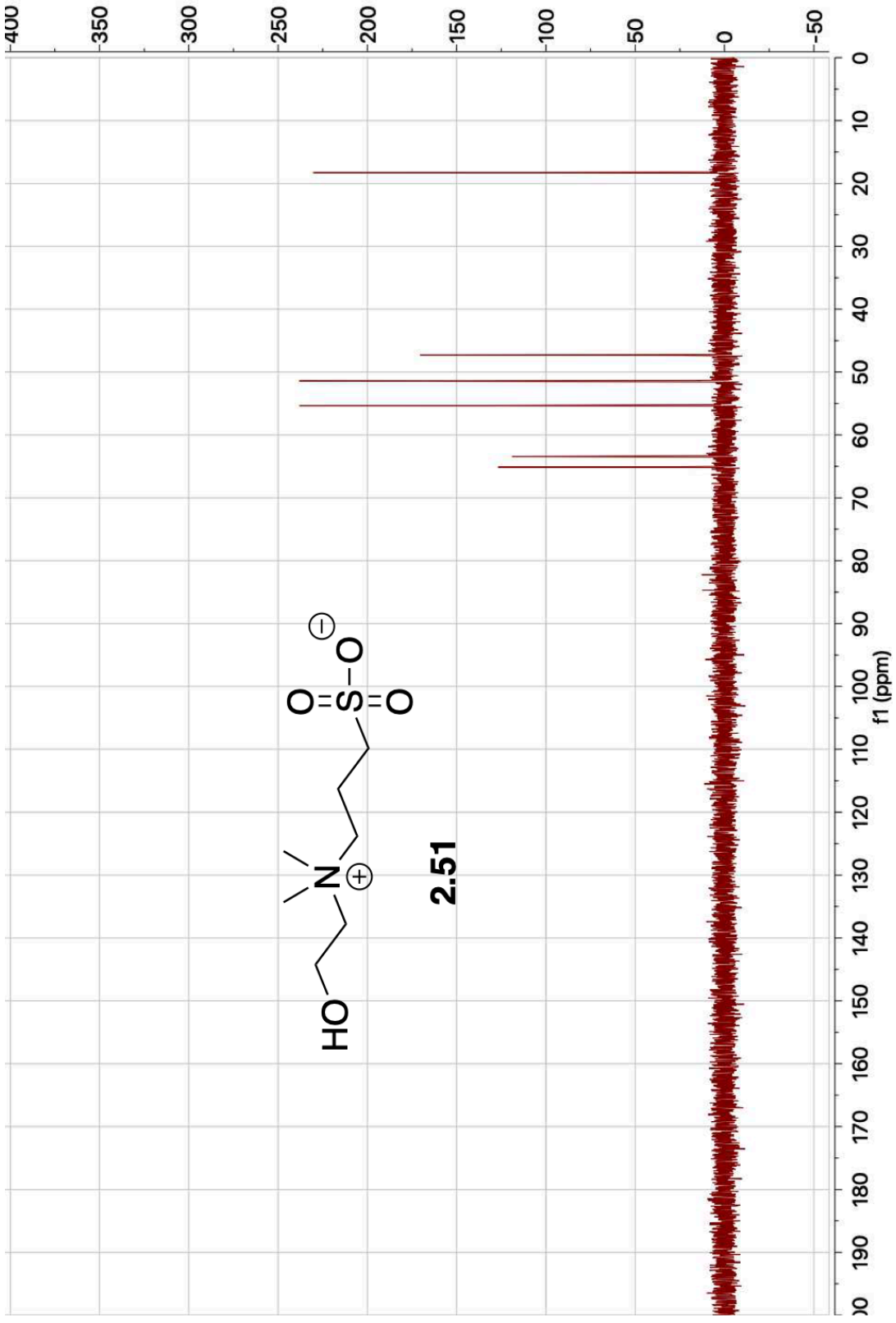
f1 (ppm)
2.51

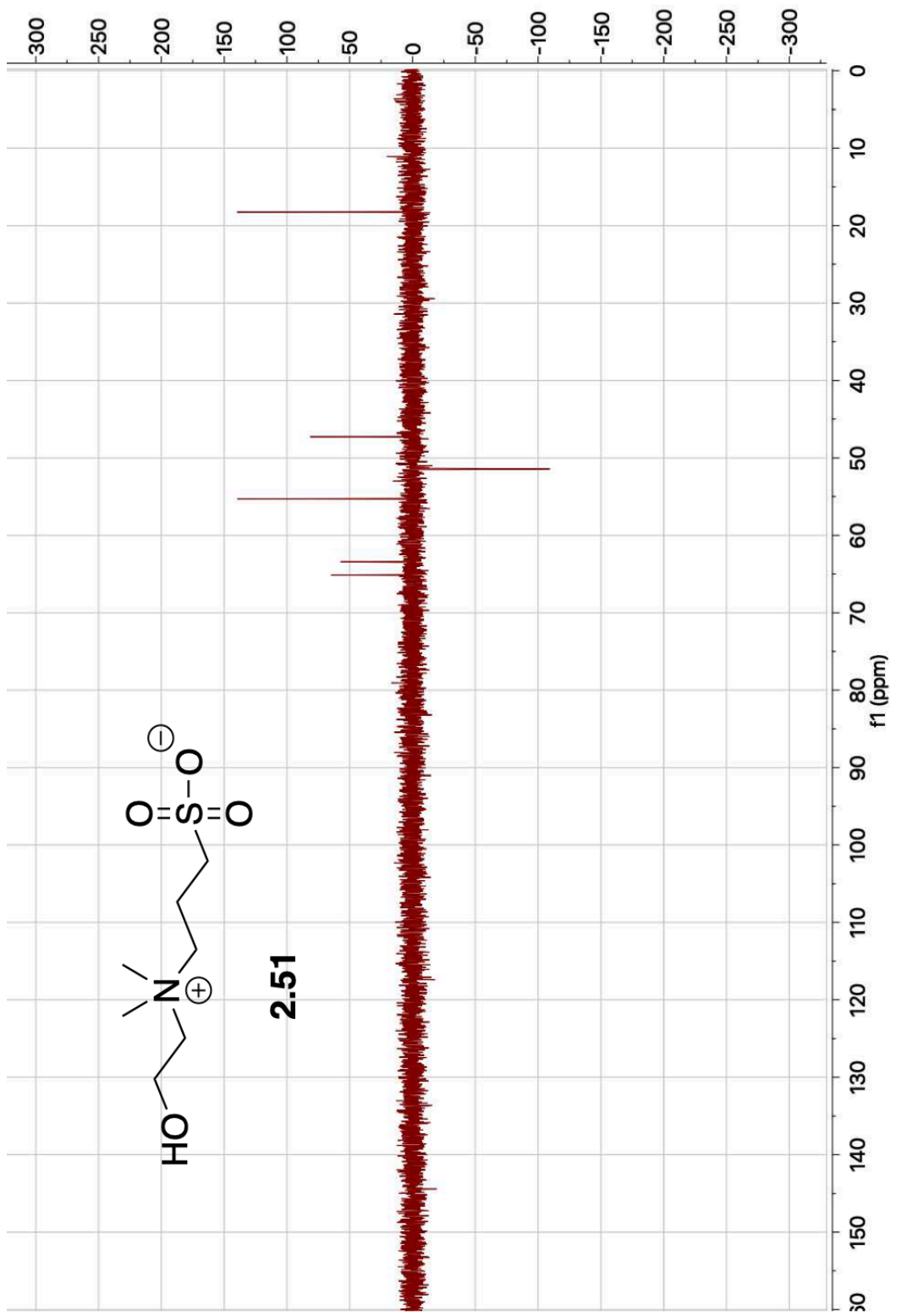
f1 (ppm)
2.51

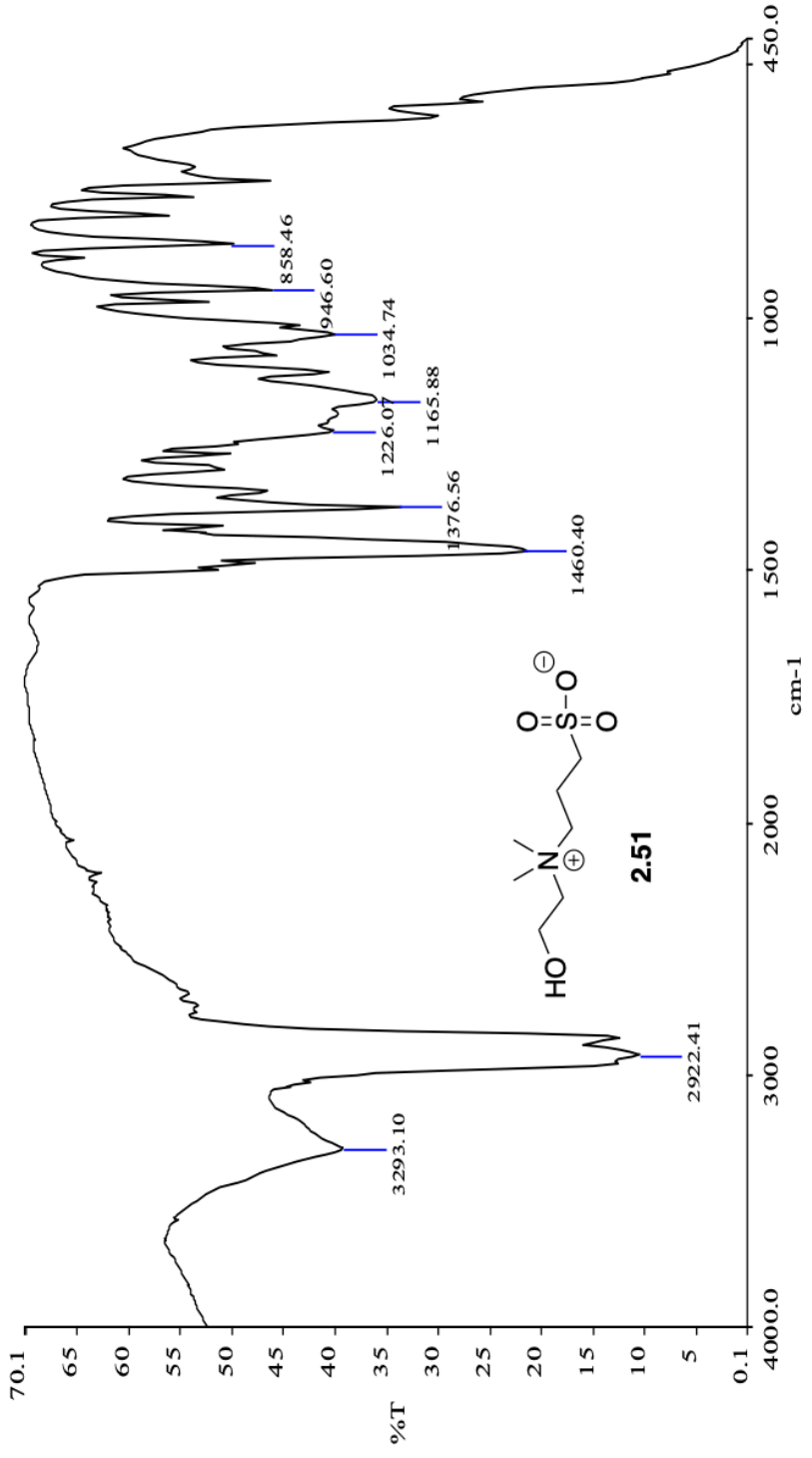
70.1
65
60
55
50
45
40
35
30
25
20
15
10
5
0.1
%T
4000.0
3000
2000
1500
1000
450.0
cm-1
3293.10
2922.41
1460.40
1376.56
1226.07
1165.88
1034.74
946.60
858.46
HO
N
O=S=O
2.51

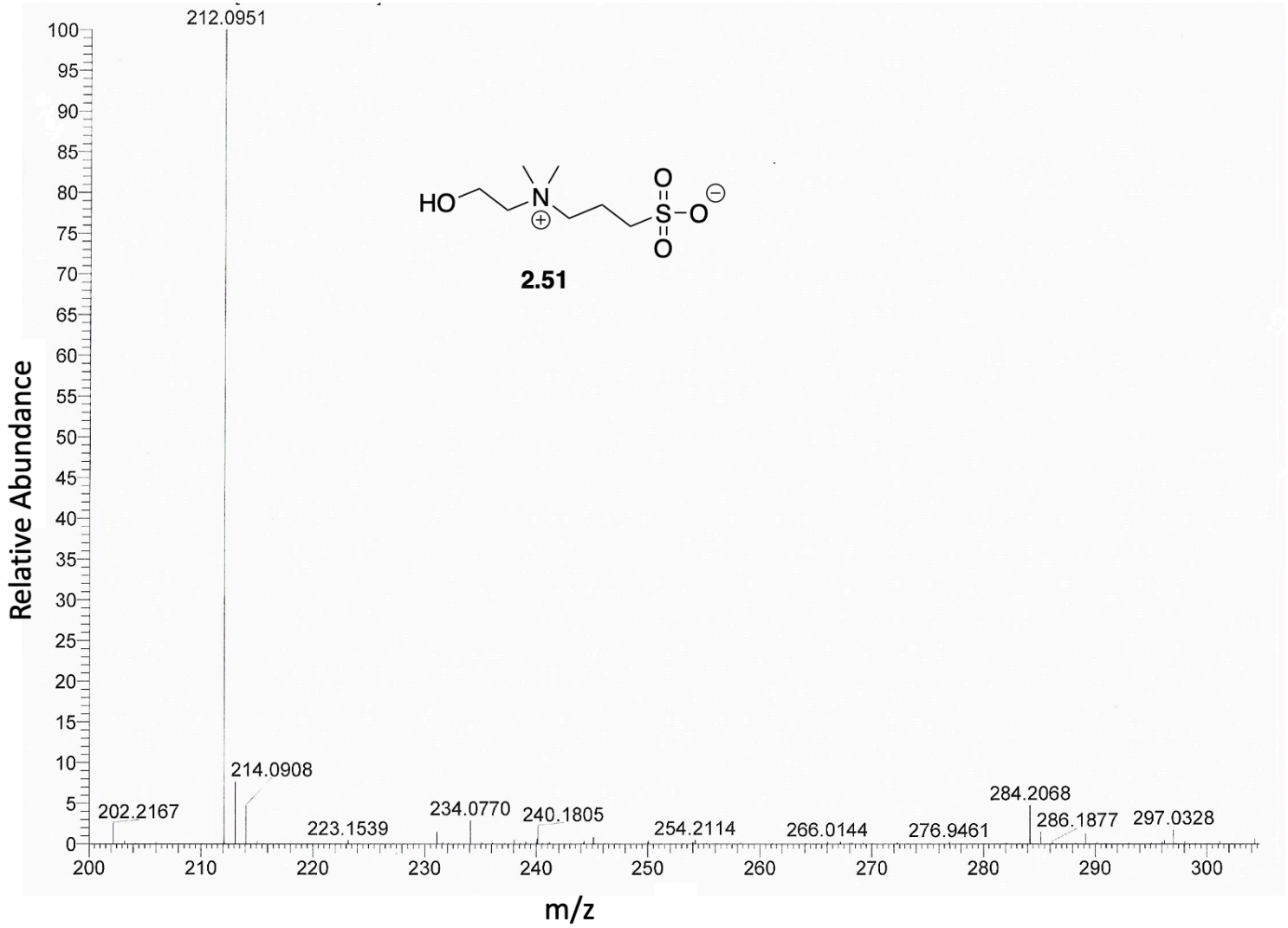
212.0951
214.0908
202.2167
223.1539
234.0770
240.1805
254.2114
266.0144
276.9461
284.2068
286.1877
297.0328
Relative Abundance
m/z
HO
N
S
O
2.51

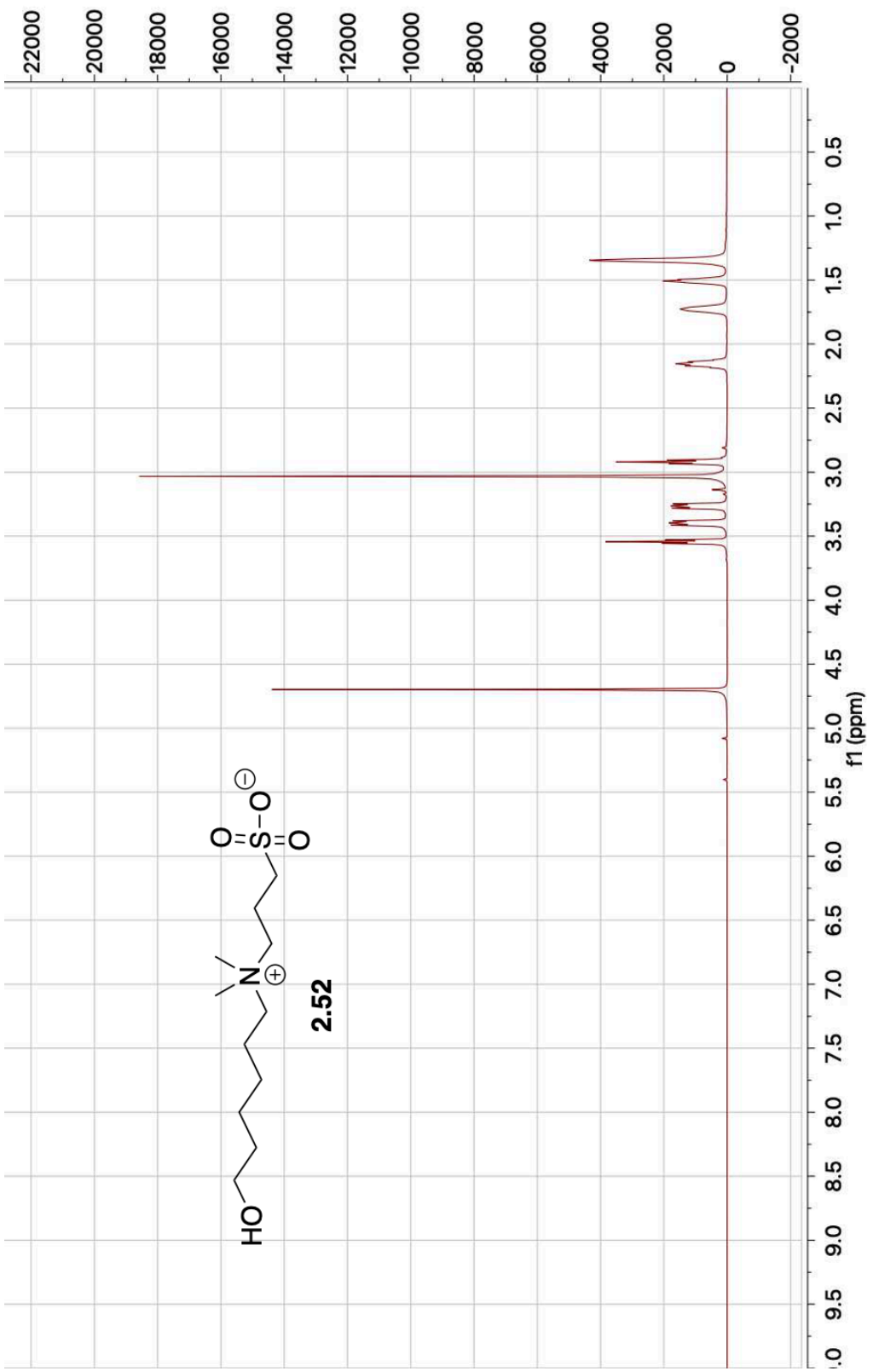
22000
20000
18000
16000
14000
12000
10000
8000
6000
4000
2000
0
-2000
0.5
1.0
1.5
2.0
2.5
3.0
3.5
4.0
4.5
5.0
5.5
6.0
6.5
7.0
7.5
8.0
8.5
9.0
9.5
f1 (ppm)
HO
N
O
S
O
O
2.52

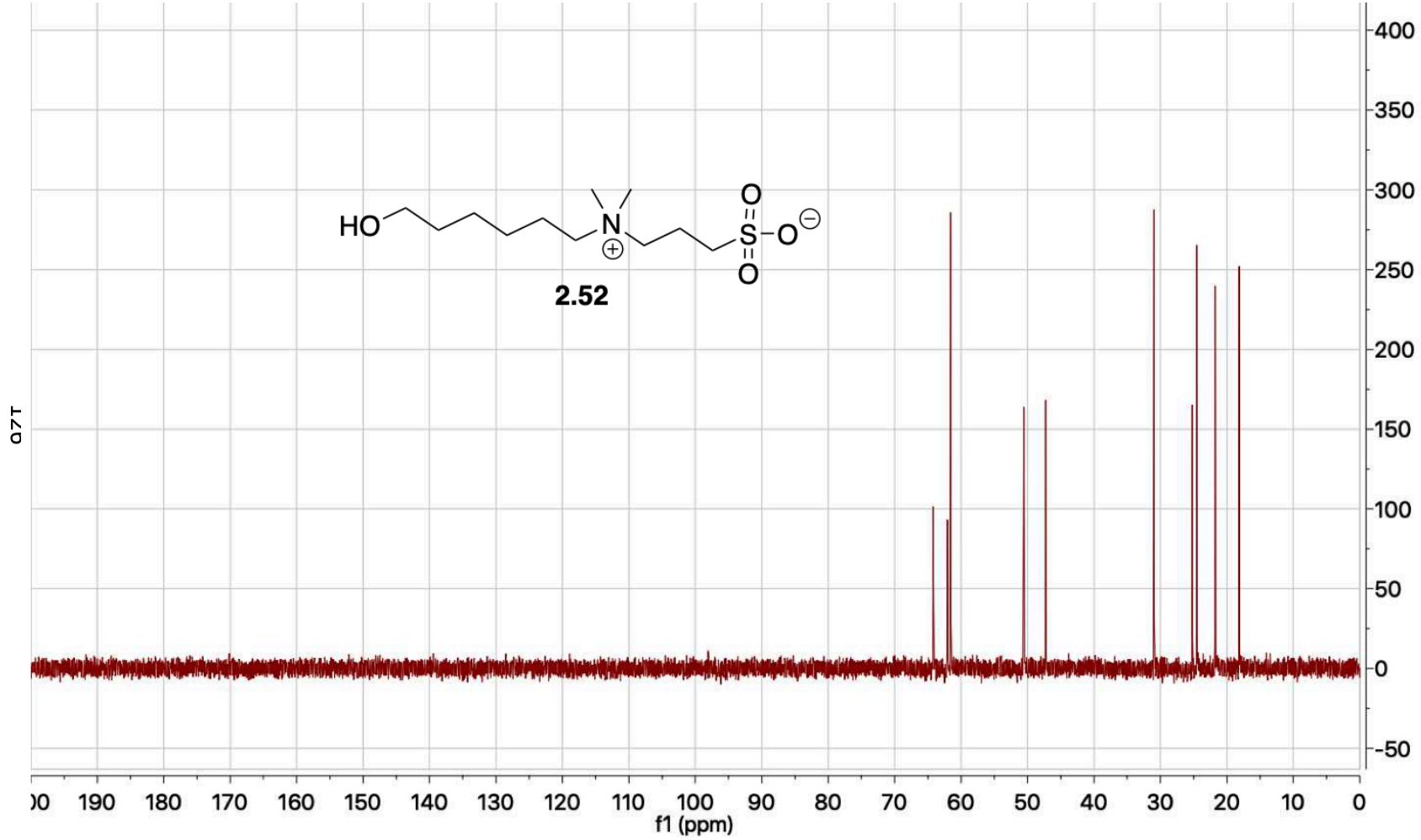
HO
N
S
O
O
O
2.52
400
350
300
250
200
150
100
50
0
-50
190
180
170
160
150
140
130
120
110
100
90
80
70
60
50
40
30
20
10
0
f1 (ppm)

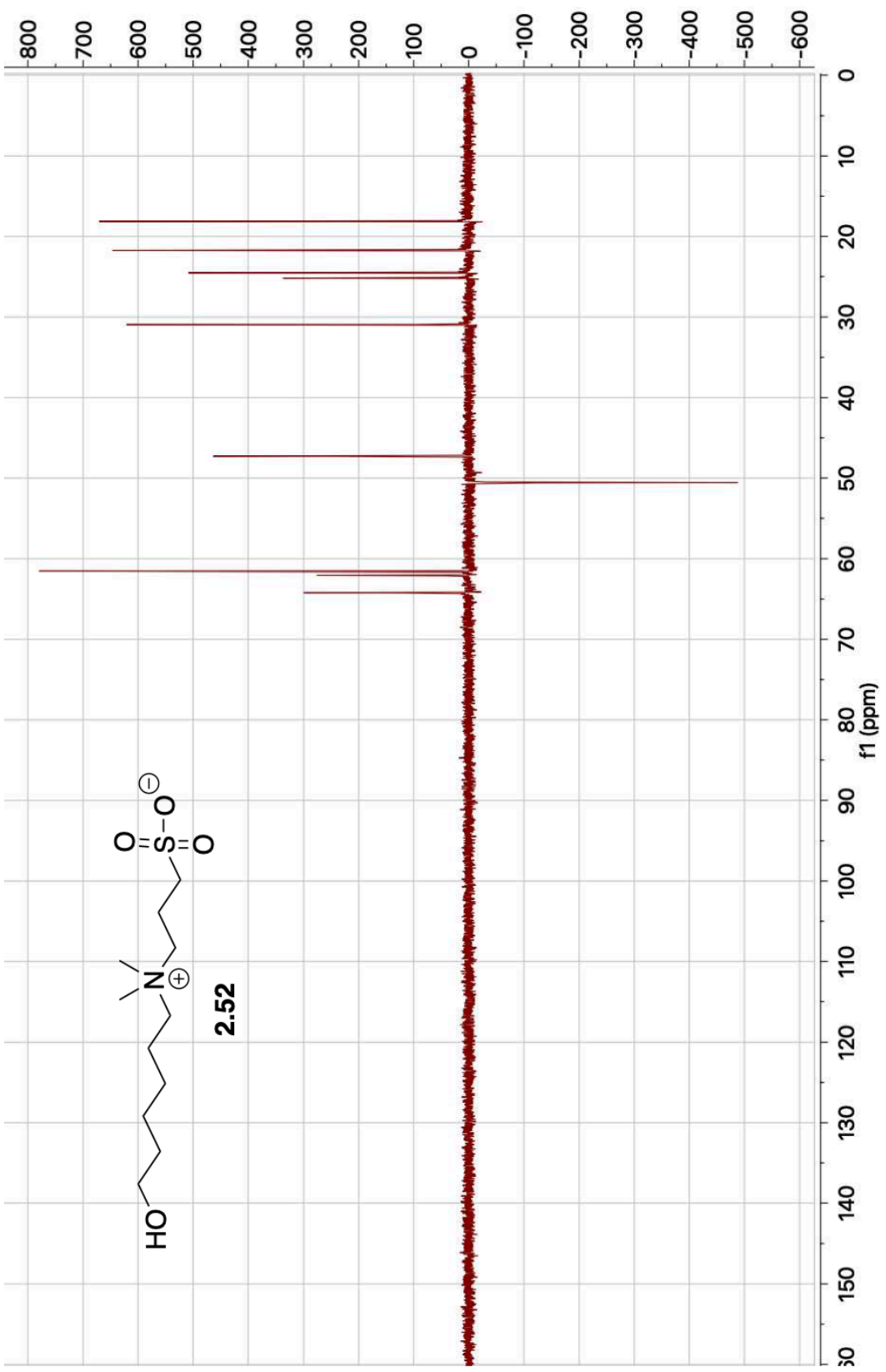
f1 (ppm)
2.52

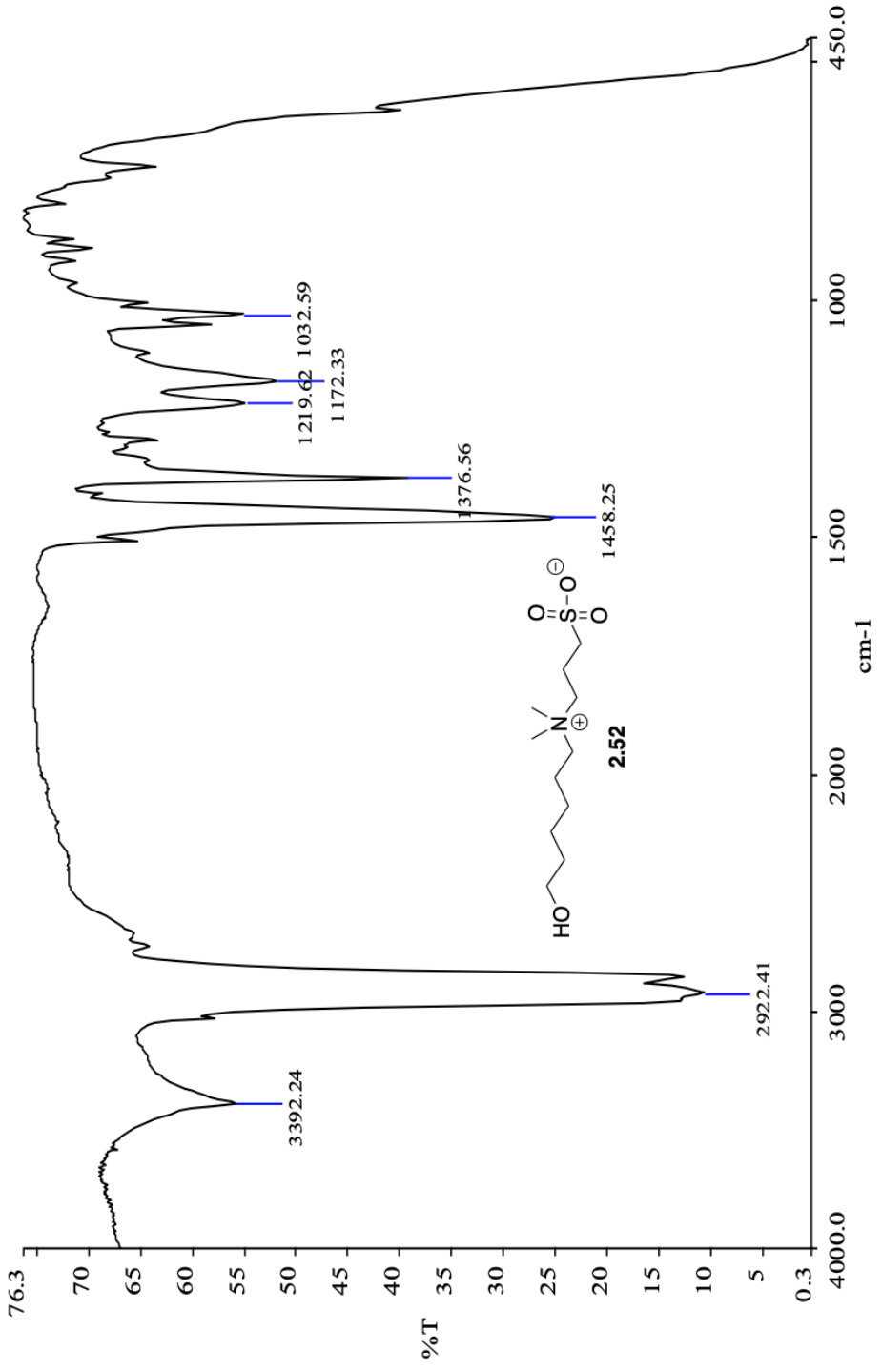
76.3
70
65
60
55
50
45
40
35
30
25
20
15
10
5
0.3
%T
4000.0
3000
2000
1500
1000
450.0
cm-1
3392.24
2922.41
1458.25
1376.56
1219.62
1172.33
1032.59
HO
N
S
O
2.52

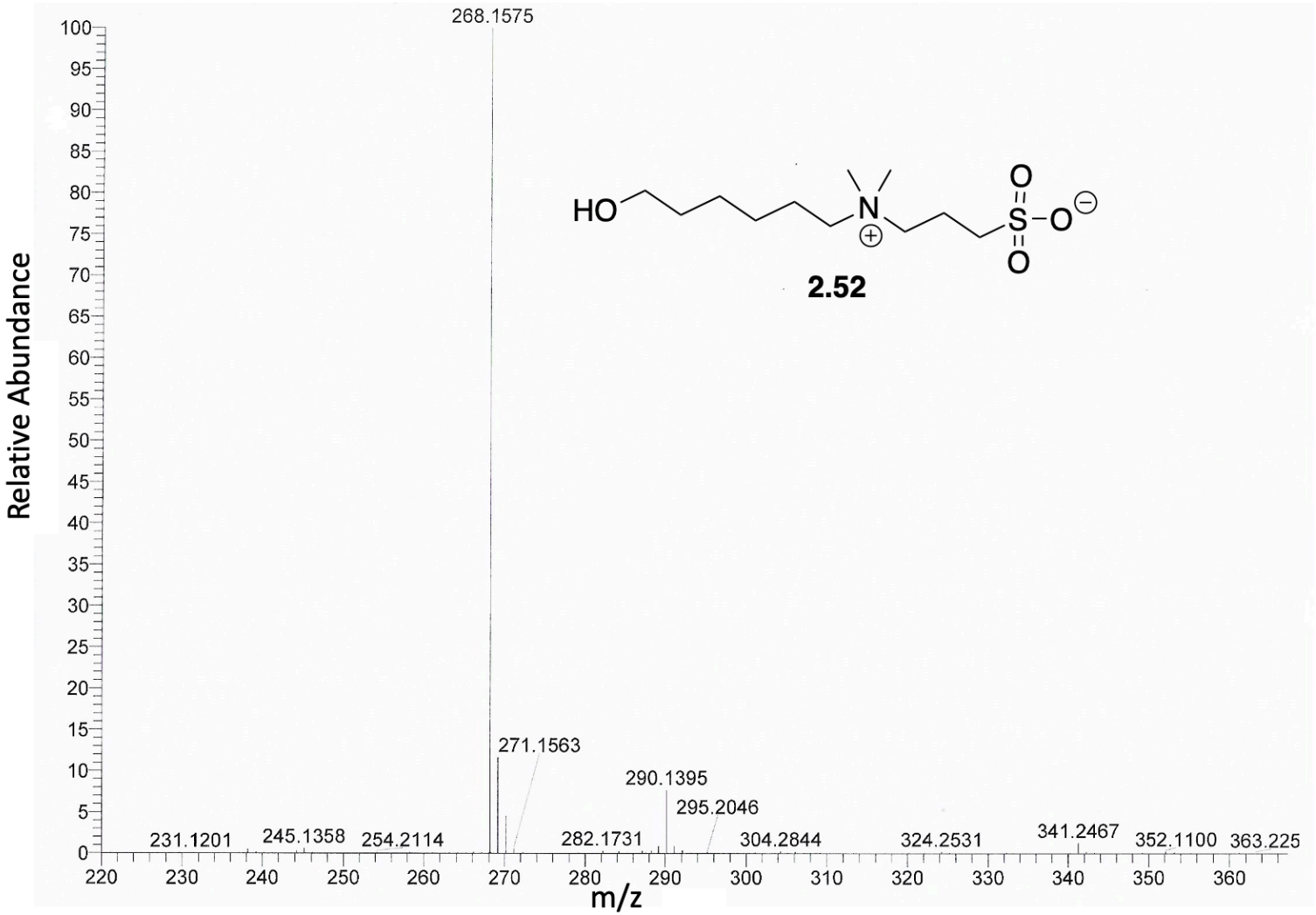
268.1575
Relative Abundance
m/z
271.1563
290.1395
295.2046
231.1201
245.1358
254.2114
282.1731
304.2844
324.2531
341.2467
352.1100
363.225
HO
N
S
O
2.52

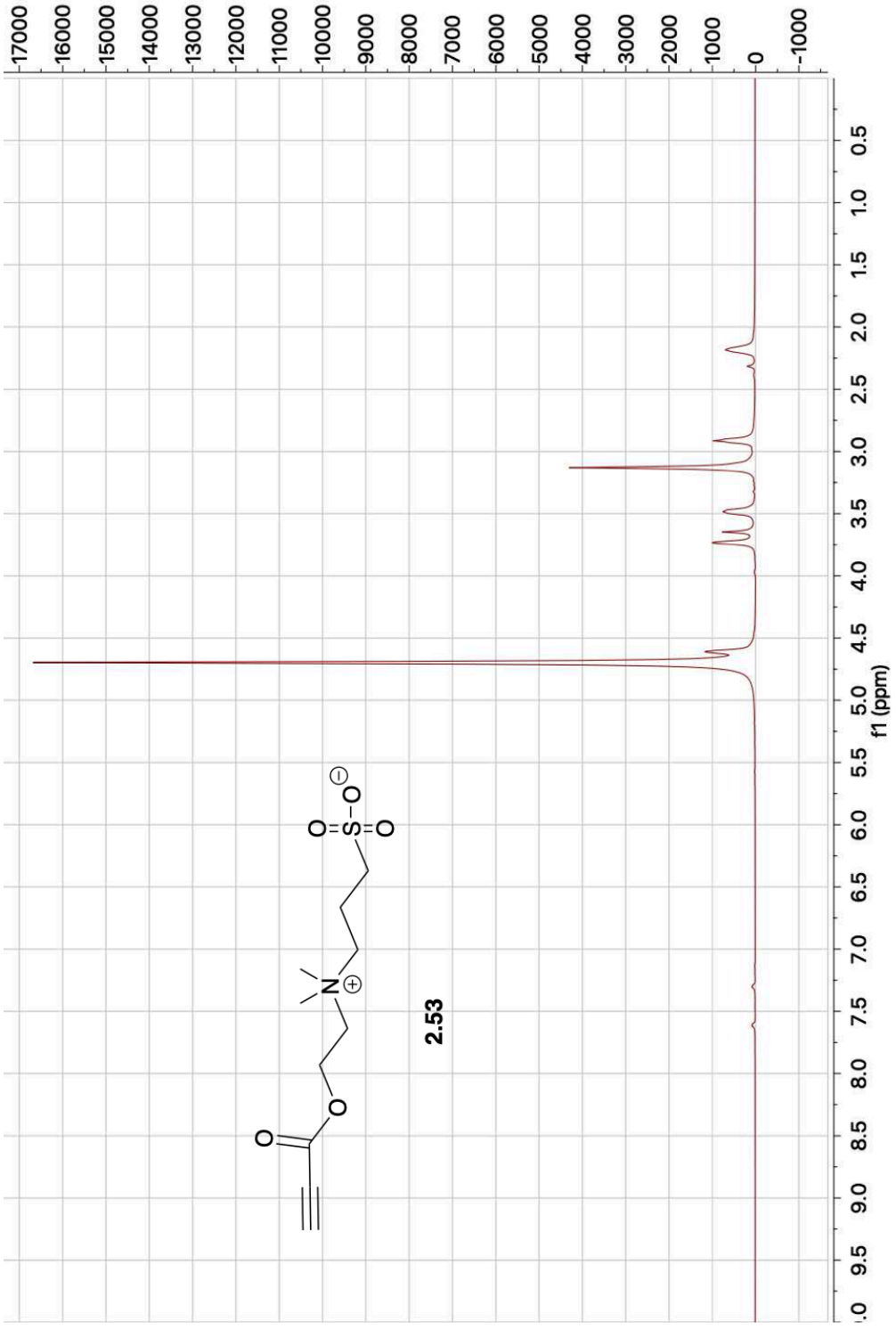
17000
16000
15000
14000
13000
12000
11000
10000
9000
8000
7000
6000
5000
4000
3000
2000
1000
0
-1000
0.5
1.0
1.5
2.0
2.5
3.0
3.5
4.0
4.5
5.0
5.5
6.0
6.5
7.0
7.5
8.0
8.5
9.0
9.5
f1 (ppm)
O
O
N
O
S
O
O
O

2.53

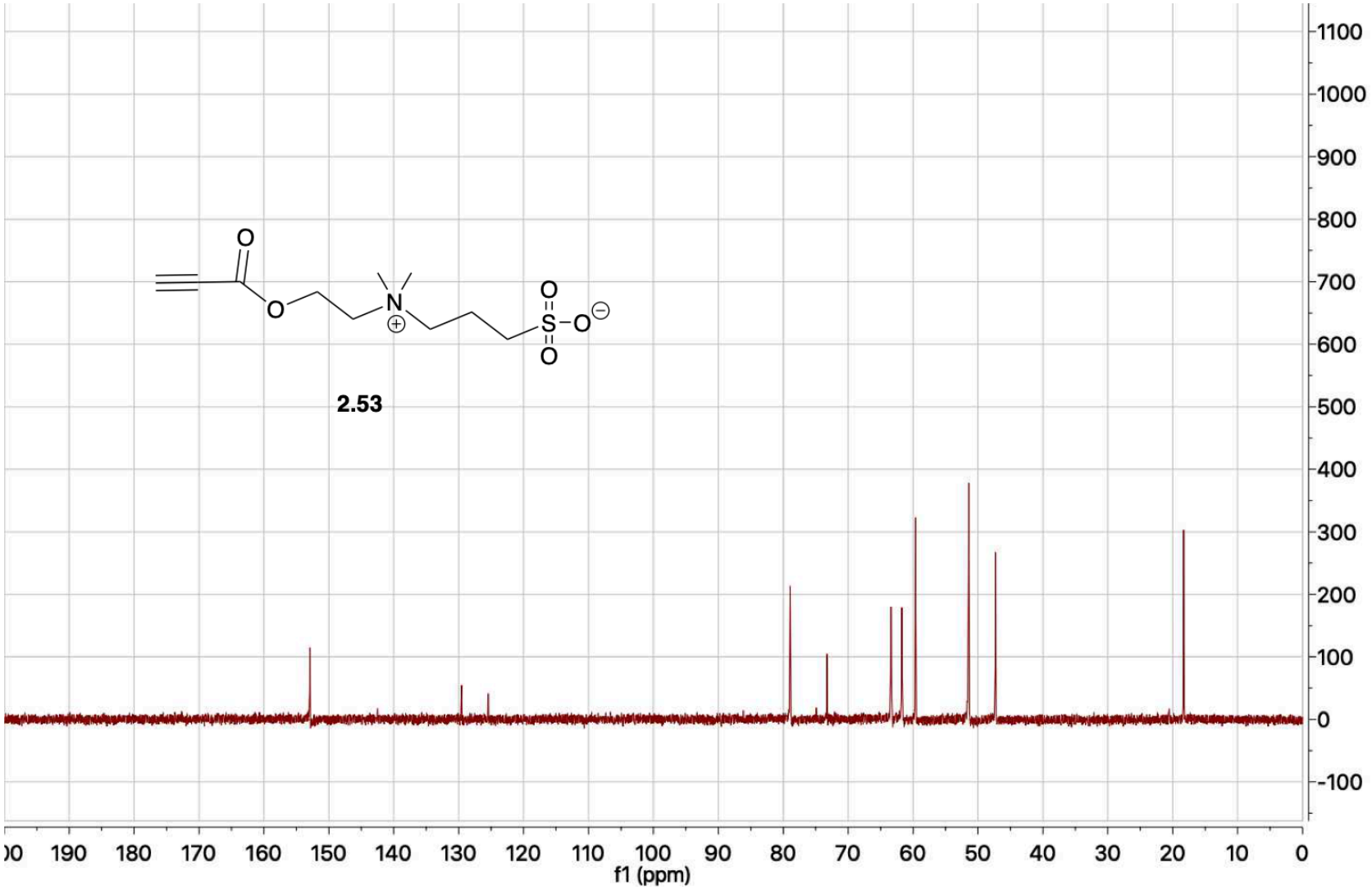
O
O
N
O
S
O
O
O
2.53
1100
1000
900
800
700
600
500
400
300
200
100
0
-100
190
180
170
160
150
140
130
120
110
100
90
80
70
60
50
40
30
20
10
0
f1 (ppm)

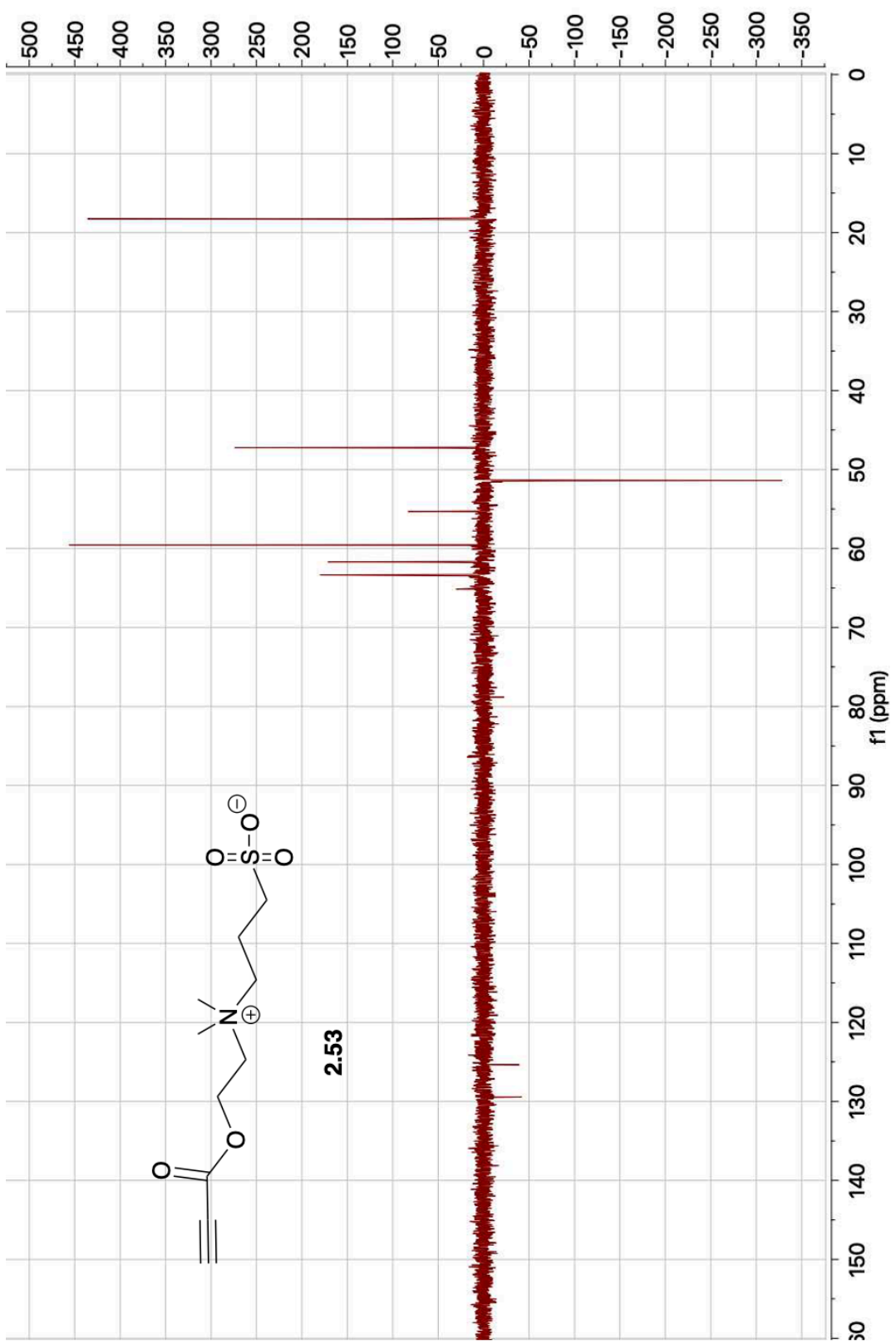
2.53
f1 (ppm)

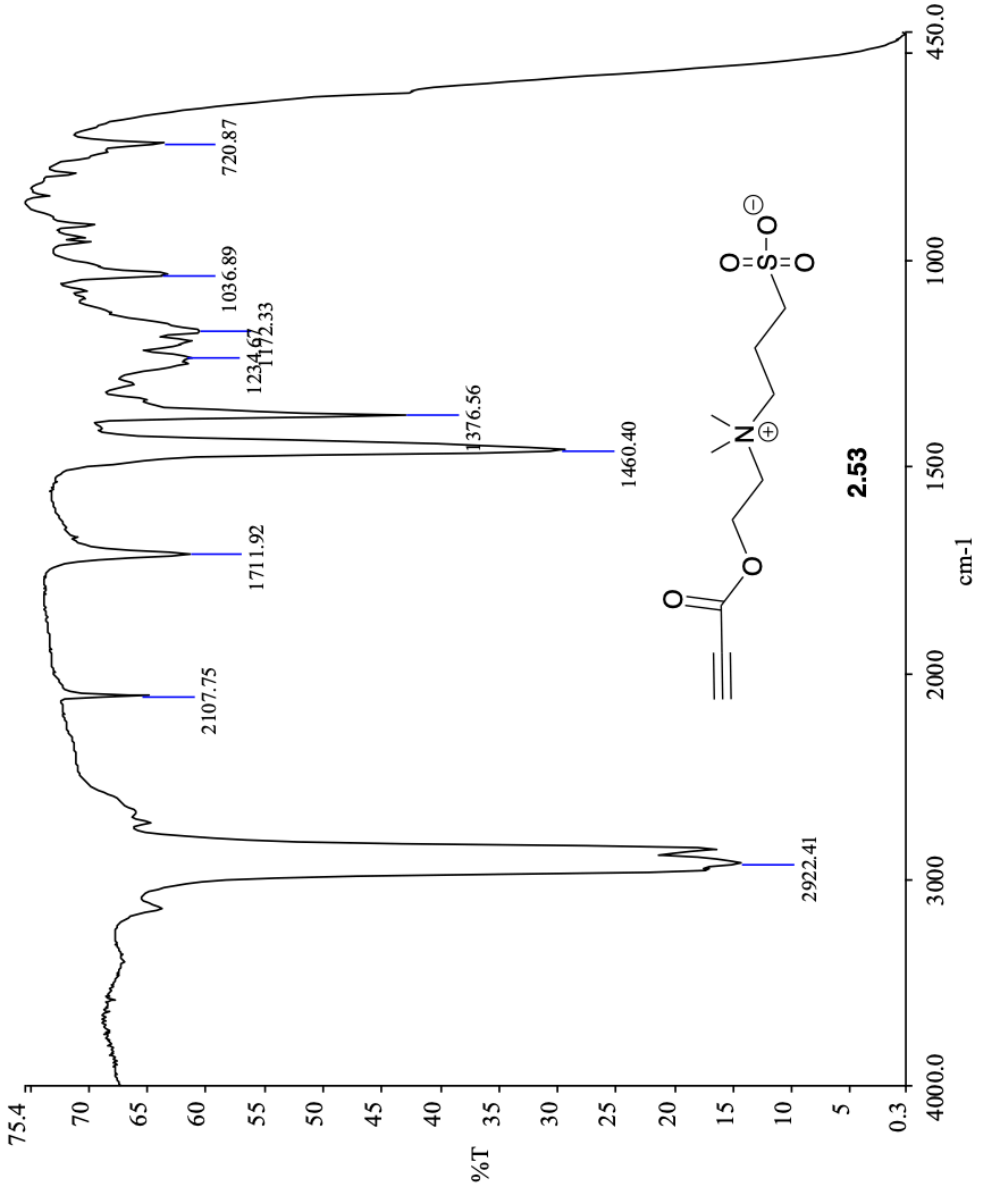
75.4
70
65
60
55
50
45
40
35
30
25
20
15
10
5
0.3
%T
4000.0
3000
2000
1500
1000
450.0
cm-1
2922.41
2107.75
1711.92
1460.40
1376.56
1234.67
1172.33
1036.89
720.87
2.53

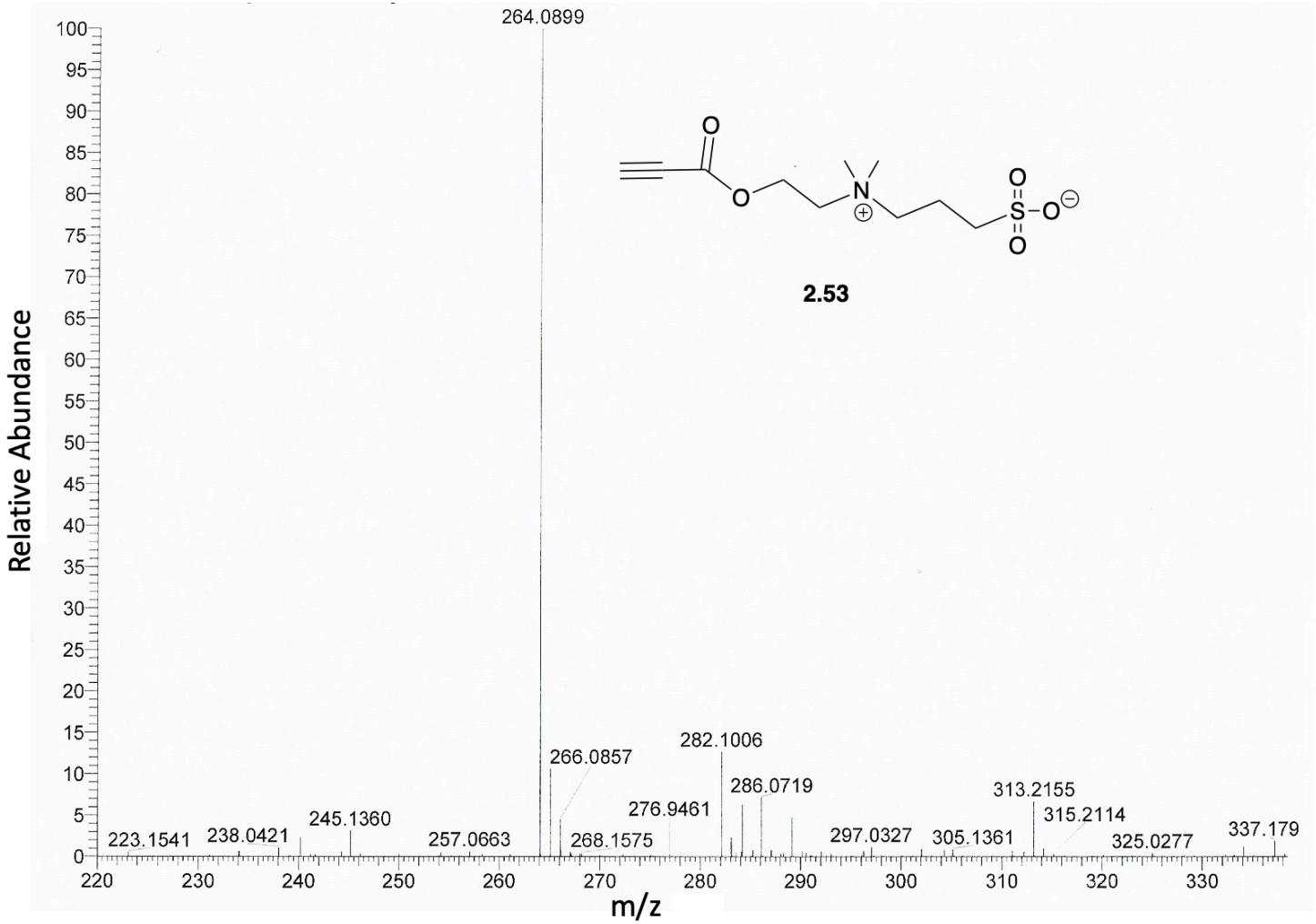
264.0899
Relative Abundance
m/z
223.1541
238.0421
245.1360
257.0663
266.0857
268.1575
276.9461
282.1006
286.0719
297.0327
305.1361
313.2155
315.2114
325.0277
337.179

2.53

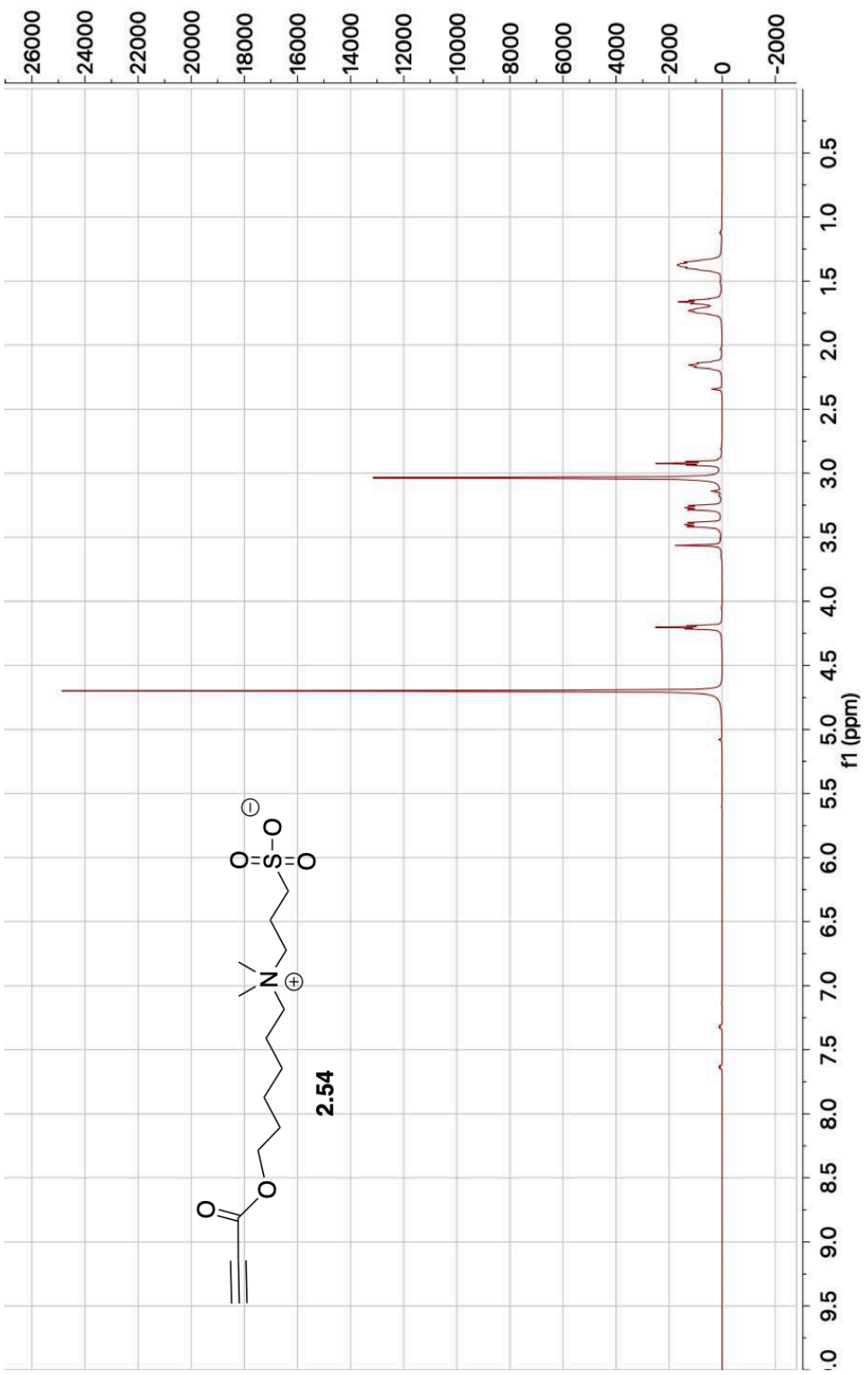
26000
24000
22000
20000
18000
16000
14000
12000
10000
8000
6000
4000
2000
0
-2000
0.5
1.0
1.5
2.0
2.5
3.0
3.5
4.0
4.5
5.0
5.5
6.0
6.5
7.0
7.5
8.0
8.5
9.0
9.5
f1 (ppm)
2.54

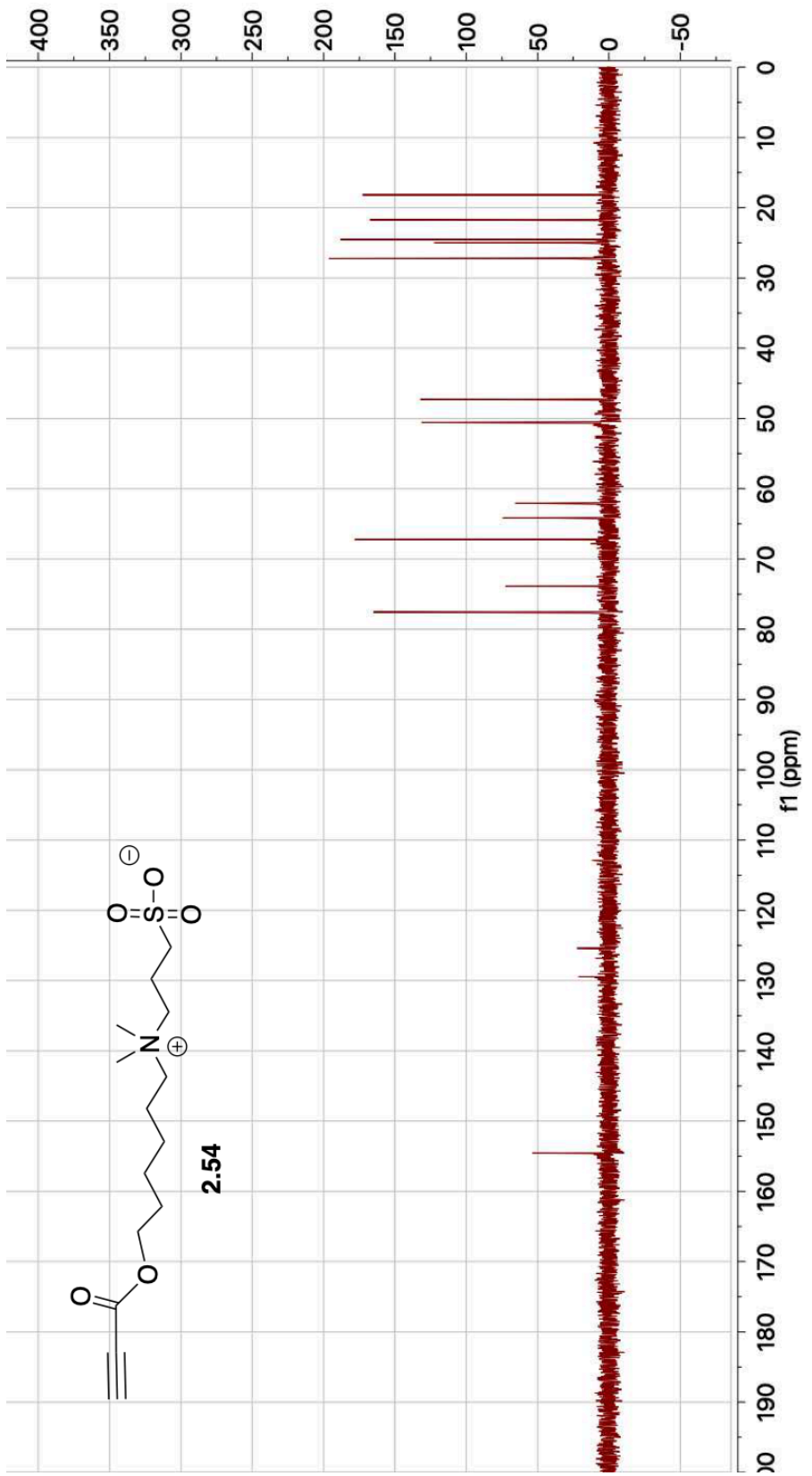
f1 (ppm)
2.54

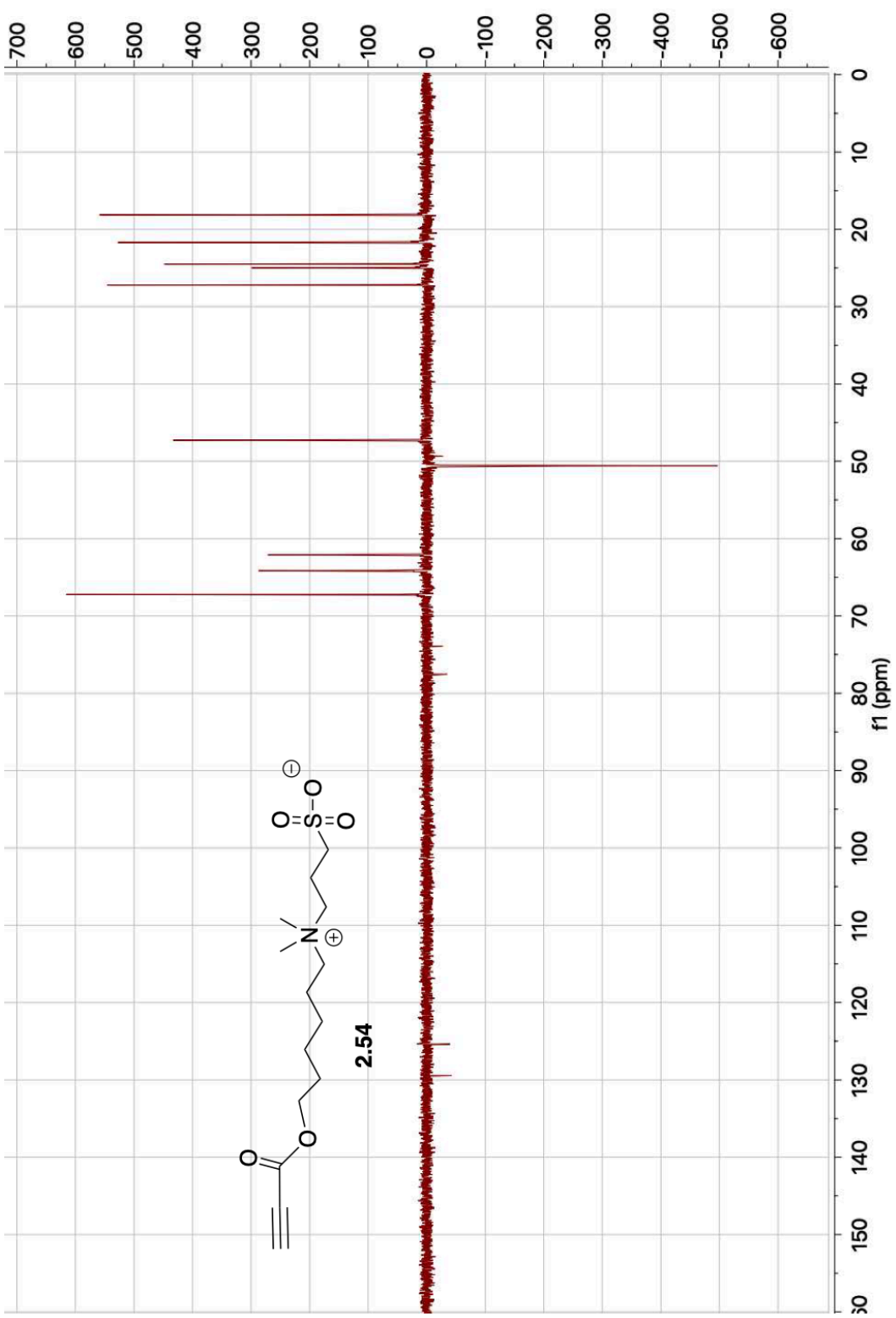
2.54
f1 (ppm)

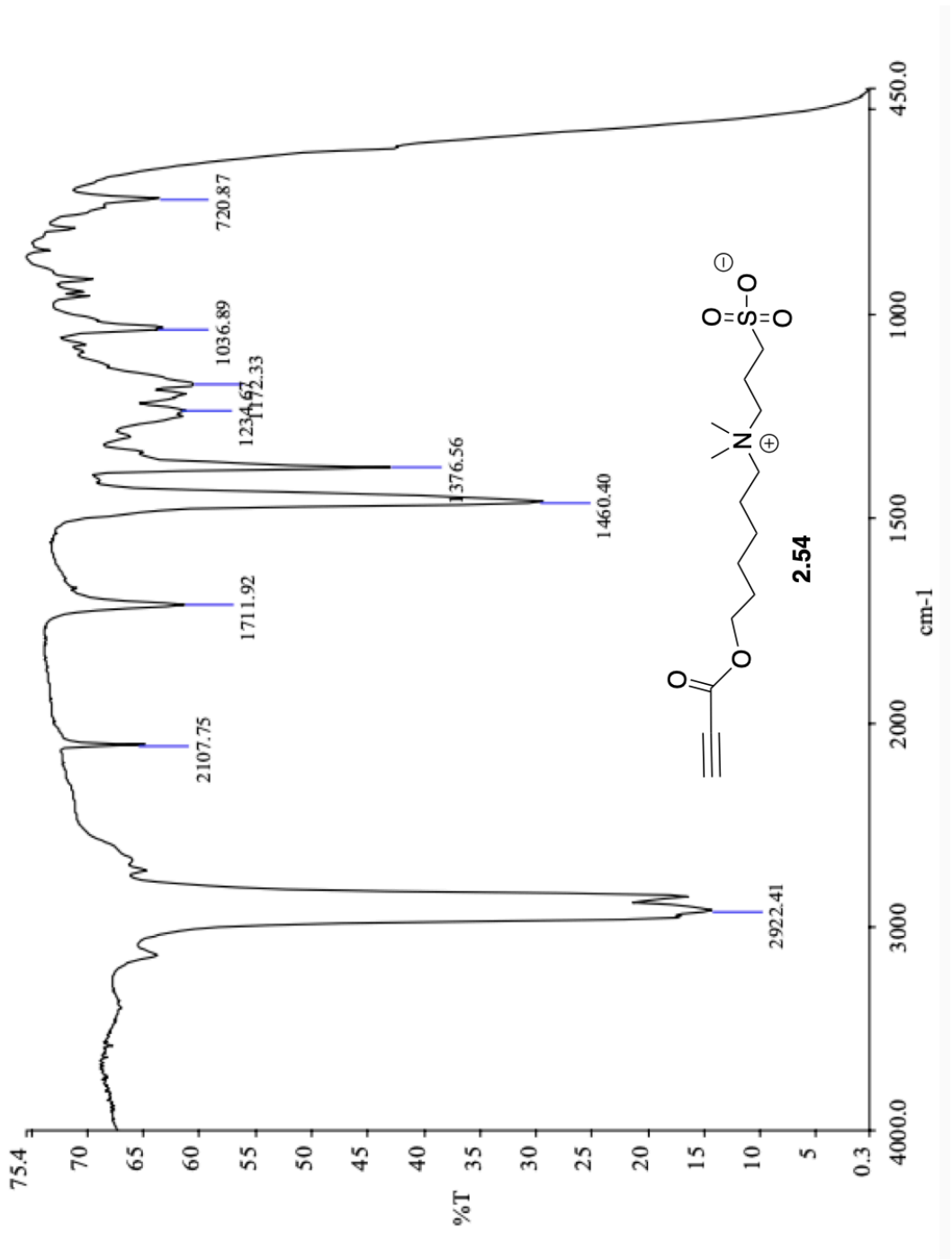
75.4
70
65
60
55
50
45
40
35
30
25
20
15
10
5
0.3
%T
4000.0
3000
2000
1500
1000
450.0
cm-1
2922.41
2107.75
1711.92
1460.40
1376.56
1234.62
1172.33
1036.89
720.87
2.54

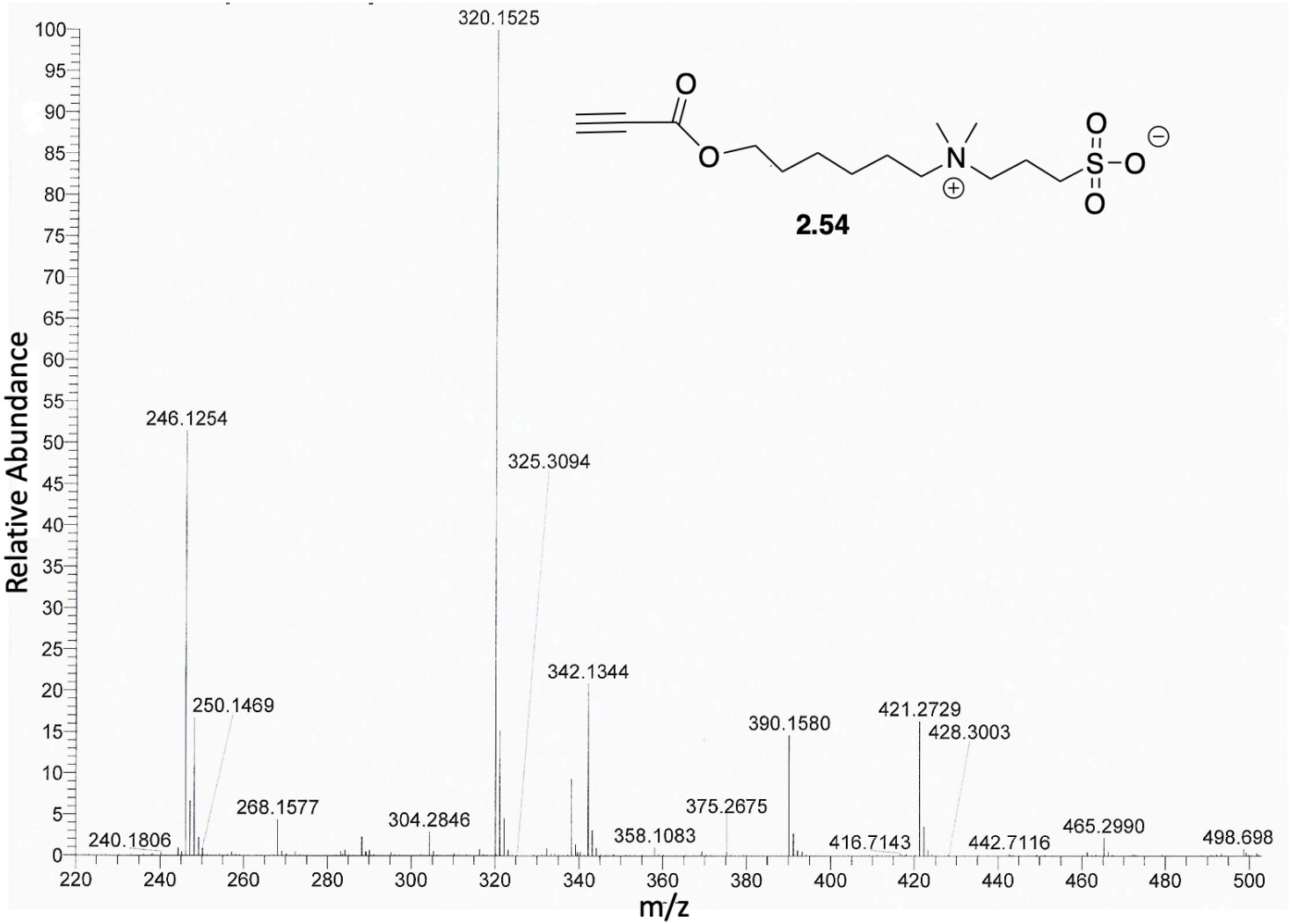
320.1525
246.1254
325.3094
342.1344
250.1469
390.1580
421.2729
428.3003
268.1577
375.2675
304.2846
240.1806
358.1083
416.7143
442.7116
465.2990
498.698
Relative Abundance
m/z
2.54

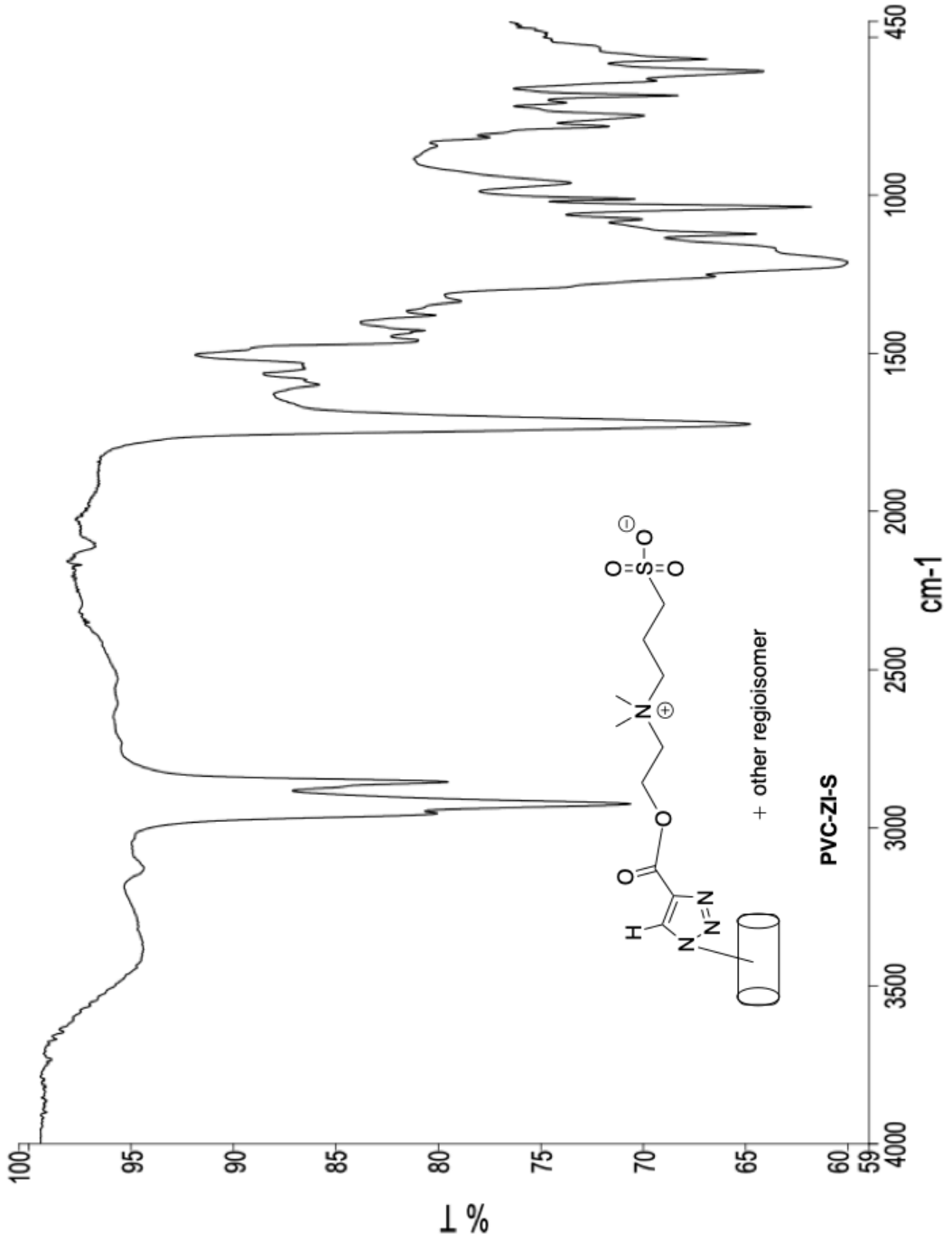
%T
100
95
90
85
80
75
70
65
60
59
4000
3500
3000
2500
2000
1500
1000
450
cm-1
PVC-ZI-S
+ other regioisomer

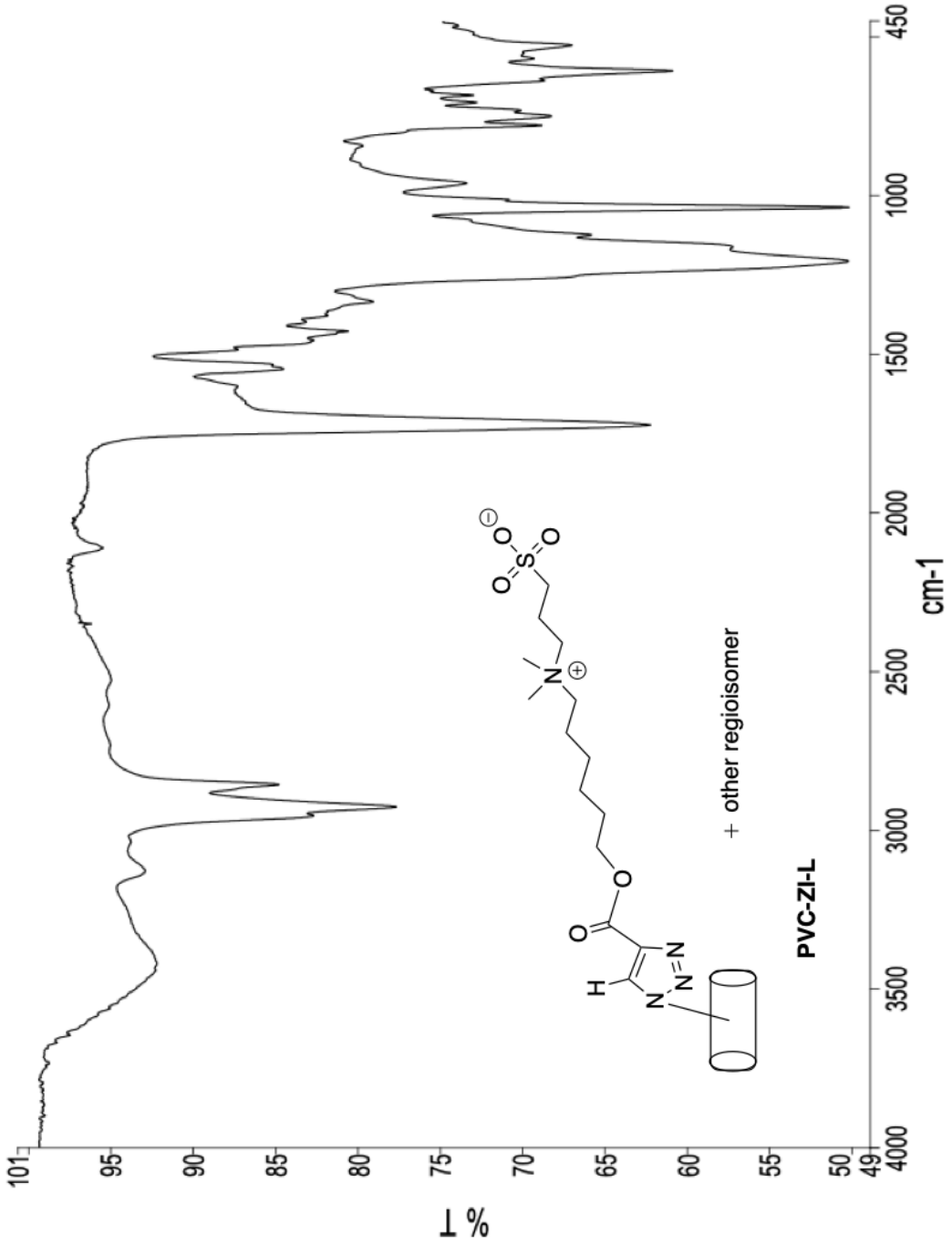
% T
cm-1
PVC-ZI-L
+ other regioisomer

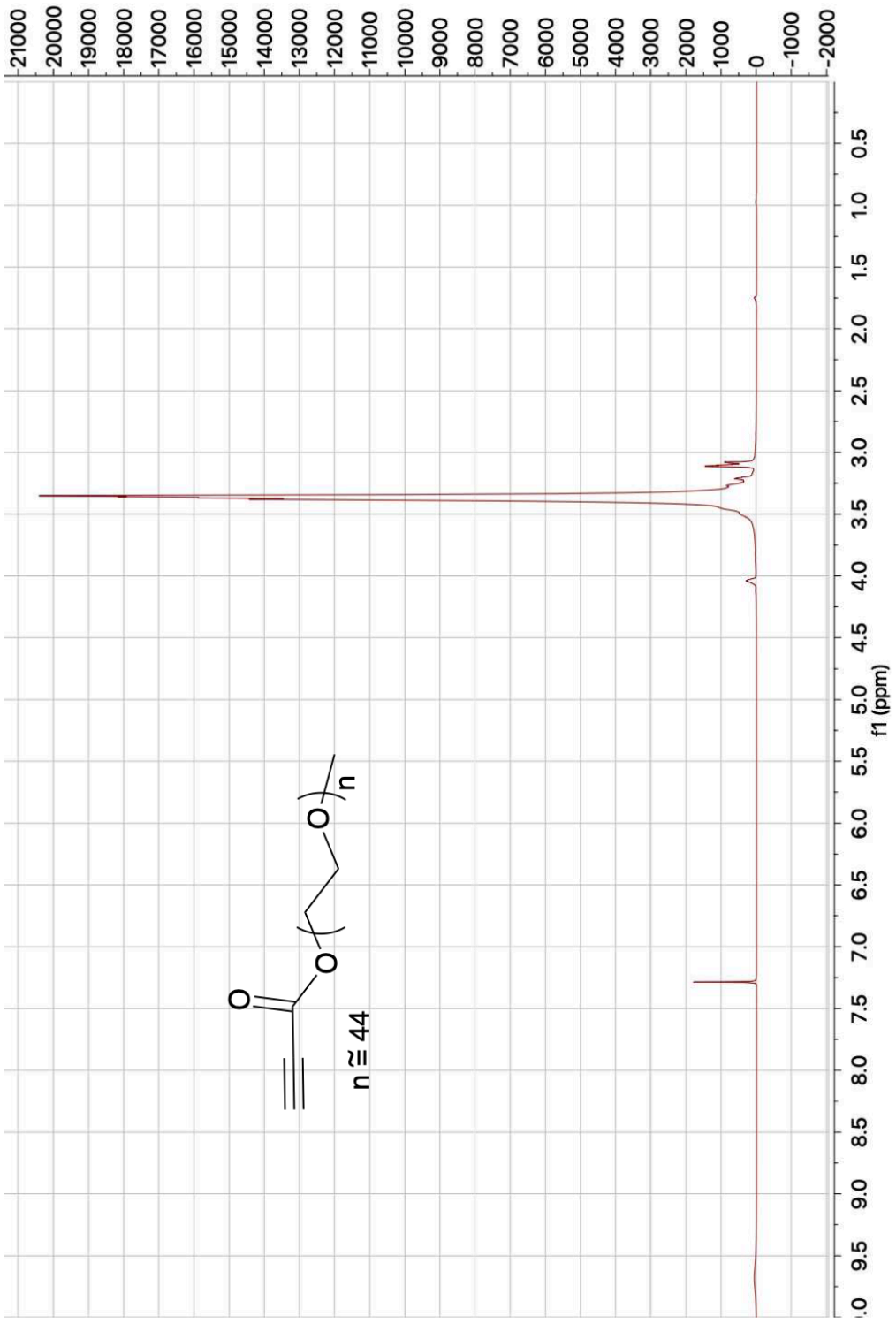
n ≅ 44
f1 (ppm)

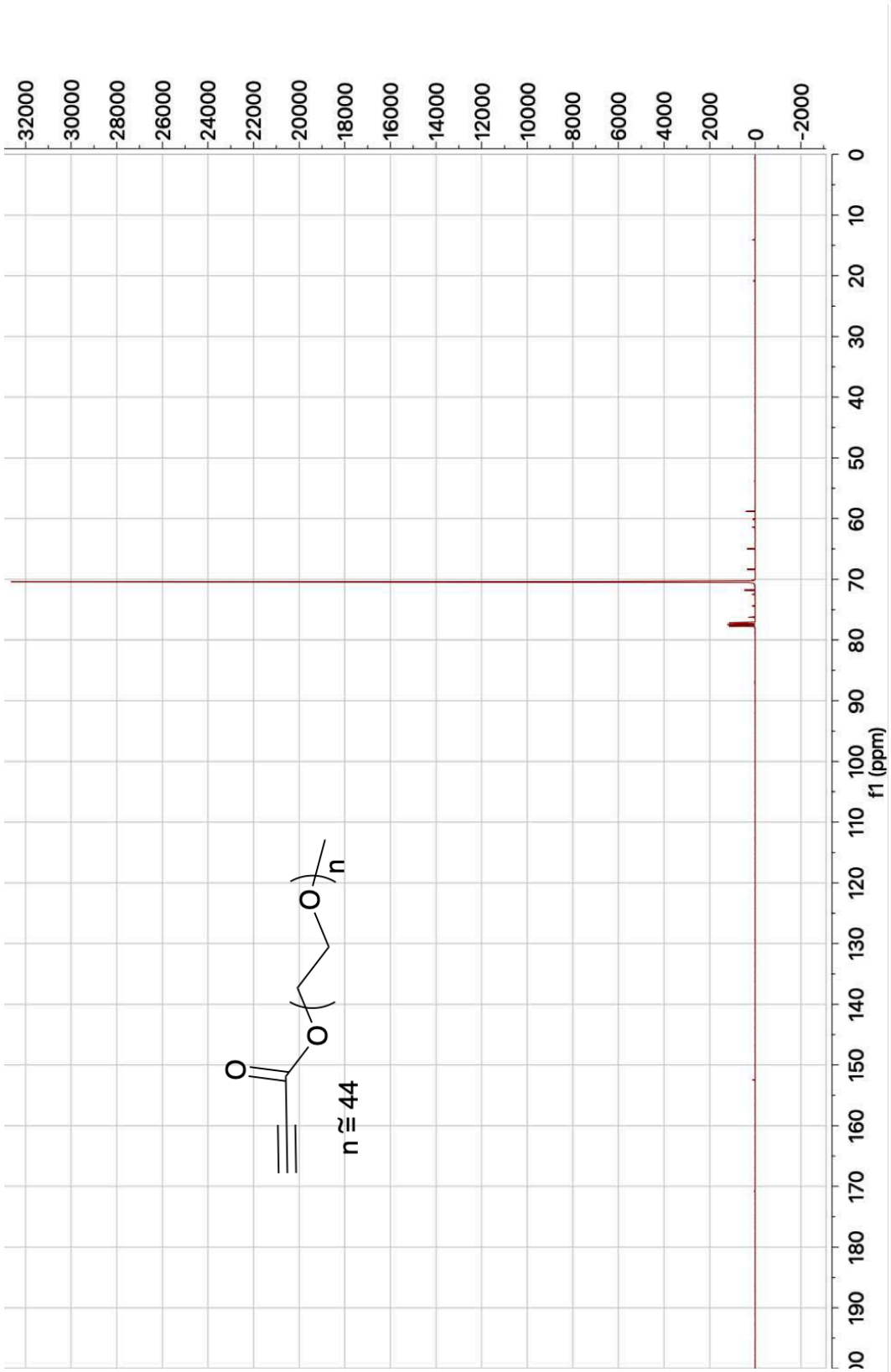
32000
30000
28000
26000
24000
22000
20000
18000
16000
14000
12000
10000
8000
6000
4000
2000
0
-2000
0
10
20
30
40
50
60
70
80
90
100
110
120
130
140
150
160
170
180
190
f1 (ppm)
O
O
O
n
n ≅ 44

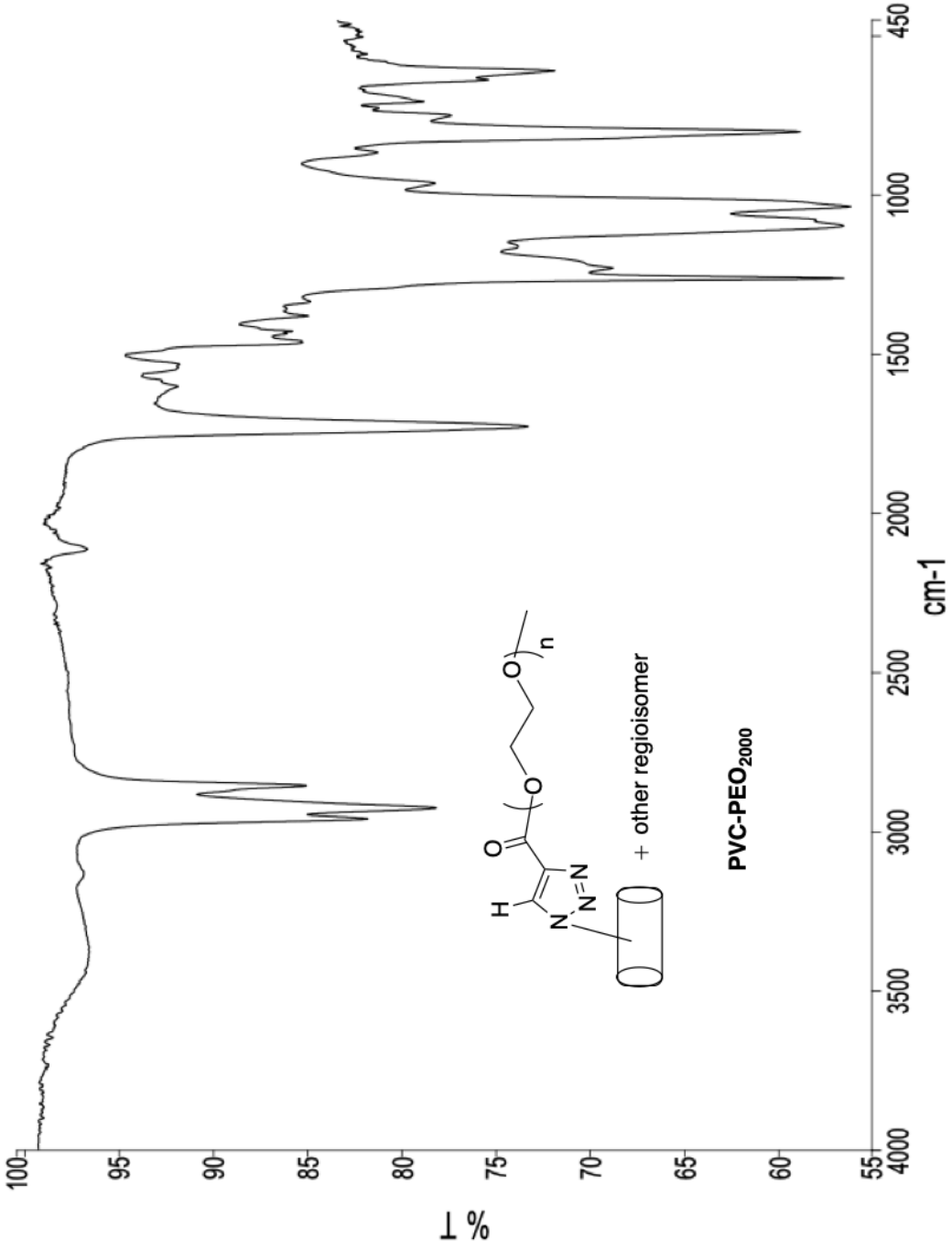
100
95
90
85
80
75
70
65
60
55
% T
4000
3500
3000
2500
2000
1500
1000
450
cm-1
O
O
n
O
O
H
N
N
N
+ other regioisomer
PVC-PEO2000


50000
45000
40000
35000
30000
25000
20000
15000
10000
5000
0
-5000
0.5
1.0
1.5
2.0
2.5
3.0
3.5
4.0
4.5
5.0
5.5
6.0
6.5
7.0
7.5
8.0
8.5
9.0
9.5
f1 (ppm)
O
O
O
O
CF3
CF3
2.56

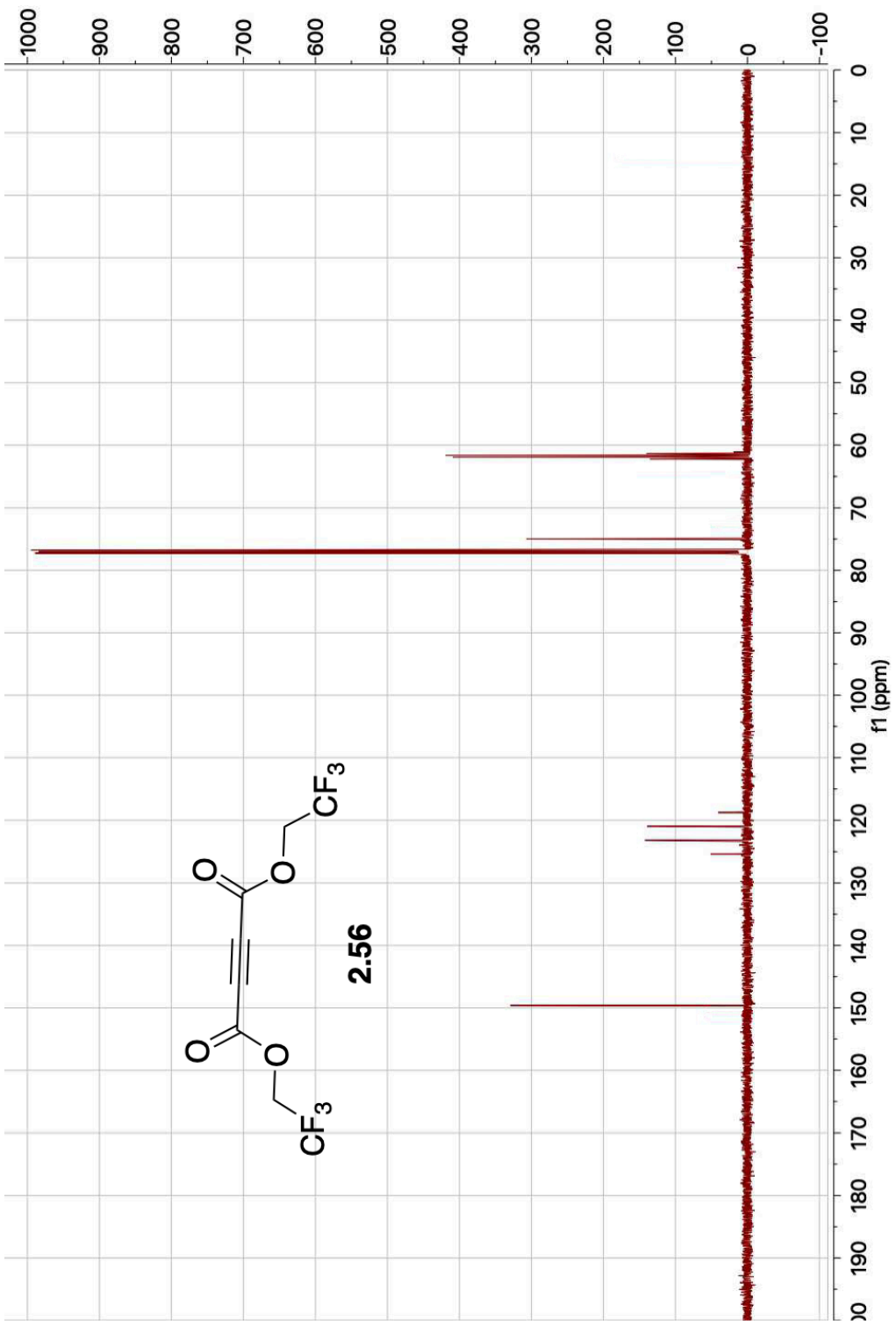
f1 (ppm)
2.56


50000
45000
40000
35000
30000
25000
20000
15000
10000
5000
0
-10
-20
-30
-40
-50
-60
-70
-80
-90
-100
-110
-120
-130
-140
-150
-160
-170
-180
-190
-200
f1 (ppm)
O
O
O
O
CF3
CF3
2.56

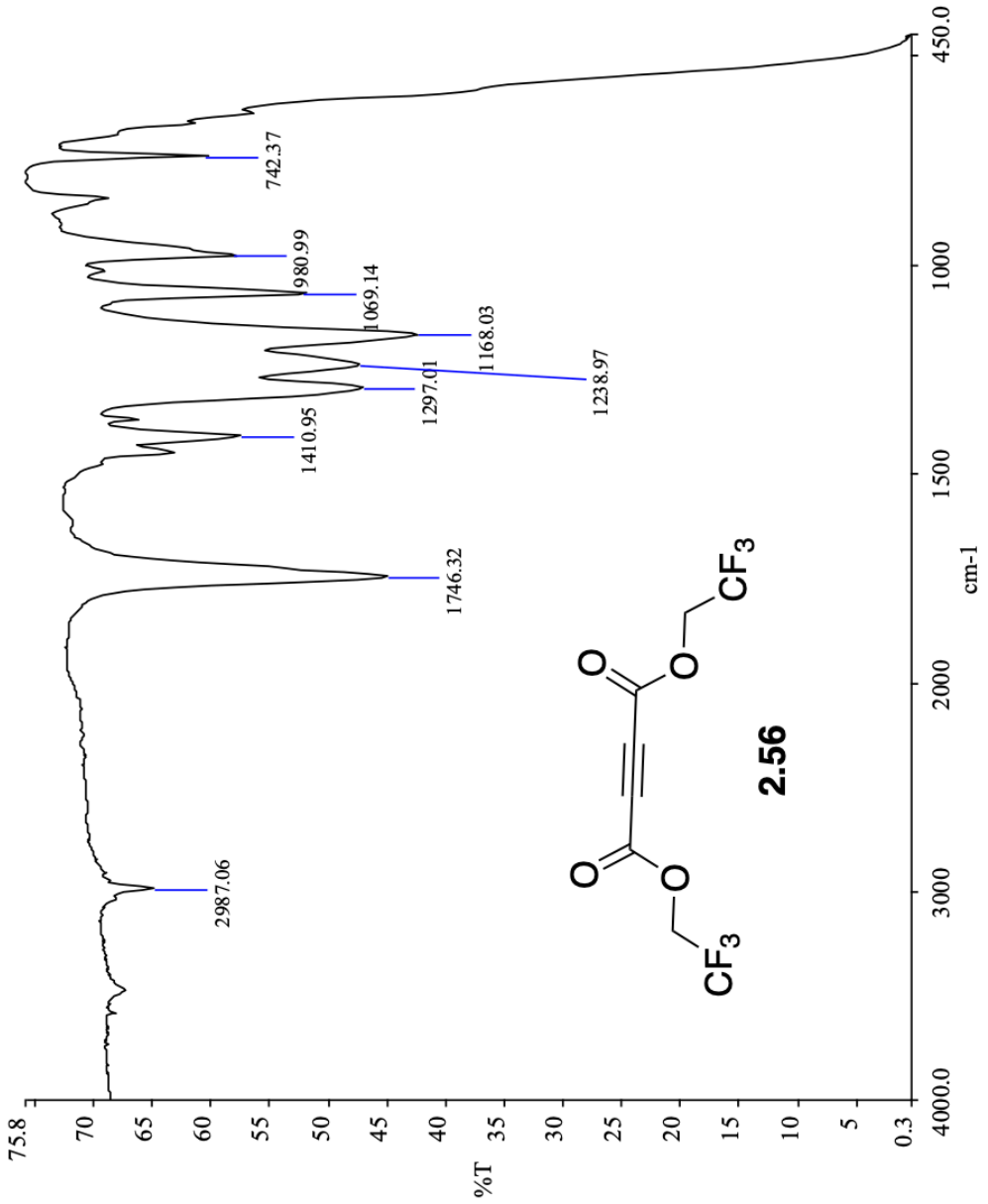
742.37
980.99
1069.14
1168.03
1238.97
1297.01
1410.95
1746.32
2987.06
%T
cm-1
2.56
CF3
CF3

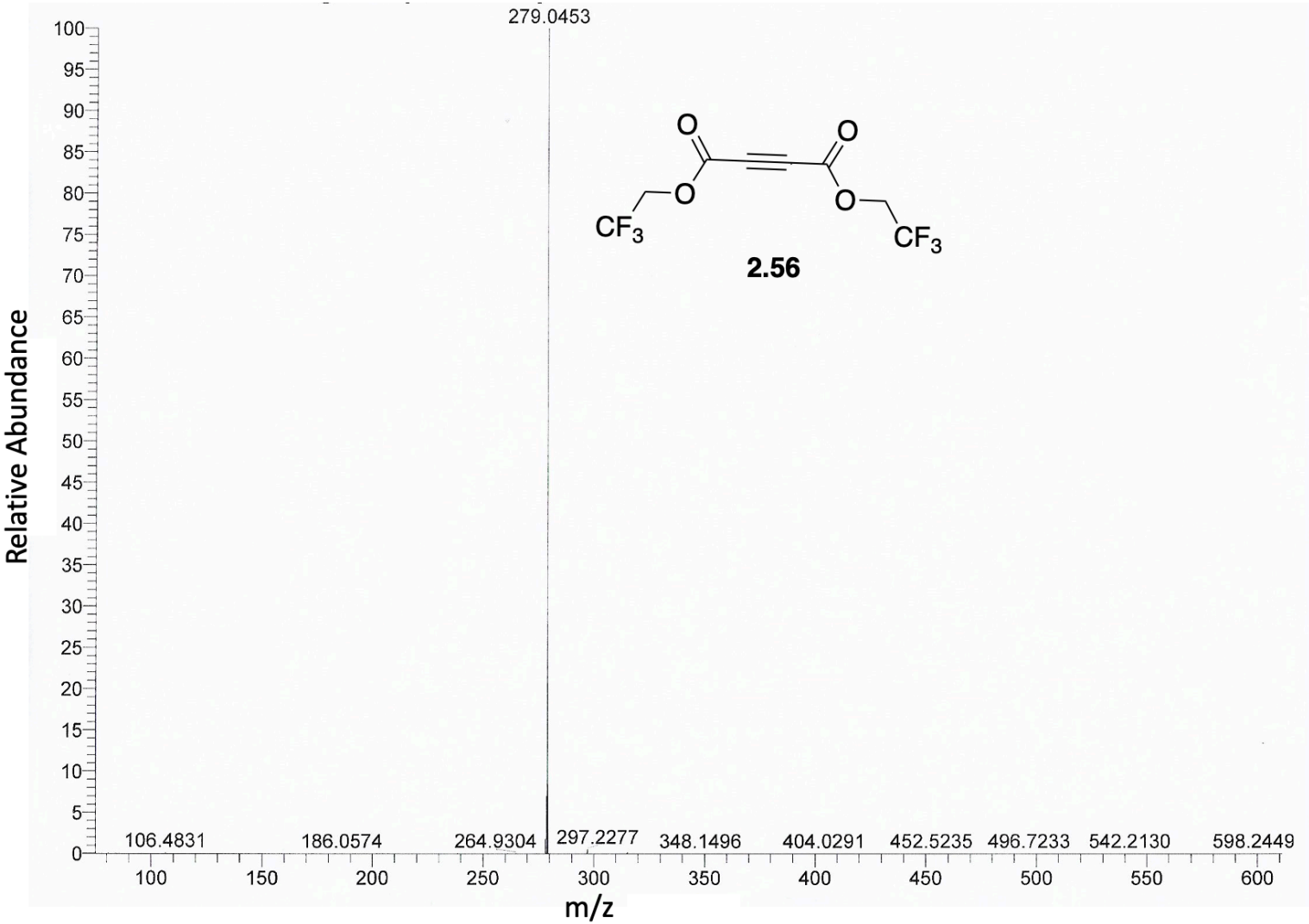
279.0453
Relative Abundance
m/z
106.4831
186.0574
264.9304
297.2277
348.1496
404.0291
452.5235
496.7233
542.2130
598.2449
O
O
O
O
CF3
CF3
2.56

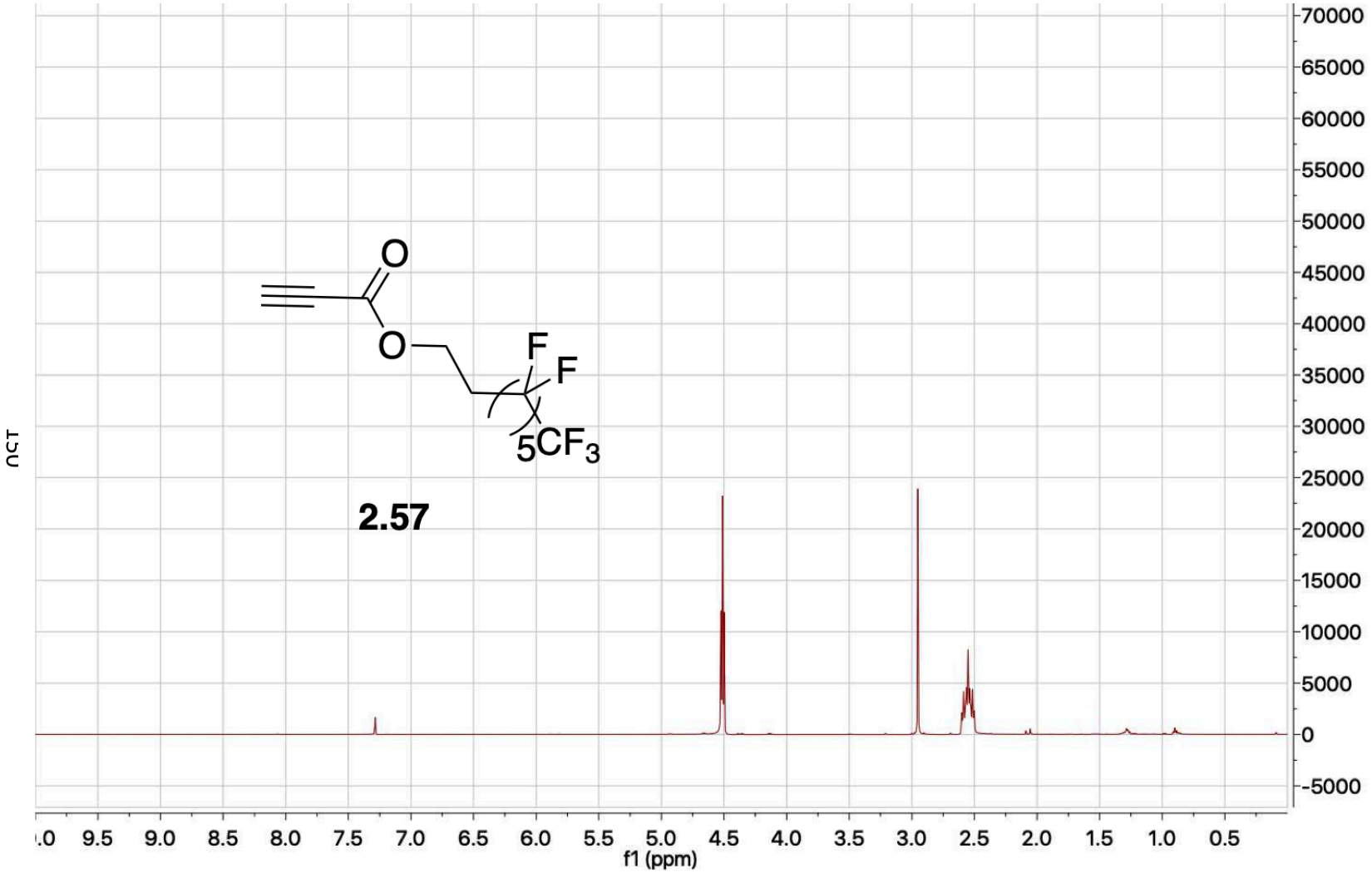
O
O
F
F
5CF3
2.57
70000
65000
60000
55000
50000
45000
40000
35000
30000
25000
20000
15000
10000
5000
0
-5000
9.5
9.0
8.5
8.0
7.5
7.0
6.5
6.0
5.5
5.0
4.5
4.0
3.5
3.0
2.5
2.0
1.5
1.0
0.5
f1 (ppm)

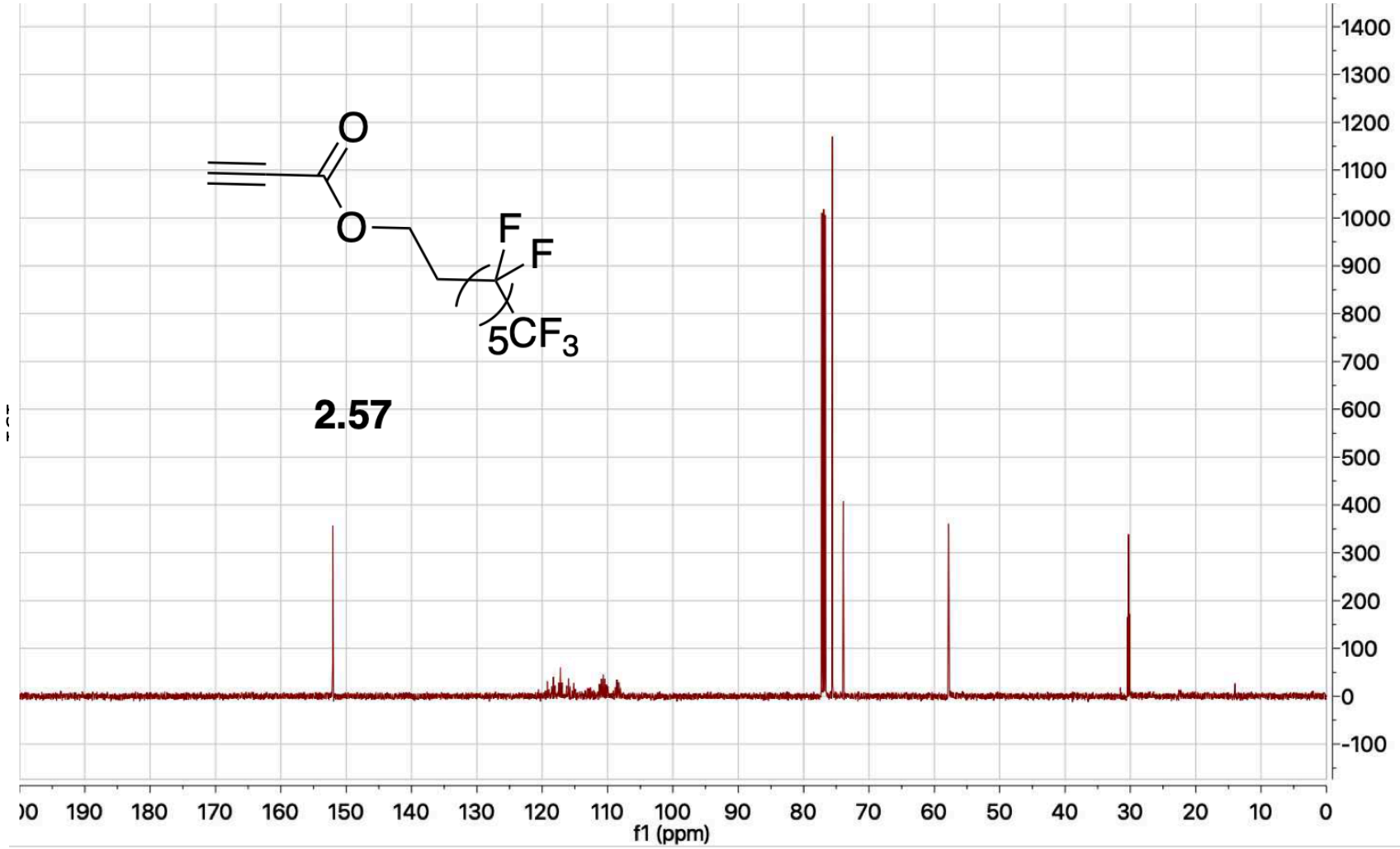
O
O
F
F
5CF3
2.57
1400
1300
1200
1100
1000
900
800
700
600
500
400
300
200
100
0
-100
190
180
170
160
150
140
130
120
110
100
90
80
70
60
50
40
30
20
10
0
f1 (ppm)

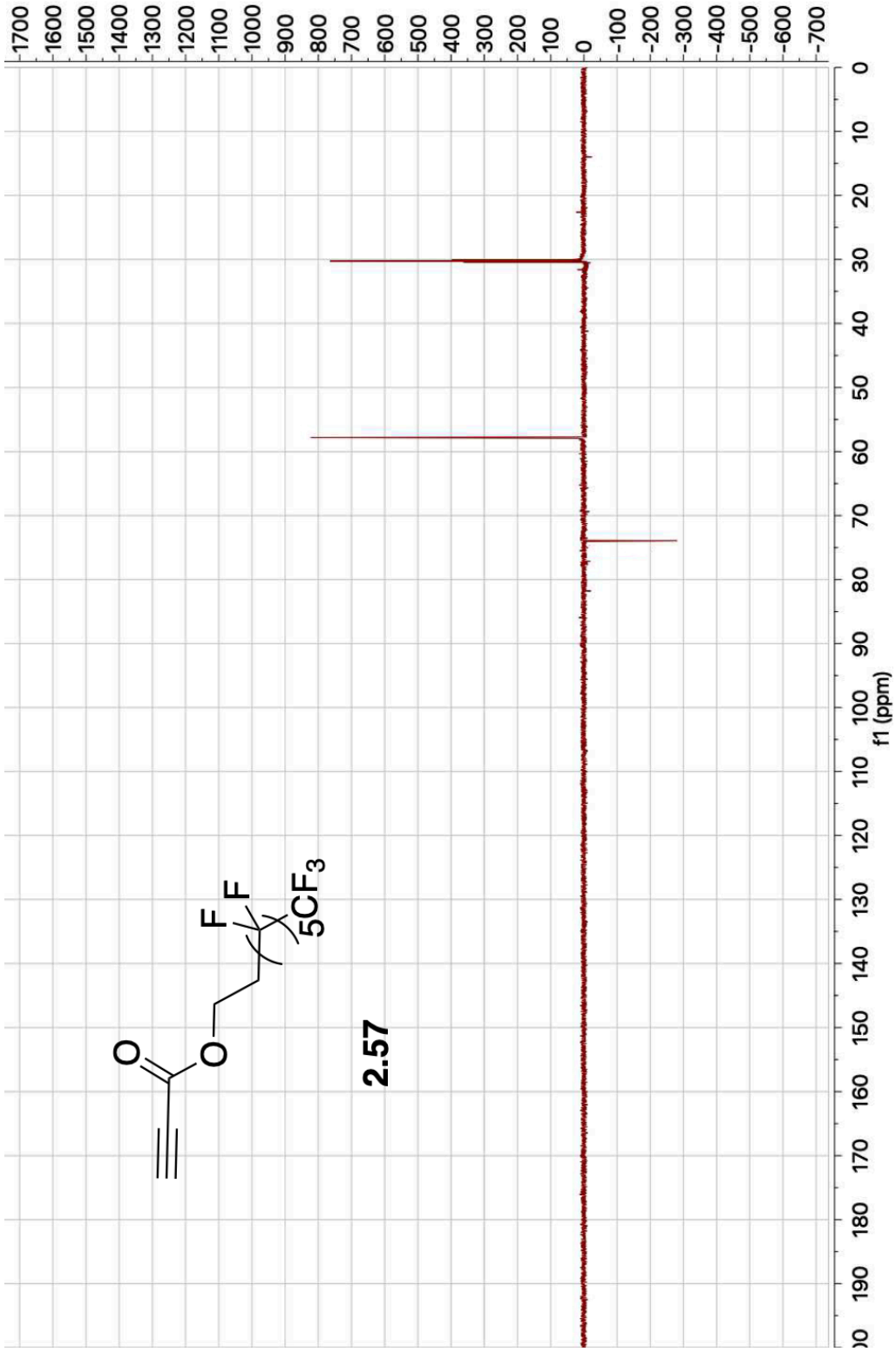
O
O
F
F
5CF3
2.57
f1 (ppm)

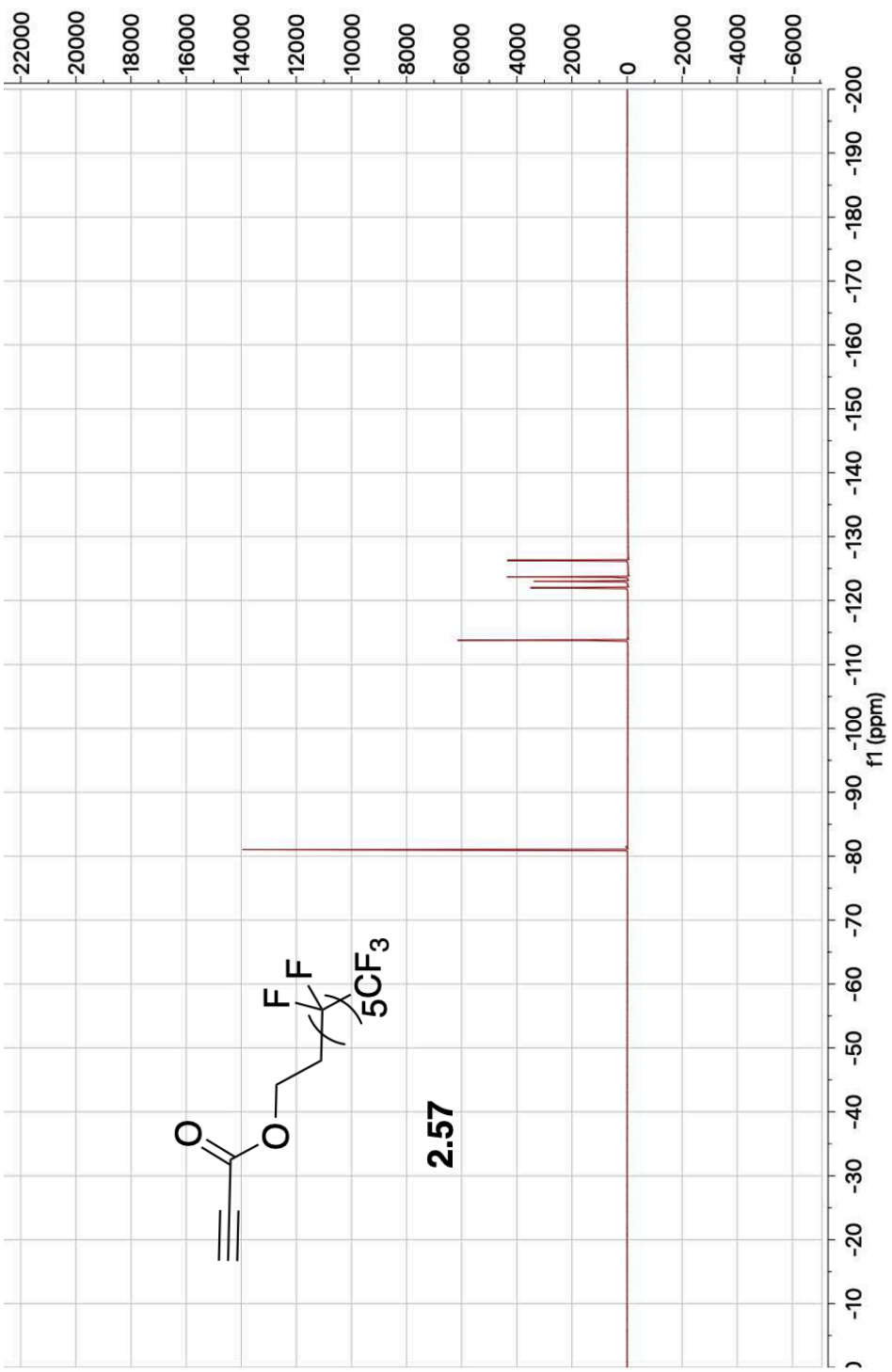
22000
20000
18000
16000
14000
12000
10000
8000
6000
4000
2000
0
-2000
-4000
-6000
-200
-190
-180
-170
-160
-150
-140
-130
-120
-110
-100
-90
-80
-70
-60
-50
-40
-30
-20
-10
f1 (ppm)
O
O
F
F
5CF3
2.57

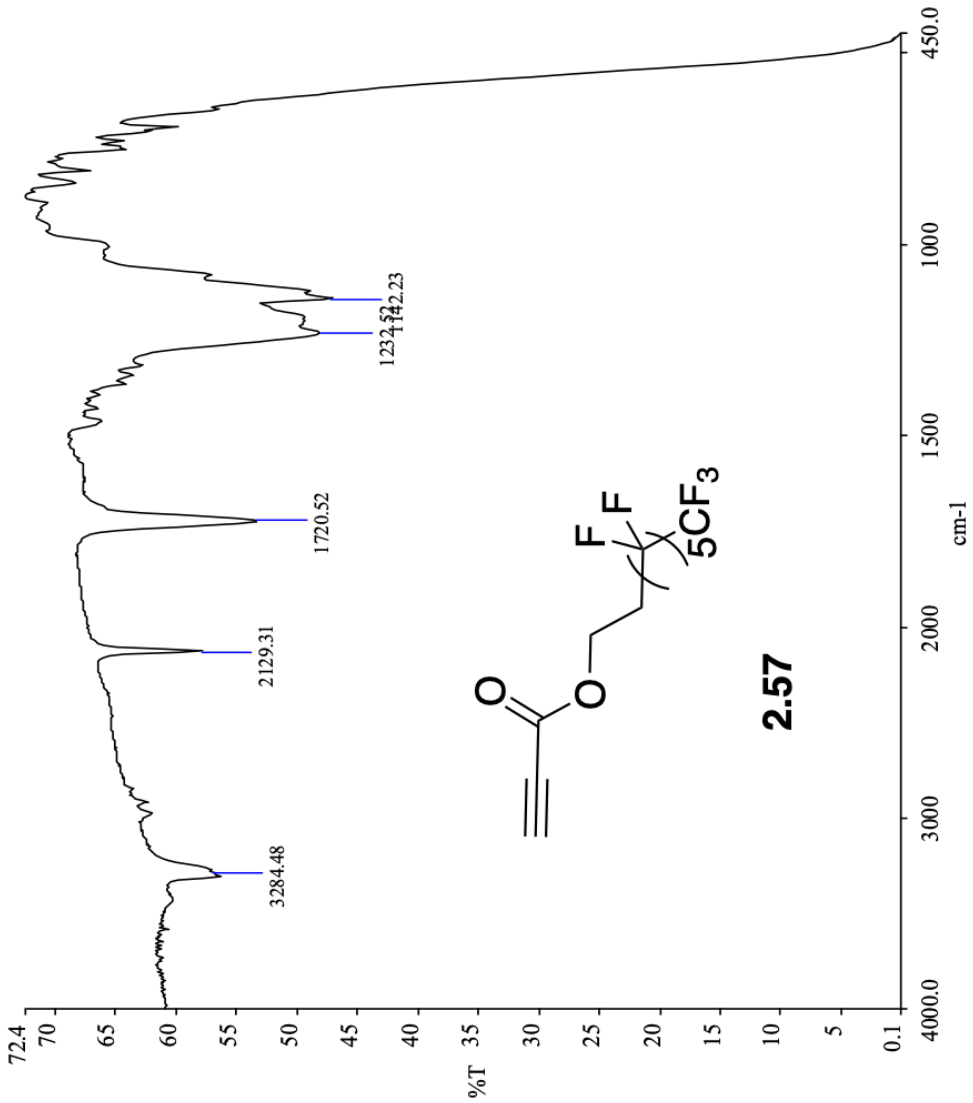
3284.48
2129.31
1720.52
1232.52
1142.23
%T
cm-1
72.4
70
65
60
55
50
45
40
35
30
25
20
15
10
5
0.1
4000.0
3000
2000
1500
1000
450.0
O
O
F
F
5CF3
2.57

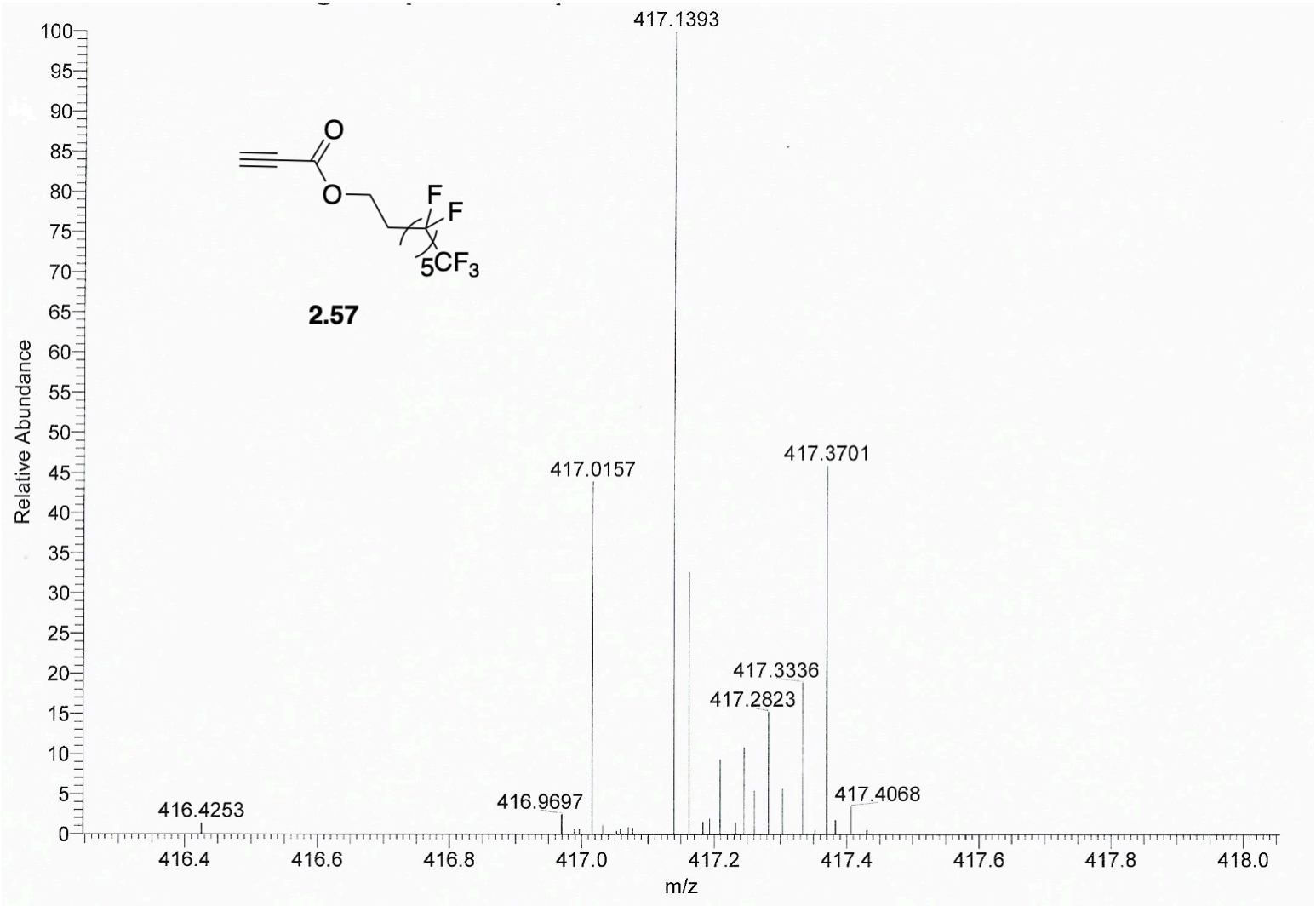
417.1393
100
95
90
85
80
75
70
65
60
55
50
45
40
35
30
25
20
15
10
5
0
Relative Abundance
O
O
F
F
5CF3
2.57
417.0157
417.3701
417.3336
417.2823
416.4253
416.9697
417.4068
416.4
416.6
416.8
417.0
417.2
417.4
417.6
417.8
418.0
m/z

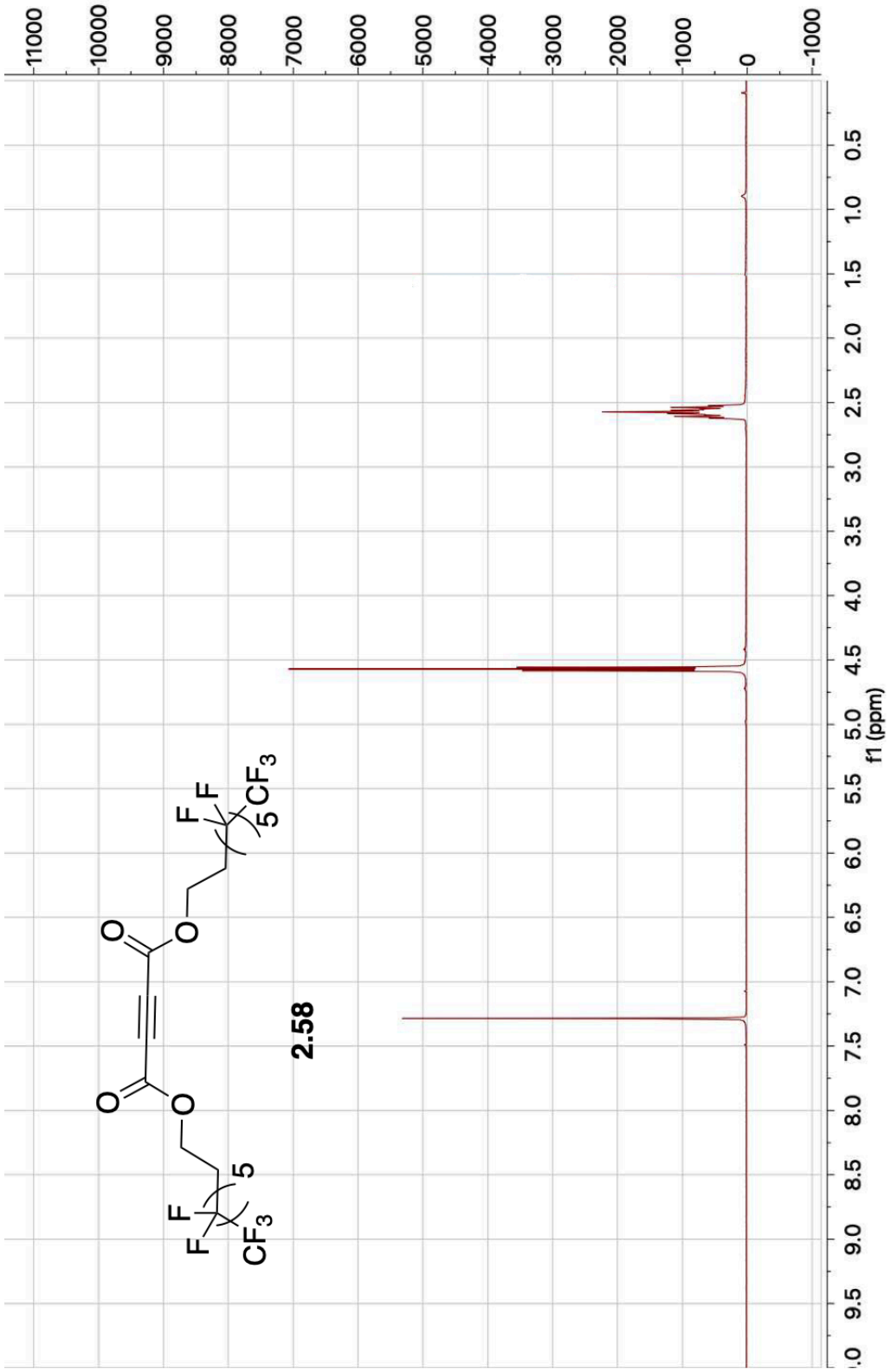
2.58
f1 (ppm)

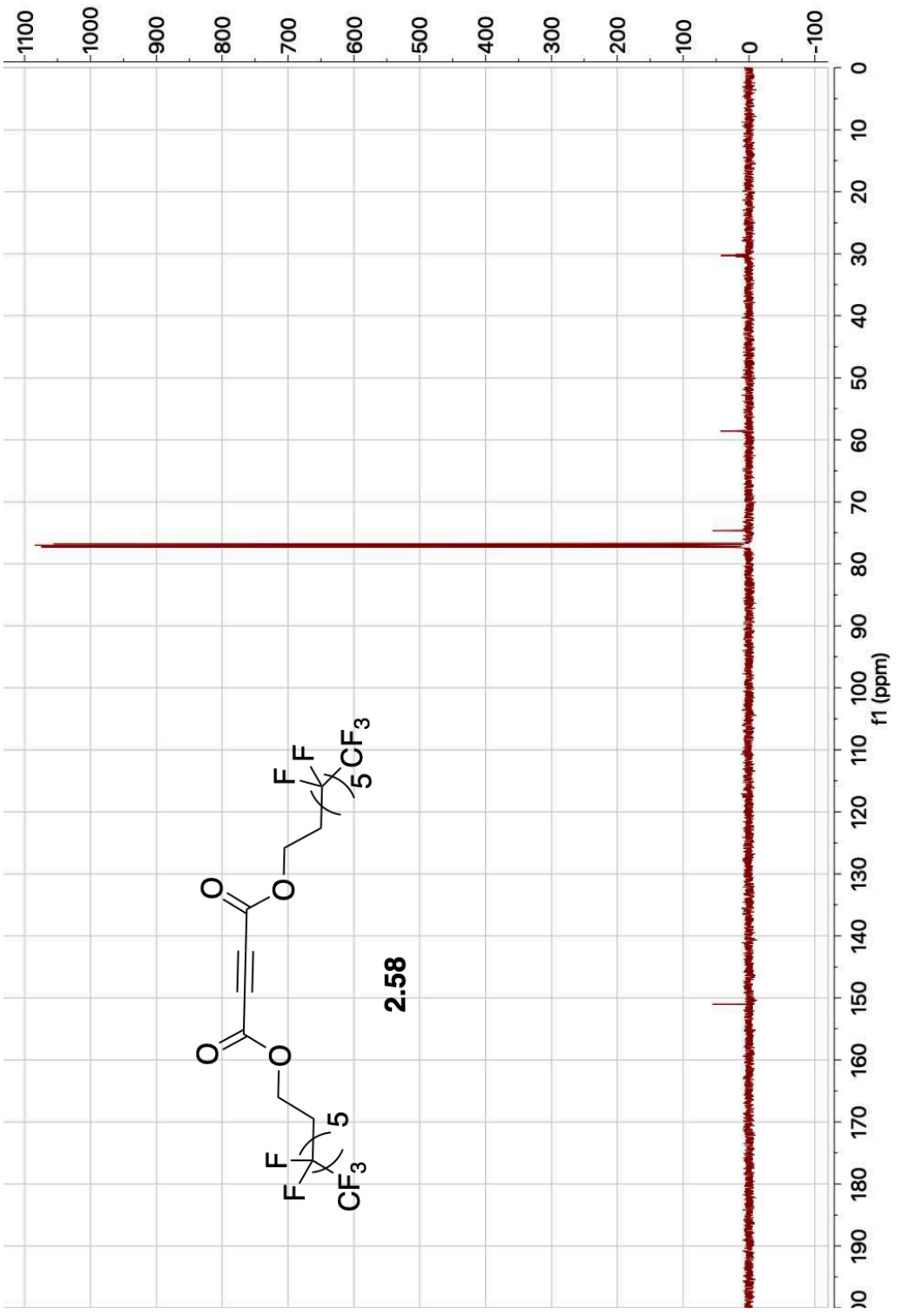
f1 (ppm)
2.58

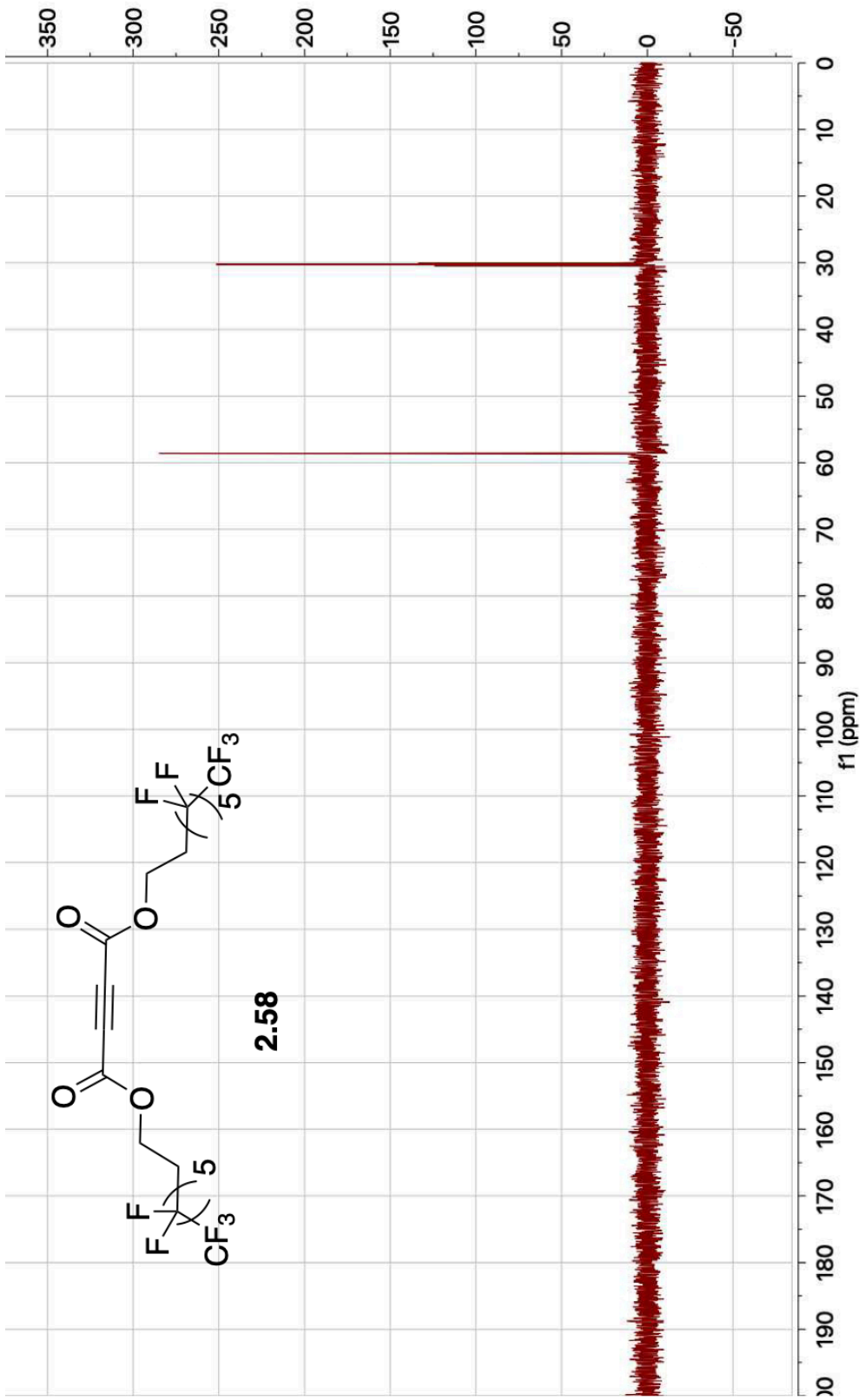
2.58
f1 (ppm)

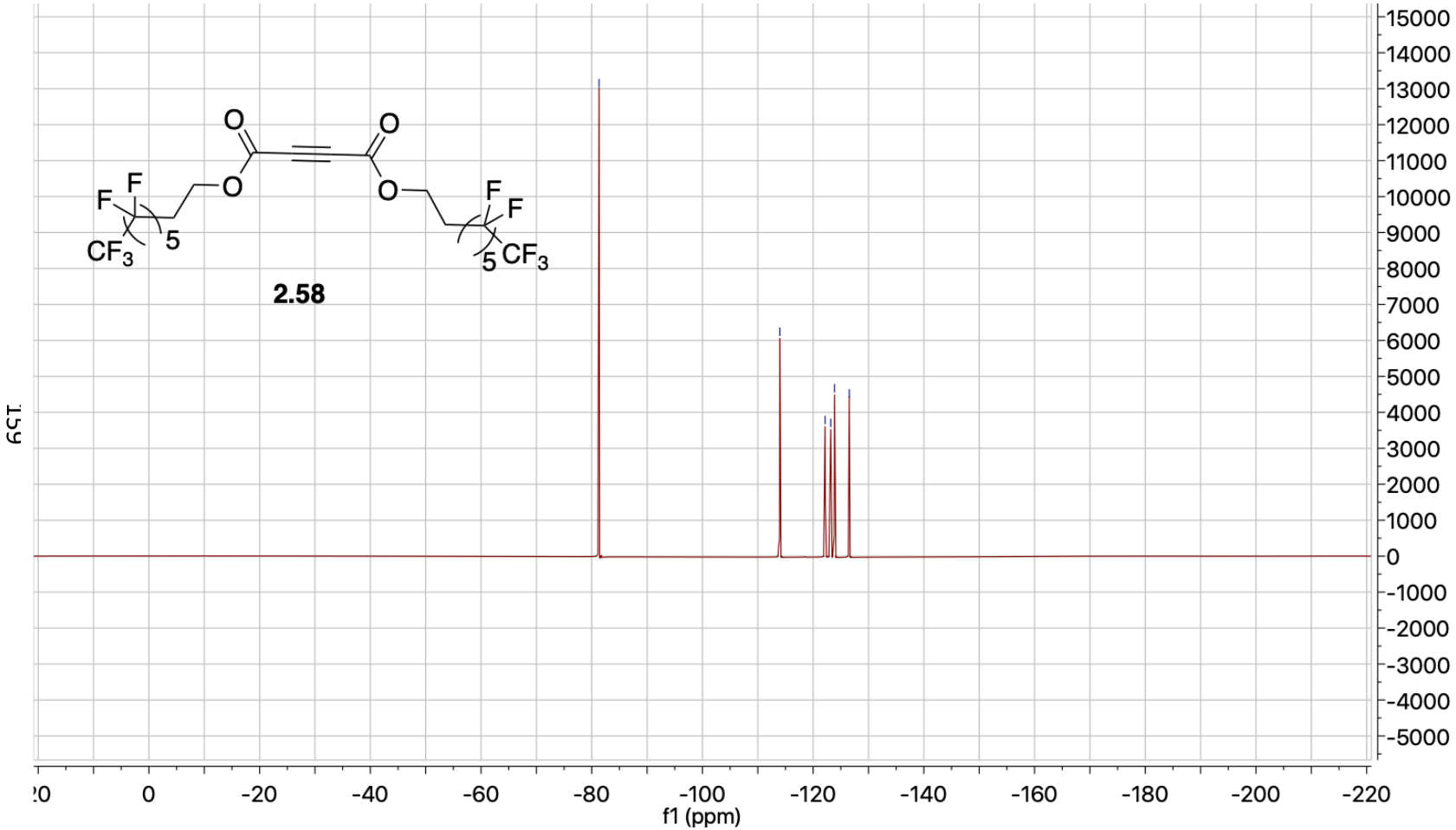
O
O
O
O
F
F
F
CF3
5
5
CF3
2.58
15000
14000
13000
12000
11000
10000
9000
8000
7000
6000
5000
4000
3000
2000
1000
0
-1000
-2000
-3000
-4000
-5000
0
-20
-40
-60
-80
-100
-120
-140
-160
-180
-200
-220
f1 (ppm)

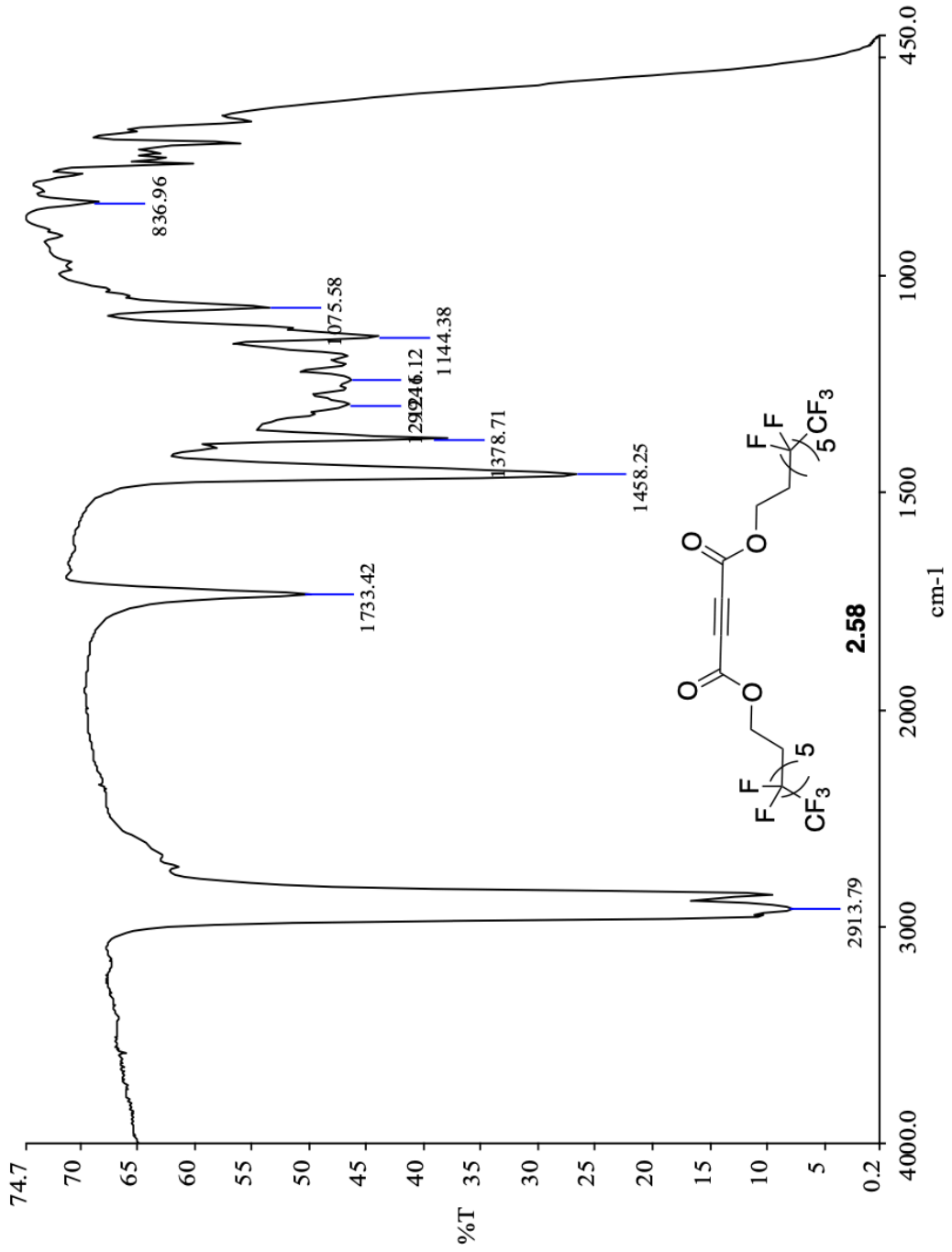
74.7
70
65
60
55
50
45
40
35
30
25
20
15
10
5
0.2
%T
4000.0
3000
2000
1500
1000
450.0
cm-1
2913.79
1733.42
1458.25
1378.71
1144.38
1075.58
836.96
2.58
O
O
O
O
F
F
CF3
5
F
F
CF3
5

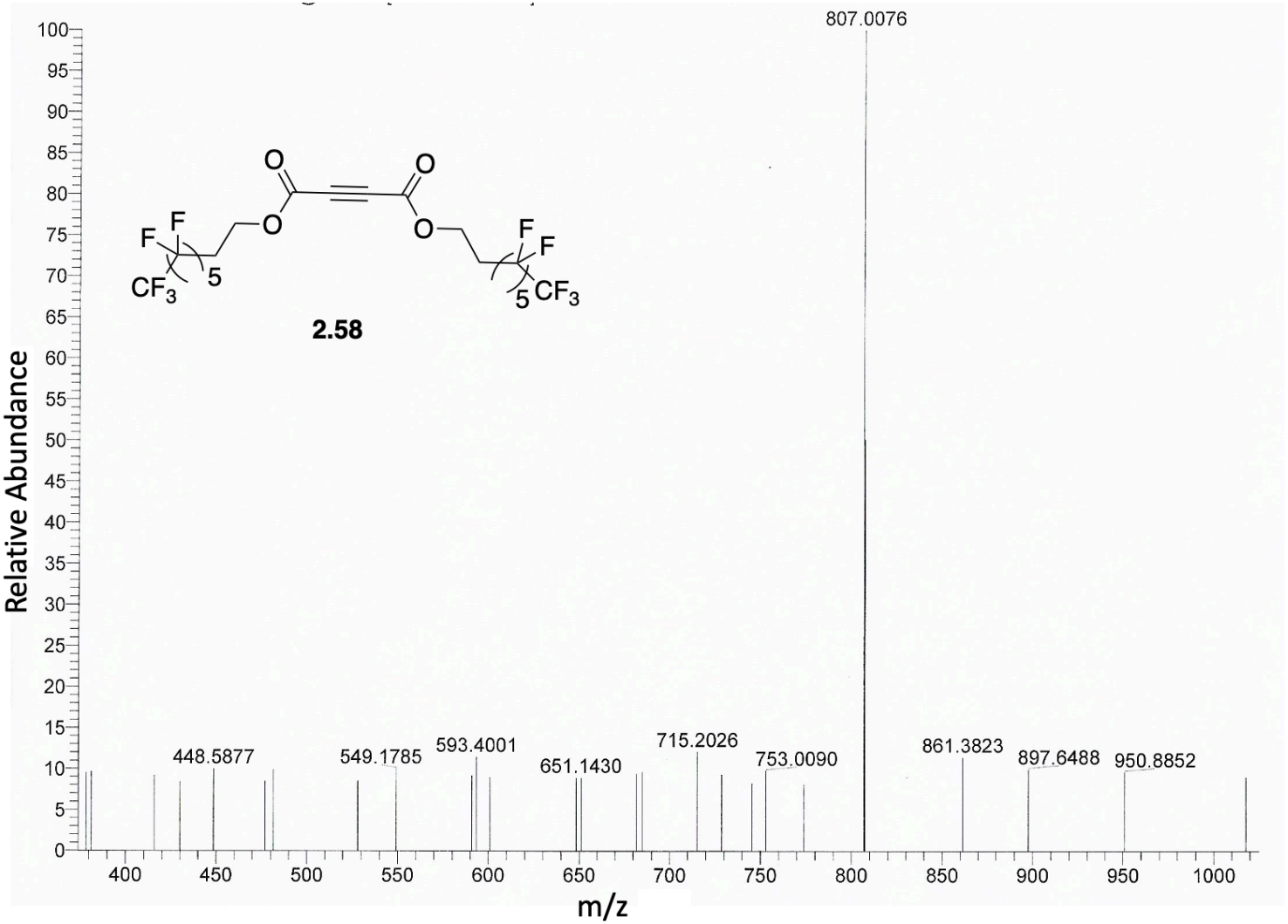
807.0076
448.5877
549.1785
593.4001
651.1430
715.2026
753.0090
861.3823
897.6488
950.8852
Relative Abundance
m/z
2.58

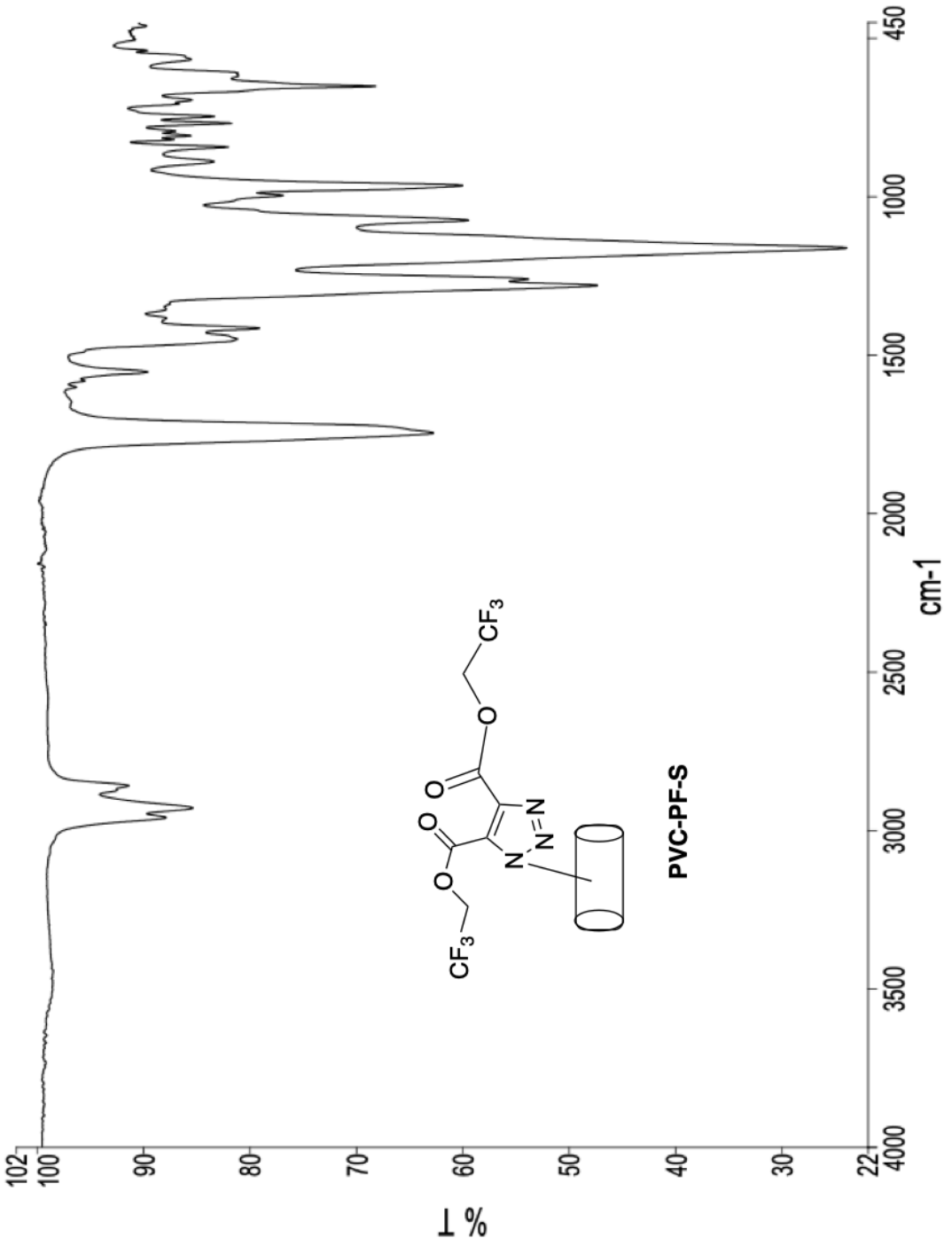
%T
cm-1
PVC-PF-S
CF3
CF3
O
O
O
O
N
N
N

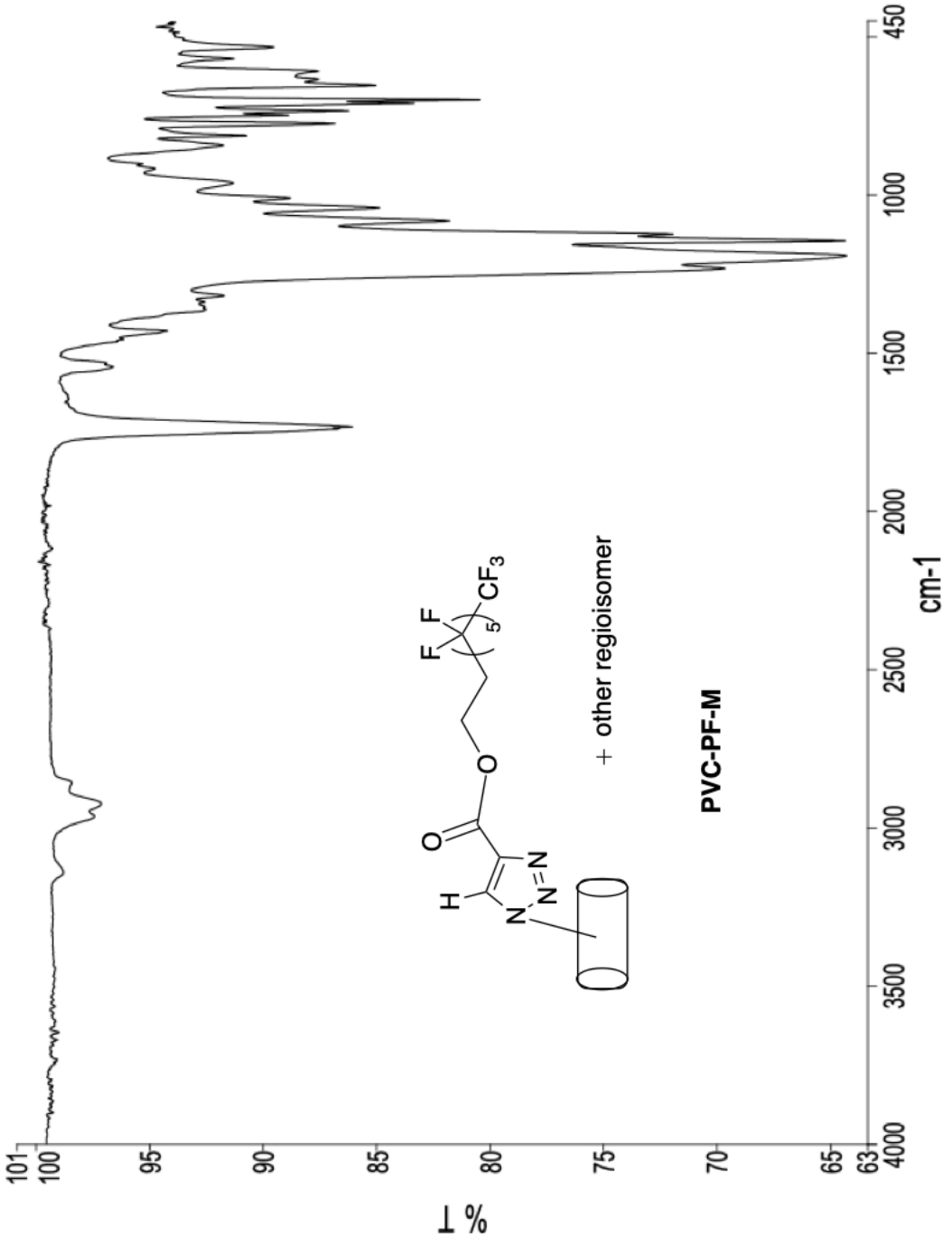
% T
cm-1
PVC-PF-M
+ other regioisomer

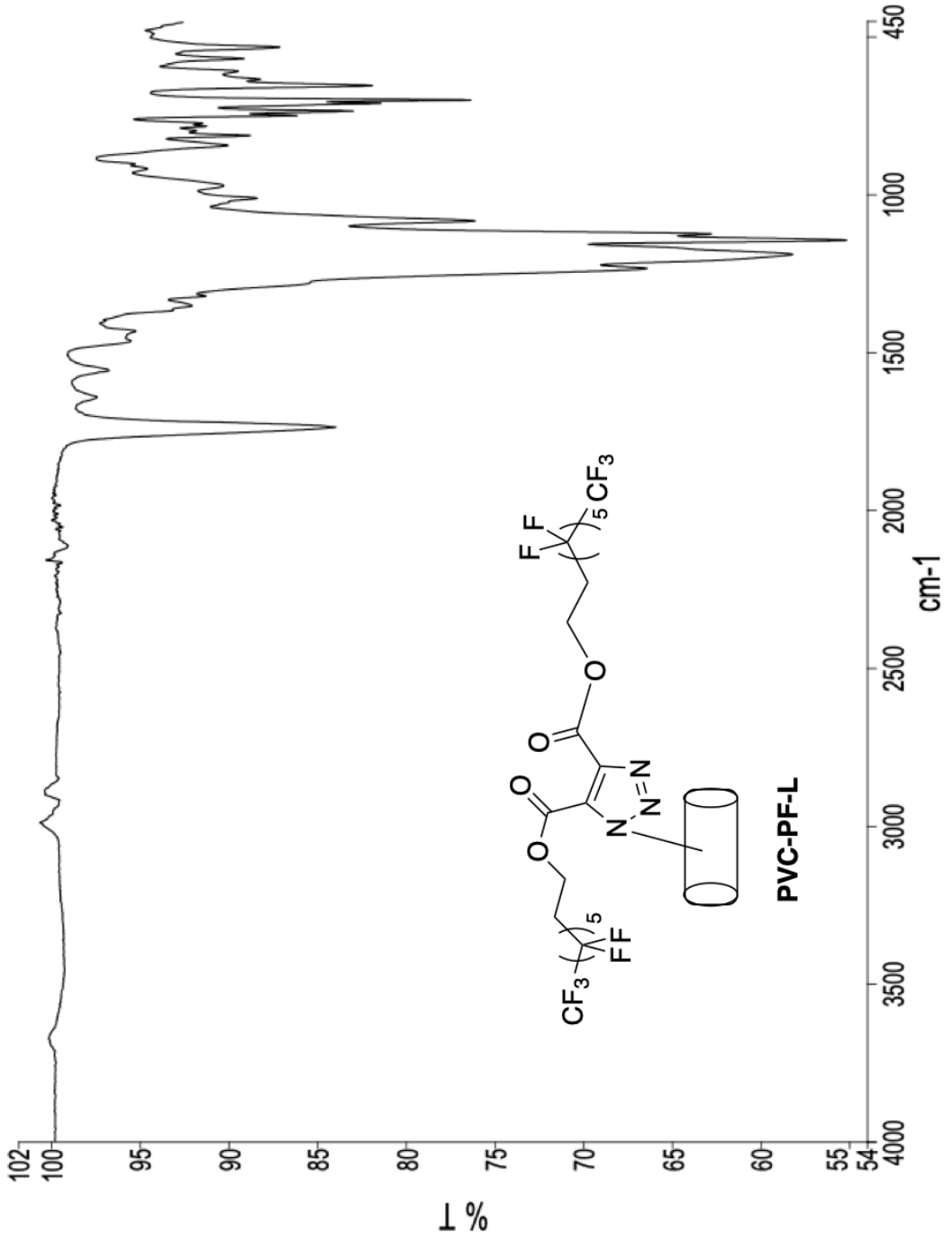
%T
cm-1
PVC-PF-L

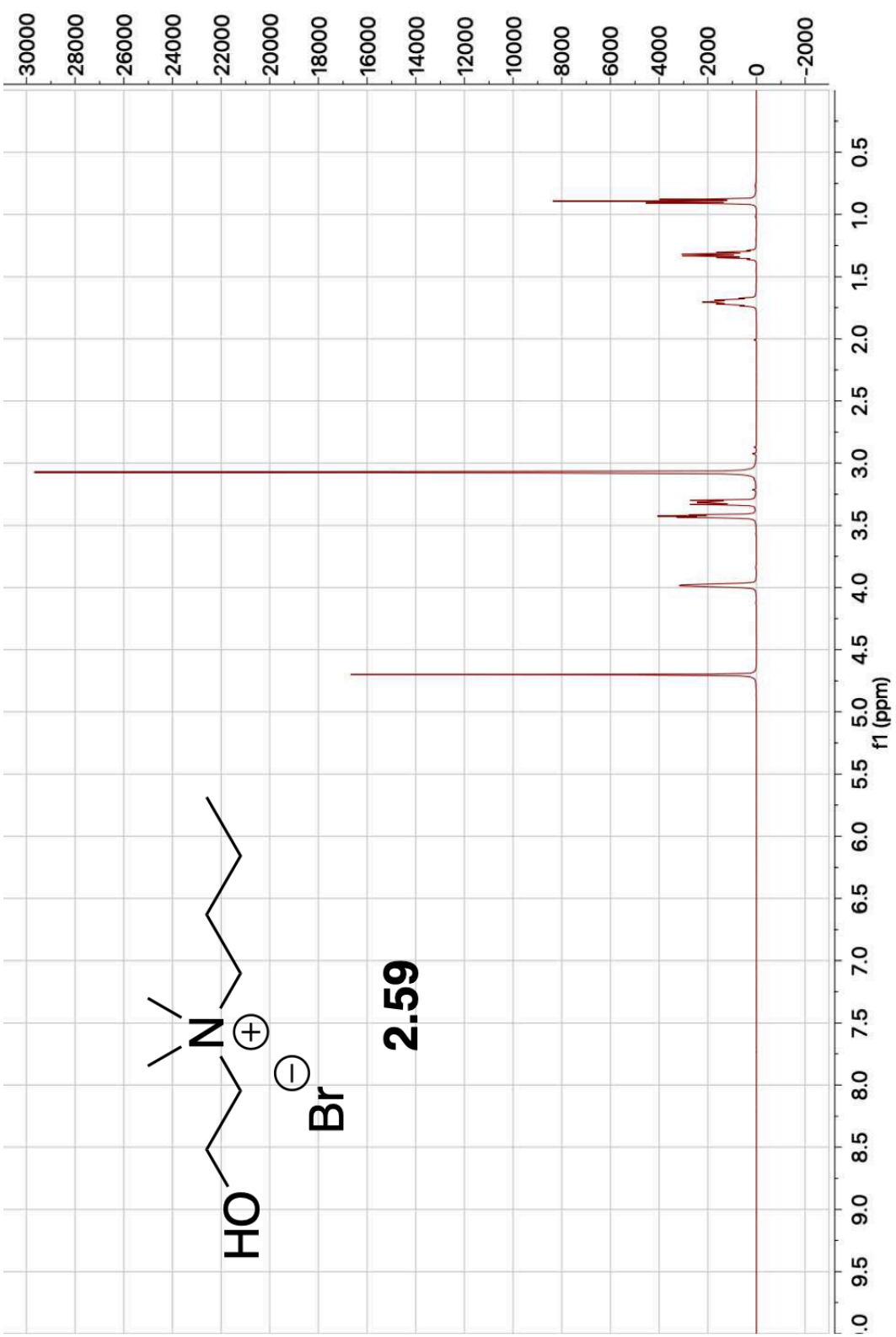
HO
N
Br
2.59
f1 (ppm)

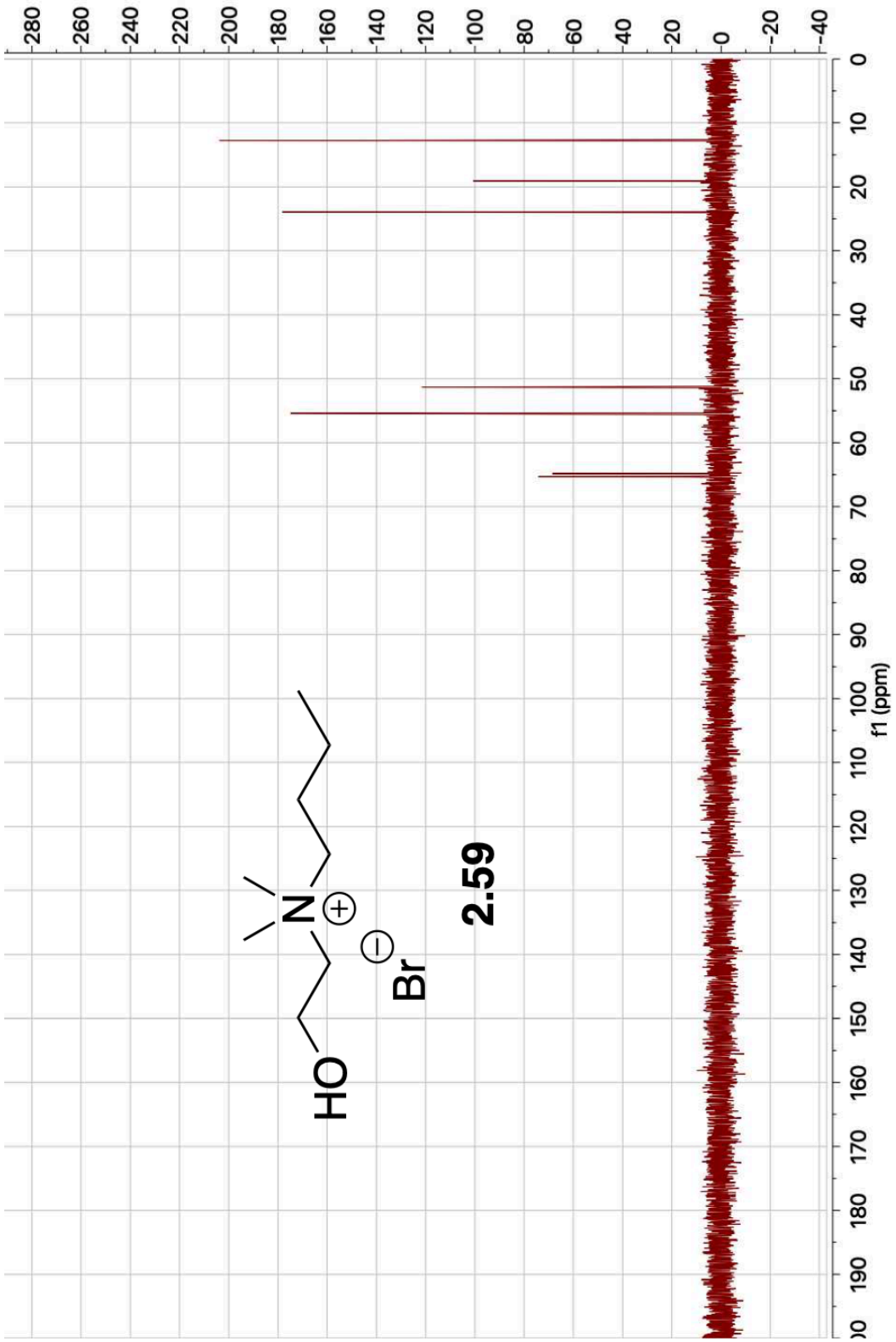
HO
N
Br
2.59
f1 (ppm)

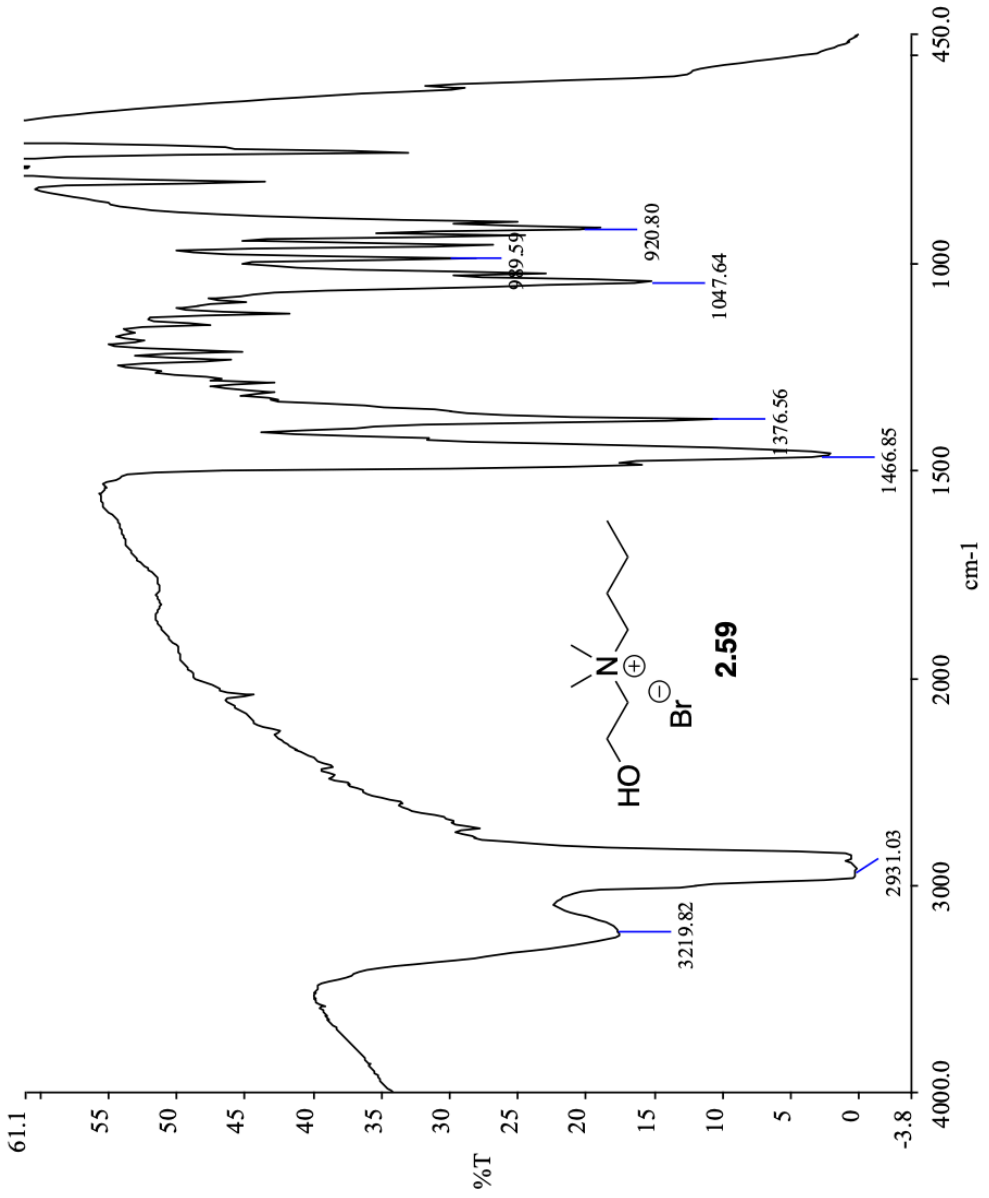
61.1
55
50
45
40
35
30
25
20
15
10
5
0
-3.8
%T
4000.0
3000
2000
1500
1000
450.0
cm-1
3219.82
2931.03
1466.85
1376.56
1047.64
989.59
920.80
HO
N
Br
2.59

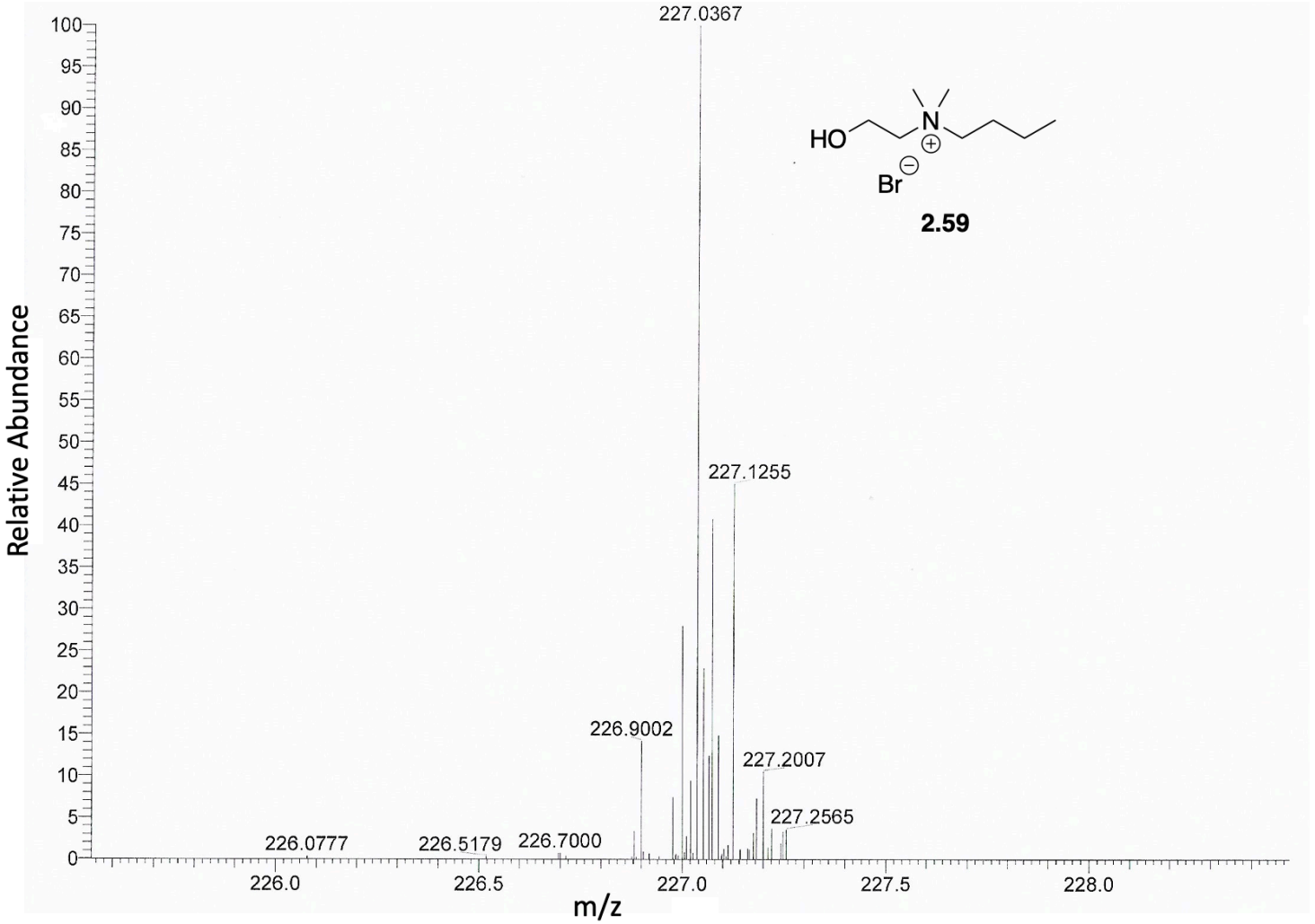
227.0367
227.1255
226.9002
227.2007
227.2565
226.0777
226.5179
226.7000
Relative Abundance
m/z
HO
N
Br
2.59

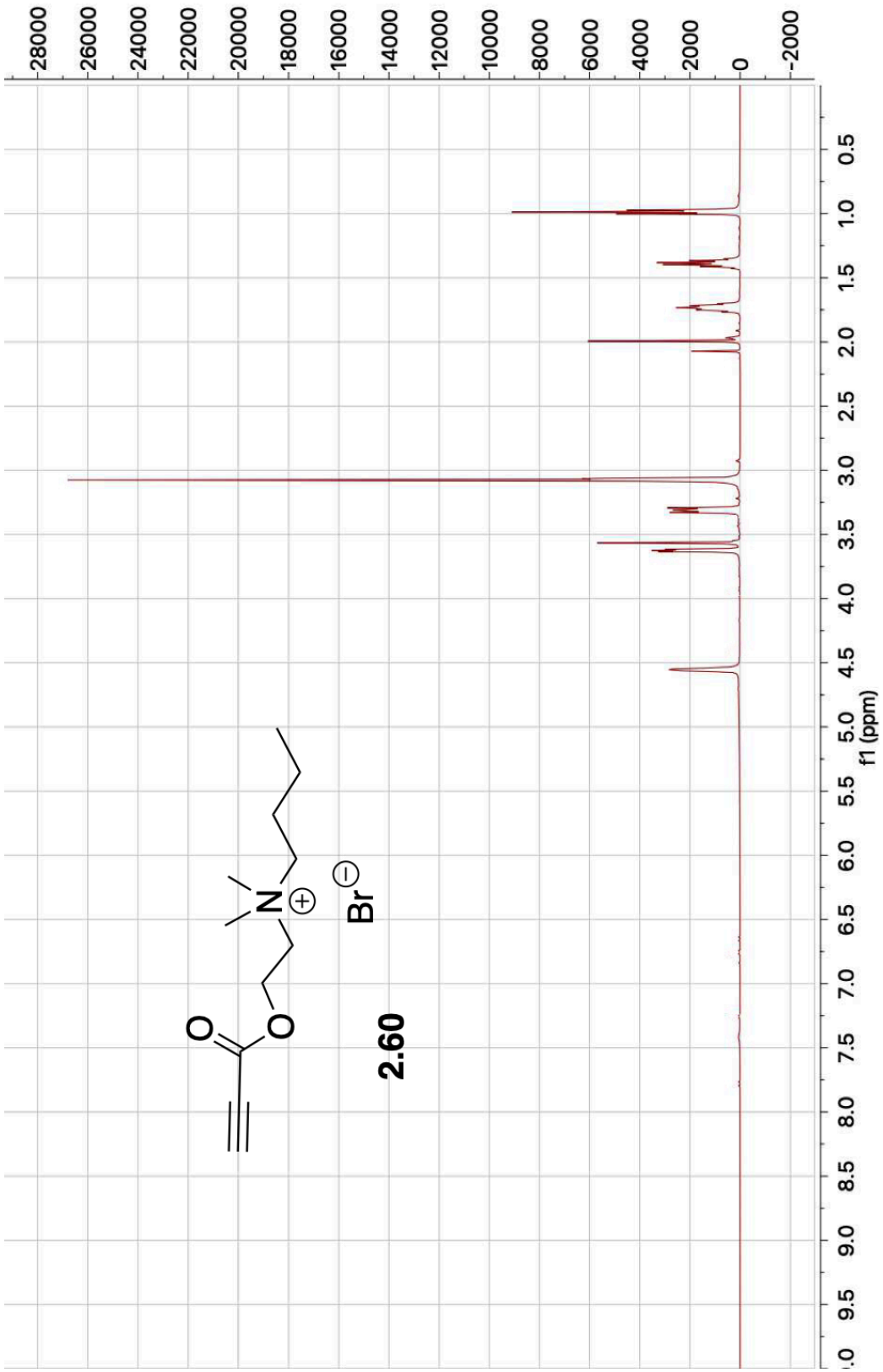
28000
26000
24000
22000
20000
18000
16000
14000
12000
10000
8000
6000
4000
2000
0
-2000
0.5
1.0
1.5
2.0
2.5
3.0
3.5
4.0
4.5
5.0
5.5
6.0
6.5
7.0
7.5
8.0
8.5
9.0
9.5
f1 (ppm)
O
O
N
Br
2.60

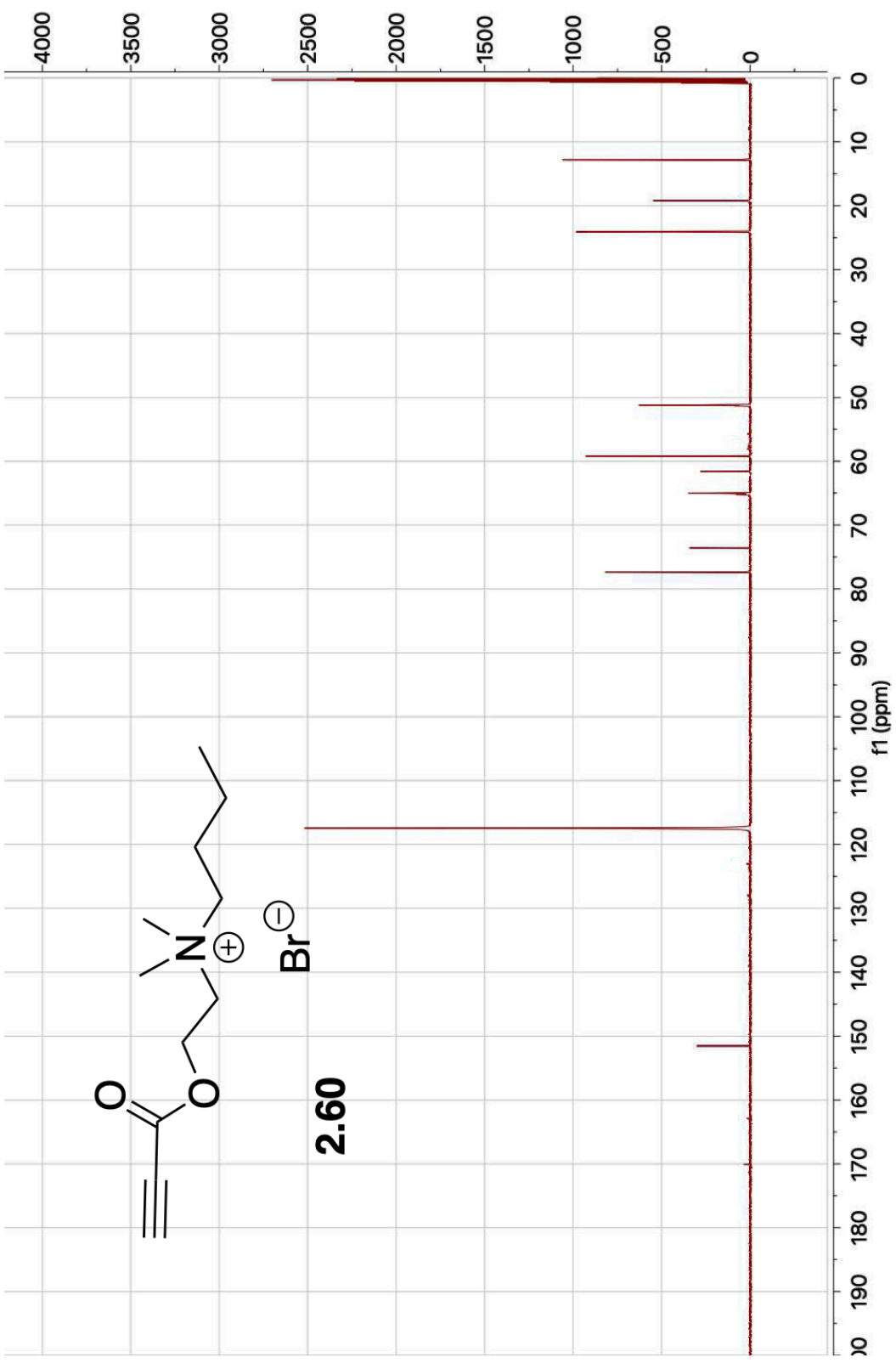
4000
3500
3000
2500
2000
1500
1000
500
0
0
10
20
30
40
50
60
70
80
90
100
110
120
130
140
150
160
170
180
190
200
f1 (ppm)
O
O
N
Br
2.60

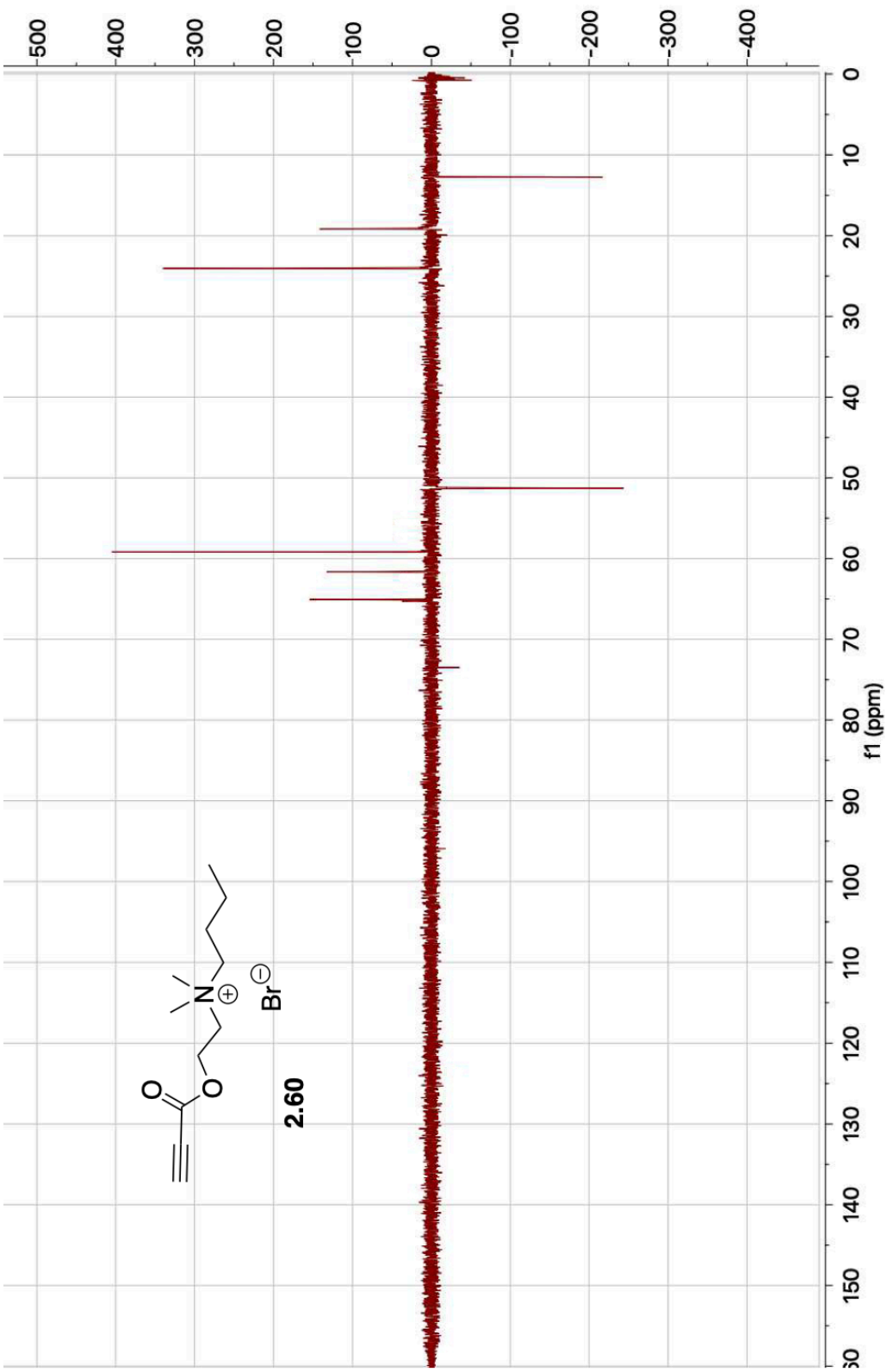
f1 (ppm)
2.60

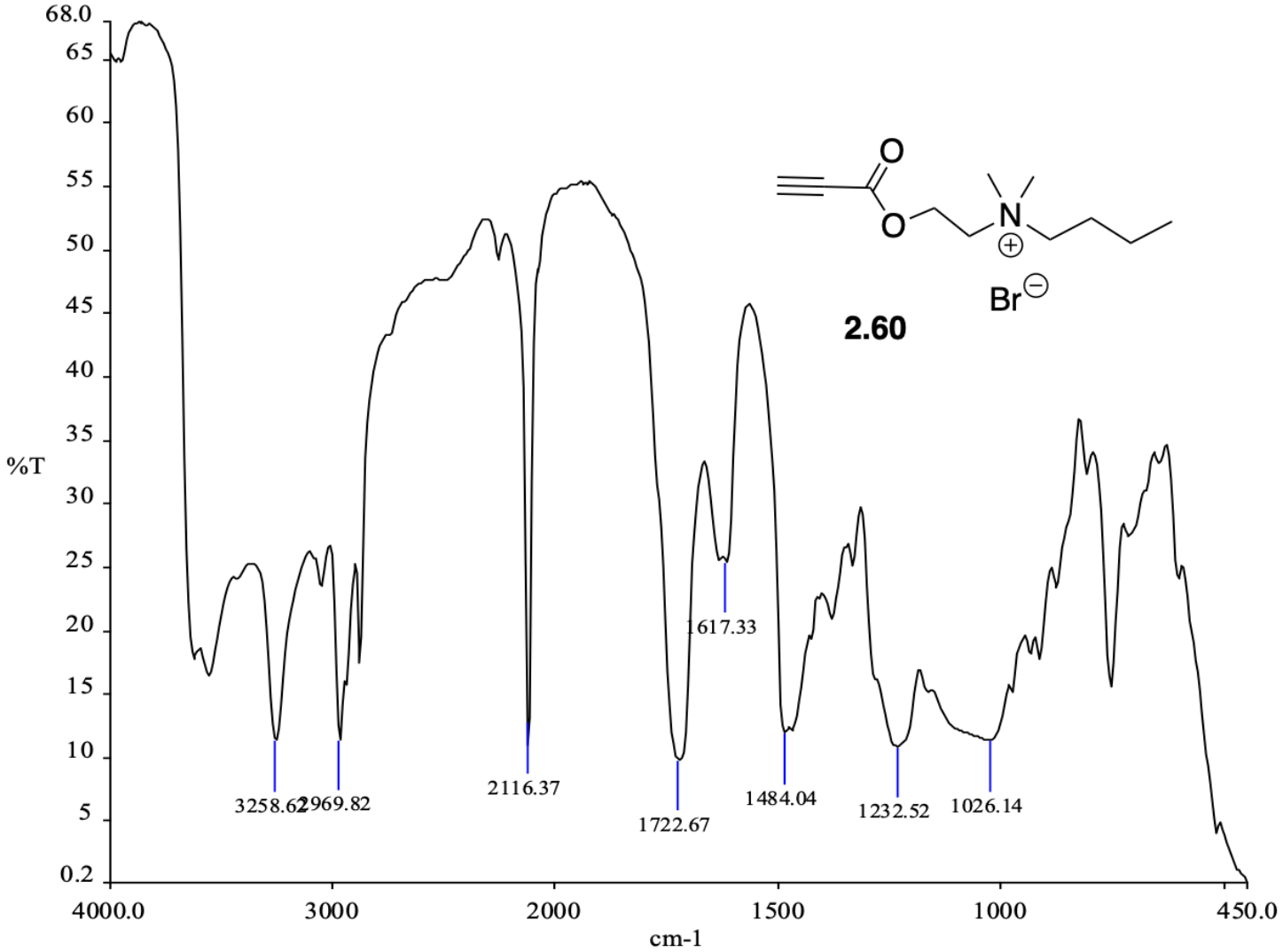
68.0
65
60
55
50
45
40
35
30
25
20
15
10
5
0.2
%T
4000.0
3000
2000
1500
1000
450.0
cm-1
3258.62
2969.82
2116.37
1722.67
1617.33
1484.04
1232.52
1026.14
O
O
N
Br
2.60

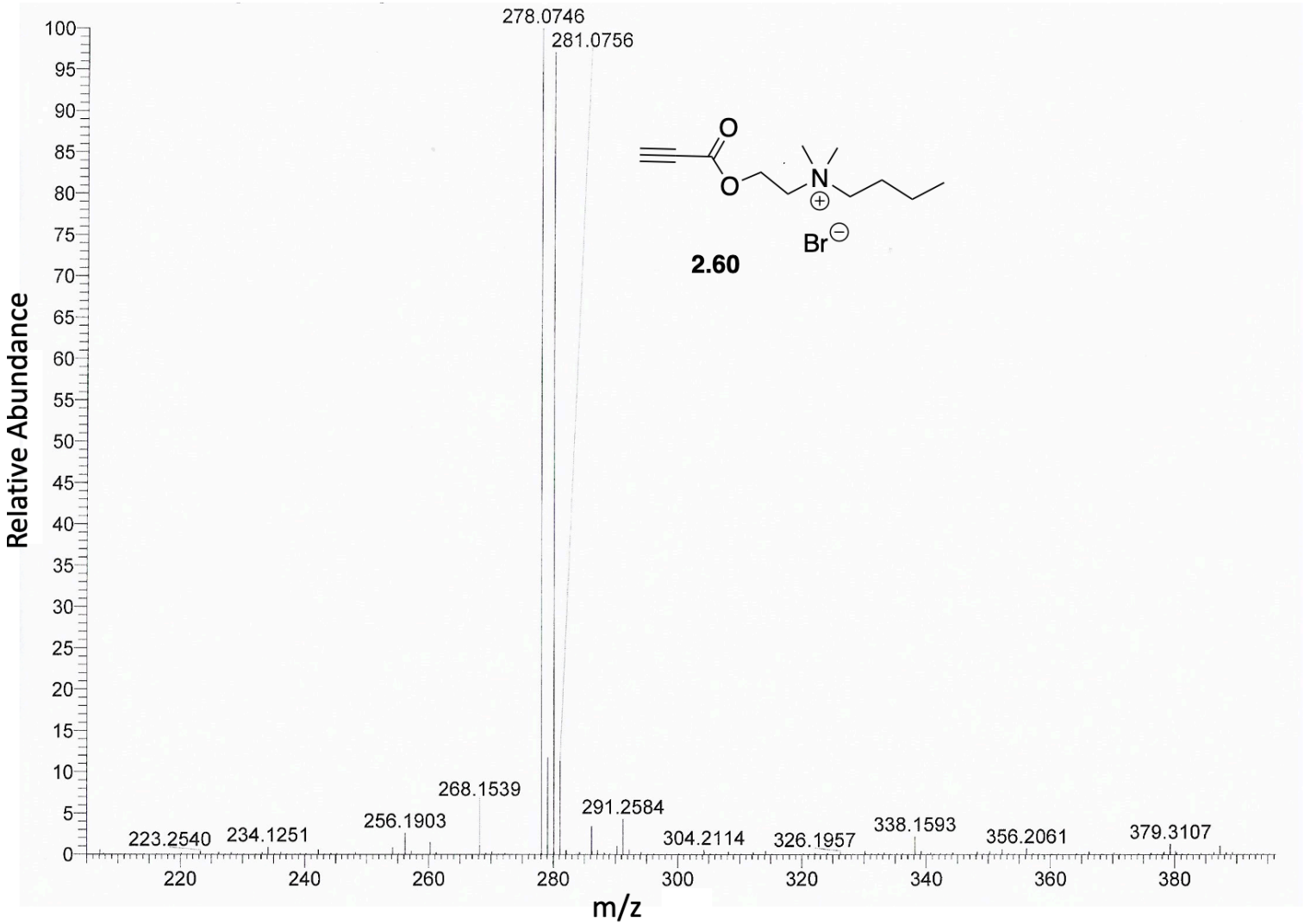
278.0746
281.0756
Relative Abundance
m/z
223.2540
234.1251
256.1903
268.1539
291.2584
304.2114
326.1957
338.1593
356.2061
379.3107
Br
2.60

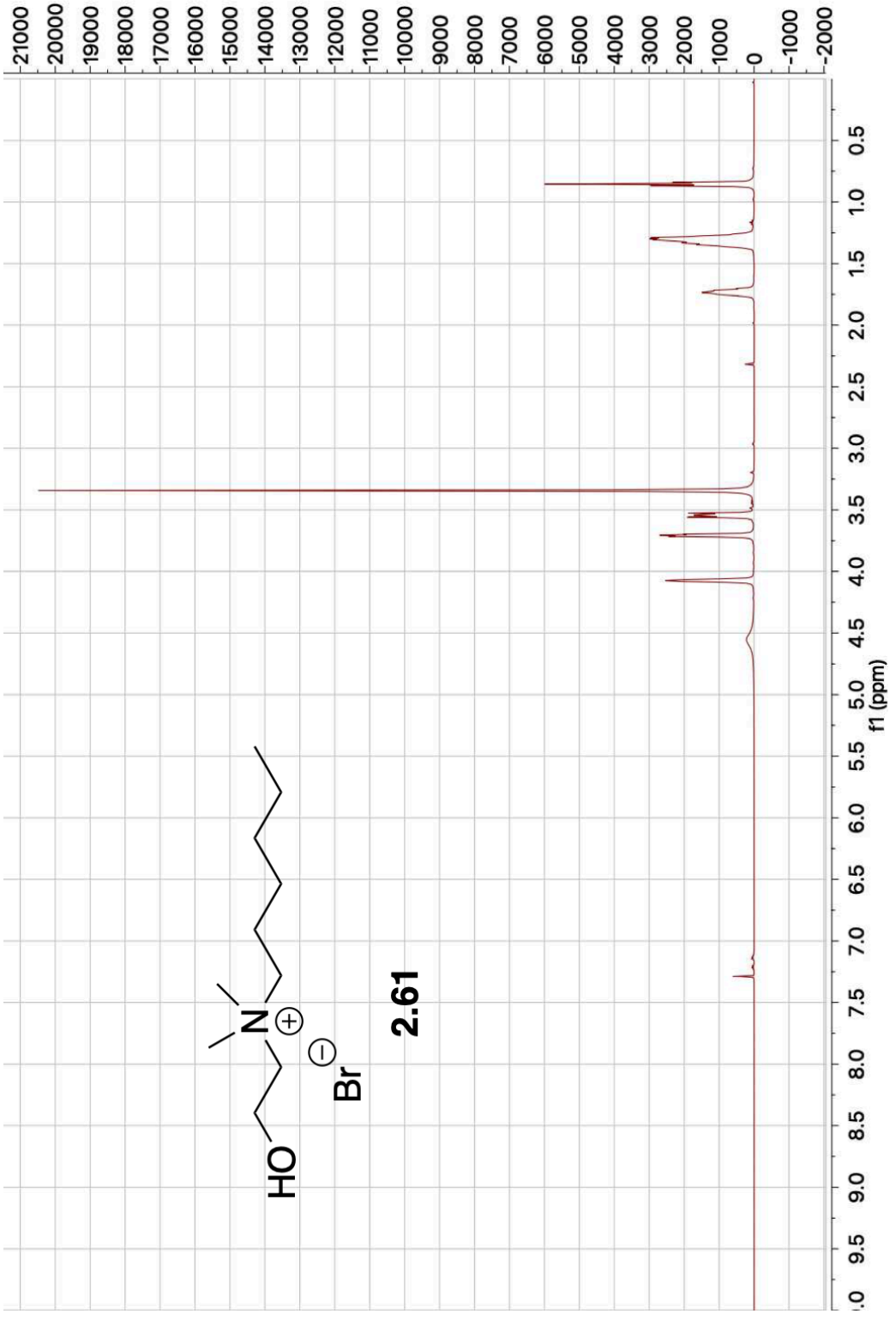
21000
20000
19000
18000
17000
16000
15000
14000
13000
12000
11000
10000
9000
8000
7000
6000
5000
4000
3000
2000
1000
0
-1000
-2000
0.5
1.0
1.5
2.0
2.5
3.0
3.5
4.0
4.5
5.0
5.5
6.0
6.5
7.0
7.5
8.0
8.5
9.0
9.5
f1 (ppm)
HO
N
Br
2.61

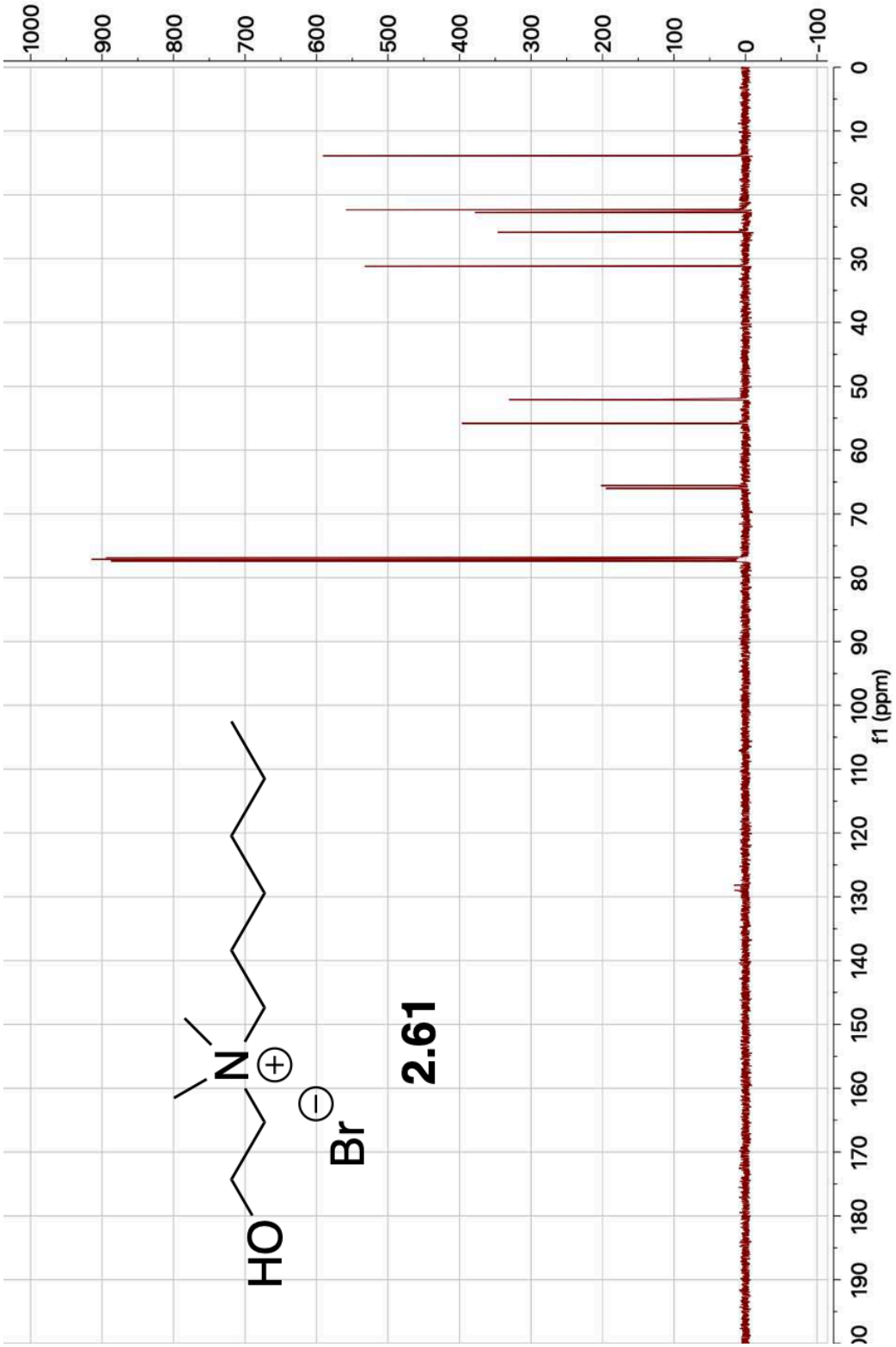
1000
900
800
700
600
500
400
300
200
100
0
-100
0
10
20
30
40
50
60
70
80
90
100
110
120
130
140
150
160
170
180
190
f1 (ppm)
HO
N
Br
2.61

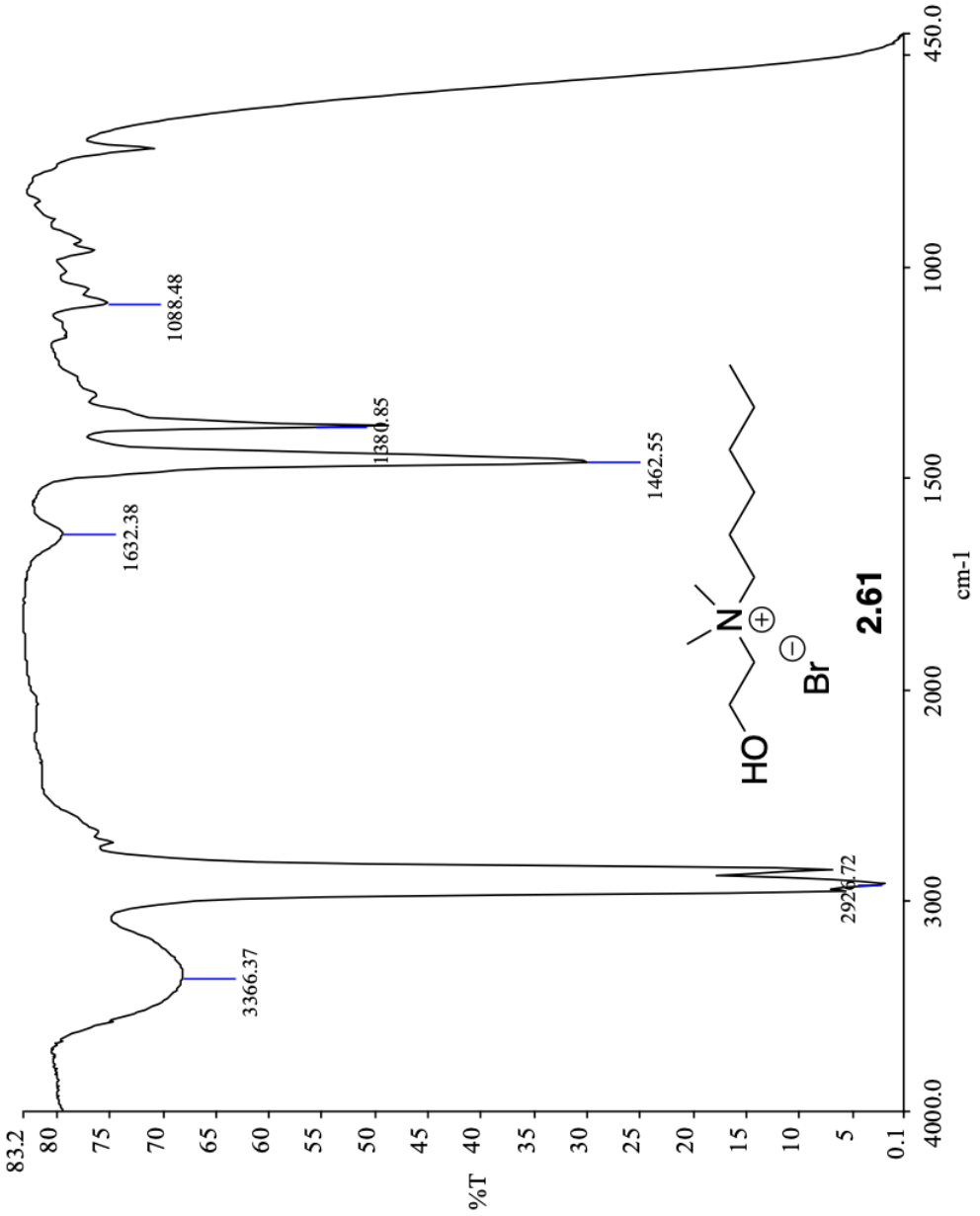
3366.37
2926.72
1632.38
1462.55
1380.85
1088.48
HO
N
Br
2.61
%T
cm-1
83.2
80
75
70
65
60
55
50
45
40
35
30
25
20
15
10
5
0.1
4000.0
3000
2000
1500
1000
450.0

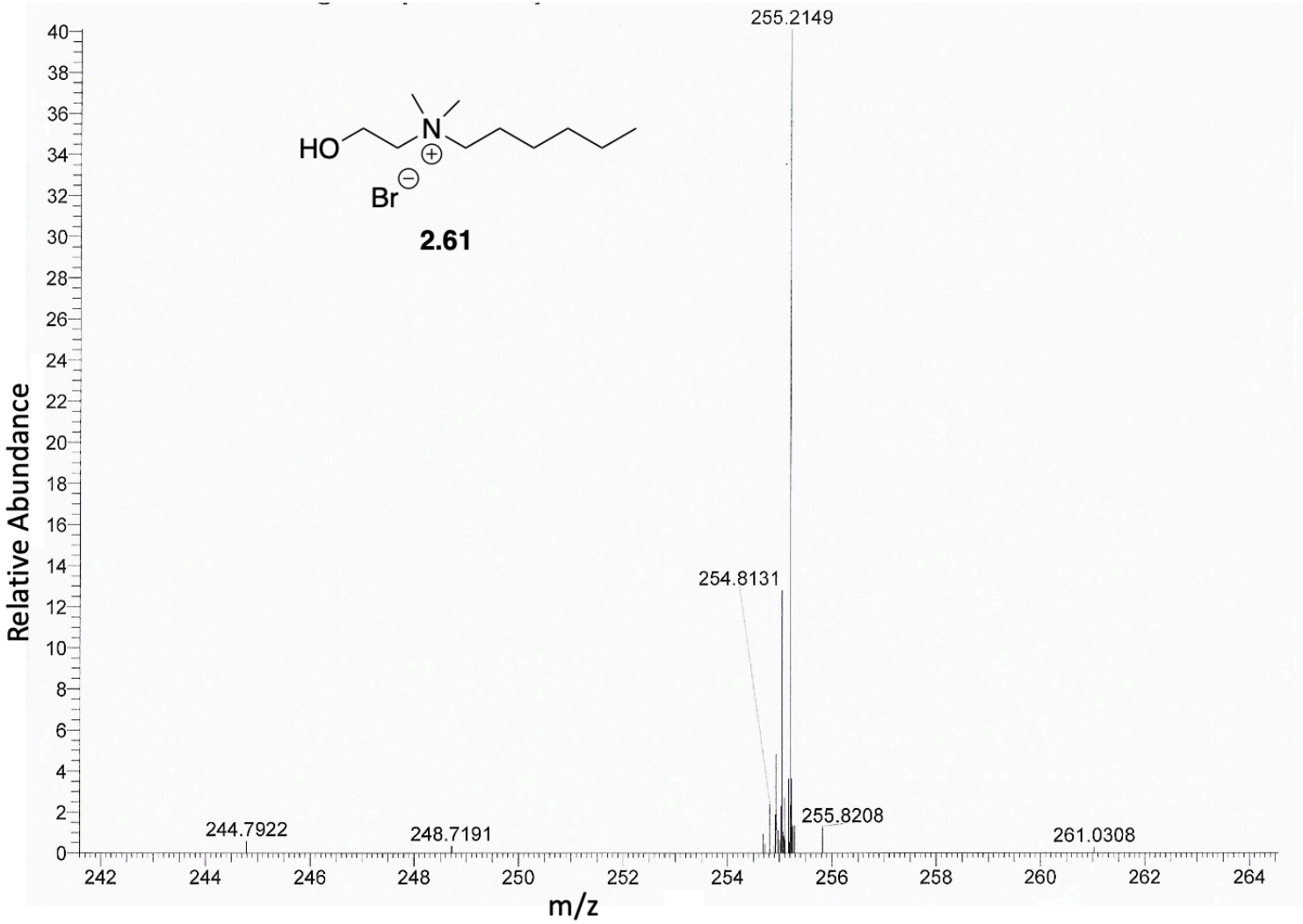
255.2149
HO
N
Br
2.61
Relative Abundance
254.8131
244.7922
248.7191
255.8208
261.0308
m/z

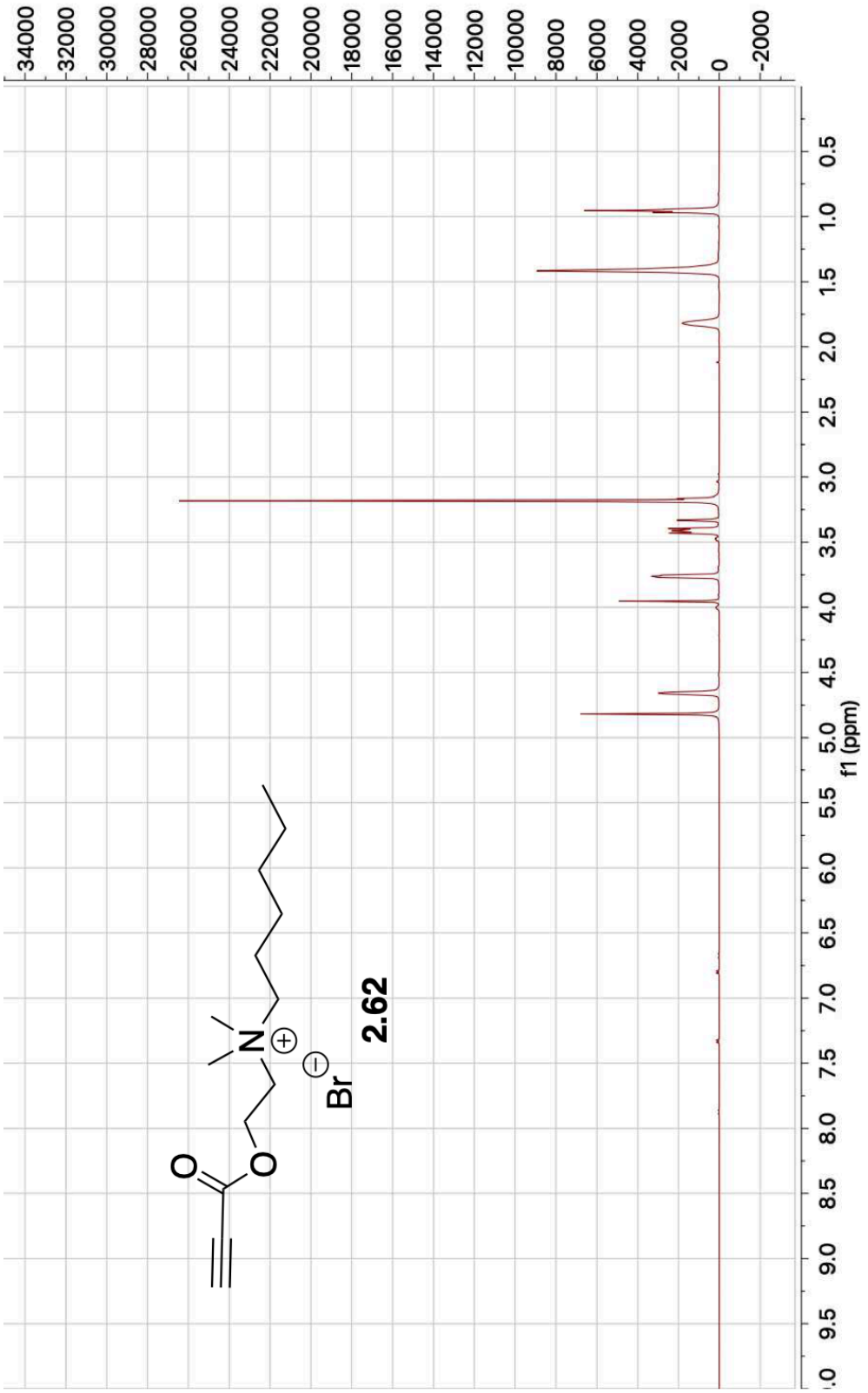
34000
32000
30000
28000
26000
24000
22000
20000
18000
16000
14000
12000
10000
8000
6000
4000
2000
0
-2000
0.5
1.0
1.5
2.0
2.5
3.0
3.5
4.0
4.5
5.0
5.5
6.0
6.5
7.0
7.5
8.0
8.5
9.0
9.5
f1 (ppm)
O
O
N
Br
2.62

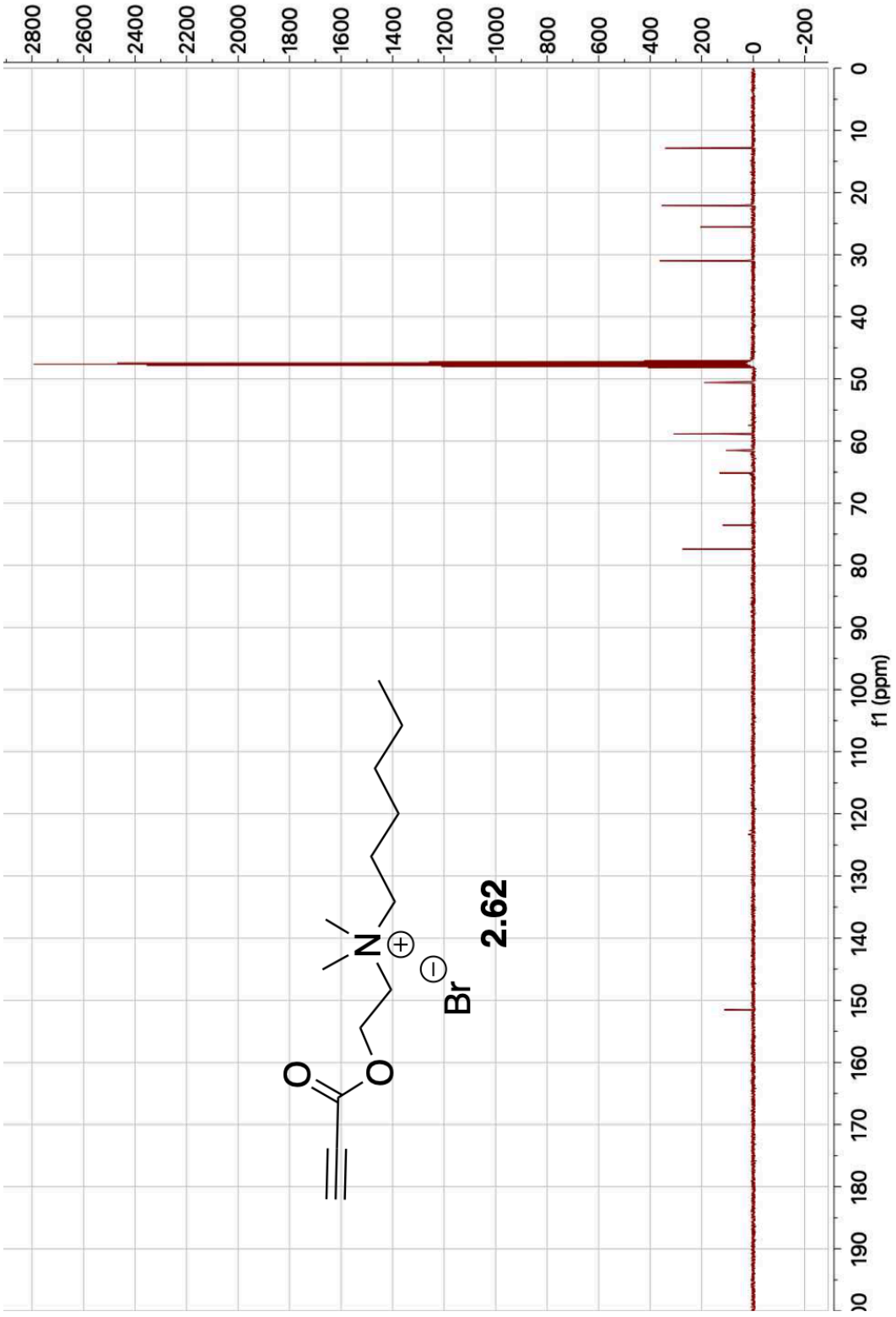
2800
2600
2400
2200
2000
1800
1600
1400
1200
1000
800
600
400
200
0
-200
0
10
20
30
40
50
60
70
80
90
100
110
120
130
140
150
160
170
180
190
f1 (ppm)
O
O
N
Br
2.62

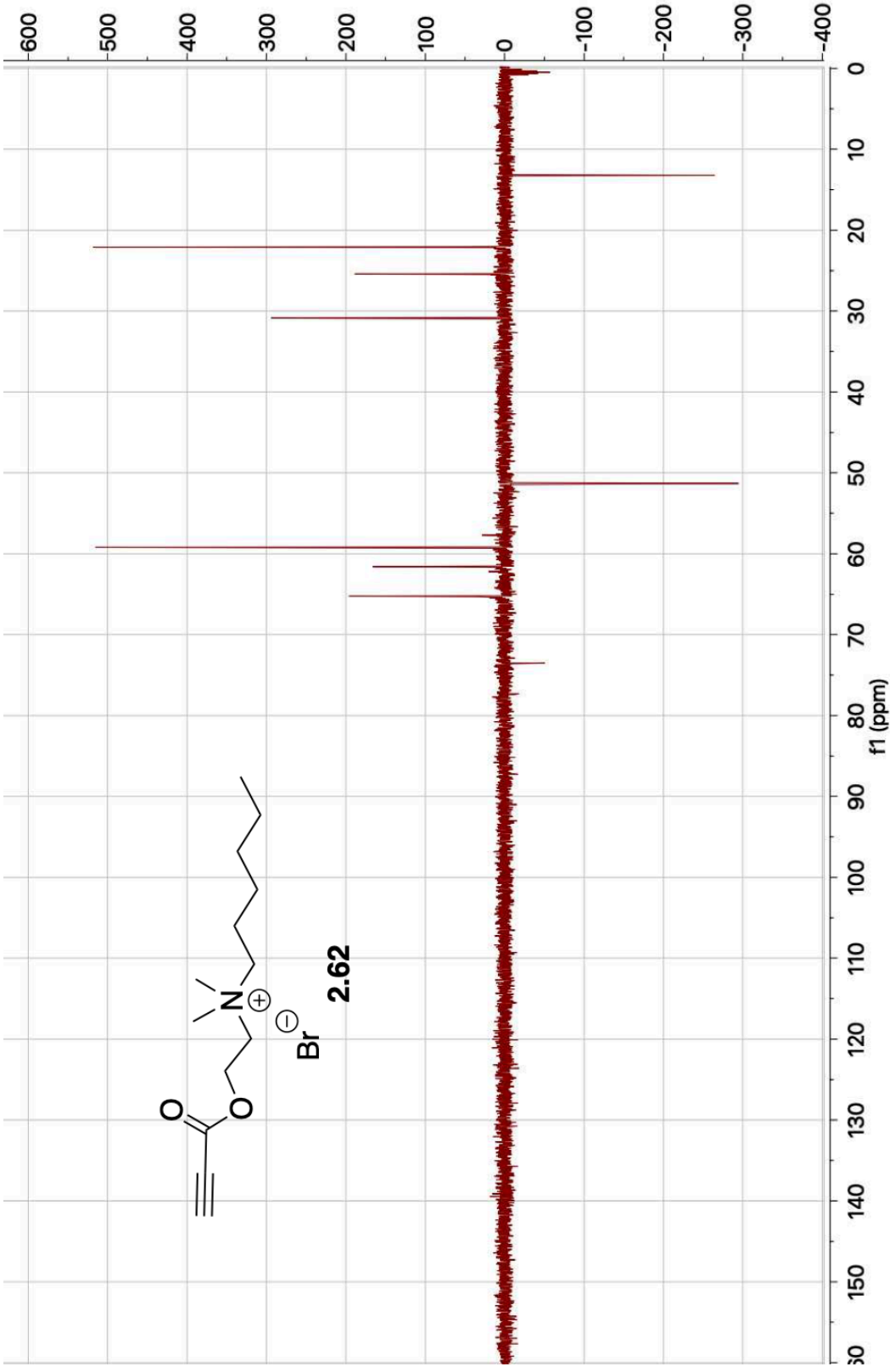
2.62
f1 (ppm)

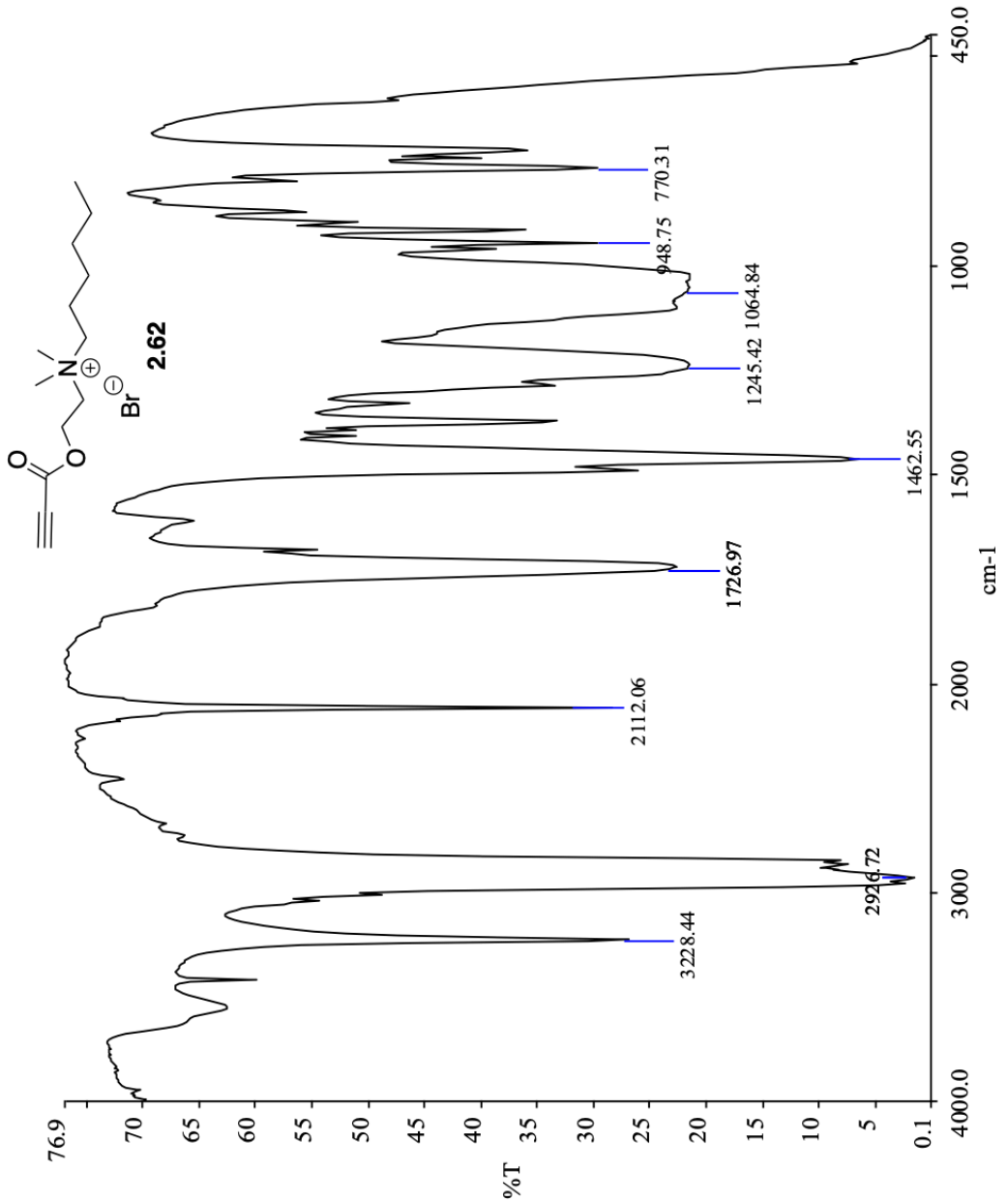
2.62
Br
3228.44
2926.72
2112.06
1726.97
1462.55
1245.42
1064.84
948.75
770.31
%T
cm-1
76.9
70
65
60
55
50
45
40
35
30
25
20
15
10
5
0.1
4000.0
3000
2000
1500
1000
450.0

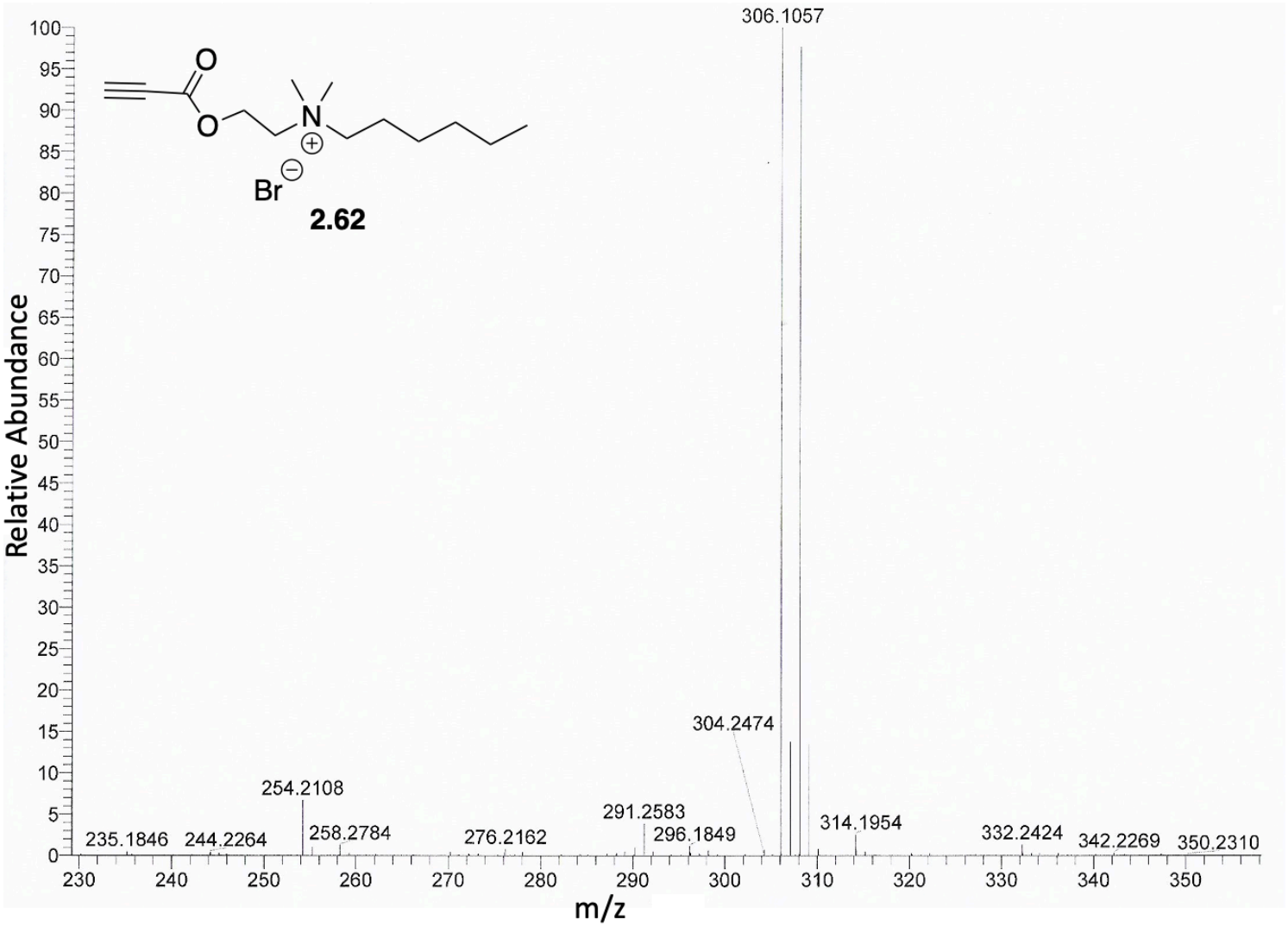
306.1057
304.2474
254.2108
291.2583
314.1954
235.1846
244.2264
258.2784
276.2162
296.1849
332.2424
342.2269
350.2310
Relative Abundance
m/z
Br
2.62

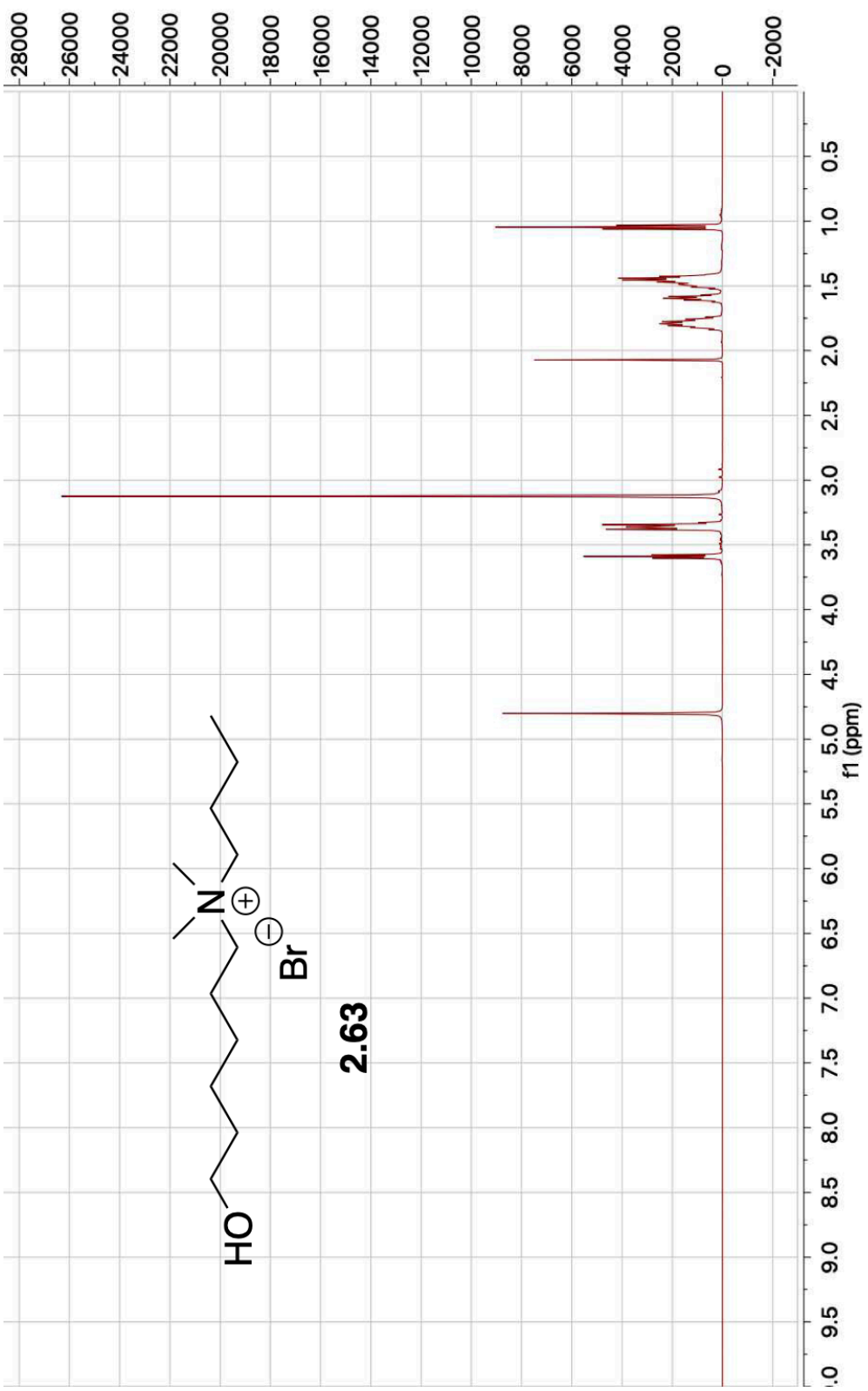
28000
26000
24000
22000
20000
18000
16000
14000
12000
10000
8000
6000
4000
2000
0
-2000
0.5
1.0
1.5
2.0
2.5
3.0
3.5
4.0
4.5
5.0
5.5
6.0
6.5
7.0
7.5
8.0
8.5
9.0
9.5
f1 (ppm)
HO
N
Br
2.63

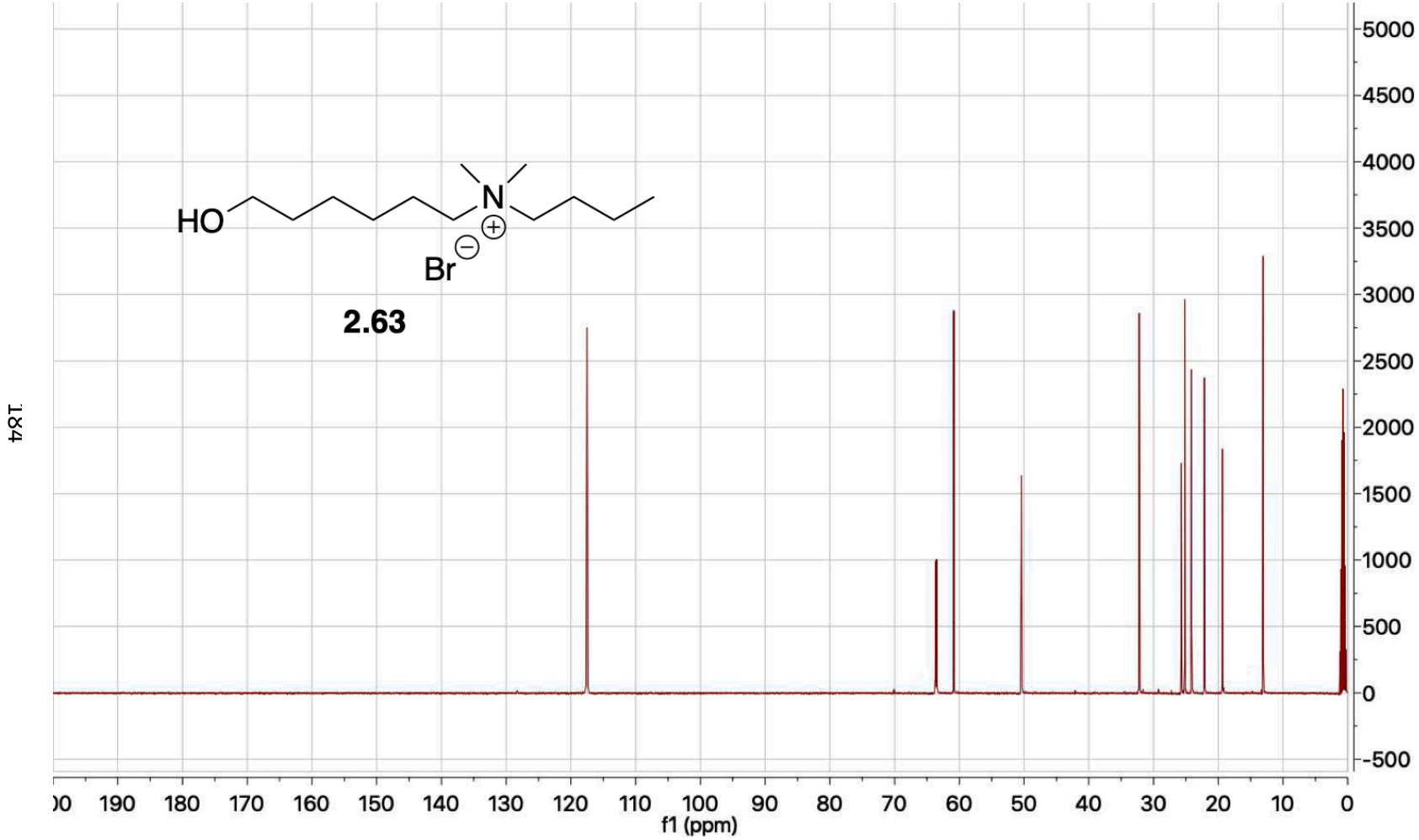
HO
N
Br
2.63
5000
4500
4000
3500
3000
2500
2000
1500
1000
500
0
-500
190
180
170
160
150
140
130
120
110
100
90
80
70
60
50
40
30
20
10
0
f1 (ppm)

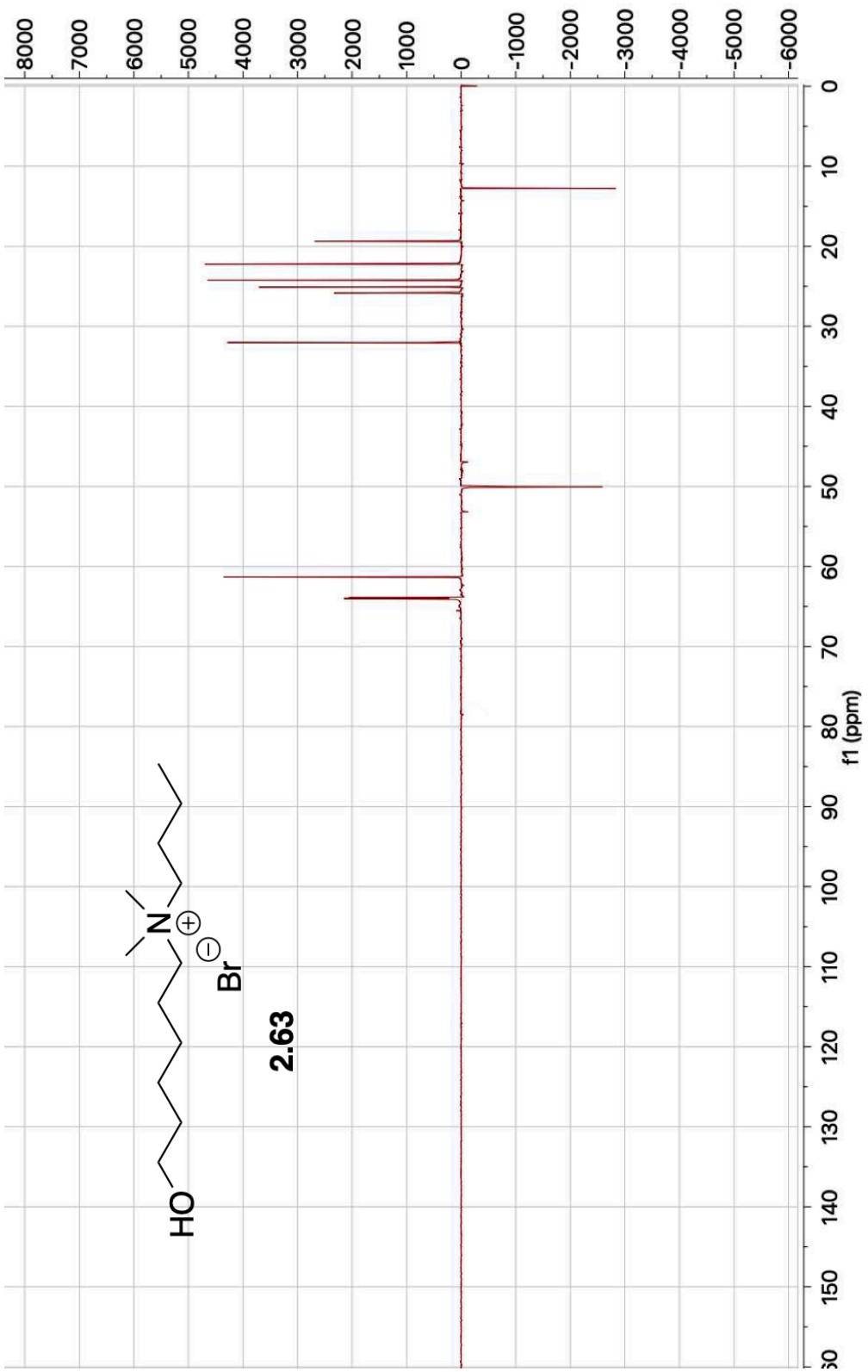
8000
7000
6000
5000
4000
3000
2000
1000
0
-1000
-2000
-3000
-4000
-5000
-6000
0
10
20
30
40
50
60
70
80
90
100
110
120
130
140
150
f1 (ppm)
HO
N
Br
2.63

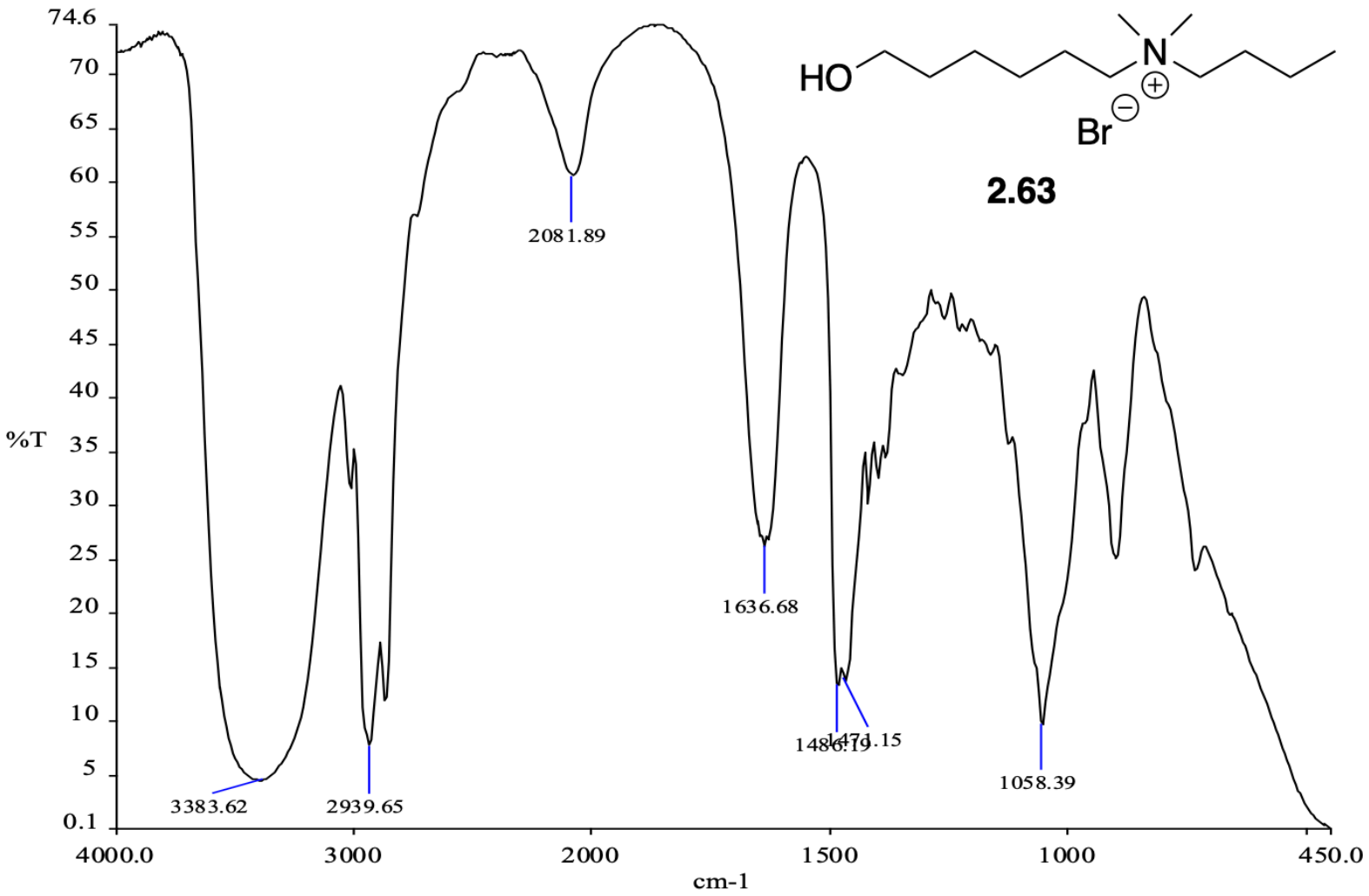
74.6
70
65
60
55
50
45
40
35
30
25
20
15
10
5
0.1
%T
4000.0
3000
2000
1500
1000
450.0
cm-1
3383.62
2939.65
2081.89
1636.68
1486.19
1471.15
1058.39
HO
N
Br
2.63

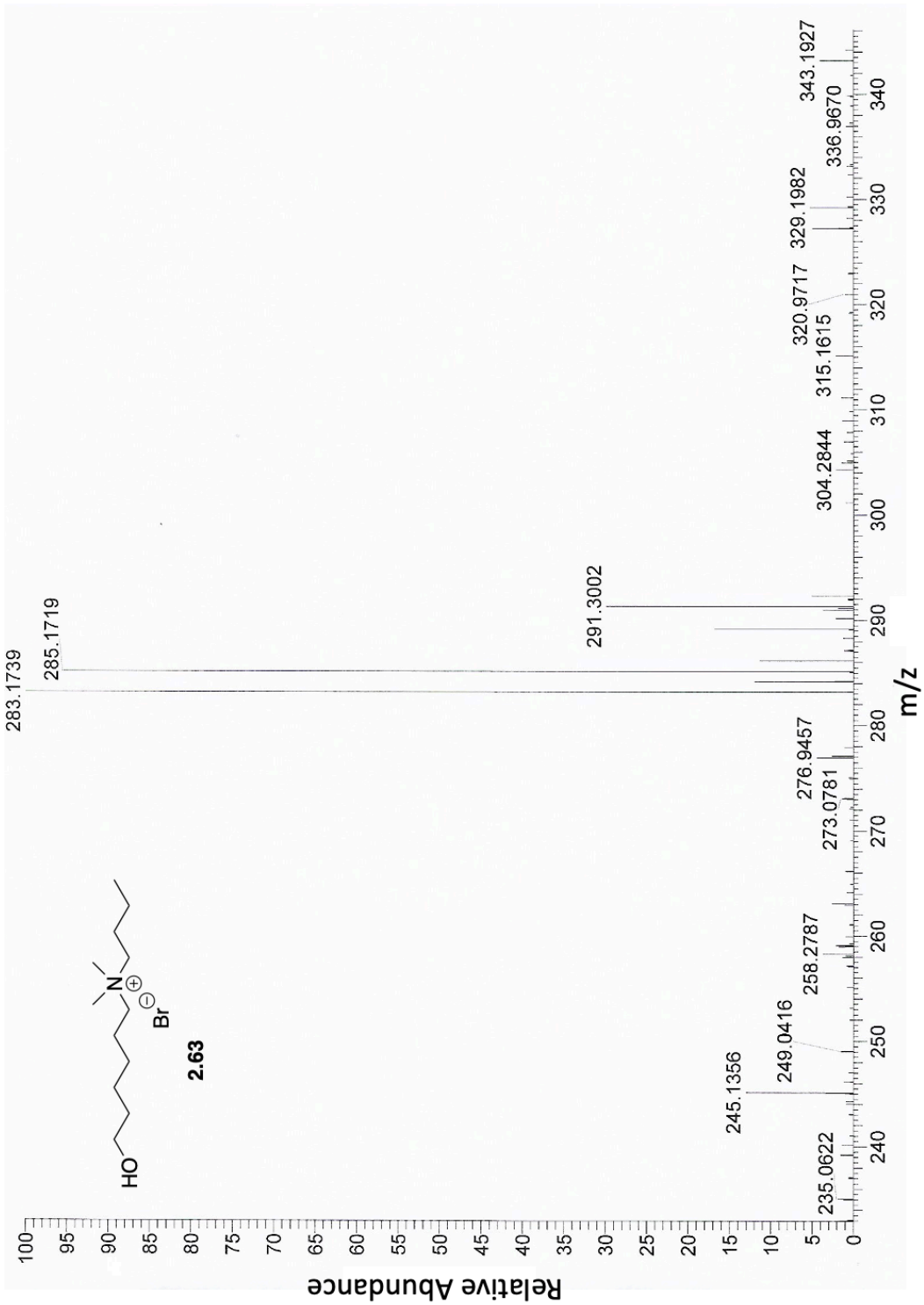
283.1739
285.1719
291.3002
304.2844
315.1615
320.9717
329.1982
336.9670
343.1927
276.9457
273.0781
258.2787
249.0416
245.1356
235.0622
HO
N
Br
2.63
Relative Abundance
m/z

2.64
Br
f1 (ppm)

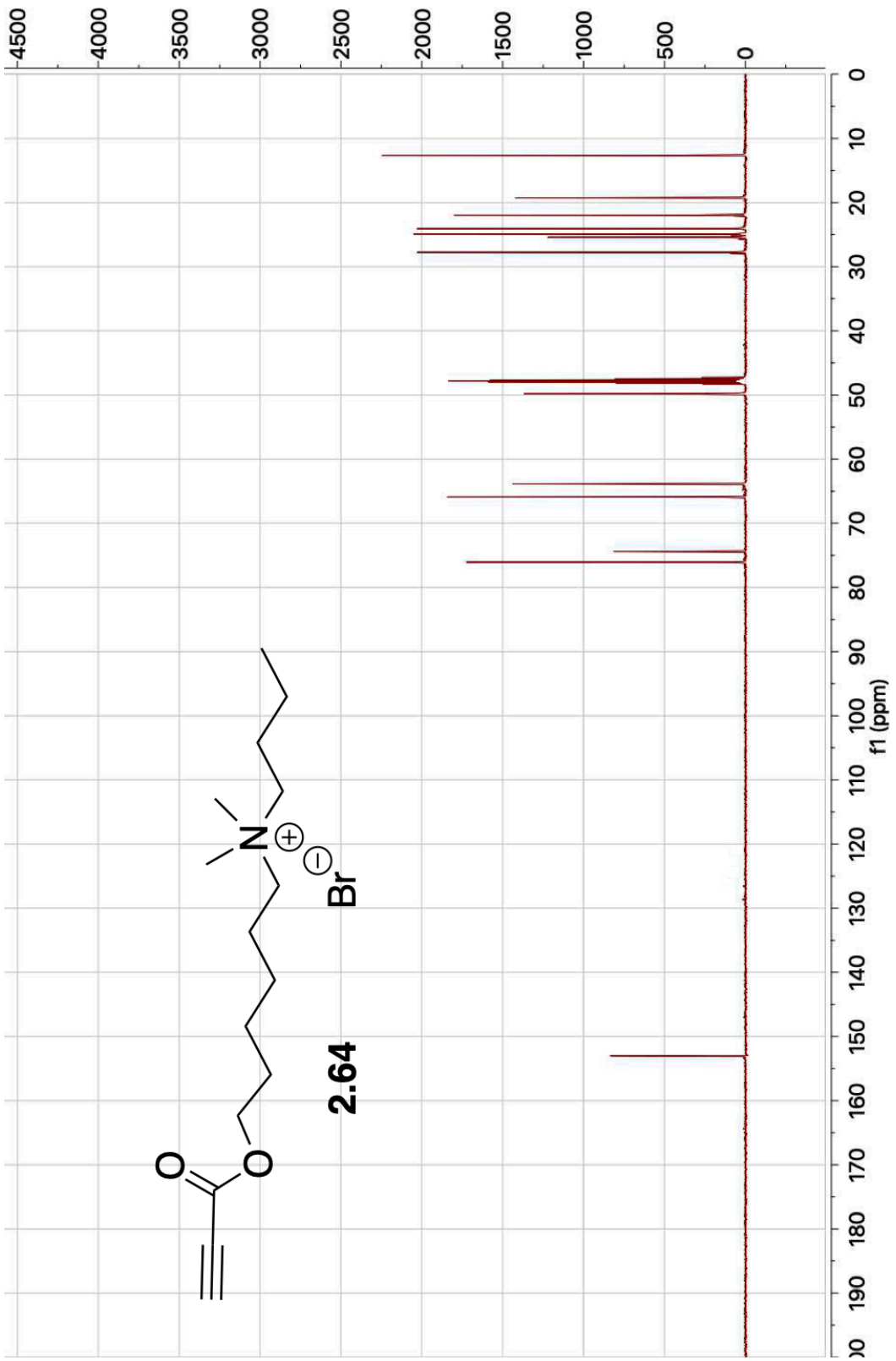
4500
4000
3500
3000
2500
2000
1500
1000
500
0
0
10
20
30
40
50
60
70
80
90
100
110
120
130
140
150
160
170
180
190
f1 (ppm)
N
Br
O
O
2.64

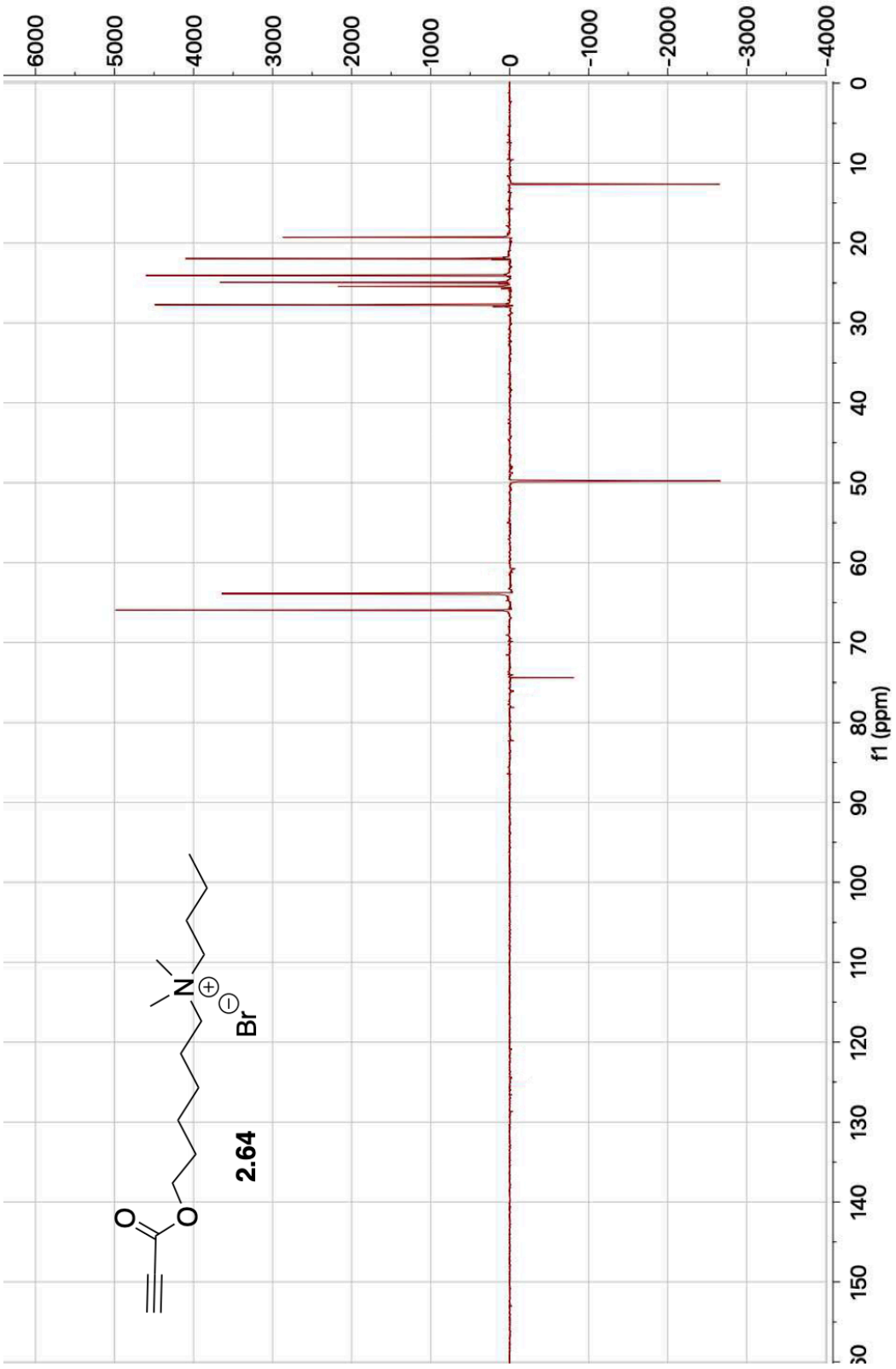
6000
5000
4000
3000
2000
1000
0
-1000
-2000
-3000
-4000
0
10
20
30
40
50
60
70
80
90
100
110
120
130
140
150
f1 (ppm)
N
Br
O
O
2.64

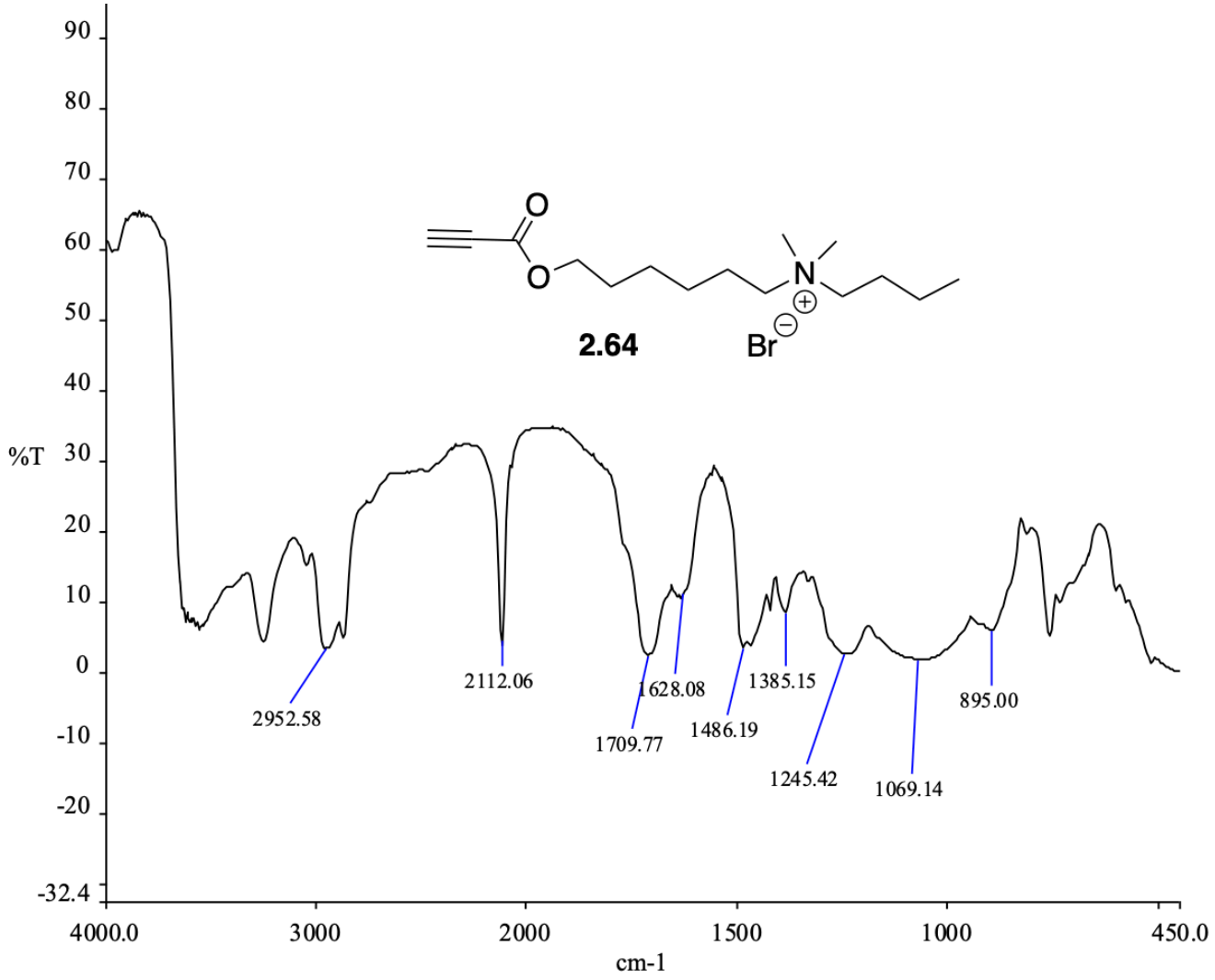
90
80
70
60
50
40
%T 30
20
10
0
-10
-20
-32.4
4000.0
3000
2000
1500
1000
450.0
cm-1
O
O
N
Br
2.64
2952.58
2112.06
1709.77
1628.08
1486.19
1385.15
1245.42
1069.14
895.00

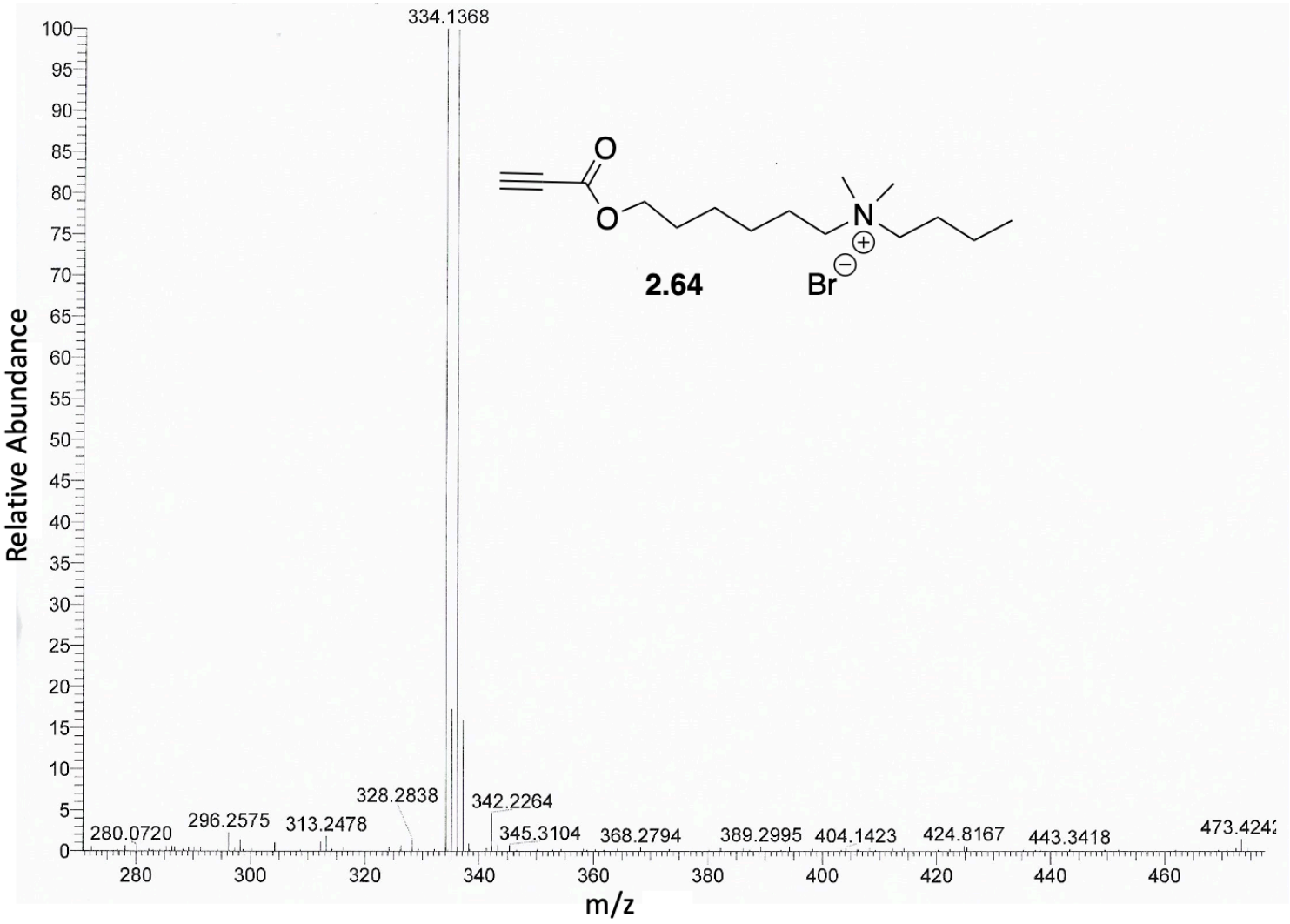
334.1368
Relative Abundance
m/z
2.64
Br
280.0720
296.2575
313.2478
328.2838
342.2264
345.3104
368.2794
389.2995
404.1423
424.8167
443.3418
473.4242

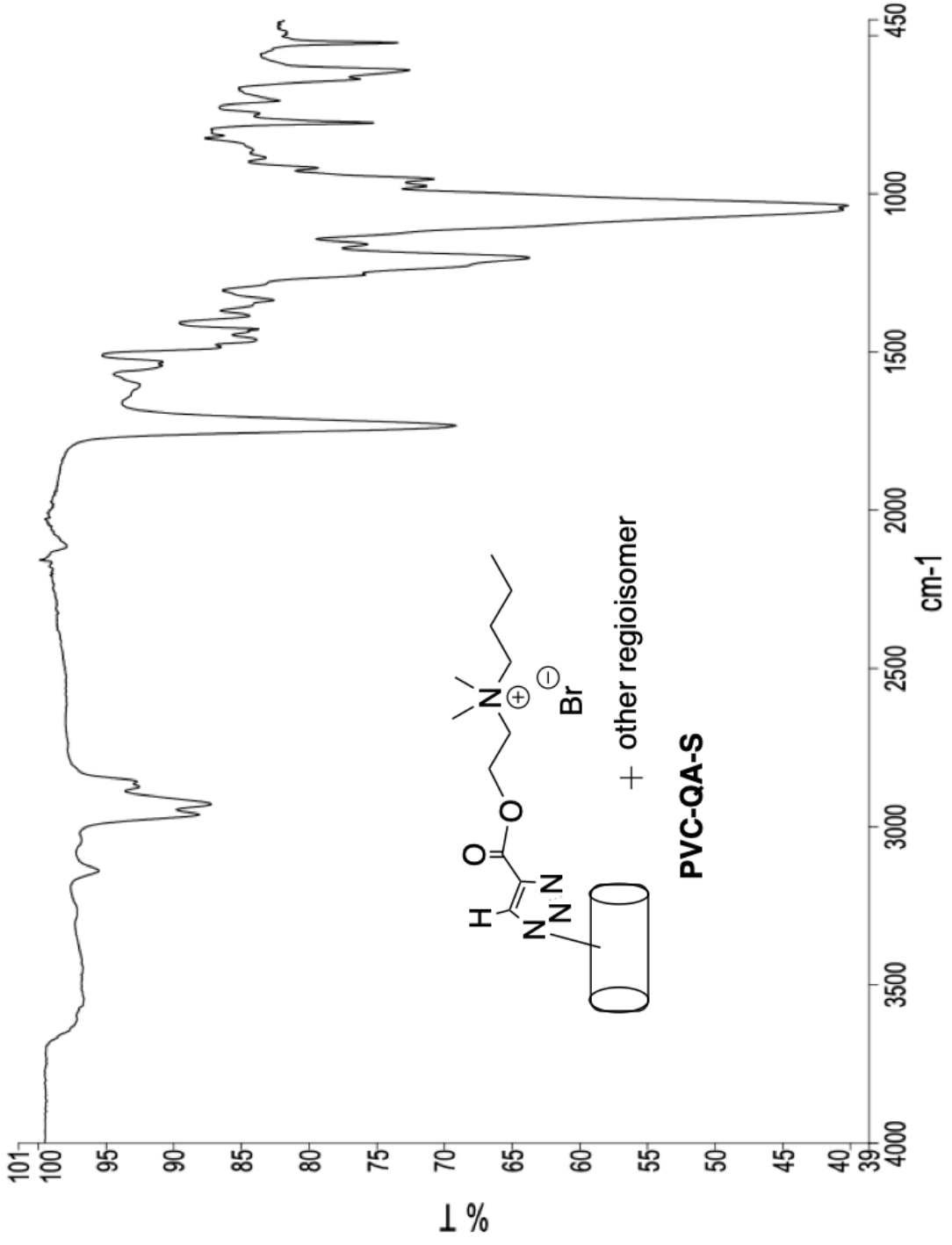
%T
cm-1
PVC-QA-S
+ other regioisomer
Br

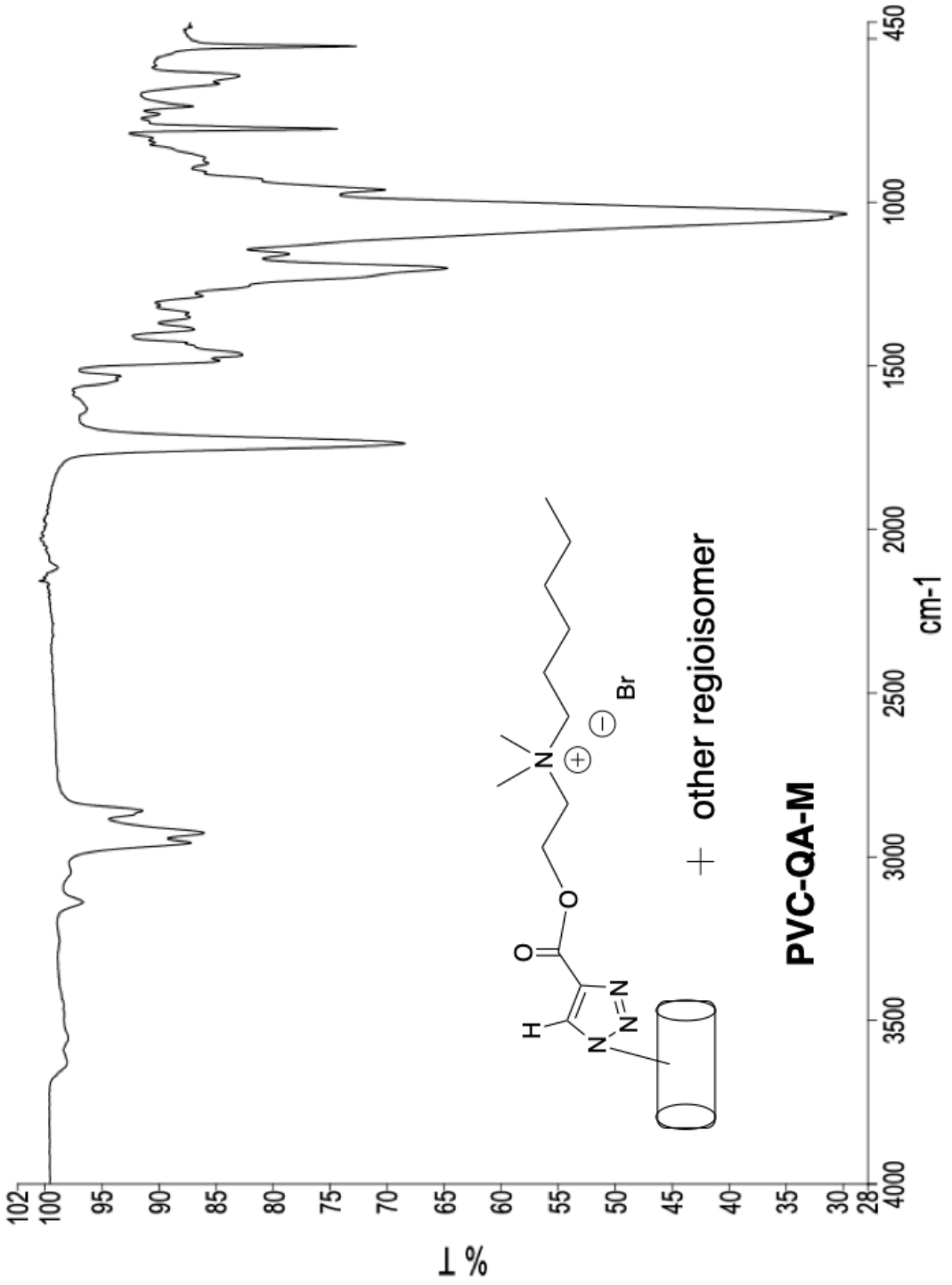
%T
cm-1
4000
3500
3000
2500
2000
1500
1000
450
PVC-QA-M
+ other regioisomer
Br

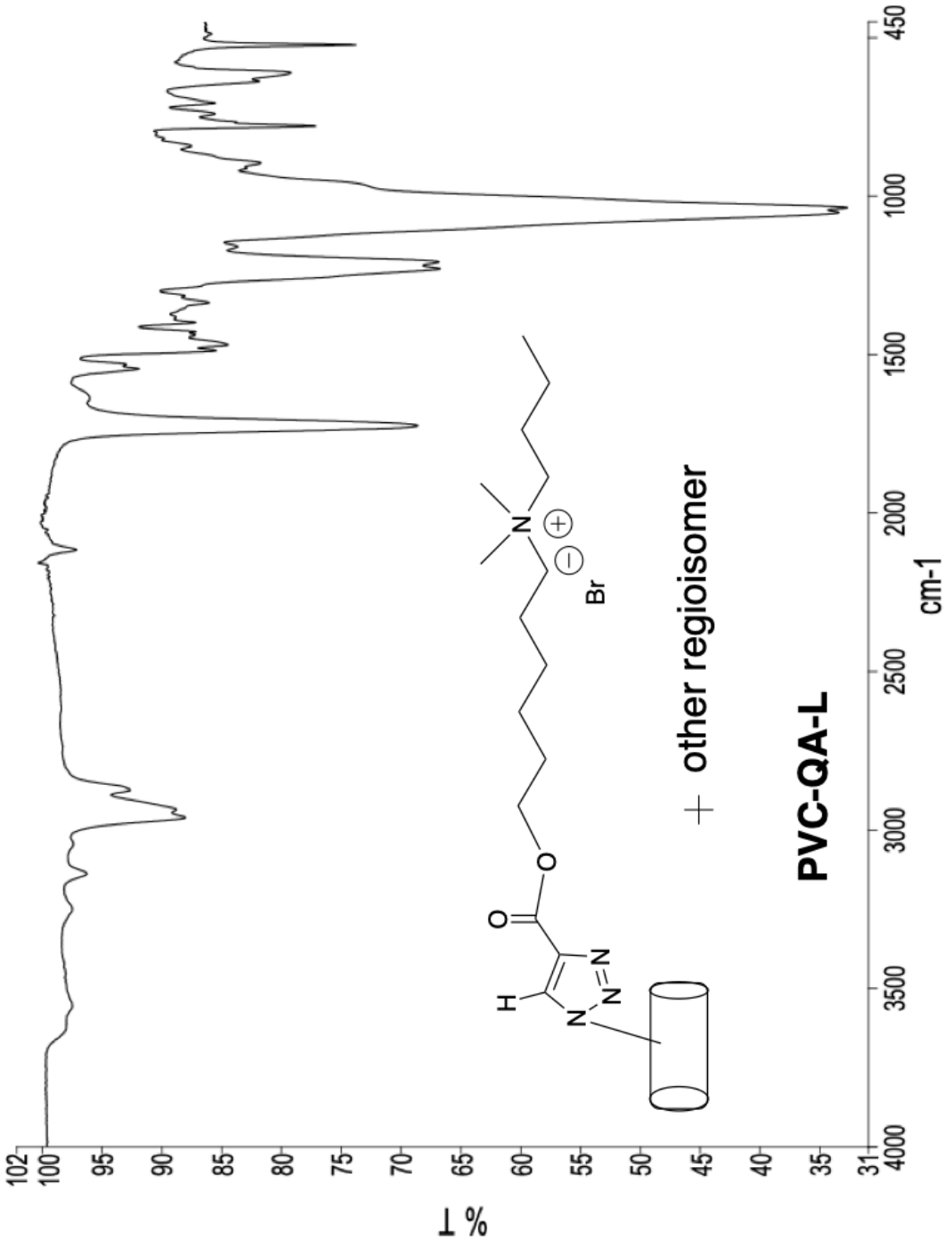
%T
cm-1
PVC-QA-L
+ other regioisomer
Br

6 Bibliography

Abdallh, M., Bufaroosha, M., Ahmed, A., Ahmed, D. S., & Yousif, E. (2020). Modification of Poly (vinyl chloride) Substrates via Schiff's Base for Photochemical Applications. *Journal of Vinyl and Additive Technology*.

Abreu, A. C., Tavares, R. R., Borges, A., Mergulhão, F., & Simões, M. (2013). Current and emergent strategies for disinfection of hospital environments. *Journal of Antimicrobial Chemotherapy, 68*(12), 2718-2732. doi:10.1093/jac/dkt281

Al-Ani, F. H., Alsalhy, Q. F., Raheem, R. S., Rashid, K. T., & Figoli, A. (2020). Experimental Investigation of the Effect of Implanting TiO(2)-NPs on PVC for Long-Term UF Membrane Performance to Treat Refinery Wastewater. *Membranes (Basel), 10*(4), 77. doi:10.3390/membranes10040077

Al-Daeif, Y., Yousif, E., & Nabi, M. A. (2012). Synthesis of New Polymers Derived from Poly (Vinyl Chloride) and Study Their Optical Properties. *Journal of Al-Nahrain University, 15*(2), 79-83.

Allan, J. T. S. (2015). The sulfonation of polyvinyl chloride: Synthesis and characterization for proton conducting membrane applications. *Journal of Membrane Science, 489*, 175-182. doi:10.1016/j.memsci.2015.03.093

Ameer, A. A., Abdallh, M. S., Ahmed, A. A., & Yousif, E. A. (2013). Synthesis and Characterization of Polyvinyl Chloride Chemically Modified by Amines. *Open Journal of Polymer Chemistry, 3*, 11-15. doi:10.4236/ojpchem.2013.31003

Arenas, E., Bucio, E., Burillo, G., & Lopez, G. P. (2007). Radiation grafting of poly(ethylene glycol) methacrylate onto poly(vinyl chloride) tubes. *Designed Monomers & Polymers, 10*(5), 459-467. doi:10.1163/156855507781833585

Balakrishnan, B., Kumar, D. S., Yoshida, Y., & Jayakrishnan, A. (2005). Chemical modification of poly(vinyl chloride) resin using poly(ethylene glycol) to improve blood compatibility. *Biomaterials, 26*(17), 3495-3502. doi:https://doi.org/10.1016/j.biomaterials.2004.09.032

Balazs, D. J., Triandafillu, K., Chevolot, Y., Aronsson, B.-O., Harms, H., Descouts, P., & Mathieu, H. J. (2003). Surface modification of PVC endotracheal tubes by oxygen glow discharge to reduce bacterial adhesion. *Surface and Interface Analysis, 35*(3), 301-309. doi:10.1002/sia.1533

Balazs, D. J., Triandafillu, K., Wood, P., Chevolot, Y., van Delden, C., Harms, H., . . . Mathieu, H. J. (2004). Inhibition of bacterial adhesion on PVC endotracheal tubes by RF-oxygen glow discharge, sodium hydroxide and silver nitrate treatments. *Biomaterials, 25*(11), 2139-2151. doi:https://doi.org/10.1016/j.biomaterials.2003.08.053

Barh, D., Jain, N., Tiwari, S., Parida, B. P., D'Afonseca, V., Li, L., . . . Azevedo, V. (2011). A novel comparative genomics analysis for common drug and vaccine targets in Corynebacterium pseudotuberculosis and other CMN group of human

pathogens. *Chemical biology & drug design, 78*(1), 73-84. doi:10.1111/j.1747-0285.2011.01118.x

Behboudi, A., Jafarzadeh, Y., & Yegani, R. (2016). Preparation and characterization of TiO2 embedded PVC ultrafiltration membranes. *Chemical Engineering Research and Design, 114*, 96-107. doi:https://doi.org/10.1016/j.cherd.2016.07.027

Beveridge, J. M., Chenot, H. M., Crich, A., Jacob, A., & Finn, M. G. (2018). Covalent Functionalization of Flexible Polyvinyl Chloride Tubing. *Langmuir, 34*(35), 10407-10412. doi:10.1021/acs.langmuir.7b03115

Bos, R., van der Mei, H. C., & Busscher, H. J. (1999). Physico-chemistry of initial microbial adhesive interactions – its mechanisms and methods for study. *FEMS Microbiology Reviews, 23*(2), 179-230. doi:10.1111/j.1574-6976.1999.tb00396.x

Campoccia, D., Montanaro, L., & Arciola, C. R. (2013). A review of the biomaterials technologies for infection-resistant surfaces. *Biomaterials, 34*(34), 8533-8554. doi:https://doi.org/10.1016/j.biomaterials.2013.07.089

Campoccia, D., Montanaro, L., Speziale, P., & Arciola, C. R. (2010). Antibiotic-loaded biomaterials and the risks for the spread of antibiotic resistance following their prophylactic and therapeutic clinical use. *Biomaterials, 31*(25), 6363-6377. doi:https://doi.org/10.1016/j.biomaterials.2010.05.005

Carroll, W. F., Johnson, R. W., Moore, S. S., & Paradis, R. A. (2017). 4 - Poly(Vinyl Chloride). In M. Kutz (Ed.), *Applied Plastics Engineering Handbook (Second Edition)* (pp. 73-89): William Andrew Publishing.

CDC. (2014). Healthcare-associated Infections. Retrieved from https://www.cdc.gov/hai/infectiontypes.html

Chen, S., Li, L., Zhao, C., & Zheng, J. (2010). Surface hydration: Principles and applications toward low-fouling/nonfouling biomaterials. *Polymer, 51*(23), 5283-5293. doi:https://doi.org/10.1016/j.polymer.2010.08.022

Cheng, Y., Hao, J., Lee, L. A., Biewer, M. C., Wang, Q., & Stefan, M. C. (2012). Thermally controlled release of anticancer drug from self-assembled γ-substituted amphiphilic poly (ε-caprolactone) micellar nanoparticles. *Biomacromolecules, 13*(7), 2163-2173

Cheng, Y.-Y., Du, C.-H., Wu, C.-J., Sun, K.-X., & Chi, N.-P. (2018). Improving the hydrophilic and antifouling properties of poly(vinyl chloride) membranes by atom transfer radical polymerization grafting of poly(ionic liquid) brushes. *Polymers for Advanced Technologies, 29*(1), 623-631. doi:10.1002/pat.4172

Corrales, M., Bierbrauer, K., Sacristan, J., & Mijangos, C. (2010). Surface Modification of PVC Membranes Using Fluorothiophenol Compounds. *Macromolecular Chemistry and Physics, 211*(18), 1990-1998. doi:doi:10.1002/macp.201000322

Darouiche, R. O., Raad, I. I., Heard, S. O., Thornby, J. I., Wenker, O. C., Gabrielli, A., . . . Hachem, R. (1999). A comparison of two antimicrobial-impregnated central venous catheters. *New England Journal of Medicine, 340*(1), 1-8.

Doyle, R. J. (2000). Contribution of the hydrophobic effect to microbial infection. *Microbes and Infection, 2*(4), 391-400. doi:https://doi.org/10.1016/S1286-4579(00)00328-2

e Silva, F. A., Siopa, F., Figueiredo, B. F. H. T., Gonçalves, A. M. M., Pereira, J. L., Gonçalves, F., . . . Ventura, S. P. M. (2014). Sustainable design for environment-friendly mono and dicationic cholinium-based ionic liquids. *Ecotoxicology and Environmental Safety, 108*, 302-310. doi:https://doi.org/10.1016/j.ecoenv.2014.07.003

Earla, A., & Braslau, R. (2014). Covalently Linked Plasticizers: Triazole Analogues of Phthalate Plasticizers Prepared by Mild Copper-Free "Click" Reactions with Azide-Functionalized PVC. *Macromolecular Rapid Communications, 35*(6), 666-671. doi:10.1002/marc.201300865

Erbil, H. Y. (2013). Bioadhesion to solids: contact angle hysteresis effect. *291*(2), 355-360.

Fang, F. C. (2012). Antimicrobial actions of nitric oxide. *Nitric Oxide, 27*, S10. doi:https://doi.org/10.1016/j.niox.2012.04.036

Fischer, I., Schmitt, W. F., Porth, H.-C., Allsopp, M. W., & Vianello, G. (2014). Poly(Vinyl Chloride). In *Ullmann's Encyclopedia of Industrial Chemistry* (pp. 1-30).

Friedman, A., & Friedman, J. (2009). New biomaterials for the sustained release of nitric oxide: past, present and future. *Expert Opinion on Drug Delivery, 6*(10), 1113-1122. doi:10.1517/17425240903196743

Fuchs, A. D., & Tiller, J. C. (2006). Contact-Active Antimicrobial Coatings Derived from Aqueous Suspensions. *Angewandte Chemie International Edition, 45*(40), 6759-6762. doi:10.1002/anie.200602738

Garside, M. (2020). U.S. PVC production volume 1990-2019. Retrieved from https://www.statista.com/statistics/975603/us-polyvinyl-chloride-production-volume/#statisticContainer

Geyer, R., Jambeck, J. R., & Law, K. L. (2017). Production, use, and fate of all plastics ever made. *Science advances, 3*(7), 1700782.

Golshan, M., Hatef, A., Socha, M., Milla, S., Butts, I. A. E., Carnevali, O., . . . Alavi, S. M. H. (2015). Di-(2-ethylhexyl)-phthalate disrupts pituitary and testicular hormonal functions to reduce sperm quality in mature goldfish. *Aquatic Toxicology, 163*, 16-26. doi:https://doi.org/10.1016/j.aquatox.2015.03.017

Hakkarainen, M. (2008). Migration of Monomeric and Polymeric PVC Plasticizers. In A.-C. Albertsson & M. Hakkarainen (Eds.), *Chromatography for Sustainable*

Polymeric Materials: Renewable, Degradable and Recyclable (pp. 159-185). Berlin, Heidelberg: Springer Berlin Heidelberg.

Handa, H., Brisbois, E. J., Major, T. C., Refahiyat, L., Amoako, K. A., Annich, G. M., . . . Meyerhoff, M. E. (2013). In vitro and in vivo study of sustained nitric oxide release coating using diazeniumdiolate-doped poly(vinyl chloride) matrix with poly(lactide-co-glycolide) additive. *Journal of Materials Chemistry B, 1*(29), 3578-3587. doi:10.1039/C3TB20277A

Handa, H., Major, T. C., Brisbois, E. J., Amoako, K. A., Meyerhoff, M. E., & Bartlett, R. H. (2014). Hemocompatibility comparison of biomedical grade polymers using rabbit thrombogenicity model for preparing nonthrombogenic nitric oxide releasing surfaces. *Journal of Materials Chemistry B, 2*(8), 1059-1067. doi:10.1039/C3TB21771J

Hanna, H., Benjamin, R., Chatzinikolaou, I., Alakech, B., Richardson, D., Mansfield, P., . . . Kantarjian, H. (2004). Long-term silicone central venous catheters impregnated with minocycline and rifampin decrease rates of catheter-related bloodstream infection in cancer patients: a prospective randomized clinical trial. *Journal of Clinical Oncology, 22*(15), 3163-3171.

He, W., Zhang, Y., Li, J., Gao, Y., Luo, F., Tan, H., . . . Fu, Q. (2016). A Novel Surface Structure Consisting of Contact-active Antibacterial Upper-layer and

Antifouling Sub-layer Derived from Gemini Quaternary Ammonium Salt Polyurethanes. *Scientific Reports, 6*(1), 32140. doi:10.1038/srep32140

Herrero, M., Quéméner, E., Ulvé, S., Reinecke, H., Mijangos, C., & Grohens, Y. (2006). Bacterial adhesion to poly(vinyl chloride) films: Effect of chemical modification and water induced surface reconstruction. *Journal of Adhesion Science and Technology, 20*(2-3), 183-195. doi:10.1163/156856106775897801

Hidalgo, M., Reinecke, H., & Mijangos, C. (1999). PVC containing hydroxyl groups: I. Synthesis, characterization, properties and crosslinking. *Polymer, 40*(12), 3525-3534. doi:https://doi.org/10.1016/S0032-3861(98)00569-2

Higa, C. M., Tek, A. T., Wojtecki, R. J., & Braslau, R. (2018). Nonmigratory internal plasticization of poly(vinyl chloride) via pendant triazoles bearing alkyl or polyether esters. *Journal of Polymer Science Part A: Polymer Chemistry, 56*(21), 2397-2411. doi:10.1002/pola.29205

Hoffman, L. R., D'Argenio, D. A., MacCoss, M. J., Zhang, Z., Jones, R. A., & Miller, S. I. (2005). Aminoglycoside antibiotics induce bacterial biofilm formation. *Nature, 436*(7054), 1171-1175. doi:10.1038/nature03912

Hron, P. (2003). Hydrophilisation of silicone rubber for medical applications. *Polymer International, 52*(9), 1531-1539. doi:10.1002/pi.1273

Huang, Z., Feng, C., Guo, H., & Huang, X. (2016). Direct functionalization of poly(vinyl chloride) by photo-mediated ATRP without a deoxygenation procedure. *Polymer Chemistry, 7*(17), 3034-3045. doi:10.1039/C6PY00483K

Imlay, J. A. (2003). Pathways of Oxidative Damage. *Annual Review of Microbiology, 57*(1), 395-418. doi:10.1146/annurev.micro.57.030502.090938

Islas, L., Alvarez-Lorenzo, C., Magariños, B., Concheiro, A., Castillo, L. F. d., & Burillo, G. (2015). Singly and binary grafted poly(vinyl chloride) urinary catheters that elute ciprofloxacin and prevent bacteria adhesion. *International Journal of Pharmaceutics, 488*(1), 20-28. doi:https://doi.org/10.1016/j.ijpharm.2015.04.036

Islas, L., Ruiz, J.-C., Muñoz-Muñoz, F., Isoshima, T., & Burillo, G. (2016). Surface characterization of poly(vinyl chloride) urinary catheters functionalized with acrylic acid and poly(ethylene glycol) methacrylate using gamma-radiation. *Applied Surface Science, 384*, 135-142. doi:https://doi.org/10.1016/j.apsusc.2016.04.169

James, N. R., & Jayakrishnan, A. (2003). Surface thiocyanation of plasticized poly(vinyl chloride) and its effect on bacterial adhesion. *Biomaterials, 24*(13), 2205-2212. doi:https://doi.org/10.1016/S0142-9612(03)00022-X

Jayakrishnan, A., & Sunny, M. C. (1996). Phase transfer catalysed surface modification of plasticized poly(vinyl chloride) in aqueous media to retard plasticizer

migration. *Polymer, 37*(23), 5213-5218. doi:https://doi.org/10.1016/0032-3861(96)00501-0

Jeon, S. I., Lee, J. H., Andrade, J. D., & De Gennes, P. G. (1991). Protein—surface interactions in the presence of polyethylene oxide: I. Simplified theory. *Journal of Colloid and Interface Science, 142*(1), 149-158. doi:https://doi.org/10.1016/0021-9797(91)90043-8

Johnson, J. R., Johnston, B., & Kuskowski, M. A. (2012). *In Vitro* Comparison of Nitrofurazone- and Silver Alloy-Coated Foley Catheters for Contact-Dependent and Diffusible Inhibition of Urinary Tract Infection-Associated Microorganisms. *Antimicrobial Agents and Chemotherapy, 56*(9), 4969-4972. doi:10.1128/aac.00733-12

Jung, W. K., Koo, H. C., Kim, K. W., Shin, S., Kim, S. H., & Park, Y. H. (2008). Antibacterial Activity and Mechanism of Action of the Silver Ion in Staphylococcus aureus and Escherichia coli. *Applied and Environmental Microbiology, 74*(7), 2171. doi:10.1128/AEM.02001-07

Kaelble, D. H. (1970). Dispersion-Polar Surface Tension Properties of Organic Solids. *The Journal of Adhesion, 2*(2), 66-81. doi:10.1080/0021846708544582

Kameda, T., Fukuda, Y., Grause, G., & Yoshioka, T. (2010a). Chemical modification of flexible and rigid poly(vinyl chloride) by nucleophilic substitution with

thiocyanate using a phase-transfer catalyst. *Materials Chemistry and Physics, 124*(1), 163-167. doi:https://doi.org/10.1016/j.matchemphys.2010.06.011

Kameda, T., Fukuda, Y., Grause, G., & Yoshioka, T. (2010b). Chemical modification of rigid poly(vinyl chloride) by the substitution with nucleophiles. *Journal of Applied Polymer Science, 116*(1), 36-44. doi:doi:10.1002/app.31452

Kawakami, H., Takahashi, T., Nagaoka, S., & Nakayama, Y. (2001). Albumin adsorption to surface of annealed fluorinated polyimide. *Polymers for Advanced Technologies, 12*(3-4), 244-252. doi:doi:10.1002/pat.134

Kilonzo, M., Vale, L., Pickard, R., Lam, T., & N'Dow, J. (2014). Cost Effectiveness of Antimicrobial Catheters for Adults Requiring Short-term Catheterisation in Hospital. *European Urology, 66*(4), 615-618. doi:https://doi.org/10.1016/j.eururo.2014.05.035

Klevens, R. M., Edwards, J. R., Richards, C. L., Horan, T. C., Gaynes, R. P., Pollock, D. A., & Cardo, D. M. (2007). Estimating Health Care-Associated Infections and Deaths in U.S. Hospitals, 2002. *Public Health Reports, 122*(2), 160-166. doi:10.1177/003335490712200205

Krylach, I. V., Kudryashov, S. I., Olekhnovich, R. O., Fokina, M. I., Sitnikova, V. E., Moskvin, M. K., . . . Uspenskaya, M. V. (2020). Fabrication of a Functional Relief on the Surface of a Polyvinyl Chloride Film by Nanosecond Laser

Microtexturing. *Optics and Spectroscopy, 128*(8), 1251-1255. doi:10.1134/S0030400X20080184

Lafarge, J., Kébir, N., Schapman, D., Gadenne, V., & Burel, F. (2013). Design of bacteria repellent PVC surfaces using the click chemistry. *Cellulose, 20*(6), 2779-2790. doi:10.1007/s10570-013-0060-y

Lantvit, S. M., Barrett, B. J., & Reynolds, M. M. (2013). Nitric oxide releasing material adsorbs more fibrinogen. *Journal of Biomedical Materials Research Part A, 101*(11), 3201-3210. doi:https://doi.org/10.1002/jbm.a.34627

Lawrence, E. L., & Turner, I. G. (2005). Materials for urinary catheters: a review of their history and development in the UK. *Medical Engineering & Physics, 27*(6), 443-453. doi:https://doi.org/10.1016/j.medengphy.2004.12.013

Lederer, J. W., Jarvis, W. R., Thomas, L., & Ritter, J. (2014). Multicenter cohort study to assess the impact of a silver-alloy and hydrogel-coated urinary catheter on symptomatic catheter-associated urinary tract infections. *Journal of wound, ostomy, and continence nursing : official publication of The Wound, Ostomy and Continence Nurses Society, 41*(5), 473-480. doi:10.1097/WON.0000000000000056

Lemire, J. A., Harrison, J. J., & Turner, R. J. (2013). Antimicrobial activity of metals: mechanisms, molecular targets and applications. *Nature Reviews Microbiology, 11*(6), 371-384. doi:10.1038/nrmicro3028

Li, L., Chen, S., Zheng, J., Ratner, B. D., & Jiang, S. (2005). Protein Adsorption on Oligo(ethylene glycol)-Terminated Alkanethiolate Self-Assembled Monolayers: The Molecular Basis for Nonfouling Behavior. *The Journal of Physical Chemistry B, 109*(7), 2934-2941. doi:10.1021/jp0473321

Li, X., Xing, Y., Jiang, Y., Ding, Y., & Li, W. (2009). Antimicrobial activities of ZnO powder-coated PVC film to inactivate food pathogens. *International Journal of Food Science & Technology, 44*(11), 2161-2168. doi:https://doi.org/10.1111/j.1365-2621.2009.02055.x

Liu, T., Li, N., Zhu, J., Yu, G., Guo, K., Zhou, L., . . . Ye, L. (2014). Effects of di-(2-ethylhexyl) phthalate on the hypothalamus-pituitary-ovarian axis in adult female rats. *Reproductive Toxicology, 46*, 141-147. doi:https://doi.org/10.1016/j.reprotox.2014.03.006

Lok, C.-N., Ho, C.-M., Chen, R., He, Q.-Y., Yu, W.-Y., Sun, H., . . . Che, C.-M. (2006). Proteomic Analysis of the Mode of Antibacterial Action of Silver Nanoparticles. *Journal of Proteome Research, 5*(4), 916-924. doi:10.1021/pr0504079

Marcilla, A., Garcia, S., & Garcia-Quesada, J. C. (2008). Migrability of PVC plasticizers. *Polymer Testing, 27*(2), 221-233. doi:https://doi.org/10.1016/j.polymertesting.2007.10.007

Marshall, K. C., & Bitton, G. (1980). *Adsorption of microorganisms to surfaces*: Wiley.

Martínez, G. (2006). Synthesis of PVC-g-PS through stereoselective nucleophilic substitution on PVC. *Journal of Polymer Science Part A: Polymer Chemistry, 44*(8), 2476-2486. doi:10.1002/pola.21346

McCoy, C. P., Cowley, J. F., Gorman, S. P., Andrews, G. P., & Jones, D. S. (2009). Reduction of Staphylococcus aureus and Pseudomonas aeruginosa colonisation on PVC through covalent surface attachment of fluorinated thiols. *Journal of Pharmacy and Pharmacology, 61*(9), 1163-1169. doi:doi:10.1211/jpp.61.09.0005

McCoy, C. P., Irwin, N. J., Hardy, J. G., Kennedy, S. J., Donnelly, L., Cowley, J. F., . . . Pentlavalli, S. (2017). Systematic optimization of poly(vinyl chloride) surface modification with an aromatic thiol. *European Polymer Journal, 97*, 40-48. doi:https://doi.org/10.1016/j.eurpolymj.2017.09.030

McGinty, K. M., & Brittain, W. J. (2008). Hydrophilic surface modification of poly(vinyl chloride) film and tubing using physisorbed free radical grafting technique. *Polymer, 49*(20), 4350-4357. doi:https://doi.org/10.1016/j.polymer.2008.07.063

Meléndez-Ortiz, H. I., Alvarez-Lorenzo, C., Concheiro, A., Jiménez-Páez, V. M., & Bucio, E. (2016). Modification of medical grade PVC with N-vinylimidazole to obtain bactericidal surface. *Radiation Physics and Chemistry, 119*, 37-43. doi:https://doi.org/10.1016/j.radphyschem.2015.09.014

Merchan, M., Sedlarikova, J., Vesel, A., Sedlarik, V., Pastorek, M., & Sáha, P. (2010). Characterization of Antibacterial, Mechanical, and Structural Properties of Polyvinyl Chloride/Silver Nitrate Composites Prepared by Thermoplastic Compounding. *International Journal of Polymer Analysis and Characterization, 15*(6), 360-369. doi:10.1080/1023666X.2010.500534

Messina, A. F., Berman, D. M., Ghazarian, S. R., Patel, R., Neustadt, J., Hahn, G., & Sibinga, E. M. S. (2014). The Management and Outcome of Spinal Implant-related Infections in Pediatric Patients A Retrospective Review. *Pediatric Infectious Disease Journal, 33*(7), 720-723. doi:10.1097/Inf.0000000000000264

Moreira, J. M. R., Ponmozhi, J., Campos, J. B. L. M., Miranda, J. M., & Mergulhão, F. J. (2015). Micro- and macro-flow systems to study Escherichia coli adhesion to biomedical materials. *Chemical Engineering Science, 126*, 440-445. doi:https://doi.org/10.1016/j.ces.2014.12.054

Nair, S., Sasidharan, A., Divya Rani, V. V., Menon, D., Nair, S., Manzoor, K., & Raina, S. (2009). Role of size scale of ZnO nanoparticles and microparticles on toxicity toward bacteria and osteoblast cancer cells. *Journal of Materials Science: Materials in Medicine, 20 Suppl 1*, S235-241. doi:10.1007/s10856-008-3548-5

Nathan, C. F., & Hibbs, J. B. (1991). Role of nitric oxide synthesis in macrophage antimicrobial activity. *Current Opinion in Immunology, 3*(1), 65-70. doi:https://doi.org/10.1016/0952-7915(91)90079-G

National Center for Biotechnology Information. PubChem Compound Summary for CID 5447130, Nitrofurazone. (2021). Retrieved from https://pubchem.ncbi.nlm.nih.gov/compound/Nitrofurazone.

Neufeld, M. J., Ware, B. R., Lutzke, A., Khetani, S. R., & Reynolds, M. M. (2016). Water-Stable Metal–Organic Framework/Polymer Composites Compatible with Human Hepatocytes. *ACS Applied Materials & Interfaces, 8*(30), 19343-19352. doi:10.1021/acsami.6b05948

Nichols, S. P., & Schoenfisch, M. H. (2013). Nitric oxide flux-dependent bacterial adhesion and viability at fibrinogen-coated surfaces. *Biomaterials Science, 1*(11), 1151-1159. doi:10.1039/C3BM60130G

Nitrofurazone. (1992). Retrieved from https://oehha.ca.gov/chemicals/nitrofurazone

North, M. L., Takaro, T. K., Diamond, M. L., & Ellis, A. K. (2014). Effects of phthalates on the development and expression of allergic disease and asthma. *Annals of Allergy, Asthma & Immunology, 112*(6), 496-502. doi:https://doi.org/10.1016/j.anai.2014.03.013

Ofek, I., & Doyle, R. J. (1994). Principles of Bacterial Adhesion. In I. Ofek & R. J. Doyle (Eds.), *Bacterial Adhesion to Cells and Tissues* (pp. 1-15). Boston, MA: Springer US.

Ona, K. R., Courcelle, C. T., & Courcelle, J. (2009). Nucleotide excision repair is a predominant mechanism for processing nitrofurazone-induced DNA damage in Escherichia coli. *Journal of Bacteriology, 191*(15), 4959-4965. doi:10.1128/jb.00495-09

Owens, D. K., & Wendt, R. C. (1969). Estimation of the surface free energy of polymers. *Journal of Applied Polymer Science, 13*(8), 1741-1747. doi:10.1002/app.1969.070130815

Ozcelik, B., Pasic, P., Sangwan, P., Be, C. L., Glattauer, V., Thissen, H., & Boulos, R. A. (2020). Evaluation of the Novel Antimicrobial BCP3 in a Coating for Endotracheal Tubes. *ACS Omega, 5*(18), 10288-10296. doi:10.1021/acsomega.9b04178

Padmavathy, N., & Vijayaraghavan, R. (2008). Enhanced bioactivity of ZnO nanoparticles-an antimicrobial study. *Science and Technology of Advanced Materials, 9*(3), 035004. doi:10.1088/1468-6996/9/3/035004

Pagliaro, M., & Ciriminna, R. (2005). New fluorinated functional materials. *Journal of Materials Chemistry, 15*(47), 4981-4991. doi:10.1039/B507583C

Park, H.-J., Kim, J. Y., Kim, J., Lee, J.-H., Hahn, J.-S., Gu, M. B., & Yoon, J. (2009). Silver-ion-mediated reactive oxygen species generation affecting bactericidal activity. *Water Research, 43*(4), 1027-1032. doi:https://doi.org/10.1016/j.watres.2008.12.002

Pascoal, M., Brook, M. A., Gonzaga, F., & Zepeda-Velazquez, L. (2015). Thermally controlled silicone functionalization using selective Huisgen reactions. *European Polymer Journal, 69*, 429-437. doi:https://doi.org/10.1016/j.eurpolymj.2015.06.026

Pawlak, M., Grygolowicz-Pawlak, E., & Bakker, E. (2010). Ferrocene Bound Poly(vinyl chloride) as Ion to Electron Transducer in Electrochemical Ion Sensors. *Analytical Chemistry, 82*(16), 6887-6894. doi:10.1021/ac1010662

Pawlak, M., Grygolowicz-Pawlak, E., Crespo, G. A., Mistlberger, G., & Bakker, E. (2013). PVC-Based Ion-Selective Electrodes with Enhanced Biocompatibility by Surface Modification with "Click" Chemistry. *Electroanalysis, 25*(8), 1840-1846. doi:https://doi.org/10.1002/elan.201300212

Percec, V., & Asgarzadeh, F. (2001). Metal-catalyzed living radical graft copolymerization of olefins initiated from the structural defects of poly(vinyl chloride). *Journal of Polymer Science Part A: Polymer Chemistry, 39*(7), 1120-1135. doi:10.1002/1099-0518(20010401)39:7<1120::Aid-pola1089>3.0.Co;2-z

Poverenov, E., Shemesh, M., Gulino, A., Cristaldi, D. A., Zakin, V., Yefremov, T., & Granit, R. (2013). Durable contact active antimicrobial materials formed by a one-step covalent modification of polyvinyl alcohol, cellulose and glass surfaces. *Colloids and Surfaces B: Biointerfaces, 112*, 356-361. doi:https://doi.org/10.1016/j.colsurfb.2013.07.032

Rabiee, H., Vatanpour, V., Farahani, M. H. D. A., & Zarrabi, H. (2015). Improvement in flux and antifouling properties of PVC ultrafiltration membranes by incorporation of zinc oxide (ZnO) nanoparticles. *Separation and Purification Technology, 156*, 299-310. doi:https://doi.org/10.1016/j.seppur.2015.10.015

Ramritu, P., Halton, K., Collignon, P., Cook, D., Fraenkel, D., Battistutta, D., . . . Graves, N. (2008). A systematic review comparing the relative effectiveness of antimicrobial-coated catheters in intensive care units. *American Journal of Infection Control, 36*(2), 104-117. doi:https://doi.org/10.1016/j.ajic.2007.02.012

Reinecke, H., & Mijangos, C. (1998). PVC modification with pyridine groups. Synthesis, characterization and transformation to ionomers. *Macromolecular Chemistry and Physics, 199*(10), 2199-2204. doi:doi:10.1002/(SICI)1521-3935(19981001)199:10<2199::AID-MACP2199>3.0.CO;2-E

Revelas, A. (2012). Healthcare - associated infections: A public health problem. *Nigerian Medical Journal, 53*(2), 59-64. doi:10.4103/0300-1652.103543

Rusen, E., Raluca, Ş., Busuioc, C., & Diacon, A. (2020). Hydrophilic modification of polyvinyl chloride with polyacrylic acid using ATRP. *RSC Advances, 10*(59), 35692-35700. doi:10.1039/D0RA05936F

Russell, A. D. (2003). Biocide use and antibiotic resistance: the relevance of laboratory findings to clinical and environmental situations. *The Lancet Infectious Diseases, 3*(12), 794-803. doi:https://doi.org/10.1016/S1473-3099(03)00833-8

Safdar, N., Crnich, C. J., & Maki, D. G. (2005). The Pathogenesis of Ventilator-Associated Pneumonia: Its Relevance to Developing Effective Strategies for Prevention. *Respiratory Care, 50*(6), 725.

Salek, M. M., & Martinuzzi, R. J. (2010). Numerical simulation of fluid flow and hydrodynamic analysis in commonly used biomedical devices in biofilm studies. *Numerical Simulations: Examples and Applications in Computational Fluid Dynamics*, 193-212.

Santos, J. C. S. d., Barbosa, O., Ortiz, C., Berenguer-Murcia, A., Rodrigues, R. C., & Fernandez-Lafuente, R. (2015). Importance of the Support Properties for Immobilization or Purification of Enzymes. *ChemCatChem, 7*(16), 2413-2432. doi:10.1002/cctc.201500310

Schaedlich, K., Schmidt, J.-S., Kwong, W. Y., Sinclair, K. D., Kurz, R., Jahnke, H.-G., & Fischer, B. (2015). Impact of di-ethylhexylphthalate exposure on metabolic

programming in P19 ECC-derived cardiomyocytes. *Journal of Applied Toxicology, 35*(7), 861-869. doi:https://doi.org/10.1002/jat.3085

Schmidt, D. L., Brady, R. F., Lam, K., Schmidt, D. C., & Chaudhury, M. K. (2004). Contact Angle Hysteresis, Adhesion, and Marine Biofouling. *Langmuir, 20*(7), 2830-2836.

Seil, J. T., Rubien, N. M., Webster, T. J., & Tarquinio, K. M. (2011). Comparison of quantification methods illustrates reduced Pseudomonas aeruginosa activity on nanorough polyvinyl chloride. *Journal of Biomedical Materials Research Part B: Applied Biomaterials, 98B*(1), 1-7. doi:10.1002/jbm.b.31821

Seil, J. T., & Webster, T. J. (2010, 26-28 March 2010). *Zinc oxide nanoparticle and polymer antimicrobial biomaterial composites.* Paper presented at the Proceedings of the 2010 IEEE 36th Annual Northeast Bioengineering Conference (NEBEC).

Seil, J. T., & Webster, T. J. (2011). Reduced Staphylococcus aureus proliferation and biofilm formation on zinc oxide nanoparticle PVC composite surfaces. *Acta Biomaterialia, 7*(6), 2579-2584. doi:https://doi.org/10.1016/j.actbio.2011.03.018

Shapiro, G. D., Dodds, L., Arbuckle, T. E., Ashley-Martin, J., Fraser, W., Fisher, M., . . . Ettinger, A. S. (2015). Exposure to phthalates, bisphenol A and metals in pregnancy and the association with impaired glucose tolerance and

gestational diabetes mellitus: The MIREC study. *Environment International, 83*, 63-71. doi:https://doi.org/10.1016/j.envint.2015.05.016

Simões, L. C., Simões, M., & Vieira, M. J. (2010). Adhesion and biofilm formation on polystyrene by drinking water-isolated bacteria. *Antonie van Leeuwenhoek, 98*(3), 317-329. doi:10.1007/s10482-010-9444-2

Singh, A., Rawat, M. S. M., & Pande, C. S. (2010). Chemical modification and characterization of poly(vinyl chloride) by crosslinking of multifunctional amines. *Journal of Applied Polymer Science, 118*(2), 876-880. doi:doi:10.1002/app.32432

Singha, P., Locklin, J., & Handa, H. (2017). A review of the recent advances in antimicrobial coatings for urinary catheters. *Acta Biomaterialia, 50*, 20-40. doi:https://doi.org/10.1016/j.actbio.2016.11.070

Starnes, W. H. (2002). Structural and mechanistic aspects of the thermal degradation of poly(vinyl chloride). *Progress in Polymer Science, 27*(10), 2133-2170. doi:https://doi.org/10.1016/S0079-6700(02)00063-1

Starnes, W. H., & Ge, X. (2004). Mechanism of Autocatalysis in the Thermal Dehydrochlorination of Poly(vinyl chloride). *Macromolecules, 37*(2), 352-359. doi:10.1021/ma0352835

Söderberg, T. A., Sunzel, B., Holm, S., Elmros, T., Hallmans, G., & Sjöberg, S. (1990). Antibacterial effect of zinc oxide in vitro. *Scandinavian Journal of Plastic and*

Reconstructive Surgery and Hand Surgery, 24(3), 193-197. doi:10.3109/02844319009041278

Thorarinsdottir, H. R., Kander, T., Holmberg, A., Petronis, S., & Klarin, B. (2020). Biofilm formation on three different endotracheal tubes: a prospective clinical trial. *Critical Care, 24*(1), 382. doi:10.1186/s13054-020-03092-1

Tsibouklis, J., Graham, P., Eaton, P. J., Smith, J. R., Nevell, T. G., Smart, J. D., & Ewen, R. J. (2000). Poly(perfluoroalkyl methacrylate) Film Structures: Surface Organization Phenomena, Surface Energy Determinations, and Force of Adhesion Measurements. *Macromolecules, 33*(22), 8460-8465. doi:10.1021/ma0008185

Tsibouklis, J., Stone, M., Thorpe, A. A., Graham, P., Peters, V., Heerlien, R., . . . Nevell, T. G. (1999). Preventing bacterial adhesion onto surfaces: the low-surface-energy approach. *Biomaterials, 20*(13), 1229-1235. doi:https://doi.org/10.1016/S0142-9612(99)00023-X

Tüzüm Demir, A. P., & Ulutan, S. (2013). Migration of phthalate and non-phthalate plasticizers out of plasticized PVC films into air. *Journal of Applied Polymer Science, 128*(3), 1948-1961. doi:https://doi.org/10.1002/app.38291

Vasudevamurthy, M. K., Lever, M., George, P. M., & Morison, K. R. (2009). Betaine structure and the presence of hydroxyl groups alters the effects on DNA melting temperatures. *Biopolymers, 91*(1), 85-94. doi:10.1002/bip.21085

Veerachamy, S., Yarlagadda, T., Manivasagam, G., & Yarlagadda, P. K. (2014). Bacterial adherence and biofilm formation on medical implants: A review. *Proceedings of the Institution of Mechanical Engineers, Part H: Journal of Engineering in Medicine, 228*(10), 1083-1099. doi:10.1177/0954411914556137

Walters, P., Cadogan, D. F., & Howick, C. J. (2020). Plasticizers. In *Ullmann's Encyclopedia of Industrial Chemistry* (pp. 1-27).

Wang, Q., & Storm, B. K. (2005). Migration of Additives from Poly(vinyl chloride) (PVC) Tubes into Aqueous Media. *Macromolecular Symposia, 225*(1), 191-204. doi:https://doi.org/10.1002/masy.200550715

Wang, R. L. C., Kreuzer, H. J., & Grunze, M. (1997). Molecular Conformation and Solvation of Oligo(ethylene glycol)-Terminated Self-Assembled Monolayers and Their Resistance to Protein Adsorption. *The Journal of Physical Chemistry B, 101*(47), 9767-9773. doi:10.1021/jp971695

Wang, Q., Sun, F.-J., Liu, Y., Xiong, L.-R., Xie, L.-L., & Xia, P.-Y. (2010). Enhancement of biofilm formation by subinhibitory concentrations of macrolides in icaADBC-positive and-negative clinical isolates of Staphylococcus epidermidis. *Antimicrobial agents and chemotherapy, 54*(6), 2707-2711.

Weaver, M. G., Bai, W.-J., Jackson, S. K., & Pettus, T. R. R. (2014). Diels–Alder Construction of Regiodifferentiated meta-Amino Phenols and Derivatives. *Organic Letters, 16*(5), 1294-1297. doi:10.1021/ol4034447

Wikipedia. Eugen Baumann. Retrieved from https://en.wikipedia.org/wiki/Eugen_Baumann

Wikipedia. Waldo Semon. Retrieved from https://en.wikipedia.org/wiki/Waldo_Semon

Wu, C., Wang, Z., Liu, S., Xie, Z., Chen, H., & Lu, X. (2018). Simultaneous permeability, selectivity and antibacterial property improvement of PVC ultrafiltration membranes via in-situ quaternization. *Journal of Membrane Science, 548*, 50-58. doi:https://doi.org/10.1016/j.memsci.2017.11.008

Wu, H., Li, T., Liu, B., Chen, C., Wang, S., & Crittenden, J. C. (2018). Blended PVC/PVC-g-PEGMA ultrafiltration membranes with enhanced performance and antifouling properties. *Applied Surface Science, 455*, 987-996. doi:https://doi.org/10.1016/j.apsusc.2018.06.056

Wypych, G. (2015). 2 - PVC MANUFACTURE TECHNOLOGY. In G. Wypych (Ed.), *PVC Degradation and Stabilization (Third Edition)* (pp. 25-45). Boston: ChemTec Publishing.

Xu, F. F., & Imlay, J. A. (2012). Silver(I), Mercury(II), Cadmium(II), and Zinc(II) Target Exposed Enzymic Iron-Sulfur Clusters when They Toxify *Escherichia coli*. *Applied and Environmental Microbiology, 78*(10), 3614-3621. doi:10.1128/aem.07368-11

Yamanaka, M., Hara, K., & Kudo, J. (2005). Bactericidal Actions of a Silver Ion Solution on Escherichia coli, Studied by Energy-Filtering Transmission Electron Microscopy and Proteomic Analysis. *Applied and Environmental Microbiology, 71*(11), 7589. doi:10.1128/AEM.71.11.7589-7593.2005

Yu, Z., Zhao, Y., Gao, B., Liu, X., Jia, L., Zhao, F., & Ma, J. (2015). Performance of novel a Ag-n-TiO2/PVC reinforced hollow fiber membrane applied in water purification: in situ antibacterial properties and resistance to biofouling. *RSC Advances, 5*(118), 97320-97329. doi:10.1039/C5RA18185B

Zarrinkhameh, M., Zendehnam, A., & Hosseini, S. M. (2013). Electrochemical, morphological and antibacterial characterization of PVC based cation exchange membrane modified by zinc oxide nanoparticles. *Journal of Polymer Research, 20*(11), 283. doi:10.1007/s10965-013-0283-5

Zhang, L., Tang, M., Zhang, J., Zhang, P., Zhang, J., Deng, L., . . . Dong, A. (2017). One simple and stable coating of mixed-charge copolymers on poly(vinyl chloride) films to improve antifouling efficiency. *Journal of Applied Polymer Science, 134*(12), 44632. doi:doi:10.1002/app.44632

Zhang, X., Li, Y., Hankett, J. M., & Chen, Z. (2015). The molecular interfacial structure and plasticizer migration behavior of “green” plasticized poly(vinyl chloride). *Physical Chemistry Chemical Physics, 17*(6), 4472-4482. doi:10.1039/C4CP05287K

Zhang, X., Shi, F., Niu, J., Jiang, Y., & Wang, Z. (2008). Superhydrophobic surfaces: from structural control to functional application. *Journal of Materials Chemistry, 18*(6), 621-633. doi:10.1039/B711226B

Zhang, Y., Zhao, Q., Li, W., Liu, J., Chen, J., Fan, Y., & Weng, Y. (2020). Substrate Independent Liquid Phase Epitaxy of HKUST-1 as Anticoagulant and Antimicrobial Coating. *Advanced Materials Interfaces, 7*(12), 1902011. doi:https://doi.org/10.1002/admi.201902011

Zhao, B., & Brittain, W. J. (2000). Polymer brushes: surface-immobilized macromolecules. *Progress in Polymer Science, 25*(5), 677-710. doi:https://doi.org/10.1016/S0079-6700(00)00012-5

Zheng, W., Jia, Y., Chen, W., Wang, G., Guo, X., & Jiang, X. (2017). Universal Coating from Electrostatic Self-Assembly to Prevent Multidrug-Resistant Bacterial Colonization on Medical Devices and Solid Surfaces. *ACS Applied Materials & Interfaces, 9*(25), 21181-21189. doi:10.1021/acsami.7b05230

Zou, Y., Kizhakkedathu, J. N., & Brooks, D. E. (2009). Surface Modification of Polyvinyl Chloride Sheets via Growth of Hydrophilic Polymer Brushes. *Macromolecules, 42*(9), 3258-3268. doi:10.1021/ma8025699

Zuñiga-Zamorano, I., Meléndez-Ortiz, H. I., Costoya, A., Alvarez-Lorenzo, C., Concheiro, A., & Bucio, E. (2018). Poly(vinyl chloride) catheters modified with pH-responsive poly(methacrylic acid) with affinity for antimicrobial agents.

Radiation Physics and Chemistry, 142, 107-114. doi:https://doi.org/10.1016/j.radphyschem.2017.02.008